

BEHAVIOUR OF RANDOMLY DISTRIBUTED FIBER-REINFORCED SAND IN SHALLOW FOUNDATIONS

A THESIS

*Submitted in partial fulfilment of the
requirements for the award of the degree*

of

DOCTOR OF PHILOSOPHY

in

CIVIL ENGINEERING

by

RAVI KANT MITTAL



DEPARTMENT OF CIVIL ENGINEERING
INDIAN INSTITUTE OF TECHNOLOGY ROORKEE
ROORKEE-247 667 (INDIA)

MAY, 2007

© INDIAN INSTITUTE OF TECHNOLOGY ROORKEE, ROORKEE, 2007

ALL RIGHTS RESERVED



INDIAN INSTITUTE OF TECHNOLOGY ROORKEE ROORKEE

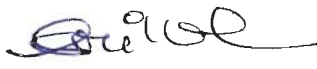
CANDIDATE'S DECLARATION

I hereby certify that the work which is being presented in this thesis entitled, **BEHAVIOUR OF RANDOMLY DISTRIBUTED FIBER-REINFORCED SAND IN SHALLOW FOUNDATIONS** in partial fulfilment of the requirements for the award of the degree of Doctor of Philosophy and submitted in the Department of Civil Engineering, of the Indian Institute of Technology Roorkee, Roorkee, is an authentic record of my own work carried out during the period from July, 2004 to May, 2007 under the supervision of Dr. Swami Saran, Emeritus Fellow, Department of Earthquake Engineering and Dr. Satyendra Mittal, Associate Professor, Department of Civil Engineering, Indian Institute of Technology Roorkee, Roorkee.

The matter presented in this thesis has not been submitted by me for the award of any other degree of this or any other Institute.


(RAVI KANT MITTAL)



This is to certify that the above statement made by the candidate is correct to the best of our knowledge.


(SATYENDRA MITTAL)
Associate Professor
Department of Civil Engineering
Indian Institute of Technology Roorkee
Roorkee-247 667, (India)


(SWAMI SARAN)
Emeritus Fellow
Department of Earthquake Engineering
Indian Institute of Technology Roorkee
Roorkee-247 667, (India)

Date: 10.05.2007

The Ph.D. Viva-Voce Examination of **Mr. RAVI KANT MITTAL**, Research Scholar, has been held on.....3/X/07.....


Signature of Supervisor(s) 


Signature of External Examiner

ABSTRACT

Ground improvement in weak soils has become necessary in view of heavy loads imposed by industrial structures, storage tanks and high-rise buildings. Due to scarcity of good land, one has to build on marginal soils or on filled up soil. Reinforced soil is one of the most popular and fastest growing techniques for improvement of poor soils. Much work has been done on bearing capacity improvement for shallow foundations using planar reinforcement. However, limited study has been carried out on use of randomly distributed fiber-reinforced sand (RDFS) in shallow foundations. Fiber reinforcement may have considerable effect on the bearing capacity improvement same as that by using oriented geogrid layers. RDFS is an emerging technology and it has been successfully used in variety of applications such as slope stabilization, road sub-grade and sub-base. The available literature indicates that this is relatively a simple technique for ground improvement which may have enormous potential for economical solutions to many geotechnical problems. But fiber-reinforced soil still has limited case histories which suggest the additional research to be done in this area.

The objective of present research programme is to explore the application of discrete fibers for bearing capacity improvement and reduction in settlement, tilt & horizontal displacement of footings. In this research work comprehensive experimental study has been carried out on fiber reinforced sand, which includes the study on strength-deformation characteristics of RDFS using triaxial set up and model footing tests under central, vertical, eccentric and inclined loads.

To study the strength - deformation characteristics of RDFS, drained triaxial tests were conducted on polypropylene fibers of different deniers (1 denier = mass in grams per 9000 m length of fiber = 1.11×10^{-7} kg/m) and lengths. In these tests it was observed that with addition of fibers in sand, there is increased peak shear strength, improvement in the post-peak response. In most of cases strain hardening effect at large strains (i.e. more ductile behaviour) was observed which suggests its suitability in foundation material where large deformations are to be tolerated such as earthquake resistant geotechnical-structures and footings subjected to eccentric-inclined loads. In RDFS, the failure does

not take place even at strain of 20% or more. Using experimental data, hyperbolic stress-strain parameters were determined and it was found that Kondner's hyperbolic stress-strain relationships are valid for RDFS.

Model footing tests under central and vertical load were conducted in test box of size 800 mm long, 77 mm wide and 400 mm deep. The Solani river sand reinforced with different type of polypropylene fibers (monofilament and fibrillated) and polypropylene mesh elements (cut from Netlon geogrid CE 121 and Netlon advanced turf system: NAF) was used in the study. A model footing of size 75 mm x 75 mm was used. To study the effect of relative density, tests were conducted at relative density of 30%, 50% and 70% for sand and RDFS. Whole tank was filled with RDFS. No lateral movement of side walls of test box was allowed by providing stiffeners all around it. Thus plane strain conditions prevailed and footing acted as strip footing of 75 mm width (B). Significant improvement in the bearing capacity and reduction in the settlement was observed due to the inclusion of discrete fibers in the sand beneath the footing. It was found that bearing capacity increased and settlement reduced with the increase in the fibre content. Improvement in pressure – settlement behaviour and bearing capacity of RDFS vary significantly for different discrete fibers and mesh elements. Lowest improvement is given by mesh elements from Netlon CE 121 and highest improvement is given by fibrillated fibers. Length or aspect ratio ($\eta = \text{length}/ \text{equivalent diameter or lateral dimension}$) of fiber or mesh may have an effect on bearing capacity but it is primarily the type of fiber or mesh element which matters most. Length appears to be more important factor than aspect ratio. The 6 denier 10 mm long ($\eta = 325$) monofilament fibers give much less improvement compared to 20 denier 20 mm long ($\eta = 350$) monofilament fibers having similar aspect ratio. Pressure – settlement curves of 6 denier 20 mm, 20 denier 20 mm, 20 denier 50 mm are almost similar. “NAF” mesh elements also gave relatively good improvement comparable to thin monofilament fibers but not better than fibrillated fibers. Thus “mesh elements perform better than fiber” is not necessarily true as reported by many investigators. However, mesh elements perform better than straight fiber cut from same mesh is true. Fibrillated fibers are though straight but during mixing these forms mesh like structure. Fibrillated fibers have shown very good improvement even at very low values of settlement ratio (settlement/width of footing) and at

high settlements, a strain hardening behaviour was observed. At a fiber content of 1% by weight, bearing capacity ratio i.e. BCR (BCR is defined as ratio of bearing capacity of RDFS to bearing capacity of sand alone at 10% settlement ratio) was around 10 at relative density of 30% for 1000 denier 50 mm long fibrillated fibers. In general it can be concluded that fibrillated fibers perform best amongst all fibers/ mesh elements used in present study.

Model footing tests were conducted at different relative densities on RDFS to study effect of density on improvement. Consistent improvement is shown at all relative densities. However BCR decreases with increase in relative density but absolute increase in bearing pressure is much high at high relative density.

To find optimum zone of reinforcement below footing, tests were conducted on varying width and depth of RDFS zone. Providing RDFS below footing in zone of 2B depth and 3B width found most effective. It would be more beneficial to reinforce sand in shallow depths with high fiber content as compared to low fiber content for deeper depth. Even providing RDFS zone of 0.5B depth and 2B width below footing is also very effective and BCR was found to increase upto 2.8 for 1% fiber content at 30% relative density.

A comparison of RDFS with horizontally placed geogrid reinforcement was also studied. Optimum and maximum increase in bearing capacity using only geogrid reinforcements was found by using 3 layers of geogrid of sizes 75mm x 375 mm each placed at spacing of 0.33B below footing. In this case bearing capacity ratio increased to 3.2 which is less than 3.3 obtained by using 0.5% of fibrillated fibers in 2B width and 1B depth only. Cost of 3 geogrid layers is about six times compared to 0.5% of fibrillated fibers in 2B width and 1B depth. Cost of single layer planar reinforcement (BCR = 2) is eight times compared to 0.25% fibers used in 2B width and 0.5B depth (BCR=2.1).

Such a high increase in bearing capacity of cohesionless soil can safely permit use of shallow foundations on RDFS in place of deep foundation or other such costly options and prove to be an economical solution for foundations subjected to heavy loads imposed by industrial structure, high rise buildings, storage tanks etc.

An analytical method based on constitutive laws of RDFS (Kondner's hyperbola) has been proposed to predict pressure-settlement behaviour of strip footing resting on fiber reinforced soil. This analytical method is able to predict pressure-settlement curve upto 2/3 of ultimate load. Predicted pressure settlement curve using this method compare very well with reported data in literature.

Tests conducted under submerged conditions record a decrease in bearing pressure of about 40% nearly at all settlement ratio which was expected due to decrease in unit weight of sand due to submergence. Under submerged condition also RDFS is equally effective as in dry condition (thus submergence under water has no adverse effect on improvements gained by RDFS).

Model tests have also been conducted on model strip footing (75 mm x 75 mm) resting on unreinforced and reinforced Solani river sand under eccentric-inclined load in two dimensional tank (plane strain condition). Tests were conducted at eccentricity ratio $e/B = 0.0, 0.1, 0.2$, load inclinations $i = 0^\circ, 10^\circ, 20^\circ$ and relative density of 30%, 50% and 70%. Fibrillated fibers of 1000 deniers 50 mm long have been used in all tests on RDFS. Some tests were conducted on 1000 deniers 20 mm and 360 deniers 20 mm fibrillated fibers also. The pressure-settlement, pressure-horizontal displacement and the pressure-tilt curves had been obtained for each model test. Pressure-settlement behaviour of footings resting on unreinforced sand under eccentric-inclined load was very poor and failure took place at very small deformations. In case of RDFS, pressure-settlement behaviour improved substantially. There was no sudden decrease in bearing pressure with increase in settlement. BCR keeps on increasing as eccentricity and inclination of load increases. Tilt and horizontal displacement decreased substantially. It suggests that for eccentric-inclined loads, beneficial effects of RDFS increased further in comparison to central-vertical loads. The depth and width of the fiber-reinforced zone had been varied and it was found that most optimum zone for eccentric-inclined load is 6 B wide and 1 B deep below footing.

The findings of model test results have been utilised to develop a regression model for strip footing on RDFS in non-dimensional form. Comparison of predicted

values of bearing capacity ratio, settlement and tilt for footings on RDFS, has shown good agreement with their respective values of model test.

To validate models developed and know the influence of size of footing on improved pressure – settlement – tilt behaviour due to RDFS, a series of tests were conducted on 50 mm, 100 mm and 150 mm wide footing in plane strain condition. Results showed that proposed regression model in non-dimensional form predicts very well the BCR and settlement for 50 mm, 100 mm and 150 mm wide footing. For eccentrically and obliquely loaded footings also and results showed that proposed model predicts very well the BCR, vertical settlement and tilt. These findings suggest that nonlinear multiple regression models developed in present research work in the non-dimensional form based on model tests can be used for design of prototype foundations resting on randomly distributed fiber-reinforced sand.

ACKNOWLEDGEMENT

It is my privilege to place on record my sincere gratitude and indebtedness to my supervisor **Prof. Swami Saran**, Emeritus fellow, Department of Earthquake Engineering, Indian Institute of Technology Roorkee, for his invaluable guidance, suggestions, encouragement and constant inspiration throughout the duration of this work. His profound knowledge, foresightedness, timely help, constructive criticism and painstaking efforts made it possible for me to present the work embodied in this thesis in its present form. His painstaking efforts in checking the manuscript are gratefully acknowledged. It was a great pleasure and the opportunity of a life time to have worked under his supervision.

I also wish to express my sincere gratitude to my supervisor **Dr. Satyendra Mittal**, Associate Professor, Department of Civil Engineering, I.I.T. Roorkee, for his continuous moral & administrative support and arranging various facilities required, during the period of this research. His painstaking efforts in checking the manuscript are gratefully acknowledged. I am also thankful to him for providing liberal access to all facilities available in his office room.

I am also grateful to Head, Department of Civil Engineering, for the facilities extended to me by the Department. Sincere thanks are also to the Coordinator, and all the faculty of Geotechnical Engineering, section, Department of Civil Engineering, I.I.T. Roorkee for their support and encouragement from time to time. I am also thankful to the technicians of Geotechnical Engineering Laboratory of Civil Engineering, Department, I.I.T. Roorkee, particularly Shri Atma Ram for his assistance in executing the experimental work.

Special mention of thanks to Prof. M. I. M. Pinto, University of Coimbra, Coimbra, Portugal, Prof. J. G. Zornberg, Civil Engineering Department, University of Texas at Austin, Austin, USA, Prof. R. L. Michalowski, Dept. of Civil and Environmental Engineering, The University of Michigan, Ann Arbor, USA,

Prof. N. C. Consoli, Dept. of Civil Engineering, Federal Univ. of Rio Grande do Sul, Rio Grande do Sul, Brazil, Mr. J. S. Tingle, Research Civil Engineer, U.S. Army Engineer Research and Development Center, Waterways Experiment Station, Vicksburg, USA, Prof. A. Kanyoza, The Polytechnic, University of Malawi, Malawi, Prof. Salah Sadek, American University of Beirut, Lebanon and Mr. Jimmy Hill, Fiber soils, U.S.A., for providing their invaluable research papers.

I wish to thank Mr. Phil Dyer of Synthetic Industries, USA and Mr. Kaushal Pareekh of Nina Industries, Mumbai, India for providing fibrillated fibers, Dr. S. R. Vengsarker, CEO of Zenith Fibers, Vadodra, India for providing monofilament polypropylene fibers and Mr. Ruben Snokes of Conwed Plastics, Belgium for providing Mesh Elements used in this research.

It is my great pleasure to acknowledge the generous support and help provided by my friends Dr. Sarbjeet Singh, P.E., New York, USA and Dr. Pramod Kumar Gupta, Assistant Professor, Department of Civil Engineering, I.I.T. Roorkee, Roorkee, India.

I am also thankful to all fellow research scholars for providing enthusiastic and enjoyable working environment during long hours of experimentation and throughout this research.

I would like to express my deep sense of gratitude and reverence to my family specially, parent in-laws and sister for their kind blessings and always being a constant source of inspiration. The work would not have seen the light of the day without all kind of support of my wife Nidhi. I greatly appreciate my wife for her understanding and unending patience. I wish to express sincere appreciation to my daughters Riju and Riddhi for their cheerful undergoing despite being deprived of the personal attention and happy moments which I otherwise would have given to them during the period of present study.

Last but not the least, I would like to express my sincere thanks to all those who helped me directly or indirectly at various stages of this research work.

(RAVI KANT MITTAL)

CONTENTS

CANDIDATE'S DECLARATION	(i)
ABSTRACT	(ii)
ACKNOWLEDGEMENT	(vii)
CONTENTS	(ix)
LIST OF TABLES	(xiii)
LIST OF FIGURES	(xv)
NOTATIONS AND ABBREVIATIONS	(xxii)
CHAPTER-1: INTRODUCTION	1
1.1 GENERAL	1
1.1.1 Different Form of Random Reinforcement	3
1.1.2 Advantages of Fiber-Reinforced Soil	4
1.2 BASIC MECHANISM	5
1.3 FIELD APPLICATIONS	7
1.4 BRIEF REVIEW OF LITERATURE	9
1.4.1 Laboratory Studies	9
1.4.2 Field Studies	10
1.5 SCOPE OF WORK	12
1.6 ORGANISATION OF THE THESIS	13
CHAPTER-2: LITERATURE REVIEW	15
2.1 INTRODUCTION	15
2.2 SHEAR STRENGTH AND STRESS-STRAIN BEHAVIOR OF RDFS	26
2.2.1 Predictive Models for Shear Strength of Fiber-Reinforced Soil	29
2.2.2 Summary	49
2.3 BEHAVIOUR OF FOOTINGS RESTING ON RDFS	51
2.3.1 Model Footing Test	58
2.3.2 Field Plate Load Test	62
2.3.3 Summary	67

CHAPTER-3: DEVELOPMENT OF EXPERIMENTAL PROGRAMME	68
3.1 GENERAL	68
3.2 SOIL USED	68
3.3 FIBERS/ MESH ELEMENTS USED	70
3.4 TRIAXIAL TESTS	73
3.4.1 Sample Preparation	73
3.4.2 Test Procedure	73
3.4.3 Tests Performed	74
3.5 MODEL FOOTING TESTS	75
3.5.1 Footings	75
3.5.2 Test Setup	76
3.5.3 Loading Assembly	78
3.5.4 Preparation of Sand and RDFS below Footing	79
3.5.5 Test Procedure	79
3.5.6 Tests Performed	80
CHAPTER-4: RESULTS AND INTERPRETATION: STRENGTH AND DEFORMATION CHARACTERISTICS OF RDFS	84
4.1 GENERAL	84
4.2 RESULTS AND INTERPRETATION ON TRIAXIAL TESTS	84
4.2.1 Stress – Strain Behaviour	84
4.2.2 Applicability of Statistical Model for Prediction of Strength of RDFS	96
4.3 CONSTITUTIVE LAWS OF RDFS	99
4.4 SUMMARY	106
CHAPTER-5: MODEL FOOTING TESTS ON RDFS: RESULTS AND INTERPRETATION	108
5.1 GENERAL	108
5.2 BEHAVIOUR OF STRIP FOOTING ON RDFS: CENTRAL – VERTICAL LOAD	108
5.2.1 Evaluation of Ultimate Bearing Capacity and Bearing Capacity Ratio	109

5.2.2	Behaviour of Strip Footing on RDFS using Different Type of Fiber / Mesh Elements	109
5.2.3	Effect of Fiber Content and Relative Density	117
5.2.4	Effect of Depth of RDFS Layer	121
5.2.5	Effect of Size of RDFS Zone below Footing	124
5.2.6	Effect of Aspect Ratio of Fiber	128
5.2.7	Effect of Denier / Diameter of Fiber	131
5.2.8	Effect of Submergence	131
5.3	COMPARISON OF RDFS WITH PLANAR REINFORCEMENT	133
5.4	BEHAVIOUR OF STRIP FOOTING ON RDFS: ECCENTRIC INCLINED LOAD	137
5.4.1	Behaviour of Strip Footing on Unreinforced Sand Subjected to Eccentric – Inclined Load	138
5.4.2	Behaviour of Strip Footing on Unreinforced RDFS Subjected to Eccentric – Inclined Load	140
5.4.3	Effect of Eccentricity and Load Inclination	142
5.4.4	Effect of Depth of RDFS Layer	144
5.4.5	Effect of RDFS Zone below Footing	146
5.5	THE INFLUENCE OF SIZE OF FOOTING ON BEARING CAPACITY – SETTLEMENT – TILT BEHAVIOUR	148
5.6	DEVELOPMENT OF MODELS FOR PREDICTION OF BEARING CAPACITY RATIO, SETTLEMENT AND TILT OF STRIP FOOTING RESTING ON RDFS	152
5.6.1	Models For Prediction of Bearing Capacity Ratio, of Strip Footing Resting on RDFS	153
5.6.2	Models For Prediction of Settlement of Strip Footing Resting on RDFS subjected to Central Vertical Load	168
5.6.3	Models for Prediction Settlement and Tilt of Strip Footing Resting on RDFS Subjected to Eccentric - Inclined Load	171
5.7	VALIDATION OF MODEL DEVELOPED FOR PREDICTED BEARING CAPACITY – SETTLEMENT – TILT BEHAVIOUR	176

5.8	ILLUSTRATIVE EXAMPLES	179
5.8.1	Strip Footing on RDFS under Central-Vertical Load	179
5.8.2	Strip Footing on RDFS under Eccentric - Inclined Load	183
CHAPTER-6: ANALYSIS OF STRIP FOOTING ON RDFS SUBJECTED TO CENTRAL – VERTICAL LOAD USING CONSTITUTIVE LAWS		186
6.1	GENERAL	186
6.2	ANALYSIS OF STRIP FOOTING ON RDFS	186
6.2.1	Introduction	186
6.2.2	Assumptions	187
6.2.3	Procedure for Development of Pressure – Settlement Curve	190
6.3	RESULTS AND VALIDATION OF PROPOSED METHOD	195
6.4	SUMMARY	198
CHAPTER-7: CONCLUSIONS		199
7.1	STRENGTH –DEFORMATION CHARACTERISTICS	199
7.2	FOOTING ON RDFS SUBJECTED TO CENTRAL – VERTICAL LOAD	200
7.3	STRIP FOOTING ON RDFS SUBJECTED TO ECCENTRIC – INCLINED LOAD	202
7.4	PREDICTION OF PRESSURE – SETTLEMENT CURVE FOR STRIP FOOTING ON RDFS USING CONSTITUTIVE LAWS OF RDFS	203
CHAPTER-8: SUGGESTIONS FOR FURTHER RESEARCH		205
	REFERENCES	206

LIST OF TABLES

Table No.	Description	Page No.
1.1	Properties of Commonly Used Fibers (Rehisi, 1988)	2
2.1	Literature Review on Strength Characteristics of RDFS	18
2.2	Literature Review on Behaviour of Footings Resting on RDFS	53
3.1	Properties of Soil Used in the Investigation	69
3.2	Properties of Fibers Used	72
3.3	Properties of Mesh Elements and Geogrid Used	72
4.1	Deviator Stress (kPa) at Failure for Unreinforced Sand (UR) and Different type of RDFS Sample - Experimental	92
4.2	Some of RDFS Samples with Similar $\eta \cdot \chi_w$	95
4.3	Deviators Stress (kPs) at Failure – Predicted	97
5.1	Bearing Capacity Ratio (BCR) Values for Different Type of Fibers and Mesh Elements	114
5.2	Comparison of BCR Values obtained for Different Footing Sizes (B) of 50 mm, 100 mm and 150 mm	151
5.3	BCR values for Different Tests under Central Vertical Load for ($D_r=30\%$)	155
5.4	BCR values for Different Tests under Central Vertical Load for ($D_r=50\%$)	157
5.5	BCR values for Different Tests under Central Vertical Load for ($D_r=70\%$)	159
5.6	BCR values for Different Tests under Eccentric – Inclined Load for ($D_r=30\%$)	162
5.7	BCR values for Different Tests under Eccentric – Inclined Load for ($D_r=50\%$)	165
5.8	BCR values for Different Tests under Eccentric – Inclined Load for ($D_r=70\%$)	167

5.9	Settlement Computation at Factor of Safety 2 & 3 for Fibrillated Fibers under Central-Vertical Load for $R_w=2B$ and $R_d=1B$ at $D_r=30\%$	169
5.10	Settlement & Tilt Computation at Factor of Safety 2 & 3 for Fibrillated Fibers under Eccentric Vertical Load	171
5.11	Settlement & Tilt Computation at Factor of Safety 2 & 3 for Fibrillated Fibers under Eccentric Inclined Load, for Load Inclination of 10°	172
5.12	Settlement & Tilt Computation at Factor of Safety 2 & 3 for Fibrillated Fibers under Eccentric Inclined Load, for Load Inclination of 20°	174
5.13	Observed and Predicted BCR Values using Models Developed by 75 mm width Footing Data for Footing sizes (B) of 50mm, 100 mm and 150 mm	177
5.14	Settlement Computation at Factor of Safety 1, 2 & 3 for 1000 Denier 50 mm Fibrillated Fibers under Central-Vertical Load for $R_w=2B$ and $R_d=1B$ for different width of footing at $D_r=30\%$	179

LIST OF FIGURES

Fig. No.	Description	Page No.
1.1.	Footing subjected to eccentric – inclined load resting on RDFS in which fiber – induced distributed tension is shown along the rupture surface	6
2.1	Shear strength envelope of fiber-reinforced soil (Gray and Ohashi, 1983)	28
2.2	Model of flexible, elastic fiber across the shear zone (Gray and Ohashi, 1983)	30
2.3	Deformation pattern of fiber-reinforced soil (Michalowski and Zhao 1996)	37
2.4	Comparison of theoretical and experimental failure criteria (after Michalowski and Zhao, 1996)	39
2.5	Macroscopic internal friction angle ϕ_r for fiber-reinforced sand	41
2.6	Model prediction and experimental results for polyamide fibers ($l_f=25.4$ mm) in fine sand: (a) fiber content = 0.5% and (b) fiber content = 2.0%	42
2.7	Representation of the equivalent shear strength according to the discrete approach	47
2.8	Footing test – effect of the sand – mesh layer depth on load-settlement behaviour (Mercer et al., 1984)	59
2.9	Pressure settlement curves for unreinforced sand and RDFS at different fiber content (Gupta et al. 2006)	60
2.10	Variation of percentage increase in the bearing capacity of the RDFS with fiber content (Gupta et al. 2006)	61
2.11	Plate load test on 300 mm diameter response directly on residual soil and on top of both sand-cement layer and sand-cement-fiber layer (Consoli et al., 2003a)	64

2.12	Failure mode for both (a) sand-cement layer and (b) sand-cement-fiber layer (Consoli et al., 2003a)	65
2.13	Load–settlement response for plate load tests (Consoli et al. 2003b)	66
3.1	Particle size distribution curve	69
3.2a	Different types of monofilament fibers	70
3.2b	Different types of fibrillated fibers	71
3.2c	Netlon CE121 geogrid and netlon advanced turf mesh elements	71
3.3	Triaxial sample in position	74
3.4	A view of model footings	76
3.5	Test set-up arrangement for model tests (plain strain condition)	77
3.6	Test set-up arrangement for model tests (three dimensional)	77
4.1	Stress- strain curves for sand ($D_r= 30\%$)	85
4.2	Stress- strain curve for sand ($D_r= 30\%$) with 0.25% fiber (6D 10mm)	86
4.3	Stress- strain curve for sand ($D_r= 30\%$) with 0.5% fiber (6D10mm)	86
4.4	Stress- strain curve for sand ($D_r= 30\%$) with 0.75% fiber (6D 10mm)	87
4.5	Stress- strain curve for sand ($D_r= 30\%$) with 1% fiber (6D 10mm)	87
4.6	Stress- strain curve for sand ($D_r= 30\%$) with 0.25% fiber (20D 20mm)	88
4.7	Stress- strain curve for sand ($D_r= 30\%$) with 0.50% fiber (20D 20mm)	88
4.8	Stress- strain curve for sand ($D_r= 30\%$) with 0.75% fiber (20D 20mm)	89
4.9	Stress- strain curve for sand ($D_r= 30\%$) with 1% fiber (20D 20mm)	89
4.10	Stress- strain curve for sand ($D_r= 30\%$) with 0.25% fiber (20D 50mm)	90
4.11	Stress- strain curve for sand ($D_r= 30\%$) with 0.50% fiber (20D 50mm)	90
4.12	Stress- strain curve for sand ($D_r= 30\%$) with 0.75% fiber (20D 50mm)	91
4.13	Stress- strain curve for sand ($D_r= 30\%$) with 1% fiber (20D 50mm)	91
4.14	Comparison of stress- strain curves for RDFS sample with 1.0% fiber content for 6 Denier 10mm and 20Denier 20mm	94
4.15	Stress- strain behaviour of fiber-reinforced sand with 0.75% fiber (6 Denier 10 mm) at different relative densities	95
4.16	Comparison of stress- strain curve for sand ($D_r= 30\%$) with 0.75% fiber of 6D 10mm and 0.25% fiber of 20D 50mm	96

4.17	Experimental versus predicted deviator stress of RDFS using Ranjan et al. (1996)	98
4.18a,b	Hyperbolic stress – strain representation (after Kondner, 1963)	101
4.19	Transformed hyperbolic stress-strain plot for RDFS ($D_r = 30\%$) with 0.25 fiber content (6D10mm)	102
4.20	Transformed hyperbolic stress-strain plot for RDFS ($D_r=30\%$) with 0.25% fiber content (20D 20mm fiber)	103
4.21	1/a for 0.25% 6D10mm fiber	104
4.22	1/b for 0.25% 6D10mm fiber	104
4.23	Stress-strain plot for Mid Ross sand and randomly reinforced with 0.18% mesh elements	105
4.24	Transformed hyperbolic stress-strain plot for Mid Ross sand and randomly reinforced with 0.18% mesh elements	106
5.1	Pressure settlement curve for different fibers / mesh elements for 0.25% fiber content ($R_w=10B$, $R_d=5B$ and $D_r=30\%$)	111
5.2	Pressure settlement curve for different fibers / mesh elements for 0.50% fiber content ($R_w=10B$, $R_d=5B$ and $D_r=30\%$)	112
5.3	Pressure settlement curve for different fibers / mesh elements for 1% fiber content ($R_w=10B$, $R_d=5B$ and $D_r=30\%$)	113
5.4	BCR for different fibers / mesh elements for 0.25% fiber content ($R_w=10B$, $R_d=5B$ and $D_r=30\%$)	114
5.5	BCR for different fibers / mesh elements for 0.50% fiber content ($R_w=10B$, $R_d=5B$ and $D_r=30\%$)	115
5.6	BCR for different fibers / mesh elements for 1% fiber content under central – vertical load	115
5.7	Pressure – settlement curve for different fiber content for 1000D 50 mm fibrillated fiber ($R_w=10B$, $R_d=5B$ and $D_r=30\%$)	118
5.8	Pressure – settlement curve for different fiber content for 1000D 50 mm fibrillated fiber ($R_w=10B$, $R_d=5B$ and $D_r=50\%$)	118
5.9	Pressure – settlement curve for different fiber content for 1000D 50 mm fibrillated fiber ($R_w=10B$, $R_d=5B$ and $D_r=70\%$)	119

5.10	Variation of BCR with relative density for 1000D 500 mm fibrillated fiber at different fiber content	119
5.11	Variation of BCR with fiber content for 1000d 500 mm fibrillated fiber at different relative densities	120
5.12	Pressure settlement curve for different depth of RDFS layer below footing ($R_w=10B$ and $D_r = 30\%$)	122
5.13	Pressure settlement curve for different depth of RDFS layer below footing ($R_w=10B$ and $D_r = 70\%$)	123
5.14	Comparison of pressure - settlement curves for different depth of RDFS layer (R_d) below footing ($R_w = 10B$ and $D_r = 30\%$)	124
5.15	Effect of variation of width of RDFS zone (R_w) below Footing for 1% fiber content of fibrillated fiber ($R_d = 1B$ and $D_r = 30\%$)	125
5.16	Effect of variation of width of RDFS zone (R_w) below Footing for 1% fiber content of fibrillated fiber ($R_d = 2B$ and $D_r = 30\%$)	125
5.17	Effect of variation of width of RDFS zone (R_w) below Footing for 1% fiber content of fibrillated fiber ($R_d = 3B$ and $D_r = 30\%$)	126
5.18	Comparison of pressure–settlement curves for 1% fiber content in 1.5B width and 1B depth and 0.25% fiber content in 2B width and 1B depth	127
5.19	Comparison of pressure – settlement curves for 1% fiber content in 1B width and 1B depth and 0.25% fiber content in 2B width and 0.5B depth	127
5.20	Variation of BCR with relative width (R_w/B) for 1% fiber content of 1000D 50mm fibrillated fiber ($R_d = 1B$ and $D_r = 30\%$)	128
5.21	Pressure-Settlement Curve for 0.25% fiber content, fibrillated fibers, $R_w = 2B$, $R_d = 1B$ and $D_r = 30\%$	129
5.22	Pressure-Settlement Curve for 0.25% fiber content, fibrillated fibers, $R_w = 2B$, $R_d = 1B$ and $D_r = 70\%$	129
5.23	BCR versus aspect ratio curve for 0.25% fiber content, fibrillated fibers, $R_w = 2B$, $R_d = 1B$ and $D_r = 30\%$	130
5.24	BCR versus aspect ratio curve for 0.25% fiber content, fibrillated fibers, $R_w = 2B$, $R_d = 1B$ and $D_r = 70\%$	130

5.25	Pressure – settlement curves for dry and submerged conditions for unreinforced sand and RDFS (0.5% of 1000D 50 mm fibrillated fibers, $R_d = 2B$ and $R_w = 10B$)	132
5.26	BCR versus (s/B) % for dry and submerged conditions for RDFS (0.5% of 1000D 50 mm fibrillated fibers, $R_d = 2B$ and $R_w = 10B$)	132
5.27	Pressure-Settlement curve for sand reinforced with Netlon CE 121, Geogrid layer at $u = S_v = 0.33B$ for $D_r = 30\%$	133
5.28	Comparison of pressure - settlement curves for sand reinforced with Netlon CE 121, three Geogrid layer at $u = S_v = 0.33B$ and 0.5% 1000D 50 mm fibrillated fibers in $R_w = 2B$ and $R_d = 1B$ ($D_r = 30\%$)	134
5.29	Comparison of pressure - settlement curves for sand reinforced with Netlon CE 121, Geogrid layer(s) at $u = S_v = 0.33B$ and 0.5% 1000D 50 mm fibrillated fibers in $R_w = 2B$ and $R_d = 1B$ ($D_r = 30\%$)	135
5.30	Comparison of pressure - settlement curves for sand reinforced with Netlon CE 121, one Geogrid layer at $u = 0.33B$ and 0.25% 1000D 50 mm fibrillated fibers in $R_w = 2B$ and $R_d = 1B$ ($D_r = 30\%$)	136
5.31	Pressure settlement curves for unreinforced sand (UR) for different load eccentricity at $i=0^\circ$ ($D_r=30\%$)	138
5.32	Pressure settlement curves for unreinforced sand (UR) for different load eccentricity at $i=10^\circ$ ($D_r=30\%$)	139
5.33	Pressure settlement curves for unreinforced sand (UR) for different load eccentricity at $i=20^\circ$ ($D_r=30\%$)	139
5.34	Pressure settlement curves for RDFS (1% fiber content) for different load eccentricity at $i=0^\circ$ ($R_w=10B$, $R_d=5B$ and $D_r=30\%$)	140
5.35	Pressure settlement curves for RDFS (1% fiber content) for different load eccentricity at $i=10^\circ$ ($R_w=10B$, $R_d=5B$ and $D_r=30\%$)	141
5.36	Pressure settlement curves for RDFS (1% fiber content) for different load eccentricity at $i=20^\circ$ ($R_w=10B$, $R_d=5B$ and $D_r=30\%$)	141
5.37	BCR for different load eccentricity ($\chi_w = 0.5\%$, $R_w=10B$, $R_d=5B$ and $D_r=30\%$)	142

5.38	BCR for different load eccentricity ($\chi_w = 1\%$, $R_w=10B$, $R_d=5B$ and $D_r=30\%$)	143
5.39	BCR for different load inclinations ($\chi_w = 0.5\%$, $R_w=10B$, $R_d=5B$ and $D_r=30\%$)	143
5.40	BCR for different load inclinations ($\chi_w = 1\%$, $R_w=10B$, $R_d=5B$ and $D_r=30\%$)	144
5.41	Pressure- settlement curves for different relative depth (1.0% 1000D 50mm fibrillated fiber, $e=0.2B$, $i=20^\circ$ and $D_r = 30\%$)	145
5.42	Pressure-tilt curves for different relative depth (1.0% 1000D 50mm fibrillated fiber, $e=0.2B$, $i=20^\circ$ and $D_r = 30\%$)	145
5.43	Pressure-horizontal displacement curves for different relative depth (1.0%, 1000D 50mm fibrillated fiber, $e=0.2B$, $i=20^\circ$ and $D_r = 30\%$)	146
5.44	Pressure- settlement curves for different sizes of RDFS zone (1.0% 1000D 50mm fibrillated fiber, $e=0.2B$, $i=20^\circ$ and $D_r = 30\%$)	147
5.45	Pressure-tilt curves for different relative depth (1.0% 1000D 50mm fibrillated fiber, $e=0.2B$, $i=20^\circ$ and $D_r = 30\%$)	147
5.46	Pressure-horizontal displacement curves for different relative depth (1.0% 1000D 50mm fibrillated fiber, $e=0.2B$, $i=20^\circ$ and $D_r = 30\%$)	148
5.47	Pressure – settlement curves for different sizes of the footings resting on sand at 30 % relative density.	149
5.48	Pressure – settlement curves for different sizes of the footings resting on RDFS (1% 1000D 50mm fibrillated fibers in $R_d=1B$ and $R_w=2B$, $D_r= 30\%$)	150
5.49	Observed BCR versus Predicted BCR for $D_r = 30\%$	156
5.50	Observed BCR versus Predicted BCR for $D_r = 50\%$	158
5.51	Observed BCR versus Predicted BCR for $D_r = 70\%$	160
5.52	Observed BCR versus Predicted BCR for under eccentric - inclined load for ($D_r=30\%$)	164
5.53	Observed BCR versus Predicted BCR for under eccentric - inclined load for ($D_r=50\%$)	166

5.54	Observed BCR versus Predicted BCR for under eccentric - inclined load for ($D_r=30\%$)	167
5.55	S_{oRDFS} / S_{oUR} versus fiber content for $R_w=2B$ and $R_d=1B$ at $D_r=30\%$	170
5.56	S_{eRDFS} / S_{oRDFS} versus e/B plot for $i=0$ ($R_w=4B$ and $R_d=1B$ at $D_r=30\%$)	172
5.57	S_{mRDFS} / S_{oRDFS} versus e/B plot for $i=0$ ($R_w=4B$ and $R_d=1B$ at $D_r=30\%$)	172
5.58	S_{eRDFS} / S_{oRDFS} versus e/B plot for $i=10^\circ$ ($R_w=4B$ and $R_d=1B$ at $D_r=30\%$)	173
5.59	S_{mRDFS} / S_{oRDFS} versus e/B plot for $i=10^\circ$ ($R_w=4B$ and $R_d=1B$ at $D_r=30\%$)	174
5.60	S_{eRDFS} / S_{oRDFS} versus e/B plot for $i=20^\circ$ ($R_w=4B$ and $R_d=1B$ at $D_r=30\%$)	175
5.61	S_{mRDFS} / S_{oRDFS} versus e/B plot for $i=20^\circ$ ($R_w=4B$ and $R_d=1B$ at $D_r=30\%$)	175
5.62	Observed BCR versus Predicted BCR for footing sizes (B) of 50 mm, 100 mm and 150 mm	178
5.63	Pressure - settlement curve for strip footing of 60 cm width	181
6.1	Hyperbolic stress-strain representation (after Kondner, 1963)	189
6.2	RDFS below footing divided into n layers	191
6.3	Uniform vertical loading on an infinite strip	191
6.4	Principal stresses at a point and their directions in the RDFS	193
6.5	Pressure versus settlement curves for strip footing on Ranipur Sand ($B=50$ mm, $D_r=84\%$), considering $5B$ Depth	196
6.6	Pressure versus settlement curves for strip footing ($B=75$ mm) on RDFS 1% fiber content of 20D 20mm ($D_r=30\%$)	196
6.7	Pressure - settlement curve for strip footing ($B=75$ mm) resting on Mid Ross sand with 0.18% mesh elements considering $4B$ depth in 40 layers (experimental data from McGown et al., 1985)	197

NOTATIONS AND ABBREVIATIONS

Symbol	Description
A	Area of footing
O.M.C.	Optimum moisture content
a	Constant of hyperbola
BCR	Bearing capacity ratio
B	Width of footing
B_f	Width of foundation
B_p	Width of plate used in plate load test
b	Constant of hyperbola
c	Cohesion
C_u	Coefficient of uniformity
C_c	Coefficient of curvature
D	Denier of fiber
D_{10}	Effective size
D_{50}	Average grain size
D_f	Depth of embedded footing from ground level
D_r	Relative density
d_f	Equivalent diameter of fiber
E	Modulus of elasticity
E_s	Secant modulus
e	Eccentricity
e_{min}	Minimum void ratio
e_{max}	Maximum void ratio
F	A factor
FOS	Factor of safety
G	Specific gravity
G_s	Specific gravity of solids at 27°C
HDPE	High density polyethylene

$(H_D/B)\%$	Horizontal displacement ratio in percent
i	Load inclination with the vertical
K_0	Coefficient of earth pressure at rest
LDPE	Low density polyethylene
l_f	Fiber length
NAF	Netlon advanced turf mesh elements
N_q	Bearing capacity factor for surcharge part
N_γ	Bearing capacity factor for weight part
P	Load
q	Pressure intensity
q_u	Ultimate bearing capacity
RDFS	Randomly distributed fiber reinforced soil. A common abbreviation used for random mixing of any discrete inclusion to any type of soil.
R_d	Depth of RDFS zone or layer below footing in terms of footing width (B)
R_w	Width of RDFS zone or layer below footing in terms of footing width (B)
S	Total settlement
S_e	Settlement at the point of load application under eccentric or eccentric-inclined load
S_f	Settlement of foundation
S_m	Maximum settlement of footing under eccentric or eccentric-inclined load
S_{oRDFS}	Settlement of footing under central vertical load for footing resting on RDFS
S_{oUR}	Settlement of footing under central vertical load for footing resting on sand
S_p	Settlement of plate used in plate load test
S_v	Vertical spacing between reinforcing layer
t	Tilt of footing
$(s/B)\%$	Settlement ratio in percent
UR	Unreinforced sand
u	Depth of topmost layer of planar reinforcement from footing base
X	Distance from centre of footing along x-axis
Y	Distance from centre of footing along y-axis

Z	Depth from footing base along z-axis
ε	Strain
ε_x	Strain in x-direction
ε_y	Strain in y-direction
ε_z	Strain in z- direction
ε_1	Major principal strain
ε_3	Minor principal strain
γ	Unit weight of soil
γ_w	Unit weight of water
η	Aspect ratio (=length / diameter) of fiber
χ_w	Fiber content by weight
χ	Fiber content by volume
μ	Poisson's ratio
ϕ	Angle of internal friction of soil
ϕ_f	Angle of internal friction of RDFS
σ	Stress
σ_u	Ultimate compressive strength in hyperbolic representation
σ_x	Normal stress in x-direction
σ_y	Normal stress in y-direction
σ_z	Normal stress in z-direction
σ_1	Major principal stress
σ_3	Minor principal stress
$(\sigma_1 - \sigma_3)_f$	Deviator stress at failure
$\tau, \tau_{xz}, \tau_{yz}, \tau_{xy}$	Shear stresses
θ	Angle
θ_1, θ_3	Inclinations of major and minor principal stresses with respect to z-axis, respectively

Note: Additional notations have been defined, wherever they emerge.

1.1 GENERAL

Ground improvement in weak soils has become necessary in view of heavy loads imposed by industrial structures, storage tanks, silos, bridge abutments, high-rise buildings etc. Due to scarcity of good land, one has to build on marginal soils or on filled up soil. Reinforced soil is one of the most popular and fastest growing techniques for improvement of poor soils. Reinforced soil means the soil formed with the inclusion of strips, sheets, nets, mats and grids of metals, synthetic fiber (polymers) or natural fibers to reduce the tensile strain. The soil reinforced with extensible reinforcement (termed Ply-Soil by McGown et al., 1978) has greater extensibility and smaller losses of post-peak strength compared to soil alone. The soil reinforced with inextensible reinforcement is termed 'Reinforced Earth' by Vidal (1969). Fiber reinforcement falls in the category of ideally extensible inclusion.

Soil randomly reinforced with discrete fibers is known as 'Fiber-reinforced Soil'. It is effective in all types of soils (i.e. sand, silt and clay). The fibers may be natural or synthetic. The properties of natural and synthetic fibres used for Civil engineering purposes are presented in Table 1.1. Synthetic fibres like Polypropylene, Nylons, and Plastics are resistant to seawater, acids, alkalies and chemicals (Setty and Rao, 1987).

The polypropylene fibres have high tensile strength and high melting temperature (165°C).

Table 1.1 Properties of Commonly Used Fibers

Fiber Type	Specific Gravity	Tensile Strength x 10 ⁴ (kPa)	Modulus of Elasticity x 10 ⁶ (kPa)	Elongation at Break (%)
Synthetic Fibers				
Polypropylene	0.91	30 to 70	3.5 to 5.5	20
Asbestos	1.9 to 3.37	180 to 350	38 to 190	2 to 3
Glass	2.7	125 to 250	70 to 80	2 to 3.5
Carbon	1.9	260	230	0.5 to 1
Kevlar	1.45	290	65 to 133	2.1 to 4
Polyester	1.3	10000 to 21000	1450 to 2500	20
Nylon	1.14	----	Up to 4	13.5
Plastic	0.92	15 to 20	30 to 50	40 to 60
Natural Fibers				
Coir	0.7 to 1.3	9 to 14	4 to 6	15 to 40
Sisal	1.3 to 1.5	100 to 200	34 to 62	3 to 7
Jute	1.36	400 to 500	17.40	1.1
Bhabar	1.8 to 1.3	5 to 7	----	----
Reed	0.47	3.3	1.52	----
Munja	1.29	20 to 75	----	----
Bamboo	1.5	----	----	----
Banana	1.3	110 to 130	200 to 510	1.8 to 3.5

Also, asbestos, glass and carbon fibres are resistant to alkalies and chemicals. But, in longer duration, they may suffer a certain amount of corrosion (Opoczky and Pentek, 1975). The natural fibres like Sisal, Jute, Bhabar, Munja and Banana suffer deterioration and lose their strength when subjected to alternate wetting in saturated lime solution or 0.1N solution of sodium hydroxide for 24 hours (Rehsi, 1988). The coir fibres do not exhibit any loss of strength when subjected to alternate wetting and drying in the solution of sodium hydroxide and possess good strength characteristics over a longer period of time (Rehsi, 1988).

1.1.1 Different Form of Random Reinforcement

Random reinforcement have been provide to different type of soils in form of mesh elements, discrete fibers, continuous yarn/ filament (Texsol), metallic powder, waste tire-chips, waste plastic strips etc. by various investigators.

- ❖ Polymeric mesh elements (e.g. Mercer et al., 1984; McGown et al., 1985; Adi, 1996; Morel and Gourc, 1997; McGown et al., 2004)
- ❖ Fibers
 - Metallic fibers (e.g. Gray and Ohashi, 1983; Bauer and Fatani, 1991; Fatani et al., 1991; Michalowski and Zhao, 1996)
 - Synthetic fibers
 - Polypropylene (e.g. Ranjan et al., 1994, 1996; Santoni, et al., 2001; Consoli, et al., 2003 a, b)
 - Polyester (e.g. Kaniraj and Havangi, 2001; Kaniraj and Gayatri, 2003; Consoli et al., 2004)
 - Polyamide (e.g. Michalowski and Cermak, 2003)

- Glass fiber (e.g. Maher and Gray, 1990; Consoli, et al., 1998)
- Waste plastic strips (e.g. Benson and Khire, 1994; Sobhan and Mashnad, 2002, 2003; Rao and Dutta, 2004)
- ‘Texsol’ (e.g. Leflaive, 1985; Khay et al., 1990)
- Natural fibers
 - Coir (e.g. Mandal and Murti, 1989; Setty and Shetty, 1989; Kurian 2001; Ranjan et al., 1996; Sivakumar Babu and Vasudevan, 2005; Rao et al., 2006b)
 - Bhabar (e.g. Ranjan et al. 1996)
 - Reed (e.g. Maher and Gray 1990)
 - Sisal (e.g. Prabhakar and Sridhar, 2002)
 - Bamboo (e.g. Khan, 2005)
 - Jute (e.g. Mandal and Murti, 1990; Kumar and Sastry, 2001)
 - Wood shavings (Lee et al., 1973)
- ❖ Metallic Powder (e.g. Verma and Char, 1978; Hosiya and Mandal, 1984; Fatani et al., 1987)
- ❖ Waste tire-chip (e.g. Edil and Bosscher, 1994; Foose et al., 1996; Cecich et al., 1996; Rao and Dutta, 2001; Mandal et al., 2005; Hataf and Rahimi, 2006; Rao and Dutta, 2006)

1.1.2 Advantages of Fiber-Reinforced Soil

Randomly distributed fiber-reinforced soil (RDFS) offers many advantages as listed below:

- Increased shear strength with maintenance of strength isotropy.
- Beneficial for all type of soils (i.e. sand, silt and clay).
- Reduced post peak strength loss.

- Increased ductility.
- Increased seismic performance.
- No catastrophic failure.
- Great potential to use natural or waste material such as coir fibers, shredded tire and recycled waste plastic strips and fibers.
- Provide erosion control and facilitate vegetation development.
- Reduce shrinkage and swell pressures of expansive soil.
- No appreciable change in permeability.
- Unlike lime, cement, and other chemical stabilization methods, the construction using fiber-reinforcement is not significantly affected by weather conditions.
- Fiber-reinforcement has been reported to be helpful in eliminating the shallow failure on the slope face and thus reducing the cost of maintenance.

1.2 BASIC MECHANISM

Randomly oriented discrete inclusions incorporated into granular soil improve its load-deformation behaviour by interacting with the soil particles mechanically through surface friction and also by interlocking. The function of the bond or interlock is to transfer the stress from the soil to the discrete inclusions by mobilizing the tensile strength of discrete inclusions. Thus, fiber-reinforcement works as frictional and tension-resistance elements. Several composite models have been proposed to explain the behaviour of randomly distributed fibres within a soil mass. The proposed models have been based on mechanistic approaches (Gray & Ohashi, 1983 and Maher & Gray, 1990), on energy dissipation approaches (Michalowski & Zhao, 1996 and Michalowski & Cermak, 2003), and on statistics based approaches (Ranjan et al., 1996). Discrete

framework is proposed by Mandal & Suresh (2001) and Zornberg (2002) to explicitly quantify the fibre-induced distributed tension which is the tensile force per unit area induced in a soil mass by randomly distributed fibres. The magnitude of the fibre-induced distributed tension is defined as a function of the properties of the individual fibres and assumed direction of fibre-induced distributed tension. Figure 1.1 depicts a case of footing subjected to eccentric – inclined load resting on RDFS in which fiber-induced distributed tension (t) is shown along the rupture surface. Due to random placement of fibers, fibre-induced distributed tension may be in a direction somewhere between the initial fiber orientation (which is random) and the orientation of the failure plane.

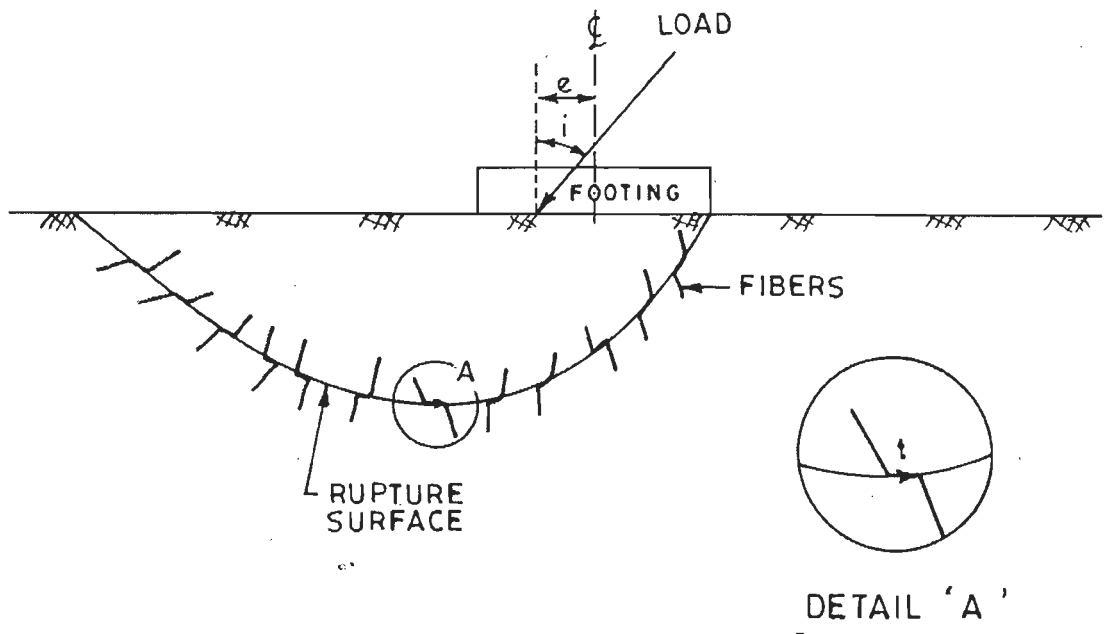


Figure 1.1 Footing subjected to eccentric – inclined load resting on RDFS in which fiber-induced distributed tension is shown along the rupture surface.

In case of randomly distributed fiber-reinforced soil, the position, the direction, the number of fibers and fibre-induced distributed tension at any plane is quite uncertain.

Further it is difficult to quantify that out of these fiber how many are active at particular deformation level. Thus, for the analysis of bearing capacity problems of randomly distributed fiber-reinforced soil, probabilistic/ statistical analysis would be more meaningful and same has been attempted in the present work.

1.3 FIELD APPLICATIONS

Based on review of literature available on laboratory tests and limited case histories, following areas are identified for field application of RDFS.

A promising application of fiber-reinforcement is in the localized repair of failed slopes (Gregory and Chill, 1998; Natraj et al. 2005). In this case, the irregular shape of the soil “patches” limits the use of continuous planar reinforcement, making the fiber-reinforcement an appealing alternative. Unlike planar reinforcement, fiber-reinforcement does not require a large anchorage length, thus minimizing the excavation depth.

Another application is the stabilization of soil veneers (e.g. landfill covers) that are too steep for stabilization using parallel-to-slope continuous reinforcements (Zornberg et al., 2001; Zornberg, 2005). Continuous horizontal reinforcement has been used, but this requires anchoring of the reinforcement into competent material underlying the soil veneer. Also, parallel-to-slope reinforcement requires anchoring the reinforcement at the slope crest. In contrast, the use of discrete fibers does not require anchoring, and is economically and technically feasible.

In pavement construction, fiber-reinforcement can be used to stabilize a wide variety of subgrade soils ranging from sand to high-plasticity clays (Lindh and Eriksson, 1990; Crockford et al., 1993; Grogan and Johnson, 1993; Santoni and Webster, 2001).

The number of passes to failure in field road test was reported to increase by fiber-reinforcement.

Fiber reinforcement has also been used in combination with planar geosynthetic for reinforced slopes or walls. By increasing the shear strength of the backfill materials, fiber reinforcement reduces the required amount of planar reinforcement and may eliminate the need for secondary reinforcement. Fiber-reinforcement has been reported to be helpful in eliminating the shallow failure on the slope face and reducing the cost of maintenance.

Fibers have also been reported to provide cracking control (Al-Wahab and El-Kedrah, 1995; Allan and Kukacka, 1995; Ziegler et al., 1998; Miller and Rifai, 2004). Earth structures constructed using clayey soils, develop desiccation cracks when subjected to wet-dry cycles. Fibers were found to reduce effectively the number and width of desiccation cracks. Fiber reinforcement can also mitigate potential cracking induced by differential settlements because fiber-reinforcement increases the ductility of the soil. Fiber reinforcement can also provide erosion control and facilitate vegetation development since the compaction effort needed for fiber-reinforced soil is less than that for unreinforced soil of equivalent strength, which makes it appealing in the design of evapotranspirative cover system for landfills.

Fiber-reinforcement has also been used for stabilization of expansive soil (Loehr, et al. 2000; Puppala and Musenda, 2000, 2001; Puppala et al. 2000; Puppala et al. 2006; Punthutaecha et al. 2006). Fibers were found to reduce shrinkage and swell pressures of expansive clays. The use of fiber was also reported to increase the free swell potential of the soils.

The inclusion of fibers was also reported to improve the response of a soil mass subjected to dynamic loading (Maher and Woods, 1990; Noorany and Uzdavines, 1989; Al-Refeai and Al-Suhaibani, 1998; Consoli et al. 2005). Reported test results have shown that fibers contribute to increase the dynamic shear modulus and decrease the liquefaction potential.

The inclusion of fibers in backfill of retaining wall has been reported to reduce the earth pressure behind the retaining walls (Arenicz, and Choudhary, 1988; Kurian, 2001; Tiwari, 2004; Park & Tan, 2005).

Another application of fiber-reinforced soil is in shallow foundations. McGown et al. (1985), Wasti & Butun (1996), Dash et al. (2004) and Gupta et al. (2006) have reported that fiber-reinforcement is effective in improving bearing capacity of shallow foundations.

1.4 BRIEF REVIEW OF LITERATURE

1.4.1 Laboratory Studies

During last twenty five years, fiber-reinforced soil has attracted researchers but most of the work has been done on evaluation of reinforced-soil through laboratory testing such as triaxial, unconfined, direct shear, CBR, model footing test, centrifuge model tests on slopes, retaining wall backfill etc. Some of the notable works are listed below.

Triaxial tests : Andersland and Khattak (1979), McGown, et al. (1985), Gray and Al-Refeai (1986), Setty and Rao (1987), Maher and Gray (1990), Al-Refeai (1991), Maher and Ho (1994), Lawton et al. (1993), Charan (1995), Michalowski and Zaho

(1996), Ranjan et al. (1996), Consoli et al.(1998, 2002), Ranjan et al. (1999), Kaniraj and Havanagi (2001), Zornberg (2002), Kaniraj and Gayatri (2003), Michalowski and Cermák (2003).

Unconfined compressive strength tests: Frietag (1986), Maher and Ho (1994), Bueno (1997), Santoni et al. (2001), Consoli et al. (2002).

Direct shear tests: Gray and Ohashi (1983), Fatani et al. (1991), Bauer and Fatani (1991), Benson and Khire, (1994), Kaniraj and Havanagi (2001), Yetimoglu and Salbas (2003), Gupta et al. (2006).

CBR Tests: Setty and Rao (1987), Lindh and Erikson (1990), Lawton et al. (1993), Charan (1995), Gosavi et al. (2004), Yetimoglu et al. (2005)

Model footing tests: McGown et al. (1985), Wasti & Butun (1996), Consoli et al. (2003 a), Consoli et al. (2003 b), Dash et al. (2004), Gupta et al. (2006).

Centrifuge model test on slopes: Li et al. (2001), Sambasivarao and Mandal (2004), Mandal et al. (2005).

Retaining structures: Arenicz and Choudhary (1988), Kurian (2001), Tiwari (2004), Park & Tan (2005).

1.4.2 Field Studies/ Case Histories

Limited field studies are available on pavement testing by Lindh and Erikson (1990), Choubane et al. (2001), Santoni and Webster (2001) and Tingle et al. (2002), slope repair by Gregory and Chill, (1998) and Natraj et al. (2005) and stabilization of soil veneers (e.g. landfill covers) by Zornberg et al., (2001), Zornberg, (2005).

Based on the review of literature the following gaps are identified:

- (i) Out of mesh elements, monofilament fibers and fibrillated fibers, which one perform best is yet to be find out? Optimum conditions for fiber type, length, and content were determined by many of the investigators but their recommendations varied widely due to differences, between experiments, in material properties and test conditions. Hence, needs further investigations in this regard.
- (ii) Effect of denier of fiber on engineering performance of RDFS is not yet established.
- (iii) Few models are available to predict shear strength parameters of RDFS, and they are of limited scope.
- (iv) Studies on RDFS application to shallow foundations are limited in scope. No study is carried out to evaluate effect of various parameters such as type of fiber/ mesh elements, fiber length, fiber aspect ratio, fiber denier, density of RDFS, size of RDFS zone below footing, submerged condition, footing size etc. on behaviour of footing resting on RDFS.
- (v) No model is available to predict bearing capacity and settlement of footing resting on RDFS.
- (vi) Neither analytical solutions nor experimental studies are available in the literature regarding the strip footings resting on sand subjected to eccentric-inclined load to study the behaviour of such footing.

1.5 SCOPE OF WORK

The objective of present research programme is to explore the application of discrete polypropylene fibers for bearing capacity improvement and reduction in settlement, tilt & horizontal displacement of footings. In this research work comprehensive experimental study has been carried out on fiber reinforced sand, which includes the study on strength-deformation characteristics of RDFS using triaxial set up and model footing tests under central, vertical, eccentric and inclined loads.

The following investigations are proposed in present study.

(A) *Studies related to strength characteristics of RDFS*

- (i) To study the strength - deformation characteristics of RDFS, in triaxial testing on polypropylene fibers of different deniers and lengths.
- (ii) Using the concept of non-linear multiple regression analysis, suitable models to be developed to evaluate strength of RDFS and comparison with existing literature.
- (iii) To develop constitutive laws of RDFS using triaxial test results and its validation.

(B) *Studies related to behaviour of strip footings subjected to central vertical load and resting on RDFS.*

- (i) Study of model strip footing behaviour resting on RDFS under central and vertical load. Effect of various parameters to be studied such as type of fibers, mesh elements, length of fiber, denier of fiber, relative density and to find optimum zone of reinforcement below footing.
- (ii) Comparison of RDFS with horizontally placed geogrid reinforcement.

- (iv) Development of an analytical method based on constitutive laws of RDFS (Kondner's hyperbola) to predict pressure-settlement behaviour of strip footing resting on fiber reinforced soil.
 - (v) Detailed nonlinear multiple regression analysis to develop models for prediction of bearing capacity and settlement of footing resting on RDFS.
 - (vi) To study the effect of submerged conditions.
 - (vii) To develop a model for strip footing on RDFS in non-dimensional form for prediction of bearing capacity and settlement.
 - (viii) To validate model developed and influence of size of footing on improved pressure – settlement behaviour due to RDFS.
- (C) Studies regarding eccentrically – obliquely loaded footings resting on RDFS*
- (i) Behaviour of footings under eccentric-inclined loads on RDFS.
 - (ii) To develop a model for strip footing on RDFS in non-dimensional form for prediction of bearing capacity, settlement and tilt.
 - (iii) To validate models developed and influence of size of footing on improved pressure – settlement – tilt behaviour due to RDFS.

1.6 ORGANISATION OF THE THESIS

The whole work carried out in this study is presented as below;

In Chapter one Introduction to the topic, brief review of the relevant literature and aim of the study are presented.

A comprehensive review of all available literature has been given in Chapter Two. Details of experimental programme, test procedures, parameters studied etc. are given in chapter three.

In Chapter Four results and interpretation of triaxial tests results are given. Strength-deformation characteristics of RDFS have been discussed which include stress-strain behaviour, effect of various parameters, development of a predictive strength model for RDFS using non-linear multiple regression analysis and comparison with existing literature. Nonlinear stress-strain curve were modeled using Kondner's constitutive laws and constitutive parameter of RDFS are determined.

Chapter Five presents results and interpretation of model footing tests. Effect of various parameters on behaviour of strip footing under different loading conditions (central - vertical load, central – inclined load, eccentric - vertical load and eccentric – inclined load) resting on RDFS is evaluated. A cost comparison is also made with strip footing resting on planar reinforcement. Using nonlinear, multiple regression analysis, mathematical models are developed using model tests to predict bearing capacity, settlement and tilt of footing resting on RDFS. Design examples also have been included to illustrate the use of the models developed.

In Chapter Six a methodology has been presented, to predict the pressure - settlement characteristic of strip footing under central - vertical loads resting on RDFS, using its constitutive laws.

Chapter Seven presents conclusions that have been drawn out from both the experimental and the analytical investigations.

Finally, the suggestions for further research work have been made and presented in Chapter Eight. At the end of the thesis the list of references has also been given.

Chapter

2

LITERATURE REVIEW

2.1 INTRODUCTION

Randomly distributed fibers reinforced soil – termed as RDFS is among the latest ground improvement techniques in which fibers of desired type and quantity are added in the soil, mixed randomly and laid in position after compaction. Thus the method of preparation of RDFS is similar to conventional stabilization techniques. RDFS is different from the other soil-reinforcing methods in its orientation. In reinforced earth, the reinforcement in the form of strips, sheets etc. is laid horizontally at specific intervals, whereas in RDFS, fibers are mixed randomly in soil thus making a homogeneous mass and maintain the isotropy in strength. Modern geotechnical engineering has focused on the use of planar reinforcement (e.g. metal strips, sheets of synthetic fabrics). However, reinforcing of soil with discrete fibers is still a relatively new technique in geotechnical projects.

Concepts involving the reinforcement of soils using fibers have been used since ancient times. For example, early civilizations added straws and plant roots to soil bricks to improve their properties, although the reinforcing mechanism may have not been fully understood. While building the Great Wall of China, the clay soil was mixed with tamarisk branches. The ancient method of addition of straw of wheat locally called “Turi” to the clay-mud plaster is still very popular in villages. Improvement of soil by tree roots

is similar to the work of fibers. Gray (1974, 1978), Waldron (1977) and Wu et al. (1988) reported that plant roots increase the shear strength of the soil and, consequently, the stability of natural slopes. Synthetic fibers have been used since the late 1980s, when the initial studies using polymeric fibers were conducted. Specifically, triaxial compression tests, unconfined compression tests, direct shear tests and CBR tests had been conducted to study the effect of fiber-reinforcement on strength characteristics and other engineering properties of RDFS. During last twenty five years much work has been done on strength deformation behaviour of RDFS and it has been established beyond doubt that addition of fiber in soil improves the overall engineering performance of soil. Among the notable properties that improve are greater extensibility, small loss of post peak strength, isotropy in strength and absence of planes of weakness. RDFS has been used in many civil engineering projects in various countries in the recent past and the further research is in progress for the many hidden aspects of it.

Several studies have been conducted to investigate the influence of randomly oriented discrete inclusions (fibers, mesh elements, waste material e.g. plastic strips, tire chips, etc.) on the geotechnical behavior of coarse grained and fine grained soils. Most of these studies were conducted on small size samples in triaxial, unconfined compression, direct shear and ring shear tests. Following laboratory studies were carried out by various investigators to study strength deformation behaviour of RDFS:

(1) Triaxial test: Andersland and Khattak (1979), Setty and Rao (1987), Maher and Gray (1990), Al-Refeai (1991), Maher and Ho (1994), Lawton et al. (1993), Michalowski and Zaho (1996), Ranjan et al. (1996), Charan (1995), Consoli et al. (1998), Ranjan et al. (1999), Prabakar & Sridhar (2002), Michalowski and Cermák (2003), Kaniraj and

Havangi (2001), Kaniraj and Gayatri (2003), Gosavi et al. (2004), Yetimoglu et al. (2005), Sivakumar Babu & Vasudevan (2005), Rao et al. (2006).

(2) **Unconfined compressive strength test:** Frietag (1986), Maher and Ho (1994), Santoni et al. (2001), Consoli et al. (2002), Tang et al. (2007), Akbulut et al. (2007).

(3) **Direct shear test:** Gray and Ohashi (1983), Fatani et al. (1991), Bauer and Fatani (1991), Yetimoglu and Salbas (2003), Gupta et al. (2006), Falorca et al. (2006), Pinto and Falorca (2006), Tang et al. (2007), Akbulut et al. (2007).

(4) **Ring shear test:** Falorca et al. (2006), Casagrande et al. (2006).

Salient features of the work of above investigators are presented in Table 2.1 in chronological order. The various abbreviations used in Table 2.1 are given below:

ϕ = angle of internal friction

ϕ_r = angle of internal friction of reinforced soil

D_{50} = average particle size of soil

LL = liquid limit

PI = plasticity index

PL = plastic limit

G, S, M and C = gravel, sand, silt and clay

γ = density

D_r = relative density

C_u = uniformity coefficient

l_f = fiber length

d_f = equivalent diameter of fiber

η = aspect ratio (=length / diameter)

χ_w = fiber content by weight

χ = fiber content by volume

δ = interfacial friction angle between fiber and soil

Table 2.1 Literature Review on Strength Characteristics of RDFS

INVESTIGATOR(S)	SOIL USED	FIBER USED	TESTS CONDUCTED AND RESULTS REPORTED
Andersland and Khattak (1979)	Kaolinite ($\phi = 20^\circ$, LL = 47.8, % PL = 20.3 %, G = 2.7)	Cellulose fiber, $l_f = 1.6$ mm, $d_f = 0.02$ mm, $\chi = 16\%$ and 40%	Triaxial tests. Addition of fiber @ 16% (dry weight basis) increases the peak stress by 43% even though the pure Kaolinite was consolidated at 1.16 times higher confining pressure than the composite. ϕ in CU test at fiber content 16 % increased to 80.4° . ϕ in CD test at fiber content of 16 % increased to 31° .
Gray and Ohashi (1983)	Dry sand $D_r = 20\%$ & 100% , $\phi = 31^\circ$ & 39° . $C_u = 1.5 D_{50}$ $= 0.23$	Reed, polypropylene (monofilament) and copper with $d_f = 1.8, 2.2$ and 1 mm respectively and fiber length of 50 mm each were used. Oriented fibers 3 to 22 in number.	Direct shear tests on all fiber types indicate that shear strength soon reaches a limiting level. This limiting increase was well below the increase predicted by assuming full mobilization of tensile strength. A mere doubling the area ratio of relatively soft reed fiber led to higher shear strength increase than that predicted by stiffer copper fiber. Low modulus fibers (extensible) do some increase in shear strength and limit the “Post failure strength loss”. They do not rupture during shear. Increase in shear strength is proportional to fiber area ratio. However for loose sand, higher strain is required to reach peak. Best orientation of inclusion is 60° with shear plane. Increase in shear strength is same for dense and loose sand. There is a “threshold confining stress”, below which fibers tend to slip. The boundary between pullout and stretching mode of fiber is indicated by a break in the shear envelope. Increasing length of fibers, increases the strength of composite, but upto some limit. Fibers do not affect the angle of internal friction of sand.
McGown, et al. (1985)	Mid –Ross sand $C_u = 5$, $D_{50} = 0.5$ mm	Polypropylene mesh elements 50 mm x 50 mm opening size 6.7 mm x 7.1 mm, $\chi_w = 0.09$ to 0.24%	Drained triaxial test and Model footing tests: Results showed that mesh increased the deviator stress developed at all strains, even at very small strains, and the peak stresses in the sand-mesh mixture occurred at slightly – higher axial strains for the sand alone.
Gray and Al-Refeai (1986)	Muskegon Dune Sand, $D_{50} = 0.41$ mm, $C_u = 1.50$, $\phi = 39^\circ$ ($D_r = 86\%$) and $\phi = 32^\circ$ ($D_r = 21\%$)	Fibers: 1) Reed, $d_f = 1.25$ mm 2) Reed, $d_f = 1.75$ mm 3) Glass fibers, $d_f = 0.30$ mm $l_f = 13, 25, 38$ mm, Geotextiles: (Fabric) Geolon 400, Geolon 200, Typar 3601, Typar 3401 and Fiberglass 196	Triaxial compression tests were run to compare the stress-strain response of a sand reinforced with continuous, oriented fabric layers as opposed to randomly distributed, discrete fibers. The influence of various test parameters such as amount of reinforcement, confining stress, inclusion modulus and surface friction were investigated. At very low strains (< 1%) fabric inclusion resulted in a loss of compressive stiffness. This effect was not observed in the case of fiber reinforcement. The increase in strength with fiber content varied linearly upto a fiber content of 2% by weight, and thereafter approached an asymptotic upper limit. The rate of increase was roughly proportional to the fiber aspect ratio. At the same aspect ratio, confining stress and fiber content, rougher (not stiffer) fibers tended to be more effective in increasing strength.

Setty and Rao (1987)	Lateritic soil (SM) G= 16 %, S = 60 %, M = 21% and C = 1 % , $\phi = 39^\circ$ at optimum moisture content of 16 % . LL = 33%, PI = 7.3 %,	Polypropylene fibers ($d_f=0.5$ mm, $\chi_w = 0,1,2, 3$ and 4 %)	Triaxial test, CBR and tensile test, each at optimum moisture content. Fibers greatly increases cohesion and slightly decreases ϕ . This was because of smooth surface of fibers. The net effect is increase in shear strength. Adding fibers improves CBR value by 2.2 times but only upto 2% fiber content. Adding fibers upto 2% improves dry strength, but afterwards there is a decrease in dry strength. Cohesion is improved to 5.7 times at χ_w of 3% but ϕ decreases to 0.78 times.
Lindh and Eriksson (1990)	Sand , $C_u = 3.5$ and $D_{50} = 0.5$	Monofilament polypropylene fiber, $\chi_w = 0.25$ % and 0.5 % , $l_f = 48$ mm	A field experiment was conducted by placing a reinforced sand layer on the existing road surface. Lindh and Eriksson observed that no rutting had taken place.
Maher and Gray (1990)	Coarse sand of nine types at $C_u = 1$ to 4, $D_{50} = 0.09$ to 0.65mm , moisture content = 10 %	Rubber, $d_f = 1.1$ mm, $\eta = 20$, $l_f = 22$ mm, glass fiber ($d_f = 1, 2.2$ & 0.6 , $\eta = 20$, $l_f = 45$) and Reed fibers (monofilament, $d_f = 0.3$, $\eta = 60$, 80,125, $l_f = 18, 24, 38$ mm) .	Drained triaxial tests. Low modulus fibers (rubber) contribute little to strength despite of high interface friction. Failure surfaces in triaxial test of RDFS are plain and oriented at $(45 + \phi / 2)$, as predicted by that of Coulomb's theory with no preferred plane of weakness. An increase in soil grain size (D_{50}), had no effect on critical confining pressure, rather it reduces fiber contribution to strength. An increase in particle sphericity resulted in higher critical confining pressure, and lower fiber contribution to strength. Poorer the soil gradation, i.e. higher the C_u value, lesser is the value of critical confining pressure. Increase in aspect ratio, resulted in lower critical confining pressure. Increasing fiber content, no effect on critical confining pressure, but increases shear strength. Higher the aspect ratio more effective is the contribution of fibers in increasing shear strength.
Fatani et al. (1991)	Silty sand , $C_u = 5$ and $D_{50} = 0.9$, $c = 10$ kN/m ² , $\phi = 47^\circ$,	Monofilament Copper and steel fiber 70 mm long, oriented (to the shear plane at 0,45 and 90°) and random . The number of inclusions varied from 5 to 32.	Drained Direct shear test at modified proctor dry density $\gamma = 20.8$ kN/m ³ and optimum moisture content 8.9 % . Most effective orientation of fiber is perpendicular to shear plane. Fibers placed parallel to slip plane of direct shear box, caused a reduction in shear strength. The residual strength of RDFS was two times that of pure sands. In randomly placed fibers, only 10-20 % of fibers cross the shear plane, which actually impart the strength. Rigid inclusions do not enhance the shear strength of soil.
Al-Refeai (1991)	Fine sand of two types(with $C_u = 1.6$ and 0.94 and $D_{50} = 0.18$, 0.78, $\phi = 35$ and 40.5° .	Fibrillated polypropylene mesh, ($d_f = 0.4$ mm, $l_f = 25$ &50 mm, $\chi_w = 0.5$ %), monofilament polypropylene pulp & glass fibers ($d_f = 0.1$ mm , $l_f = 2 - 100$ mm $\chi_w = 0.5$ %)	Triaxial test at R.D. = 50 % and 60 % at moisture content = 6 % . Fine sand gives better results than medium sand. Rounded sand particles give higher strength than angular sand particles. Polypropylene mesh type reinforcement gives best results among polypropylene fibrillated and glass fibers mesh. Changing type of soil do not improve ϕ_r/ϕ . ϕ_r is influenced by friction angle between fibers and soil. Strength of RDFS is proportional to extensibility of fibers. Optimum value of polypropylene fiber is 2%, afterwards the strength decreases. Optimum aspect ratio is 75. The tensile force in fiber is proportional to its length. Short fibers require greater confining stress to prevent pullout. Short fibers require greater confining pressure than long fibers to prevent

			slippage. Mesh type is far better than any other type at optimum fiber content of 1% in improving major principal stress at failure. The value of critical confining stress was same for both soils. Contact efficiency of soil is proportional to angularity and fineness. Mixing problem arises as the fiber length and content increased.
Bauer and Fatani (1991)	Silty sand – $C_u = 5$, $D_{50} = 0.9$ c = 10 kN/m^2 , $\phi = 47$, at optimum moisture & modified Proctor	Steel (rigid, $d_f = 3$ mm, $l_f = 40$ mm, random) & copper (flexible $d_f = 0.8$ mm, $l_f = 70$ mm, 5, 6 & 32 fibers aligned) surface area of inclusions in each test was kept same for comparison. Fiber orientation with shear plane was 90° , 60° and 45°	Direct shear test and pullout tests, at modified proctor density of 2.08 t/m^3 and corresponding moisture content of 8.9 %, $\phi = 37^\circ$ and $\delta = 23^\circ$. Results of direct shear test reveal that residual strength of composite was 200 % to 300 % higher than unreinforced soil. Best orientation of fiber was 60° to shear plane. Pullout test revealed that well graded sand gave highest anchorage capacity or friction δ .
Maher and Ho (1994)	Kaoloine LL = 45, PI=15	Polypropylene (monofilament, $d_f = 0.03$ mm, $l_f = 2.5$ to 20 mm $\chi_w = 1$ to 5%) and glass fibers ($d_f = 0.05$ mm, $l_f = 6$ to 25 mm, $\chi_w = 1$ to 5 %)	Unconfined compression test, splitting tension and three point bending. The baseline behaviour of clay is that at low moisture content clay is strong and brittle. Addition of water reverses these properties linearly. Addition of polypropylene fibers (from 1% to 5%) improves the unconfined compressive strength linearly (from 1.2 times to 1.4 times). Increasing the fiber length, decrease the strength (opposite to the effect in granular soils). Increasing fiber length from 5 mm to 20 mm, decrease q_u from 1.4 to 1.2 times. Fibers increase the unconfined compressive strength and reduced post peak loss in strength. This benefit is more at lower moisture content. Increasing fiber content from 0.5% to 4.0 % and the aspect ratio had no effect on optimum moisture content and maximum dry density of composite. Tensile strength of fiber-reinforced clay is inversely proportional to fiber content and fiber length.
Michalowski and Zaho (1995)	Coarse and poorly graded sand . $D_{50} = 0.89$, $C_u = 1.52$ and $\phi = 37^\circ$	25 mm long polyamide and steel fiber at aspect ratio 40, 85 and 180. Oriented fibers at fiber content (volume basis) of 0.4 %, 0.5 %	An energy based homogenisation technique was used to evolve a design criterion. The failure condition of RDFS consists of two parts; first the tensile failure of fiber and second the slip of fiber. The transfer from one part to another is smooth. Theoretical and experimental results were in good agreement.
Michalowski and Zaho (1996)	Dry sand with $C_u = 1.52$ and $D_{50} = 0.9$ mm	Polyamide and steel fibers (dia 0.3, 0.4 mm, aspect ratio 85 and 180 , fiber length = 25 and $\chi = 0.5$ %)	Triaxial test. Addition of steel fibers, increases the peak shear stress by 20% (at aspect ratio = 40, fiber content = 1.25%). This benefit was maximum at low confining pressure (50 kPa). Presence of fibers inhibited the sample dilation and made the sample stiff, before reaching failure. Adding polyamide fibers, increases peak shear but loss of stiffness before failure. This increases the strain. Increasing fiber content and / or aspect ratio, increases peak shear strength significantly.
Charan (1995) and	Cohesionless soils (sand,	Polypropylene (monofilament, $d_f = 0.3$ mm, $\eta = 50$ to 125, $l_f = 15$	Consolidated undrained triaxial test and CBR test. At confining pressure less than critical confining pressure, strength of composite is due to surface friction and at confining

Ranjan et al. (1996)	medium sand, fine sand, silty sand, silt). $C_u = 2.3$ to 2.4 , $c = 18$ to 31 kPa and $\phi = 32^\circ$ to 34°	to 37 mm, $\chi_w = 0.5$ to 4%) coir (monofilament $d_f = 0.2$ mm, $\eta = 50$ to 125 , $\chi_w = 0.5$ to 4 %) and Bhabar ($d_f = 0.2$ mm, $\eta = 50$ to 125 , $\chi_w = 0.5$ to 4 %)	pressure greater than critical confining pressure, due to tensile stress in fibers. Critical confining pressure is unaffected with fiber content and D_{50} . Critical confining pressure decreases with increase in aspect ratio and soil fiber surface friction (δ). The RDFS composite fails before fibers could break. Optimum value of aspect ratio is 100 (afterwards fibers tend to ball up). Optimum value of fiber content is 2% (beyond this value there is difficulty in mixing). Gain in shear strength is 2.4 times at all optimum values of fibers. Critical confining pressure for all soil-fiber parameter was < 100 kPa. Addition of silt by 10 % to 70% decreases shear strength by 10% to 20%. Strength of composite is unaffected by improving density of composite. The CBR value is improved by 2 times at fiber content of 1.5%. A model was developed to predict major principal stress at failure of RDFS using regression analysis of experimental data.
Nataraj and McManis (1997)	Sand: $D_{50} = 0.17$ mm, $C_u = 1.56$, $C_c = 0.95$, $\phi = 33.5^\circ$, O.M.C. = 15.2% Clay: LL = 44%, P.L. = 25%, $c = 84$ kPa, $\phi = 19.5^\circ$, O.M.C. = 17.9%	Fibrillated polypropylene fibers, $l_f = 25$ mm, $\chi_w = 0.1$ to 0.3%	Compaction, unconfined compression, direct shear, CBR test were conducted. Compaction characteristics of the fiber reinforced soils were similar to that of the unreinforced soils. The addition of fibers to clay and sand specimens results in substantial increase in the measured value of the peak friction angle and cohesion. The increase in compression strength is a function of fiber content and moisture content. The CBR values also increase significantly with the addition of fibers. Finally, the test results indicated that optimum fiber content is 0.3% of the dry unit weight of the soil specimen.
Consoli et al. (1998)	Non plastic silty sand (S M), $C_u = 4.8$, $S = 61\%$, $M = 31\%$, $C = 7.5$ %). LL = 22% and PI = 7 %	Glass fibers $l_f = 12.8$ mm, $\chi_w = 3\%$	Drained triaxial test at complete saturation. Addition of cement makes soil brittle whereas adding fibers makes soil ductile. Addition of fibers improves ϕ from 35° to 46° , and ϕ is very much dependent upon confining pressure. Cohesion intercept is practically unaffected by fibers. For uncemented soil ratio of deviator stress for reinforced to non reinforced is 1.65, but for cemented (1%) sands it falls to 1.3. It means fiber reinforcement is more effective for uncemented soils.
Ranjan et al. (1999)	Clay (CH) LL = 58 % PL = 37 % and Sand (SP), $\gamma = 18$ kN/m ² . $\phi = 34^\circ$ and cohesion 10.5 kPa.	Polypropylene monofilament - dia = 0.3 mm and $\delta = 21^\circ$	Moist sample of clay was drilled to make a central hole ,which was filled with a moist mixture of sand and fiber. Fibers inclusion improves both, strength and stiffness of cohesionless soil. In triaxial tests unreinforced soil shows peak of normal stress at 10-20% of axial strain, but reinforced soil do not show any peak, so 15-20% of strain is taken as failure. In principal stress envelope, below the critical confining pressure, fibers tend to slip/pull out. Increasing aspect ratio of fiber, decreases critical confining pressure. Critical confining pressure is unaffected by fiber content. Shear strength increases linearly with increasing the amount of fibers upto 2%, afterwards gain is smaller. Residual strength of reinforced soil is higher than that of unreinforced soil.
Santoni et al. (2001)	Six type of non plastic	Polypropylene, monofilament denier = 4, 15, 20, $l_f = 13$ to 51	Unconfined compressive strength.. Performance of RDFS at base moisture content (2.6 %) and saturation (14%) was found to be same. q_u at 9% is about 2 times the q_u at 14%.

	cohesionless soils , ranging from coarse medium to fine sand with $C_u = 1.44$ to 6.98	mm, $\chi_w = 0$ to 1% , and fibrillated (denier= 260 & 1000 with same l_f and χ_w)	Best fiber shape is fibrillated. q_u fibrillated / q_u mono = 1.5 , Optimum length of fibrillated fiber was 51 mm. Optimum fiber content is 0.8% at Fiber content $< 0.6\%$ caused strain softening (q_u decreases). Fiber content $> 0.8\%$ causes strain hardening. Within sand, changing the D_{50} , shows no difference in results. Adding silt upto 8% leaves the results unaffected. At silt content greater than 12% , q_u decreases. q_u improves slightly by increasing aspect ratio.
Consoli et al. (2002)	Sand (SP), effective size= 0.16 , $C_u = 1.9$	Polyethylene tetraphalate (PT) fiber, monofilament , $d_f = 0.2$ mm . $\chi_w = 0-0.9\%$, $l_f = 0- 36$ mm, moisture content = 10% and cement	Unconfined compression tests, drained triaxial tests. Fiber inclusion improves both the peak strength and ultimate strength for uncemented and cemented sands. Fiber length strongly improves the unconfined compressive strength. Uncemented sand shows a proportionally greater increase. For cemented sand longer the fiber, higher is its efficiency (in increasing the ultimate strength). Addition of fibers only (36 mm fibers) increases the peak friction angle ; for uncemented sands 37 to 43° (1.16 times)and for cemented sands 43 to 49° (1.11 times)secondly it improves the peak failure stress by 1.8 times and ultimate by 1.6 times and thirdly it improves unconfined compressive strength 2 times. Fiber inclusions reduced the brittle behaviour of cemented sand. Cohesion was practically unaffected by fiber inclusion.
Prabakar & Sridhar (2002)	Clay (CL) LL = 31.36 PL = 17.47 PI = 14.09	Sisal $l_f = 10,15,20$ & 25 mm $\chi_w = 0.25,0.5,0.75$ and 1%	Triaxial compression test. When the soil is reinforced with the sisal fibre, it reduces the dry density of the soil due to a low specific gravity and unit weight of sisal fibre. The increase in the fibre length and fibre content also reduces the dry density of the soil. The shear stress of fibre reinforced soil is improved due to the addition of sisal fibre. The shear stress of reinforced soil is also increased with increase in confining pressure. The value of cohesion is increased due to the inclusion of sisal fibre. The non-linear variation of ϕ with percentage of fibre content leads to a conclusion that the behaviour of the fibre included soil may be non-linear in high stress regions.
Pinto and Falorca (2002)	Granular soil	Polypropylene fibre	Compaction, CBR and permeability tests. Reinforced sand provided a significantly greater penetration resistance at large plunger displacements than the unreinforced sand, which indicates that the reinforced sand is the right material when large deformations are expected. The level of improvement depends on the deformation level. A fibre percentage of 0.50% can be used to improve shear strength and bearing capacity of sand with no reduction on its permeability.
Beena (2002)	Red Soil $q_u = 31.2$ kN/m ² $\phi = 39$ Marine Clay LL = 120 PL = 36	Coir fiber pith $\chi_w = 3,5,10\%$	Unconfined compressive strength tests. As percentage pith increases the maximum dry density decreases. It is also found that aging of soil pith mixture will not have much effect on maximum dry density. When coil pith is added to soil it shows a considerable increase in the value of unconfined compressive strength initially at 3% and then decreases as percentage pith increases.

Kaniraj and Gayathri (2003)	Fly Ash collected from Dadri & Rajghat	Polyester Fibers : ($d_f=0.0203\text{mm}$, $l_f=6\text{ mm}$ and $d_f=0.075\text{ mm}$, $l_f=20\text{ mm}$) $\chi_w = 1\%$	Compaction, unconfined compression, unconsolidated undrained and consolidated drained triaxial test were conducted. They observed that fiber inclusion of 1% did not effect the maximum dry density (MDD) and optimum moisture content (OMC) of the Dadri flyash appreciably. However, in Rajghat fly ash, the fiber inclusion of 1% increased the MDD and decreased the OMC. Fiber reinforced flyash specimens exhibited a highly ductile behaviour and fiber inclusions had a significant effect on the stress –strain behaviours of the specimens. When short fibers were used, there was a loss in the strength of the specimens after the attainment of peak stress. The fiber inclusions increased the failure deviator stress and the shear strength parameter C_{uu} and ϕ_{uu} . Values of axial stress at failure determined by the empirical equation of Ranjan et al. (1996) were higher than the measured values by about 16 to 19% on the average for different specimens.
Kumar and Tabor (2003)	Silty clay (CL), P.L = 18, LL = 34, O.M.C.=17%	Nylon fibers $l_f = 51\text{ mm}$, χ_w , 0.05, 0.15 and 0.3%	Unconfined compression tests were performed on soil specimens prepared at degrees of compaction of 93, 96 and 99% at the maximum dry unit weight determined using the Standard Proctor test. Samples compacted at 93% showed higher increase in the peak and residual strength compared to the samples compacted to higher densities. For samples compacted to 93% of maximum dry density obtained from standard proctor test with 0.3% fibers, the residual strength increase was approximately 20 times the residual strength of unreinforced sample, compared to approximately 4 times strength increase in the peak strength.
Gosavi et al. (2004)	Black Cotton Soil (Cl) LL = 38%, PL = 14%, $c = 41\text{ kN/m}^2$, $\phi = 14^\circ$ and CBR=4.9%	Fiber glass ($d_f = 0.1\text{ mm}$, aspect ratio = 250 and 500 mm). Pieces cut from woven fabric (thread diameter = 0.5 mm, aspect ratio = 25 and 50), $\chi_w = 1, 2$ and 3% mixed randomly.	Standard Proctor Test, Direct shear test and Laboratory soaked CBR test. Value of OMC increases and MDD decreases upto $\chi_w = 2\%$ than trends were reversed on further increase in fiber content value of cohesion (c) increases and angle of internal friction of soil (ϕ) decreases with χ_w upto 2%). With further increase χ_w , c decreases and ϕ increases. CBR increases by 42% to 55% for $\chi_w=1\%$. With increase in χ_w , CBR values decreases. Safe bearing capacity increased by 33.58% and 29.67% due to addition of 2% woven fibers and fiber glass with aspect ratio 50 and 500 respectively.
Ghiassain et al. (2004)	Silty sand (SM) $G_s=2.675$, $S=85.8\%$, $M=12\%$, $C=2.2\%$, $C_u=2.84$, $C_c=0.71$, $PL=0$	Waste carpet tape fibers $l_f=5, 15, 25, 35$ and 45mm . $\chi_w = 0, 0.4, 0.6, 0.8$, and 1% . $\eta = 1, 3, 5, 7, 9$.	Triaxial tests. Inclusion of strips increased the peak and residual compressive strengths, maximum modulus, and ductility of fine sand. At any constant aspect ratio (or constant strip contents), the peak strength and total volume change increase with strip content (or aspect ratio) whereas the rate of increase reduces with increasing strip content (or aspect ratio). At any constant strip content, the influence of reinforcement on strength and volume change is more pronounced at higher aspect ratio. Unlike plain soil specimens, the maximum dilation rate in reinforced specimens does not coincide with the onset of failure time but instead occurs earlier.

Yetimoglu et al. (2005)	Uniform quartz river sand $D_{50} = 0.3$ mm $C_u = 1.65$ $C_c = 1.02e_{max} = 0.67$ $e_{min} = 0.57$ Clay: LL = 80% PL = 31%	Polypropylene fibers (Duomix F20) $l_f = 20$ mm $d_f = 0.05$ mm $\chi_w = 0.0625$ to 1%	Laboratory California Bearing Ratio (CBR) tests were performed to investigate the load-penetration behavior of sand fills reinforced with randomly distributed discrete fibers overlying soft clay. Randomly distributed fiber inclusions in sand fill increased the peak piston load considerably. The initial stiffness was insignificantly affected by the fiber inclusions. The penetration value at which the piston load was the highest tended to increase with increasing reinforcement content. Increasing fiber reinforcement content could increase the brittleness of the system providing higher loss of post-peak strength.
Sivakumar Babu & Vasudevan (2005)	Red Soil-Clay LL = 39% PL = 25%	Coir fibre $l_f = 15$ mm $d_f = 0.15, 0.25, 0.35$ mm $\chi_w = 0.5$ to 2.5%	Unconsolidated undrained triaxial test. Major principal stresses at failure increased upto 3-times. Deviator stress for coir fibre reinforced soil (CFRS) increases as the diameter of fibres increases. This trend in contradiction to the synthetic fibres. As the fibre content increases the deviator stress also increases. This was observed upto a fibre content of 2.5%. Beyond 2.5% of fibre, the specimen preparation becomes difficult.
Falorca et al. (2006)	Sandy Clay PI = 19 LL = 35	Polypropylene fiber $l_f = 25, 50, 100$ mm $\chi_w = 0.25$ and 0.5%	Direct shear tests and ring shear tests. Fibre reinforcement increases the shear strength and modifies significantly shear stress displacement behaviour of the soil. Increases in shear strength higher than 20% were observed. The increase in shear strength of soils due to fibres depends on the shear displacement induced. During shear deformation the fibre orientation varies, which influences significantly the increase of shear strength of fibre reinforced soils. Results indicate that progressive strength increase is an outcome of the evolution of the fibre orientation.
Pinto and Falorca (2006)	Granular soil	Polypropylene fiber	Direct shear tests. Influence of both cement and fibre were evaluated. Choice of the most appropriate material to improve the shear strength of the sand depends on the expected level of shear deformation for small deformation (about 3%) cement is advised; for shear deformation up to 10% cement plus fibers are preferable; and finally for higher deformations very extensible polypropylene fibres should be added to the sand.
Casagrande et al. (2006)	Sodium Bentonite-clay (CH) PL = 55% LL = 550% PI = 495%	Polypropylene fibers $l_f = 12, 24$ mm $d_f = 0.023$ mm $\chi_w = 1.5$ or 3%	Ring shear test. The inclusion of randomly distributed fibers increased the peak shear strength of the Bentonite, but the increase in strength deteriorated at large displacements and the residual strengths of both the non-reinforced and fiber-reinforced bentonite were similar. The peak shear strengths were found to increase both with increasing fiber length and content. After testing it was found that the fibers had both extended and broken with a predominance of broken fibers.
Rao et al. (2006b)	Yamuna River Sand $D_{50} = .24$ mm $C_u = 1.76$ $C_c = 1.09$	Coir Fibers $l_f = 25$ mm $d_f = 0.20$ mm (Type A1) $d_f = 0.14$ mm (Type A2) $\chi_w = 0.5$ to 1%	Triaxial compression tests. Coir fibers improve the performance of sand specimens. The deviator stress at failure increases with reinforcement, which conforms the fibre to strengthen the sand, and more with increase in fibre content. The deviator stresses at failure in the sand-coir fibres random inclusion mixture occurred at higher axial strain than sand alone at lower confining pressure. In general the volume change behaviour is

	$e_{min} = 0.64$ $e_{max} = 1.04$		similar to that of unreinforced sand. The effect of reinforcement is to decrease the volumetric expansion. Sand with randomly distributed coir fibre exhibited higher increase in strength parameters than layered one.
Tang et al. (2007)	Clay (CL) PL = 18.6% LL = 36.4% PI = 17.8%	Polypropylene fibers $l_f = 12$ mm $d_f = 0.034$ mm $\chi_w = 0.05$ to 0.25%	Unconfined compressive strength (UCS) and direct shear tests on fiber-reinforced uncemented and cemented clayey soil. The increase in strength of combined fiber and cement inclusions is much more than the sum of the increase caused by them individually. The “bridge” effect of fiber can efficiently impede the further development of tension cracks and deformation of the soil. Bond strength and friction at the interface seem to be the dominant mechanisms controlling the reinforcement benefit. In fiber-reinforced uncemented soil, interactions occur at the interface between the fiber surface and the clay grains play key roles in the mechanical behavior. However, in fiber-reinforced cemented soil, the interactions between the fiber surface and the hydrated products make main contribution to the strength at the interface. The micromechanical behavior of the fiber/matrix interface depends on binding material properties in the soil, normal stress around the fiber body, effective contact area and fiber surface roughness. It is known that the interface roughness plays an important role in reinforced soil systems.
Akbulut et al. (2007)	Three types of clay soil (CH)	Scrap tire rubber fibers $l_f = 2 - 5, 5 - 10, 10 - 15$ mm, $\chi_w = 1, 2, 3, 4, 5$ % Polyethylene fibers $l_f = 5, 10, 15, 30, 40, 60$ mm $\chi_w = 0.1, 0.2, 0.3, 0.4, 0.5$ % Thickness 0.25mm, Width 2.5 mm Polypropylene fibers $l_f = 5, 10, 15, 30, 40, 60$ mm $\chi_w = 0.1, 0.2, 0.3, 0.4, 0.5$ % $d_f = 1$ mm	Unconfined compressive strength (UCS), direct shear test and resonant frequency tests. UCS values increased with increasing tire rubber fibers contents upto 2% and then decreased. The polyethylene and polypropylene fibers increase the UCS values for all contents with a maximum at 0.2%. The UCS values of all samples significantly increased with fiber contents at optimum fiber length. The maximum cohesion values were observed for 10 – mm long fibers. The internal friction angle value of each reinforced sample increased in a non-linear way. The tire rubber, polyethylene, and polypropylene fibers increased damping ratio and shear modulus. The maximum values were observed for 2% tire rubber fibers of 10 – mm length and 0.2% polyethylene and polypropylene fibers of 15 mm.

Works of many notable investigators (e.g., Gray and Ohashi 1983; Gray and Al Refeai 1986; Maher and Gray 1990; Al Refeai 1991; Maher and Ho, 1994; Ranjan et al. 1994, 1996; Michalowski and Zhao 1996; Consoli et al. 1998, 2003a, 2003b; Zornberg, 2002; and Michalowski and Cermak 2003) have improved understanding of the mechanisms involved and the parameters affecting the behavior of fiber-reinforced soils. The following are the factors on which the strength characteristics and other engineering properties of RDFS depend:

- (i) Type of soil: It includes soil sphericity, soil gradation expressed in terms of mean grain size (D_{50}) and uniformity coefficient (C_u).
- (ii) Type of fiber: Monofilament or fibrillated
- (iii) Fiber content: It is expressed in percentage with respect to weight of soil
- (iv) Denier of fiber: It is the weight (in gm) of 9000 m long fiber
- (v) Fiber length
- (vi) Aspect ratio: It is defined as the ratio of the length of fiber to its diameter
- (vii) Fiber-soil surface friction

In the subsequent sections significant works of previous investigators related to shear strength characteristics of RDFS have been discussed.

2.2 SHEAR STRENGTH AND STRESS-STRAIN BEHAVIOR OF RDFS

Previous research has shown that fiber-reinforcement can significantly increase the peak shear strength and limit the post-peak shear strength loss of a soil mass. Most of the experimental studies were conducted using granular soils. Gray and Ohashi (1983) studied the mechanisms of fiber-reinforcement using direct shear tests. Fibers were placed at different specific orientations with respect to the shear plane. The fiber content,

orientation of fibers, and modulus of fibers were found to influence the contribution of fibers to the shear strength. Al-Refeai (1991) studied the effect of fiber-reinforcement using different types of granular soils and fibers. The effect of fiber-reinforcement was found to be more significant in fine sand with sub-rounded particles than in medium grained sand with sub-angular particles. The extensibility of the fibers was also found to influence the soil-fiber interaction.

Research on the use of fiber-reinforcement with cohesive soils has been more limited. Although fiber-reinforcement was reported to increase the shear strength of cohesive soils, such improvement needs additional evaluation because the load transfer mechanisms on the interface between fibers and clayey soils are not clearly understood. Andersland and Khattak (1979) performed tests on kaolinite clay reinforced with cellulose pulp fibers. The shear strength under various testing conditions (undrained, consolidated drained, and consolidated undrained) increased with increasing fiber content. The ductility of the specimen was also found to increase with increasing fiber content. The load transfer mechanism on the fiber-soil interface was explained as an attraction between soil particles and fibers. Maher and Ho (1994) reported that randomly distributed fibers increase the peak unconfined compressive strength, ductility, splitting tensile strength and flexural toughness of kaolinite clay. The contribution of fiber-reinforcement was found to be more significant for specimens with lower water contents. Some researchers have studied the use of fibers to improve the ductility of cement-stabilized soils. Consoli et al. (1998) reported that fiber-reinforcement increases the peak and residual shear strength of cement-treated soil, and reduces its brittleness. Kaniraj and Havanagi (2001) reported similar behaviour when using fibers with soils stabilized with

cement or fly ash. Traditionally, the design of fiber-reinforcement has been performed using a ‘composite’ approach, in which the fiber-soil composite is treated as a homogeneous material. An ‘equivalent’ shear strength envelope has been generally used to quantify the response of the composite under shearing. Gray and Ohashi (1983) reported that the shear strength envelopes of fiber sand mixture show a bilinear trend. The shear strength envelope of fiber-reinforced specimens was found to be parallel to the envelope of unreinforced soil, once the confining pressure exceeds a critical or ‘threshold’ value. Below the critical confining pressure, the reinforced soil showed a higher friction angle than in the unreinforced soil (Figure 2.1).

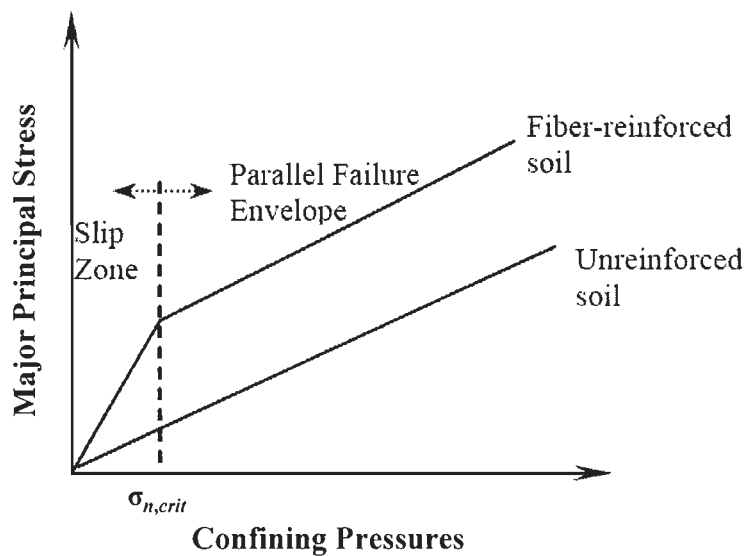


Figure 2.1: Shear strength envelope of fiber-reinforced soil (Gray and Ohashi, 1983)

Gray and Al-Refeai (1986) reported that the critical confining pressure is a function of the surface friction properties of fiber and soils. Nataraj and McManis (1997) reported shear strength results for clay and sand reinforced with polypropylene fibrillated fibers obtained using direct shear tests. The addition of fibers was reported to increase

both the friction angle and cohesion. The shear strength envelope of fiber-reinforced clay was found to be slightly nonlinear. The friction angle at low confining pressures was found to be slightly larger than that at higher confining pressure. The phenomenon was explained as an effect of dilatancy, which increases the interface shear strength between fiber and soil. This effect is more pronounced at low confining stresses than at high confining stresses.

2.2.1 Predictive Models for Shear Strength of Fiber-Reinforced Soil

Soil structures reinforced with randomly distributed fibers have been conventionally designed using composite approaches to characterize the contribution of fibers to stability. In these cases, the mixture is treated as a homogenous composite material. The contribution of the fibers has been typically quantified by an equivalent friction angle and cohesion of soil. Composite models have been proposed by several investigators towards the understanding of the behavior of fibers within a soil mass. These include mechanistic models (Gray and Ohashi, 1983; Maher and Gray, 1990), a statistical model (Ranjan, et al., 1996), and an energy-based limit analysis model (Michalowski and Zhao, 1996). A recently proposed discrete design methodology (Mandal and Suresh, 2001 and Zornberg, 2002) uses concepts derived from limit equilibrium, and requires independent characterization of soils and fibers. An overview of these composite models is presented in subsequent sections.

Gray and Ohashi (1983) proposed a force equilibrium model based on the results of a series of direct shear tests conducted on sands reinforced with fibers placed at fixed orientations. Along the shear plane, the shearing of soils is assumed to cause fiber distortion, thereby mobilizing its tensile resistance (See Figure 2.2).

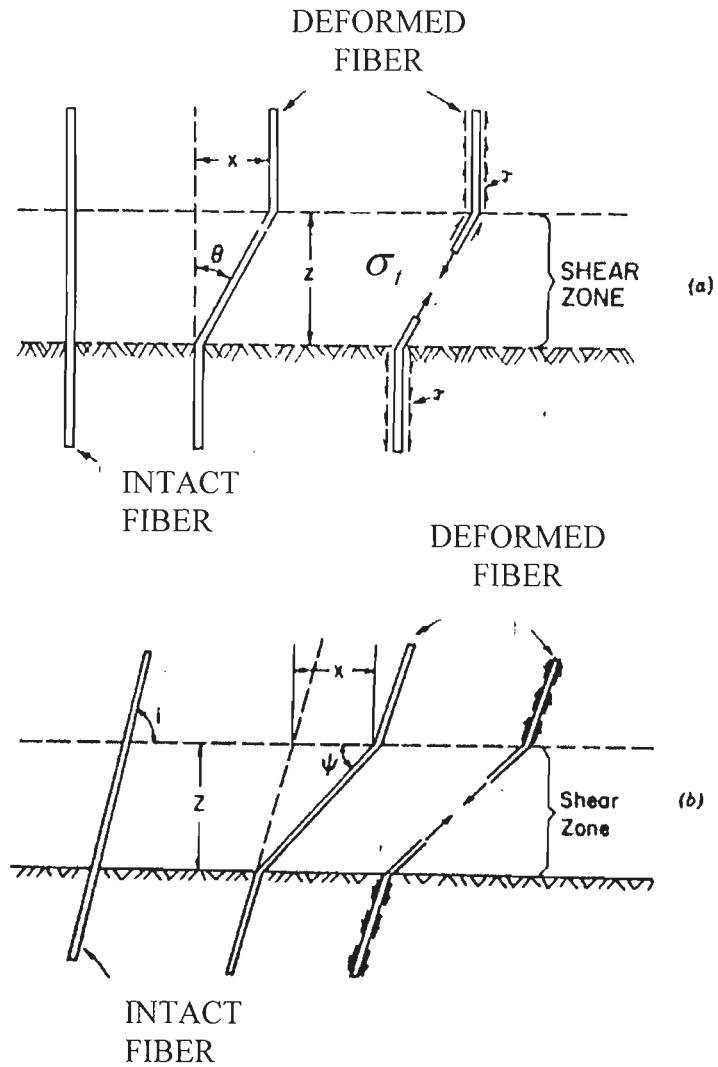


Figure 2.2 Model of flexible, elastic fiber across the shear zone (Gray and Ohashi, 1983): (a) Vertical fiber; (b) Oblique fiber with given orientation angle to the direction of shear

The fiber-induced tension was determined from the extension of fibers by assuming that fibers length, interface friction and confining pressure are large enough to avoid pullout failure. In this case, the fiber-induced tension can be expressed as a function of fiber modulus, interface friction, fiber diameter and thickness of the shear zone, as follows:

$$\sigma_t = \left(\frac{4E_f \tau_f \cdot z}{d_f} \right)^{1/2} (\sec \phi - 1)^{1/2} \quad (2.1)$$

where σ_t = tensile stress within a single fiber,

τ_f = interface frictional resistance along fiber,

E_f = modulus of elasticity of fiber,

d_f = diameter of fiber,

ϕ = friction angle of soil and

z = thickness of shear zone.

The contribution of the fiber-induced tension to the shear strength of the composite was determined from force equilibrium considerations, and was proposed by the following equation if fibers are perpendicular to the shear plane (Fig. 2.2 a):

$$\Delta S = \sigma'_t (\sin \theta + \cos \theta \tan \phi) \quad (2.2)$$

where θ = angle of shear distortion and

σ'_t = mobilized tensile strength of fibers per unit area of soil in shear.

The mobilized tensile strength of fiber per unit area of soil, σ'_t is given by:

$$\sigma'_t = (A_f / A) \sigma_t \quad (2.3)$$

where A_f = area of fibers in shear, and

A = total area of the shear plane.

Also, the following equation was developed for the case in which the fibers are oblique, showing an angle i in relation to the direction of shear:

$$\Delta S = \sigma'_t [\sin(90^\circ - \psi) + \cos(90^\circ - \psi) \tan \phi] \quad (2.4)$$

ψ = orientation angle of the distorted fibers, given by:

$$\psi = \tan^{-1} \left[\frac{1}{(x/z) + (\tan^{-1} i)^{-1}} \right] \quad (2.5)$$

where i = initial orientation of fiber with respect to the shear plane and

x = horizontal shear displacement;

Equation (2.1) calculates the fiber-induced tension force in terms of the fiber extension, which is valid only for extensible fiber with a frictional surface. Commonly used polymeric fibers have relatively high tensile strength and deformation modulus but relatively low interface friction. Consequently, this model may be inadequate when failure is governed by the pullout of fibers. In addition, this model requires determination of the thickness of the shear zone as an input parameter, which is difficult to quantify.

Maher and Gray (1990) further expanded the model proposed by Gray and Ohashi (1983) to randomly-distributed fibers by incorporating statistical concepts. The average embedment length for randomly distributed fiber, which is the smaller portion of the fiber length on either side of the failure plane, was adopted as $1/4$ of the fiber length. The expected average fiber orientation (i) with respect to the slip plane was estimated to be 90° . The average number of fibers N_s , intersecting the unit area of the shear plane was obtained as:

$$N_s = \frac{2\chi}{\pi d_f^2} \quad (2.6)$$

where χ is the volumetric fiber content. And the fiber area ratio was estimated as:

$$\frac{A_f}{A} = N_s \left(\frac{\pi}{4} d_f^2 \right) \quad (2.7)$$

The tensile stress developed in fibers was defined as:

$$\sigma_t = 2(\sigma_n \tan \delta) \frac{l_f}{d_f}, \text{ for } \sigma_n < \sigma_{n,crit} \quad (2.8a)$$

$$\sigma_t = 2(\sigma_{n,crit} \tan \delta) \frac{l_f}{d_f}, \text{ for } \sigma_n \geq \sigma_{n,crit} \quad (2.8b)$$

where σ_n = confining stress acting on the fibers,

δ = angle of skin frictional resistance, and

$\sigma_{n,crit}$ = critical confinement corresponding to the break on the shear strength envelope.

The shear strength increase ΔS , due to fiber-reinforcement was obtained by substituting Equations (2.8a & b) into (2.2), as follows:

For $\sigma_3 < \sigma_{n,crit}$

$$\Delta S = N_s \left(\frac{\pi d_f^2}{4} \right) \left[2(\sigma_n \tan \delta) \frac{l_f}{d_f} \right] (\sin \theta + \cos \theta \tan \phi)(\xi) \text{ for } \sigma_n < \sigma_{n,crit} \quad (2.9a)$$

For $\sigma_3 \geq \sigma_{n,crit}$

$$\Delta S = N_s \left(\frac{\pi d_f^2}{4} \right) \left[2(\sigma_{n,crit} \tan \delta) \frac{l_f}{d_f} \right] (\sin \theta + \cos \theta \tan \phi)(\xi) \text{ for } \sigma_n \geq \sigma_{n,crit} \quad (2.9b)$$

where ξ is an empirical coefficient depending on sand granulometry.

In the force equilibrium model proposed by Gray and Ohashi (1983), the model proposed by Maher and Gray (1990) still requires the thickness of shear zone as input, which is difficult to quantify. The expression of $\sigma_{n,crit}$ and ξ was derived empirically using the results from triaxial tests.

Statistical Model

Ranjan et al. (1996) used the multi-regression analysis of consolidated undrained triaxial compression test results performed on cohesionless soils reinforced with different fibers and proposed an empirical model to predict the contribution of these fibers to major principal stresses at failure. Five hundred tests were performed with three different types of fibers (Polypropylene fibers, Coir fibers, Bhabar fibers) and five sand types (Fine sand, sandy silt, silty sand and medium sand). The purpose was the quantification of the effect of fiber properties, soil characteristics, and confining pressure on the shear strength of fiber reinforced soils using a statistical best – fit model.

Fiber content, fiber aspect ratio, fiber-soil interface friction, and shear strength of unreinforced soil were identified as the main variables influencing the shear strength. These variables were used in a regression analysis, which led to the following relationships for shear strength of fiber-reinforced soil:

For $\sigma_3 < \sigma_{n,crit}$

$$\sigma_{1f} = 12.3(\chi_w)^{0.4} (l_f / d_f)^{0.28} (f^*)^{0.27} (f)^{1.1} (\sigma_3)^{0.68} \quad (2.10a)$$

For $\sigma_3 \geq \sigma_{n,crit}$

$$\sigma_{1f} = 8.78(\chi_w)^{0.35} (l_f / d_f)^{0.26} (f^*)^{0.06} (f)^{0.84} (\sigma_3)^{0.73} \quad (2.10b)$$

where σ_{1f} = major principal stress at failure; χ_w = gravimetric fiber content. The coefficient of interface friction f^* and coefficient of internal friction f is defined as follows:

$$f^* = \frac{a}{\sigma_N} + \tan \delta \quad (2.11a)$$

$$f = \frac{c}{\sigma_N} + \tan \phi \quad (2.11b)$$

where a = adhesion intercept of surface friction; c = cohesion of soil; and σ_N is a normal confining stress level (100 kPa was suggested). The shear strength envelope predicted by equation (2.10) is curvilinear with a transition at certain confining stress (instead of a sharp break). Two expressions were derived depending on the confining stress (below or above the critical confining stress). The critical confining ($\sigma_{n,crit}$) stress usually becomes less when aspect ratio increased.

The model predictions were compared to experimental results by Maher and Gray (1990) and the comparison was reasonably good especially for uniformly graded cohesionless soils. This model is useful for preliminary estimation of fiber reinforcement contribution to strength.

Energy Dissipation Model

Michalowski and Zhao (1996) proposed an energy based homogenization technique to determine a failure criterion for discrete randomly distributed fiber reinforced sand. In this technique, only the fibers are supposed to contribute to energy dissipation. The established failure criterion is then used to predict the major principal stress at failure.

The model requires five parameters for prediction of the major principle stress at failure: fiber content χ , fiber aspect ratio η (the length should be at least one order of magnitude larger than the sand grain size; the diameter of the fiber should be of the same order of magnitude as the sand grain size), fiber yield stress ($\sigma_{f,ult}$), soil-fiber interface friction angle (ϕ_w) and soil angle of internal friction (ϕ). The fibers were assumed to have

a deformation pattern as shown in Figure 2.3, in which fiber slippage takes place on the both ends of the fibers and tensile rupture takes place in the middle of the fibers. The energy dissipation rate during plastic deformation of soil was assumed to conform to the associate flow rule, which is zero. Therefore, only energy dissipation due to fiber-soil slippage and to fiber tensile rupture needs to be considered.

The energy dissipation rate, \dot{d} due to fiber slippage and extension in a single fiber oriented in direction θ is given by:

$$\dot{d} = \pi \cdot d_f \cdot s^2 \sigma_n \tan \delta \langle \dot{\epsilon}_\theta \rangle + \frac{1}{4} \pi \cdot d_f^2 (l_f - 2s) \alpha_{f,ult} \langle \dot{\epsilon}_\theta \rangle \quad (2.12)$$

where d_f = diameter of the fiber,

σ_n = normal stress acting on fiber,

$\sigma_{f,ult}$ = yield stress of the fiber material,

δ = interface friction angle,

s = length of the portion of fiber over which slippage occurs (see Figure 2.3).

$\langle \dot{\epsilon}_\theta \rangle$ = The strain rate in the direction of the fiber

$$= |\dot{\epsilon}_\theta| \text{ if fiber is in tension}$$

$$= 0 \text{ if fiber is in compression} \quad (2.13)$$

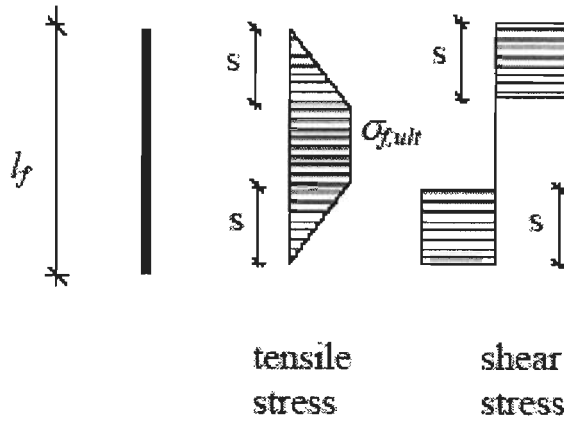


Figure 2.3 Deformation pattern of fiber-reinforced soil (Michalowski and Zhao 1996)

The total energy dissipation rate per volume of the soil, \dot{D} , is the integral of (2.12) over the volume of fiber soil composite. This is given by:

$$\dot{D} = \frac{\chi \sigma_{f,ult}}{3} M \left(1 - \frac{1}{4\eta} \frac{\sigma_{f,ult}}{p \tan \delta} \right) \varepsilon_1 \quad (2.14)$$

where χ = volumetric fiber content; η = aspect ratio; p = mean of the maximum and minimum principal stresses, which is given by:

$$p = (\bar{\sigma}_1 + \bar{\sigma}_3) / 2 \quad (2.15)$$

where $\bar{\sigma}_1$ and $\bar{\sigma}_3$ are the stresses within the homogenized material, different from the stresses within soil (σ_1 and σ_3); and

$$M = \left(\frac{1}{2} + \frac{\phi}{\pi} + \frac{1}{\pi} \cos \phi \right) \tan^2 \left(\frac{\pi}{4} + \frac{\phi}{2} \right) - \frac{1}{2} - \frac{\phi}{\pi} + \frac{1}{\pi} \cos \phi \quad (2.16)$$

If pure slippage occurs with no yielding of fibers, Equation (2.14) can be simplified to:

$$\dot{D} = \frac{1}{3} \chi \cdot \eta \cdot M \cdot p \cdot (\tan \delta) \cdot \varepsilon_1 \quad (2.17)$$

The energy dissipation rate is equal to the work rate of the macroscopic stress for $\bar{\sigma}_{ij}$

$$\dot{D} = \bar{\sigma}_{ij} \dot{\varepsilon}_{ij} \quad (2.18)$$

For plane strain condition, the energy dissipation rate is

$$\dot{D} = \dot{\varepsilon}_1 \bar{\sigma}_1 + \dot{\varepsilon}_3 \bar{\sigma}_3 \quad (2.19)$$

The kinematics of the soil is governed by the flow rule associated with the Mohr-Coulomb yield criterion, which leads to the following relationship for the strain rate:

$$\frac{\dot{\varepsilon}_1 + \dot{\varepsilon}_3}{\dot{\varepsilon}_1 - \dot{\varepsilon}_3} = -\sin \phi \quad (2.20)$$

A failure criterion was derived from (2.19) by substituting (2.20) into (2.19), as follows :

$$\frac{R}{\chi \sigma_{f,ult}} = \frac{P}{\chi \sigma_{f,ult}} \sin \phi + \frac{1}{3} N \left(1 - \frac{1}{4\pi\chi} \frac{\cot \delta}{\frac{P}{\chi \sigma_{f,ult}}} \right) \quad (2.21)$$

where R = radius of the Mohr's circle; and

$$N = \frac{1}{\pi} \cos \phi + \left(\frac{1}{2} + \frac{\phi}{\pi} \right) \sin \phi \quad (2.22)$$

When pure slippage takes place, (2.21) can be simplified to:

$$R = p \left(\sin \phi + \frac{1}{3} N \chi \eta \tan \delta \right) \quad (2.23)$$

The model predictions were in good agreement with experimental results (Figure 2.4).

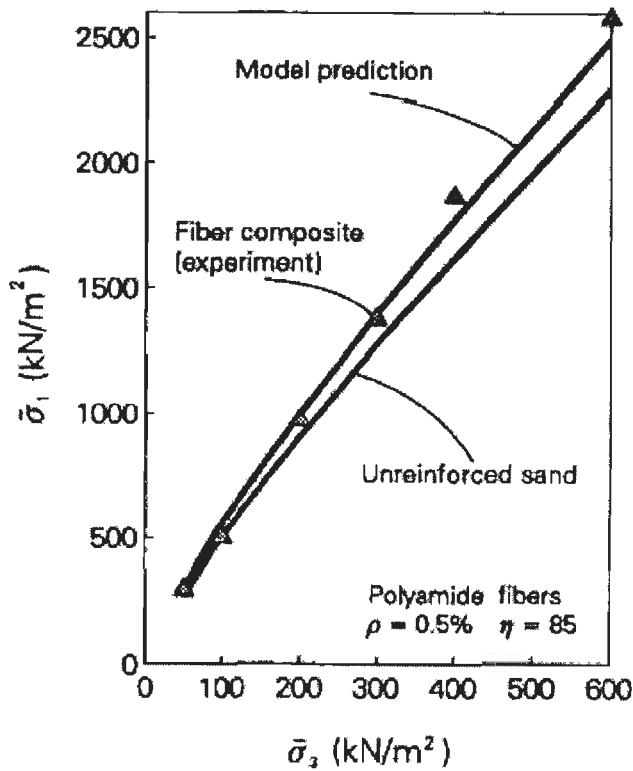


Figure 2.4 Comparison of theoretical and experimental failure criteria (after Michalowski and Zhao, 1996)

Michalowski and Cermak (2003)

To complete the modeling work of Michalowski and Zhao (1996), Michalowski and Cermak (2003) performed laboratory tests and proposed the concept of “macroscopic angle of internal friction (ϕ_r)” as a way of describing the shear strength of fiber – reinforced soils. This angle included the influence of both the sand and the fibers.

The critical confining stress was also derived as

$$\sigma_{n,crit} = \frac{6 - M \cdot \chi \cdot \eta \tan \phi_w}{6(1 + K_p) \cdot \eta \cdot \tan \phi_w} \sigma_{f,ult} \quad (2.24)$$

For practical analyses, one can replace fiber-reinforced sand with an equivalent granular material characterized by the angle ϕ_r .

$$\phi_r = 2 \tan^{-1} \sqrt{\frac{\chi \cdot \eta \cdot M \cdot \tan \phi_w + 6 \cdot K_p}{6 - \chi \cdot \eta \cdot M \cdot \tan \phi_w}} - \frac{\pi}{2} \quad (2.25)$$

where,

ϕ_r = angle of internal friction of equivalent granular material reinforced with fiber,

η = fiber aspect ratio,

χ = volumetric fiber concentration,

$M = K_p \cdot \sin \theta_o$,

$\theta_o = \tan^{-1} \sqrt{K_p / 2}$,

$K_p = \tan^2 (45^\circ + \phi / 2)$,

ϕ = friction angle of un-reinforced sand, and

ϕ_w = peak interface friction angle.

The angle ϕ_r is presented in Figure 2.5 as a function of the product of fiber concentration and fiber aspect ratio. This angle has a physical sense only when the confining stress is less than $\sigma_{n, \text{crit}}$. An equivalent friction angle beyond this stress is no longer constant and no convenient closed-form representation was found. In practical applications the minor principal stress in fiber-reinforced soil is likely to be of the order of 100 kPa, whereas the critical stress is beyond 1000 kPa.

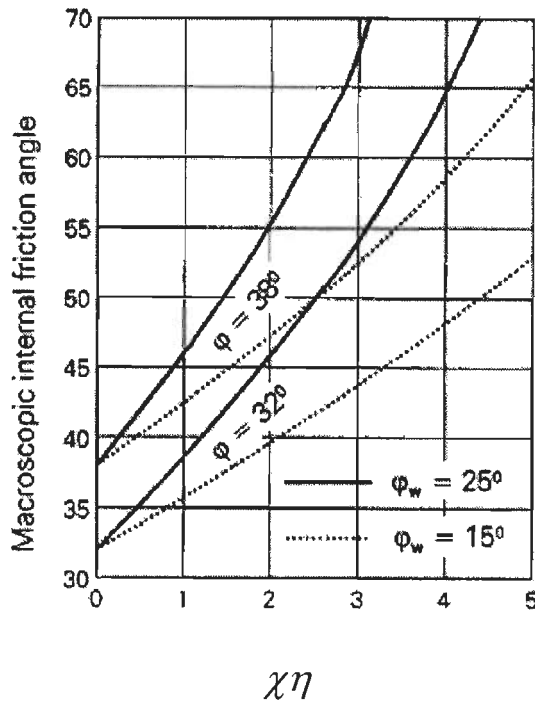


Figure 2.5 Macroscopic internal friction angle ϕ_r for fiber-reinforced sand

The triaxial testing program implemented by Michalowski and Cermak (2003), included two types of sand and different fiber geometries and concentrations. During the testing, the void ratio, not the relative density, was chosen as the most suitable parameter to describe the compaction of the reinforced sand because the addition of fibers affected the maximum and minimum void ratios of the mixture which made the relative density a rather impractical parameter. The shear strength was improved by as much as 70% with a

volumetric fiber content of 2%. Whereas, when the fiber concentration was 0.5% the reinforcement effect dropped to about 20% or less. The reinforcing effect in fine sand is stronger, compared to that in the coarse sand, when the fiber concentration is small (0.5%). However, the relative increase in strength of coarse sand is greater for large fiber concentration (2%). The reinforcing effect is dependent on the fiber aspect ratio. The larger the aspect ratio, the more effective are the fibers. However, if the fiber aspect ratio and concentration are kept constant but the length is varied, longer fibers contribute more to the composite strength than do the shorter fibers. The reinforcement is more effective when the fiber length is larger compared with the size of the grains. The model predictions were in good agreement with experimental results (Figure 2.6).

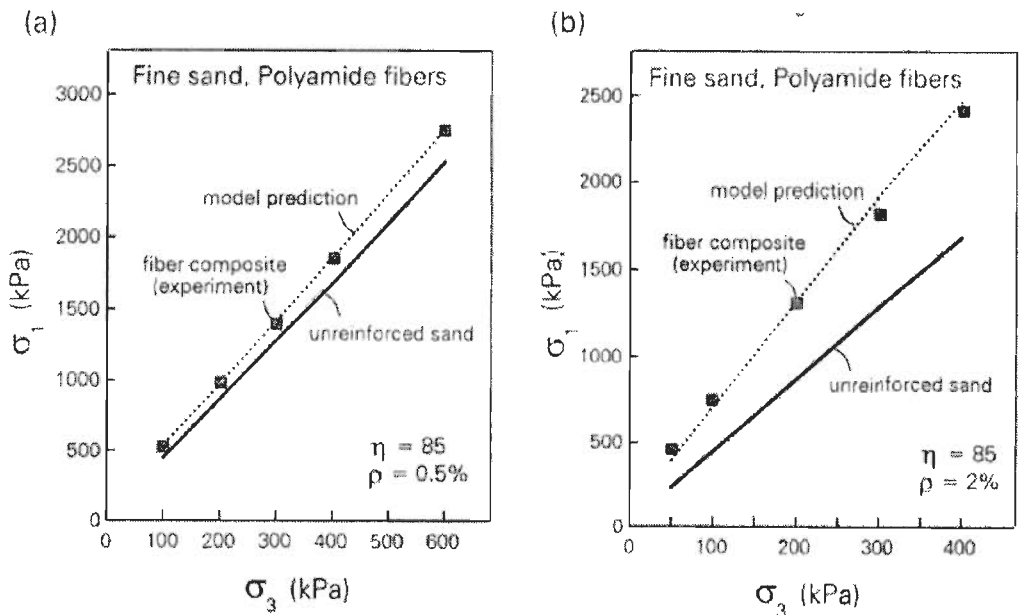


Figure 2.6 Model prediction and experimental results for polyamide fibers ($l_f = 25.4$ mm) in fine sand: (a) Fiber content = 0.5% and (b) Fiber content = 2.0%

Discrete Framework (Mandal and Suresh, 2001 and Zornberg, 2002)

A discrete approach for the design of fiber-reinforced soil slopes was recently proposed to characterize the contribution of randomly distributed fibers to stability (Mandal and Suresh, 2001; Zornberg, 2002). The proposed methodology treats the fibers as discrete elements that contribute to stability by mobilizing tensile stresses along the shear plane.

The contribution of fibers to stability leads to an increased shear strength of the “homogenized” composite reinforced mass. However, the reinforcing fibers actually work in tension and not in shear. The discrete framework explicitly quantifies the fiber-induced distributed tension, t , which is the tensile force per unit area induced in a soil mass by randomly distributed fibers. Specifically, the magnitude of the fiber induced distributed tension is defined as a function of properties of the individual fibers. In this way, as in analyses involving planar reinforcements, limit equilibrium analysis of fiber-reinforced soil can be explicitly account for by the tensile forces.

The interface shear strength of individual fibers can be expressed as:

$$f_f = c_{i,c'} \cdot c' + c_{i,\phi'} \cdot \tan \phi' \cdot \sigma'_{n,ave} \quad (2.26)$$

where c' and ϕ' are the cohesive and frictional components of the soil shear strength and $\sigma_{n,ave}$ is the average normal stress acting on the fibers. The interaction coefficients, $c_{i,c'}$ and $c_{i,\phi'}$ commonly used in soil reinforcement literature for continuous planar reinforcement, are adopted herein to relate the interface shear strength to the shear strength of the soil. The interaction coefficients are defined as:

$$c_{i,c'} = \frac{a'}{c'} \quad (2.27)$$

$$c_{i,\phi'} = \frac{\tan \delta'}{\tan \phi'} \quad (2.28)$$

where a' is the adhesive component of the interface shear strength between soil and the polymeric fiber, and $\tan \delta'$ is the frictional component.

The pullout resistance of a fiber should be estimated over the shortest side of the two portions of a fiber intercepted by a failure plane. The length of the shortest portion of a fiber intercepted by a failure plane varies from zero to half of the fiber length. Statistically, the average embedment length of randomly distributed fibers,

$l_{e,ave}$, can be defined by:

$$l_{e,ave} = \frac{l_f}{4} \quad (2.29)$$

where l_f is the total length of the fibers.

The average pullout resistance can be quantified along the average embedment length, $l_{e,ave}$, of all individual fibers crossing a soil control surface A . The ratio between the total cross sectional area of the fibers A_f and the control surface A can be defined by the volumetric fiber content χ . That is:

$$\chi = \frac{A_f}{A} \quad (2.30)$$

When failure is governed by pullout of the fibers, the fiber-induced distributed tension, t_p , is defined as the average of the tensile forces within the fibers over the control area A . Consequently, t_p can be estimated as:

$$t_p = \chi \cdot \eta \cdot (c_{i,c'} \cdot c' + c_{i,\phi'} \cdot \tan \phi' \cdot \sigma'_{n,ave}) \quad (2.31)$$

where η is the fiber aspect ratio.

When failure is governed by the yielding of the fibers, the distributed tension, t_t , can be determined from the tensile strength of the fiber:

$$t_t = \chi \cdot \sigma_{f,ult} \quad (2.32)$$

where $\sigma_{f,ult}$ is the ultimate tensile strength of the individual fibers.

The fiber-induced distributed tension, t , to be used in the discrete approach to account for the tensile contribution of the fibers in limit equilibrium analysis is:

$$t = \min(t_p, t_t) \quad (2.33)$$

The critical normal stress, $\sigma_{n,crit}$, which defines the change in the governing failure mode, is the normal stress at which failure occurs simultaneously by pullout and tensile breakage of the fibers. That is, the following condition holds at the critical normal stress:

$$t_t = t_p \quad (2.34)$$

An analytical expression for the critical normal stress can be obtained as follows:

$$\sigma'_{n,crit} = \frac{\sigma_{f,ult} - \eta \cdot c_{i,c'} \cdot c'}{\eta \cdot c_{i,\phi'} \cdot \tan \phi'} \quad (2.35)$$

In analyses involving planar inclusions, the orientation of the fiber-induced distributed tension should also be identified or assumed. Specifically, the fiber induced distributed tension can be assumed to act: a) along the failure surface so that the discrete fiber-induced tensile contribution can be directly “added” to the shear strength contribution of the soil in a limit equilibrium analysis; b) horizontally, which would be consistent with design assumptions for reinforced soil structures using planar reinforcements; and c) in a direction somewhere between the initial fiber orientation

(which is random) and the orientation of the failure plane. Assumption a) is adopted in this study for simplicity.

The equivalent shear strength of fiber-reinforced specimens, S_{eq} , can be defined as a function of the fiber-induced distributed tension t , and the shear strength of the unreinforced soil, S :

$$S_{eq,p} = c_{eq,p} + (\tan \phi')_{eq,p} \cdot \sigma'_n \quad (2.36)$$

where α is an empirical coefficient that accounts for the effect of fiber orientation and the mobilization on fiber-induced distribution tension. For the case of randomly and uniformly distributed fibers, α is assumed to be 1.

Depending on whether the mode of failure is fiber pullout or breakage, the equivalent shear strength can be derived by combining (2.31) or (2.32) with (2.36). It should be noted that the average normal stress acting on the fibers, $\sigma'_{n,ave}$, does not necessarily equal the normal stress on the shear plane σ'_n . For randomly distributed fibers, $\sigma_{n,ave}$ could be represented by the octahedral stress component.

However, a sensitivity evaluation undertaken using typical ranges of shear strength parameters shows that $\sigma_{n,ave}$ can be approximated by σ_n without introducing significant error (Zornberg, 2002).

Accordingly, the following expressions can be used to define the equivalent shear strength when failure is governed by fiber pullout:

$$S_{eq,p} = c_{eq,p} + (\tan \phi')_{eq,p} \cdot \sigma'_n \quad (2.37)$$

$$c'_{eq,p} = (1 + \alpha \cdot \eta \cdot \chi \cdot c_{i,c'}) \cdot c' \quad (2.38)$$

$$(\tan \phi')_{eq,p} = (1 + \alpha \cdot \eta \cdot \chi \cdot c_{i,\phi'}) \cdot \tan \phi' \quad (2.39)$$

Equivalently, the following expressions can be obtained to define the equivalent shear strength when failure is governed by tensile breakage of the fibers:

$$S_{eq,t} = c'_{eq,t} + (\tan \phi')_{eq,t} \cdot \sigma'_n \quad (2.40)$$

$$c'_{eq,t} = c' + \alpha \cdot \chi \cdot \sigma_{f,ult} \quad (2.41)$$

$$(\tan \phi')_{eq,t} = \tan \phi' \quad (2.42)$$

The above expressions yield a bilinear shear strength envelope, which is shown in Figure 2.7.

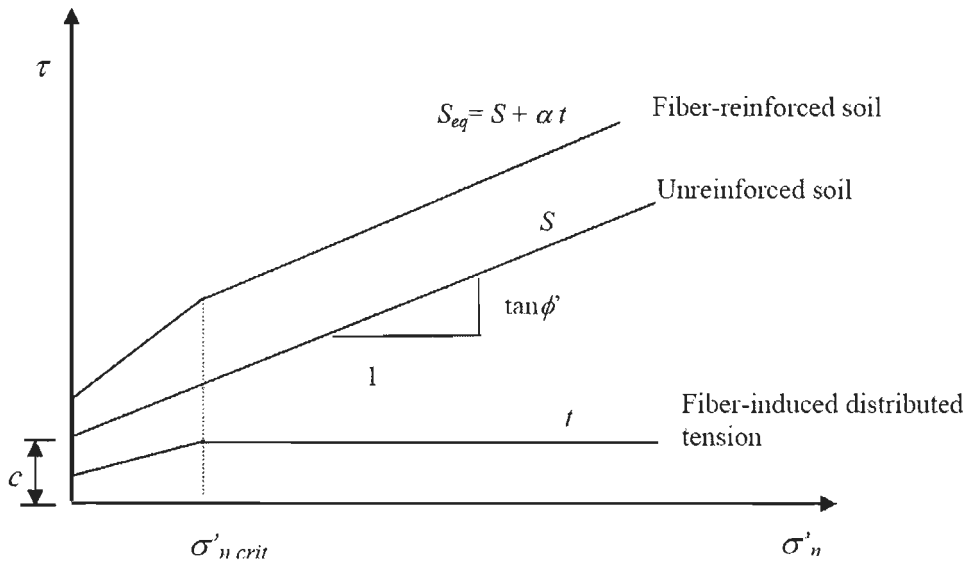


Figure 2.7 Representation of the equivalent shear strength according to the discrete approach

Usually, a geotechnical designer dealing with soil improvement and soil reinforcement techniques requires simple straight forward methods to estimate the efficiency and usability of each technique and therefore wants a direct method to estimate the level of improvement associated with each technique. From what was previously

presented, the Zornberg (2002) method and Michalowski and Cermak (2003) model appear to be two of the most interesting theories in matter of “shear strength improvement estimation” for soils mixed with fibers.

Zornberg (2002) proposed discrete framework which omits to account for a number of major parameters, yet it still offers the possibility of predicting fiber reinforced soil behavior and strength improvements, be it for a cohesive or cohesionless soil, and that, by simply conducting independent tests on soil and fiber specimens. Heineck and Consoli (2004) discussed shortcoming of this model. When failure is governed by fibre pullout, this method is inaccurate in determining both the equivalent cohesion and the friction angle. For the failure envelope governed by tensile breakage of the fibres, the cohesion intercept was overestimated, whereas the friction angle was almost exact. However, it accurately determines the critical normal stress. The discrete framework assumes that the mixture is homogeneous and that the fibres are randomly distributed (empirical coefficient α is assumed to be equal to 1.0). Difficulty in achieving good fibre mixing may compromise the validity of the discrete framework for comparatively high fibre aspect ratios and for comparatively high fibre contents (Zornberg, 2004). Major drawback of discrete framework is to quantify value of α for which one has to do laboratory testing on RDFS sample for particular fiber and soil used in field. Then using laboratories results α is to be back calculated. Thus, major objective of discrete approach, avoiding testing of RDFS specimen is defeated.

On the other hand, the energy dissipation model introduced by Michalowski and Zhao in 1996 and completed by Michalowski and Cermak in 2003 also seems to offer a very simple method for the estimation of a “macroscopic internal friction angle” that

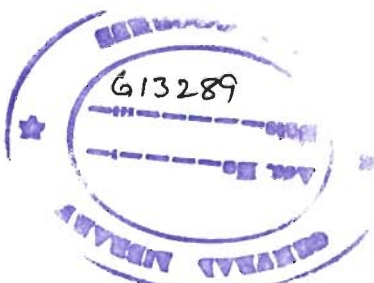
directly accounts for the effect of the random addition of fibers on granular soils particularly sands and silty sands.

2.2.2 Summary

From the literature it is evident that there has been no general consensus among researchers on what type of reinforcing material is suitable for any particular type of soil, what should be the optimum length of reinforcement, or how exactly the properties of the reinforcement influence the behavior of reinforced soil. Important findings are summarized as follows.

- (i) The addition of fibers can significantly increase the peak shear strength and limit the post peak strength loss of both cohesive and granular soil. An increase in fiber content leads to increasing strain at failure and, consequently, to a more ductile behavior.
- (ii) It is evident from Table 2.1 that most of the work on RDFS is done using sand as soil. However, good amount of work has been done on silt and clay also. Unlikely to planar reinforced soil and soil nailing, RDFS technique is beneficial in all types of soil (e.g. sand, silt and clay) and in waste products also (e.g. flyash).
- (iii) The fiber reinforcement tends to restrain the volume dilation of the soil in drained condition, or equivalently, increase the positive water pressure in undrained condition.
- (iv) Depending on the type of soil and fiber, there is a maximum limit of fiber content (χ_w) beyond which mixing of fibers in soil becomes very difficult. This limit is usually around 1 to 2% fiber content.

- (v) There is a minimum length of the fiber to get mobilize its full tensile strength. This is referred as critical length of fiber (l_{fc}). If fiber length (l_f) is greater than l_{fc} , fiber shall first yield and then rupture at shear plane. If l_f is lesser than l_{fc} , then fibers will be pulled out without yielding. It was observed that for best results, fiber length should be more than l_{fc} .
- (vi) Mohr's envelope of RDFS obtained through shear tests were found as bi-linear with a break occurring at a particular confining pressure. This is termed as critical confining pressure. It is found independent of the fiber content and D_{50} of soil. The critical confining pressure decreases with the increase in aspect ratio and increases with increase in tensile strength of the fiber. Further it was observed that it is more in well graded soil and rough fibers. Further, critical confining pressure is directly proportional to particle sphericity.
- (vii) There is a value of aspect ratio (η), beyond which the gain in strength of RDFS is nominal. This is referred as optimum aspect ratio. The peak shear strength increases with increasing aspect ratio. The strain at peak deviator stress increases with increasing fiber aspect ratio.
- (viii) Shear strength improves with the increase in aspect ratio, fiber content, roughness and extensibility of fiber.
- (ix) Fibrillated shape of fiber is better than mono-filament. RDFS prepared with fibrillated fibers possess higher strength.
- (x) CBR (soaked/unsoaked) values are found to be directly proportional to fiber content (χ_w).



- (xi) Various models are proposed to predict shear strength parameters. Additional experimental results are needed to validate these proposed design models and further modifications are required. The accuracy of the prediction of these models also relies on the proper understanding of the mechanism of interface interaction between fibers and soils. Available models are limited in scope involving some parameters either difficult to estimate or some value is suggested applicable to particular soil-fiber studied. Yet, no complete model is available to account for all parameters affecting strength of RDFS.

2.3 BEHAVIOUR OF FOOTINGS RESTING ON RDFS

Horizontally oriented geosynthetic reinforced soil (GRS) and RDFS are two reinforcing techniques for increasing bearing capacity and reducing settlements. GRS technique is very well established based on last thirty years research on it. Many investigators have studied the behaviour of footings resting on reinforced earth (Binquet and Lee, 1975; Akinmusuru and Akinbolade, 1981; Fragaszy and Lawton, 1984; Guido et al., 1986; Van Impe and Silence, 1986; Samatani and Sonpal, 1989; Huang and Tatsuoka, 1990; Sridharan et al., 1988; Dixit and Mandal, 1993; Khing et al., 1993; Shukla and Chandra (1994a, b); Huang and Menq, 1997; Yetimoglu et al. 1994; Adams and Collin, 1997, Kumar and Saran, 2001, 2002, 2003). All of them have reported improvement in bearing capacity of soil with the inclusion of horizontal layers of reinforcement in the foundation soil. Maximum increase in bearing capacity is found to be 3 to 4 times of virgin soil depending upon size, position and number of layer etc. of reinforcement.

Past research has demonstrated that random inclusion of discrete fibers significantly improves the engineering properties of soils. Very few studies of limited scope are available on application of RDFS for shallow foundations under central – vertical load. Model footing tests and field plate load tests (Mercer et al. 1984; McGown et al. 1985; Setty and Chandrashekar, 1988; Shamsher, 1992; Wasti and Butun, 1996; Purohit et al., 1997a, b; Agarwal and Chandra, 1997; Consoli et al., 2003 a, b; Dash et al., 2004; Rao et al., 2005; Hataf and Rahimi, 2006; Gupta et. al.. 2006 and Rao et al., 2006b) have been conducted on soil improved by randomly mixing mesh elements, fibers, tire-chip etc. under central - vertical load. Salient features of the work of above investigators are presented in Table 2.2 in chronological order.

Various theoretical solutions and sufficient experimental investigations data, to predict the behaviour of shallow footings subjected to eccentric - inclined loads on unreinforced soils, are available in the literature. Very few experimental studies are available in the literature to predict the pressure settlement and pressure tilt characteristics for shallow footings (Prakash et al., 1984; Agarwal, 1986; Saran and Agarwal, 1989, 1991; Kezdi, 1961; Jumikis, 1956, 1961; Lee, 1965; Meyerhof, 1953, 1956; Muhs and Weiss, 1969, 1973; Prakash and Saran. 1971, 1973; Saran and Singh, 1976; Purkayastha & Char, 1977, 1978; Hanna and Meyerhof, 1980).

Table 2.2 Literature Review on Behaviour of Footings Resting on RDFS

INVESTIGATORS	SOIL USED	FIBERS USED	TESTS CONDUCTED AND RESULTS REPORTED
Mercer et al. (1984) and McGown et al. (1985)	Mid-Ross sand $C_u=5$, $D_{50}=0.5$ mm	Polypropylene mesh elements 50 mm x 50 mm, opening size 6.7 mm x 7.1 mm . $\chi_w=0.19\%$	The test tank of size 640 mm long x 300 mm deep x75 mm wide was filled with dry Mid-Ross sand placed in a dense state. Footing size was 75 mm x 75 mm made of smooth metal. Sand below footing was reinforced by 0.18% of mesh elements, and the depth of this reinforced layer was varied in each test from 0.5 to 4.0 times the breadth. Very large improvements were obtained at all strain levels which were similar to triaxial tests in terms of both strength and deformation characteristics. No further improvements were noticed beyond a depth of more than 1.5 B of reinforced layer. BCR at failure of 2 and 2.44 was observed for depth of reinforced zone of 1B and 2 B respectively.
Setty and Chandrashekar (1988)	Lateritic soil (SM) G= 17 %, S = 61 % , M = 15% and C= 7 % , $\phi = 38.4^\circ$ at OMC = 13.5 % . LL=33.6%, PI=9.6%,	Polypropylene fibers: $l_f=20$ mm, dia 0.5 mm, tensile strength 127.4 N/mm ² and fiber content of 0,1,2 and 3 %	Plate load test on RDFS compacted in a rectangular box of size 1m x 1.5m x 0.95m, on 150 mm diameter concrete footing. Ultimate bearing capacity of lateritic soil increased to 6.36% and 38.2% by addition of 1% and 2% fibers respectively. A decrease of 20% was found in ultimate bearing capacity of lateritic soil by addition of 3% fibers. This reduction was reported due to insufficient amount of soil matrix resulting in free fiber.
Shamsher (1992)	Poorly Graded Sand(SP), $C_u=1.76$ $C_c=1.09$, $D_{50}=0.24$ mm	The Netlon geogrid CE121 cut in to pieces of sizes 30 mm x 30 mm and 50 mm x 50 mm were used as micro-mesh elements. $\chi_w = 0.72$ and 1.4%	Model footing tests were conducted in a rigid mild steel tank of size 1240x910x800 mm, on a square plate of width B=125 mm. Sand below footing was reinforced by 0.72% and 1.4% of mesh elements, and the depth of this reinforced layer was varied in each test from 0.5B, 1B, 1.5B. The tests were performed in loose ($D_r=20\%$) as well as dense ($D_r=65\%$) conditions. BCR increased with increase in depth of reinforced zone upto a depth of 1B beyond which increase in BCR was not significant. BCR was 2.5 and 2.53 at 1.4% mesh elements in 1B and 1.5 B depths respectively in dense condition. In loose state for same condition BCR was 2.36 and 2.55 respectively. Results were compared with planar reinforcement of same geogrid and found more economical compared to randomly reinforced sand by mesh elements.
Rao et al. (1994)	Yamuna sand (S1) $C_u = 1.76$ $C_c = 1.09$ Crust stone dust (S2) $C_u = 3.35$ $C_c = 0.84$	Geogrid cut into pieces of 50 mm x 50 mm as micro mesh (GMM) reinforcement	A square footing (width, B) placed at depth, D_f below ground level and resting on sand layer overlying a clay bed. The values of B and D_f were 1.25 m and 1 m respectively. The ultimate bearing capacity has been completed using Meyerhof's theory (1974). For GMM reinforce sand (S2) BCR increases with increase in H/B (where H = thickness of granular layer, below the foundation) upto a value of around 1.5, beyond this increase is insignificant. The maximum BCR obtained was 3 for 1.4 % GMM at H/B of 1.25. Similar findings were found for GMM reinforce sand (S1) in loose and dense conditions. Higher BCR values were observed for sand in loose condition. Contribution of GMM reinforcement towards settlement reduction was marginal.

Wasti and Butun (1996)	Sand, $C_u=3.995$, $C_e=1.132$, $D_{60}=0.819\text{mm}$ $C'=6.98$, $\phi'=47.8^\circ$	Polypropylene mesh, 30x50 mm (small) and 50x100 mm(big) with opening 10x10 mm. 50 mm long fiber by cutting mesh	Laboratory model test on a strip footing 50 mm (width) x250 mm (length) supported by sand reinforced by randomly distributed polypropylene fiber and mesh elements were conducted. Reinforced sand sample was of 1.2 m x 0.51 m x 0.75 m (depth) size. Results indicated that reinforcement of sand caused an increase in the ultimate bearing capacity values and the settlement at the ultimate load in general. The big mesh size was found to be superior to other inclusions considering the increase in ultimate bearing capacity values.
Purohit et al. (1997a)	Non plastic uniformly graded fine sand	Natural fibers of 'coconut jute', $l_f=0$ to 10mm, $\chi_w = 0.2\%$	The size of the circular footing used in the test programme was 5.0 cm, 6.0cm and 7.0 cm. The density of the sand fiber matrix was kept as 1.59 gm/cm ³ . diameter. The fiber layer was placed at a depth of $D/B = 0.5$ and 1.0 where D is the depth of fiber layer from top, and B = diameter of footing. The lengths of the natural fibers were also varied from 0.0 cm to 1.0 cm in length. About 60 tests were conducted. It has been observed from load-settlement tests that bearing capacity increase is very high when fibers are mixed with sand. When the fibers are placed in layer then there is increases in the bearing capacity of sand but after $D/B = 1.25$ the increase is not sufficient to be taken into account.
Purohit et al. (1997b)	Non plastic uniformly graded fine sand	Tyre shreds $\chi = 0\%$ to 10% by volume	A series of load tests were conducted on mixture of sand and tyre shreds to determine various factors which influence their strength. The size of the circular footing used in the test programme was 5.0 cm, 6.0 cm and 7.0 cm diameter. The shredded tyre layer was placed at $D/B = 0.5$ and 1.0, where B is the depth of shredded tyre layer from top, and B-diameter of footing. It has been observed that the bearing capacity is 5.07, 7.61 and 9.61 t/m ² for 5 cm, 6 cm and 7 cm diameter footing respectively on dune sand. The bearing capacity was increased to 9.00, 12.07 and 17.40 t/m ² on addition of 10% shredded tyres by volume randomly for 5 cm, 6 cm and 7 cm diameter footings respectively. The bearing capacity of above stated footings was increased 9.13, 12.5 and 17.78 t/m ² when 10% shredded tyres were placed in a layer at depth $D = 0.5 B$ where B is diameter of footing.
Agarwal and Chandra (1997)	Kaolin, Clay fraction – 57%	Polypropylene fibers and jute fibers ($l_f=10$ mm and 20 mm, $\chi_w = 0, 1, 2\%$)	Model footing test, triaxial compression and unconfined compression tests : Moist soil – fiber mix samples were prepared in a seasoned teak wooden frame having inside dimensions (470 x 200 x 78) mm. Size of footing was (20 x 78) mm and placed at the middle of wooden box along the width. Results indicated that increase in strength and bearing capacity was a function of length, content and type of fibers. Increase in bearing capacity, unconfined compressive strength and undrained cohesion is more for jute fibers compared to polypropylene fiber reinforced kaolin.

<p>Consoli et al. (2003a)</p>	<p>Non plastic silty sand (S M), $C_u = 4.8$, $S = 61\%$, $M = 31\%$, $C = 7.5\%$. $LL = 22\%$ and $PI = 7\%$</p>	<p>Monofilament polypropylene fiber, $d_f = 0.023$ mm, $\chi_w = 0.5\%$ $l_f = 24$ mm</p>	<p>The load-settlement response from three plate load tests on 300 mm diameter, 25.4 mm thick carried out directly on a homogeneous residual soil stratum, as well as on a layered system formed by two different top layers 300 mm thick—sand-cement and sand-cement fiber—overlaying the residual soil stratum. The utilization of a cemented top layer increased bearing capacity, reduced displacement at failure, and changed soil behavior to a noticeable brittle behavior. After maximum load, the bearing capacity dropped towards approximately the same value found for the plate test carried out directly on the residual soil. The addition of fiber to the cemented top layer maintained roughly the same bearing capacity but changed the post failure behavior to a ductile behavior. A punching failure mechanism was observed in the field for the load test bearing on the sand-cement top layer, with tension cracks being formed from the bottom to the top of the layer. A completely distinct mechanism was observed in the case of the sand-cement-fiber top layer, the failure occurring through the formation of a thick shear band around the border of the plate, which allowed the stresses to spread through a larger area over the residual soil stratum.</p>
<p>Consoli et al. (2003b)</p>	<p>Sand (SP), Effective size = 0.16, $C_u = 1.9$</p>	<p>Monofilament polypropylene fiber, $d_f = 0.023$ mm, $\chi_w = 0.5\%$ $l_f = 24$ mm</p>	<p>Two plate load tests on steel plate 0.3 m diameter, 25 mm thick, on a thick homogeneous stratum of compacted sandy soil, reinforced with polypropylene fibers, as well as on the same soil without the reinforcement. One layer was improved by compaction only, while to the other 0.5% by weight of polypropylene fiber was also added. Both layers were 1.2 m thick and were built in twelve consecutive lifts of 0.1 m each by using a steel roller to reach the maximum dry density of 17.4 kN/m^3 for standard Proctor energy. The field load tests were conducted by using 0.30 m diameter smooth circular steel plates, which were 25 mm in thickness. Figure 2.12, shows the load–settlement curves for the plate load tests carried out using 0.30 m diameter steel circular plates directly on the two compacted layers. Comparing the load–settlement curves, it is clearly observed that fiber reinforcement improved the behavior of the compacted soil, and that the improvement increased with increasing settlement.</p>
<p>Dash et al. (2004)</p>	<p>Uniformly graded river sand (SP), $C_u = 2.318$; $C_c = 1.03$; $D_{10} = 0.22$ mm; $\gamma_{max} = 17.4$ kN/m³; $\gamma_{min} = 14.3$ kN/m³. $D_r = 70\%$.</p>	<p>Mesh elements of size 41 mm x 120 mm obtained from biaxial geogrid made of polypropylene and having aperture opening size of 35 x 35 mm. $\chi_w = 0.1\%$ Reinforced sand was placed throughout the test tank.</p>	<p>The model tests were conducted in a steel tank measuring 1200 mm long x 332 mm wide x 700 mm high. The long sides of the tank were made of 15 mm thick Perspex sheet and were braced with mild steel angle to avoid lateral yielding during the tests. The model footing used was made of steel and measured 330 mm long x 100 mm wide x 25 mm thick. The ultimate bearing pressure for the reinforced sand bed with 0.1% randomly distributed reinforcement increased by 1.8 times higher than that of the unreinforced case (i.e. BCR = 1.8). Tests were conducted using planar reinforcement and compared these results. At failure BCR was 4 for planar reinforcement.</p>

<p>Rao & Dutta (2004)</p>	<p>Badarpur Sand (SP-SW) $D_{50}=0.42$ mm $C_u = 2.11$ $C_c = .96$ $\gamma_{d \max} = 16.7$ $\gamma_{d \min} = 12.3$ $e_{\max} = 1.12$ $e_{\min} = .56$ $D_r = 66$</p>	<p>Waste plastic strips Type-1 Size 12 mm x 12 mm 24mm x 12 mm Thickness 0.05 mm $\chi_w = 0.05$ to 0.15%</p> <p>Type-2 Same size as type-1 Thickness 0.45 mm $\chi_w = 0.25$ to 2%</p>	<p>A theoretical analysis has been carried out to assess the improvement in bearing capacity of a footing on waste plastic strip reinforced sand bed resting on clay soil. Analysis was based on $c-\phi$ values obtained from triaxial test. The analysis reveals that plastic strips in sand were found to improve only the bearing capacity. The influence on settlement is negligible. The bearing capacity ratio (BCR) increases with increase in relative depth (Rd) upto a value of around 2, beyond which the increases in significant.</p>
<p>Rao et al. (2005)</p>	<p>Sand (SP), overlying Soft marine clay (CH) $PL = 30$, $LL = 104$ $PI = 74$, $OMC = 27\%$</p>	<p>Discrete fibers of 3 mm width are cut from cement bags made of low density polyethylene (LDPE) $l_f = 25.4$ mm, 50.8 mm and 76.2 mm. $\chi_w = 0.5\%$, 0.75 %, 1.0 % and 1.25%.</p>	<p>Model footing tests were conducted on surface footing of 50 mm diameter resting on top and layer randomly reinforced with LDPE fibers overlying soft clay bed in test tanks of 300 mm diameter and 380 mm deep. The total thickness of the gravel layer has been maintained at 76 mm. Gravel layer was overlying 250 mm thick clay layer compacted to a dry unit weight of 14 kN/m³ The load-carrying capacity of reinforced soil system increases with increase in the fiber length. With increase in the fiber content the load-carrying capacity of the system increases only up to 1.0% fiber content beyond, which the load-carrying capacity decreases. At 1.0% fiber content bearing capacity increased to 255%</p>
<p>Hataf and Rahimi (2006)</p>	<p>Uniformly graded sand $C_u = 1.0$ $C_c = 8.0$</p>	<p>Tire shreds with rectangular shape and widths of 2 and 3 cm with aspect ratios 2, 3, 4 and 5 are mixed with sand. Five shred contents of 10%, 20%, 30%, 40% and 50% by volume were selected.</p>	<p>A series of laboratory test have been carried out on the model of shallow footing resting on reinforced sand. Tire shreds were used as reinforcement elements. Two parameters were selected to identify their influence on bearing capacity of sand: shred content and shred aspect ratio. It was found that addition of 10% shreds by volume increases BCR from 1.17 to 1.83 (increasing bearing capacity from 17% to 83%), 20% tire shreds increases BCR from 1.6 to 2.2, 30% tire shreds increase BCR from 2.15 to 3, 40% tire shreds increases BCR from 3.2 to 3.9 and 50% tire shreds increases BCR from 2.95 to 3.9 with respect to shreds width and aspect ratio.</p> <p>Aspect ratio of 4 was found as the best aspect ratio for two widths used in this study (i.e., 2 and 3 cm). Shreds of 4 cm length and smaller work improperly as reinforcement because of the small length. Optimum shred content found in this study is 40%, further addition of shreds will not increase the BCR significantly.</p>

Gupta et.al. (2006)	Poorly graded sand (SP) $D_{50} = 0.31$ mm $C_u = 2$ $e_{max} = 0.673$ $e_{min} = 0.519$	Polypropylene fibers $l_f = 24$ mm $\chi_w = 0.05, 0.1, 0.2$ and 0.3%	Model footing tests were conducted to study the pressure settlement behaviour of square footing of size 150 mm X 150 mm resting on randomly distributed fibre reinforced sand (RDFS) at different fibre contents in a tank of size 1000 mm X 1000 mm X 450 mm depth. From the footing tests it has been found that the bearing capacity of the RDFS increases with increase in fibre content. The percentage increase in the bearing capacity with the increase in the fibre content shows almost a linear trend. However, direct shear and triaxial tests do not show linear trend in increase of strength with increase in fiber content. These findings suggest that results from small sample in direct shear and triaxial test may not be true indicator for prediction of improved strength of RDFS.
Rao et al. (2006a)	Gravel (GW), overlying Soft marine clay (CH) PL = 30, LL = 104	Discrete fibers of 3 mm width are cut from cement bags made of low density polyethylene (LDPE) $l_f = 25.4$ mm, 50.8 mm and 76.2 mm. $\chi_w = 0.5\%$, 0.75 %, 1.0 % and 1.25%.	Model footing tests were conducted on surface footing of 76 mm diameter resting on top gravel layer randomly reinforced with LDPE fibers overlying soft clay bed in test tanks of 380 mm diameter and 400 mm deep. The total thickness of the gravel layer has been maintained at 76 mm. Gravel layer was overlying 300 mm thick clay layer compacted to a unit weight of 14 kN/m ³ The load-carrying capacity of reinforced soil system increases with increase in the fiber length. With increase in the fiber content the load-carrying capacity of the system increases only up to 1.0% fiber content beyond, which the load-carrying capacity decreases. At 1.0% fiber content bearing capacity increased to 130.6 %.

Experimental study conducted under eccentric - vertical loads, central – inclined loads and eccentric - inclined load on planar reinforced sand are available in literature to investigate the behaviour of footing (Saran et al., 1985; Dembicki et al., 1986; Manjunath and Dewaikar, 1996; Galav, 1997; Al-Smadi, 1998; Mutgi et al., 2001 and Saran et al., 2007). However, no study is reported in literature on study of footing resting on RDFS subjected to eccentric - inclined load.

In the subsequent sections, significant works of previous investigators related to behaviour of footing resting on RDFS have been discussed.

2.3.1 Model Footing Tests

Mercer et al. (1984) and McGown et al. (1985) carried out small plane footing tests on dry sand with and without Mesh Elements at mesh content of 0.19%. The bearing capacity increased with increase in soil-mesh layer up to a thickness of $2B$, beyond this point there was no significant increase in the bearing capacity of the footing. The test tank of size 640 mm long x 300 mm deep x 75 mm wide was filled with dry Mid-Ross sand placed in a dense state. Footing size was 75 mm x 75 mm made of smooth metal. Sand below footing was reinforced by 0.18% of mesh elements, and the depth of this reinforced layer was varied in each test from 0.5 to 4.0 times the breadth. Significant improvements were obtained and increased with increase in strain levels which were similar to triaxial tests in terms of both strength and deformation characteristics. No further improvements were noticed beyond a depth of more than 1.5 to $2B$ of reinforced layer (Fig. 2.8). Bearing capacity ratio (at failure) of 2 and 2.44 was observed for depth of reinforced zone of $1B$ and $2B$ respectively.

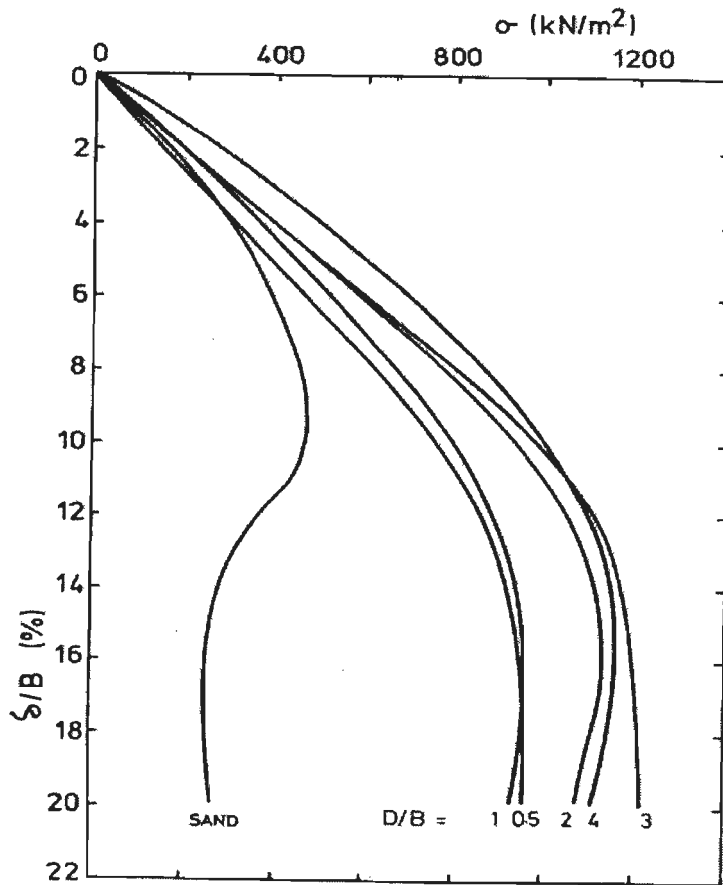


Figure 2.8 Footing test – effect of the sand – mesh layer depth on load-settlement behaviour (Mercer et al., 1984)

Gupta et al. (2006) carried out an experimental study using model footing (150 mm x 150 mm) test on large samples (1000 mm x 1000 mm x 450 mm deep) of RDFS. Model footing tests on the fiber reinforced sand were conducted to investigate the pressure settlement behaviour of RDFS and effect of fiber content on the bearing capacity of the RDFS. All tests were conducted on the square footing of size 150 mm resting on poorly graded sand (SP) or sand randomly reinforced with the polypropylene fibers (specific gravity 0.92, tensile strength 1.5×10^5 kPa, and tensile modulus 3×10^6 kPa) in a square tank of size 1000 mm x 1000 mm x 450 mm (deep). The fiber reinforced sand

was placed in tank in three layers and each layer was compacted using weight of hand rammer - 12.5 kg to achieve the relative density of 50%. A total of four model footing tests were performed under vertical load to study the pressure settlement curves of the RDFS and effect of fiber content on the bearing capacity of the RDFS. One test was performed on the unreinforced sand at relative density of 50%. Three tests were performed on randomly distributed fiber reinforced sand at 50% relative density with fiber length of 30 mm and fiber content of 0.05%, 0.1% and 0.2% by weight of sand. Pressure versus settlement curves are shown in Figure 2.9.

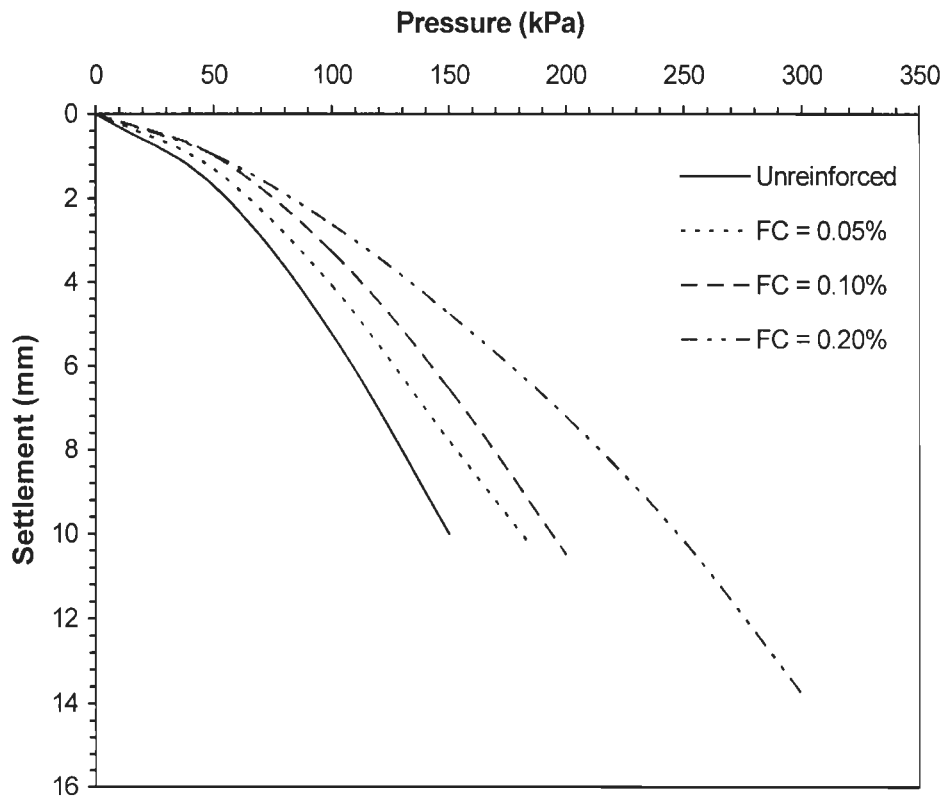


Figure 2.9 Pressure settlement curves for unreinforced sand and RDFS at different fiber content (Gupta et al. 2006)

Percentage increase in the bearing capacity of the RDFS in comparison to unreinforced sand was 17.6% at 0.05% fiber content, 35.3% at 0.1% fiber content and 64.7% at 0.2% fiber content. The percentage increase in the bearing capacity with the increase in the fiber content is almost linear as shown in the Figure 2.10. However, shear strength parameters obtained from direct shear and triaxial tests by Gupta et al. (2006) did not show linear trend in increase of strength with increase in fiber content. Which suggest that shear strength parameters obtained from direct shear and triaxial tests results may not be true indicator for prediction of improved strength of RDFS.

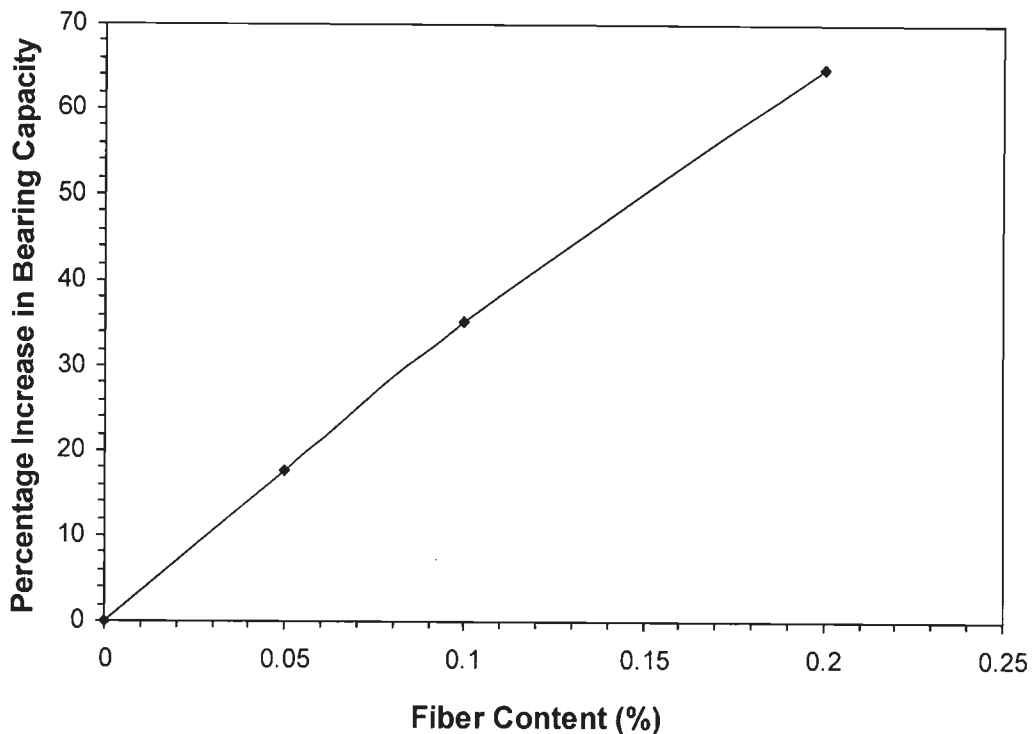


Figure 2.10 Variation of percentage increase in the bearing capacity of the RDFS with fiber content (Gupta et al. 2006)

2.3.2 Field Plate Load Test

Consoli et al. (2003a) obtained the load-settlement characteristics of soil from three plate load tests conducted on 300 mm diameter, 25.4 mm thick plate placed directly on a homogeneous residual soil stratum, as well as on a layered system formed by two different top layers (300 mm thick) sand-cement and sand-cement fiber, overlaying the residual soil stratum. The site consisted of homogeneous upper layer (3.5 m depth) of sandy-silty red clay, which is classified as low plasticity clay according to the Unified Soil Classification System. Grain size data indicated that the soil was 6% medium sand, 38% fine sand, 32% silt, and 24% clay. The average bulk unit weight ranged between 17.7 and 18.2 kN/m³; the moisture content was typically 24.5–26.0%; the degree of saturation was around 78%, and the void ratio varied between 0.80 and 0.86. Atterberg limits were: liquid limit 43% and plastic limit 22%, which yield a plasticity index of 21%.

The sand used, (borrowed from a coastal region near the city of Osorio, in southern Brazil), was fine sand classified as nonplastic, uniform fine sand according to the Unified Soil Classification System. The other parameters of sand were specific gravity of solids as 2.62, 100% effective diameter of 0.16 mm; the uniformity and curvature coefficients as 1.9 and 1.2, respectively, the minimum and maximum void ratios as, 0.57 ($\gamma_{d \max} = 16.7 \text{ kN/m}^3$) and 0.85 ($\gamma_{d \max} = 14.2 \text{ kN/m}^3$) respectively. At this point, it is important to mention that the use of the local residual soil instead of the uniform sand in the improved top layers was not considered, given that it had a certain

plasticity that might bring difficulties in the mixing process and make it impossible to ensure a uniform soil-fiber-cement mixture.

Rapid-hardening Portland cement, potable water, and chopped polypropylene fibers were used in this investigation. The average characteristics of the fiber were: 24 mm length, 0.023 mm diameter, specific gravity of 0.91, tensile strength and elastic modulus of 120 and 3,000 MN/m², respectively, and linear strain at failure of 80%.

Before the construction of the sand-cement and the sand-cement-fiber top layers, a 1.2-m-thick layer of the upper residual soil was removed from the testing area. After removal, two improved soil layers, 300 mm thick and 2.25 m² each (1.5 m x 1.5 m), were built over the residual soil in three consecutive layers, each 100 mm thick, by using a vibratory plate to reach the specified relative density of 70% established as a reference value for comparison among the mixtures, and then allowed to cure for 28 days before being tested. The improved soils were prepared in a rotating drum mixer, by mixing air-dried sand, Portland cement 7% by weight of dry sand, water 10% as moisture content, and polypropylene fiber 0.5% by weight of dry sand plus cement when appropriate. The utilization of a cemented top layer increased bearing capacity, reduced displacement at failure, and changed soil behavior to a noticeable brittle behavior (Figure 2.11). After maximum load, the bearing capacity dropped towards approximately the same value found for the plate test carried out directly on the residual soil. A punching failure mechanism was observed in the field for the load test bearing on the sand-cement top layer, with tension cracks being formed from the bottom to the top of the layer.

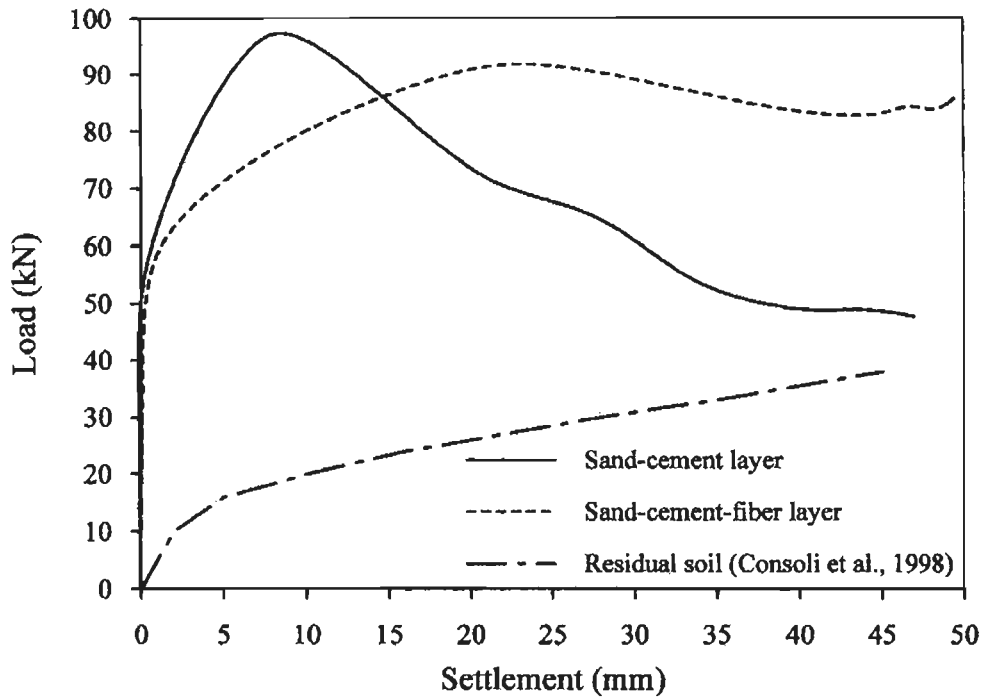


Figure 2.11 Plate load test on 300 mm diameter response directly on residual soil and on top of both sand-cement layer and sand-cement-fiber layer (Consoli et al., 2003a).

The addition of fiber to the cemented top layer maintained roughly the same bearing capacity but changed the post failure behavior to a ductile behavior. A completely distinct mechanism was observed in the case of the sand-cement-fiber top layer, the failure occurring through the formation of a thick shear band around the border of the plate, which allowed the stresses to spread through a larger area over the residual soil stratum (Figure 2.12).

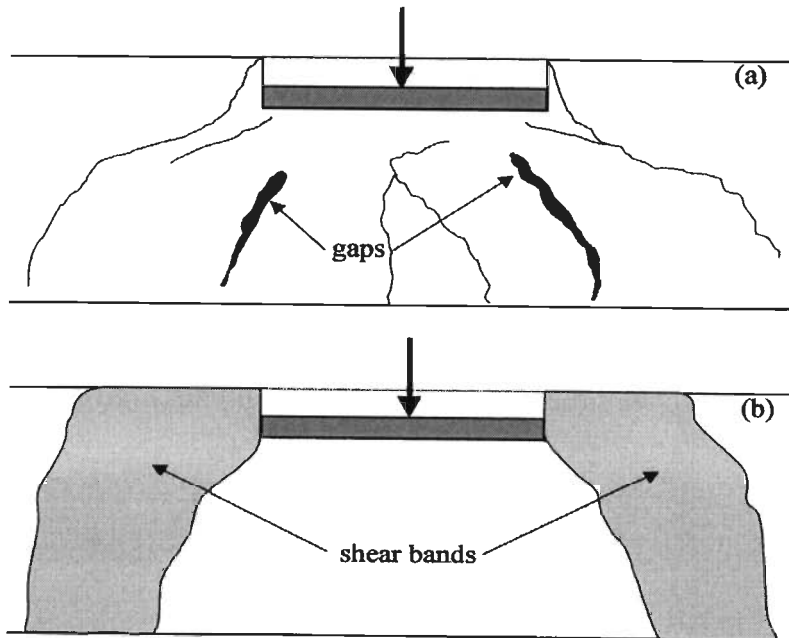


Figure 2.12 Failure mode for both (a) sand-cement layer and (b) sand-cement-fiber layer (Consoli et al., 2003a).

Consoli et al. (2003b), carried out the field plate load tests on steel plate 0.3 m diameter, 25 mm thick, on a thick homogeneous stratum of compacted sandy soil, reinforced with polypropylene fibers, as well as on the same soil without the reinforcement. Soil and soil-fiber layers were built on the top of a residual soil stratum. Before the construction of the compacted soil and the soil-fiber layers, a 1.2 m thick residual soil layer was removed throughout the testing area. After removal, two top improved soil layers each of 4 m² area (2mx2m) were prepared by mixing in a drum rotating mixer, dry soil and water to the optimum moisture content of 16% as determined from the standard Proctor energy. One layer was improved by compaction only, while to the other 0.5% (by weight) of polypropylene fiber was also added. Both layers were 1.2 m thick and were built in twelve consecutive lifts of 0.1 m each by using a steel roller to reach the maximum dry density of 17.4 kN/m³ for standard Proctor energy. The field load

tests were conducted by using 0.30 m diameter smooth circular steel plates, which were 25 mm in thickness.

Figure 2.13, shows the load–settlement curves for the plate load tests carried out using 0.30 m diameter steel circular plates directly on the two compacted layers. Comparing the load–settlement curves, it is clearly observed that fiber reinforcement improved the behavior of the compacted soil, and that the improvement increased with increasing settlement. This behavior is consistent with the triaxial laboratory test results for the fiber-reinforced soil in which the strength increased continuously even at large deformations.

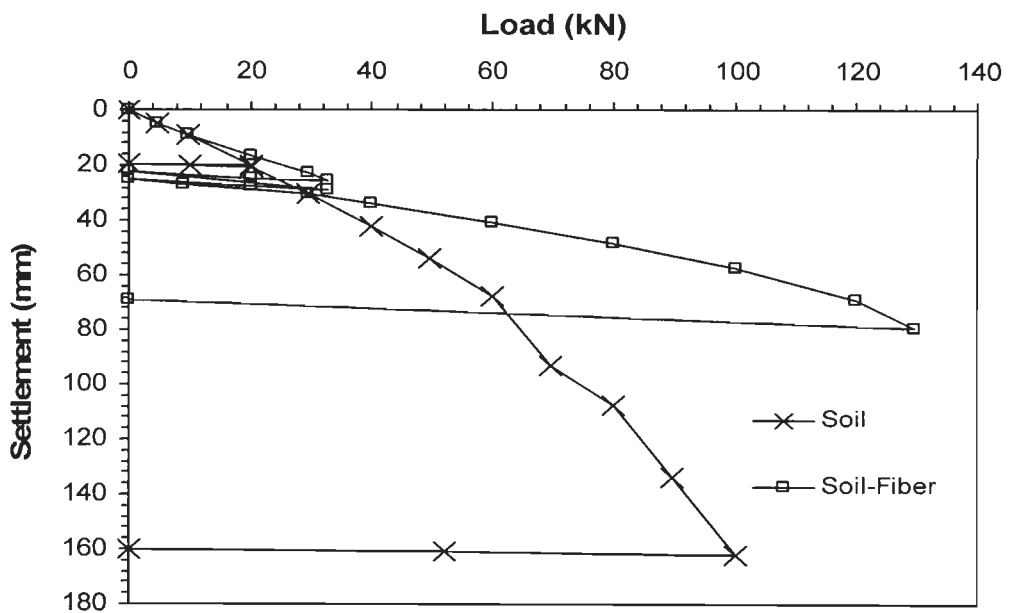


Figure 2.13 Load–settlement response for plate load tests (Consoli et al., 2003b)

In the case of the non-reinforced stratum, a punching failure was characterized. A vertical shear zone was observed just below the plate borders. No heave adjacent to the plates was detected, and the load–settlement curve showed a gradually increasing resistance even at very large displacements. For the fiber-reinforced soil stratum, the

fibers seemed to redistribute the stresses over a broader area, acting similarly to plant roots. As a result, the load–settlement response was considerably improved when compared to that obtained for the plate bearing on the non-reinforced soil stratum.

2.3.3 Summary

An extensive review of literature revealed that very meager information is available on the behaviour of shallow footings subjected to central - vertical load, resting on RDFS. No study is available on the behaviour of shallow footings subjected to eccentric - inclined load, resting on RDFS

From the literature it is evident that there has been no general consensus among researchers on what type of reinforcing material is suitable for any particular type of soil, what would be the optimum length of reinforcement ,or how exactly the properties of the reinforcement influence the behavior of RDFS. Important findings are summarized below.

1. Reinforcing shallow depths below footing may be sufficient to get high improvements.
2. No significant improvements were observed beyond 1.5B to 2B (for square footing, Rao et al., 1991, Rao et al., 1994, Rao and Dutta, 2004) or 2B (for strip footing, Mercer et al., 1984) depth of RDFS zone.
3. Footing resting on RDFS failed at higher strain compared to unreinforced sand or has not shown any failure even at large strain
4. Only few investigators have carried out study on behaviour of footing resting on RDFS under central – vertical loads and are of limited scope.

3.1 GENERAL

This chapter describes in detail the plan of experimental work carried out to study the strength - deformation characteristics of RDFS, in triaxial testing and behaviour of strip footings resting on RDFS subjected to central-vertical, central-eccentric and eccentric-inclined load.

The main purpose of the triaxial tests performed in this study is to develop a method for prediction of load-settlement characteristics of strip footing resting on RDFS. The effect of various parameters of fibers and sand such as fibers type (monofilament, fibrillated, mesh elements etc.), fiber content, fiber aspect ratio, fiber denier, fiber length, density of sand, effect of depth of RDFS, size of RDFS zone below footing is studied on bearing capacity, vertical settlement (s), horizontal displacement (H_d) and tilt (t) of the footings.

3.2 SOIL USED

Locally available Solani river sand has been used in present investigations. Various preliminary tests i.e. particle size analysis, specific gravity and maximum and minimum void ratio tests have been carried out in accordance with the relevant Indian Standard of practices to identify and classify the soil. Figure 3.1 shows the particle size

distribution curve and its various properties are given in Table 3.1. As per the Indian Standards (IS- 1498-1970), the soil is classified as poorly graded sand (SP).

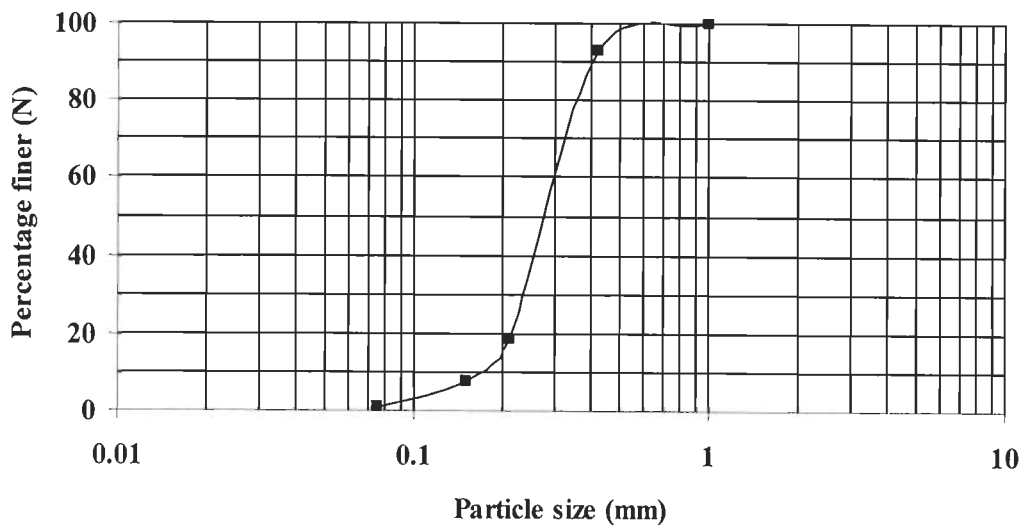


Figure 3.1 Particle size distribution curve

Table 3.1 Properties of Soil Used in the Investigation

S.No	Characteristics	Value
1	Soil Classification	SP (Poorly graded sand)
2	Effective size (D_{10})	0.165 mm
3	Average grain size (D_{50})	0.27 mm
4	Coefficient of uniformity (C_u)	1.8
5	Coefficient of curvature (C_c)	1.09
6	Specific gravity of solids (G_s) at 27°C	2.61
7	Minimum void ratio (e_{min})	0.54
8	Maximum void ratio (e_{max})	0.84

3.3 FIBERS/ MESH ELEMENTS USED

The reinforcement used consists of monofilament polypropylene fibers, fibrillated polypropylene fibers, mesh elements cut from Netlon geogrid CE121 and Netlon advanced turf mesh elements (Figure 3.2a, b and c). Netlon CE 121 geogrid was also used as planar reinforcement for comparison with RDFS in model footing test programme. Monofilament and fibrillated fibers were supplied in ready to used cut sizes. Mesh elements (NAF) were supplied in 50 mm x 100 mm sizes. The properties of fibers used in this investigation are given in Table 3.2 and properties of Netlon CE 121 geogrid and Netlon advanced turf mesh elements (NAF) are given in Table 3.3.

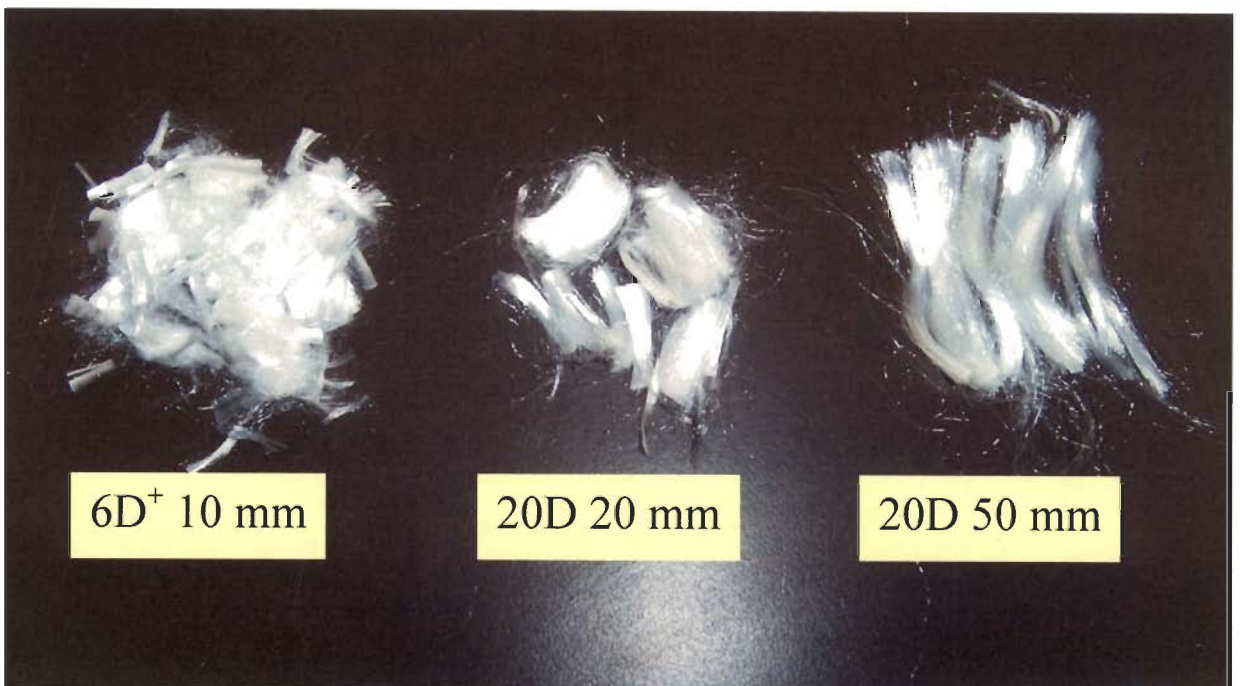


Figure 3.2a, Different types of monofilament fibers

+ Symbol D is used for denier of fiber (e.g. 6D 10mm means 6 denier 10 mm long fiber).

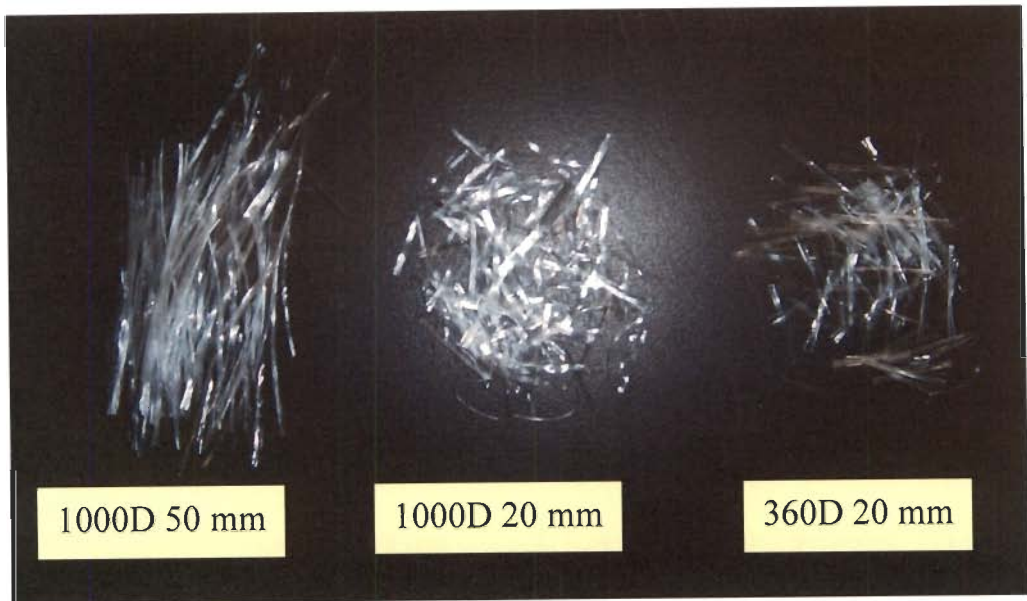
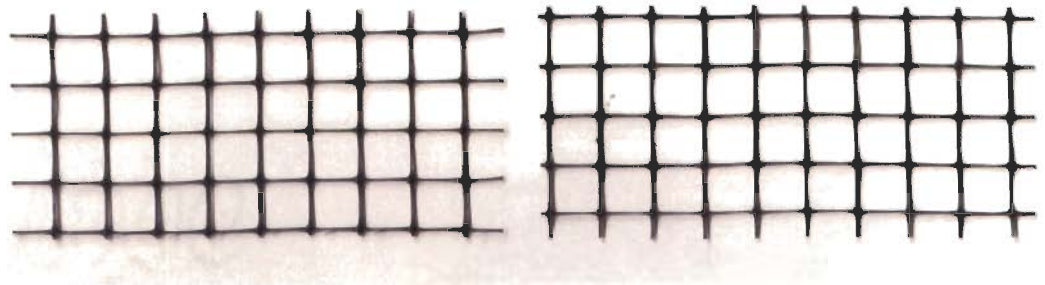
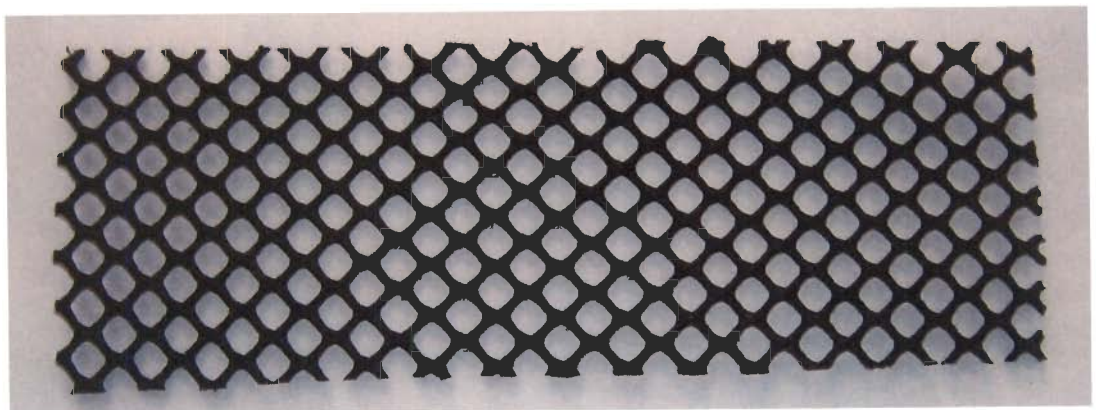


Figure 3.2b Different types of fibrillated fibers



Netlon Advanced Turf Mesh Elements (NAF)



Netlon CE 121 Geogrid

Figure 3.2c Netlon CE121 Geogrid and Netlon Advanced Turf Mesh Elements

recorded. Visual examination of exhumed specimens confirmed the mixtures to be satisfactorily uniform.



Fig. 3.3 Triaxial sample in position

3.4.3 Tests Performed

A total of 72 different triaxial tests were conducted under varying fibre contents (0.25, 0.5, 0.75 and 1%), fibre aspect ratios (325, 350 and 900) and confining pressure (25, 50, 100, 200, 300 and 400 kN/m²) on three different type of monofilament fibers as mentioned earlier. Six tests were conducted on unreinforced sand at six confining pressure of 25, 50, 100, 200, 300 and 400 kN/m². In all above mentioned tests a relative density of 30% was maintained. Twenty four tests were conducted on 6 denier 10mm monofilament fiber at relative density of 50% also.

3.5 MODEL FOOTING TESTS

Model tests were conducted on strip footings subjected to central-vertical, central-eccentric and eccentric-inclined load, resting on sand bed having relative density of 30%, 50% and 70% and reinforced with fibers or mesh elements or geogrid. Similar tests were also carried out for comparison purposes, on unreinforced sand at the same density.

3.5.1 Footings

Model footings made of mild steel were used. These footings were machined to the correct size. Footing was made up of mild steel plate of thickness 12.5 mm and was converted into a box of 50mm height. The bottom sides of model footings were knurled, in order to simulate the roughness of the actual foundations.

Grooves of about 2 mm depth were made on the footings so that the ratios of eccentricity to width, $e/B = 0.0, 0.1$ and 0.2 can be achieved to apply the eccentric load. Rectangular plates were welded on two edges at the top of each footing (box) for fixing the tilt-meter.

The following sizes of footings were used as shown in Figure 3.4.

- i) 50 mm x 75 mm
- ii) 75 mm x 75 mm
- iii) 100 mm x 75 mm
- iv) 150 mm x 75 mm
- v) 75 mm x 450 mm

Most of tests were conducted using 75 mm x 75 mm footing in plane strain conditions. Other sizes of footings were used to study scale effect and validation of models developed for predicting BCR, settlement and tilt.

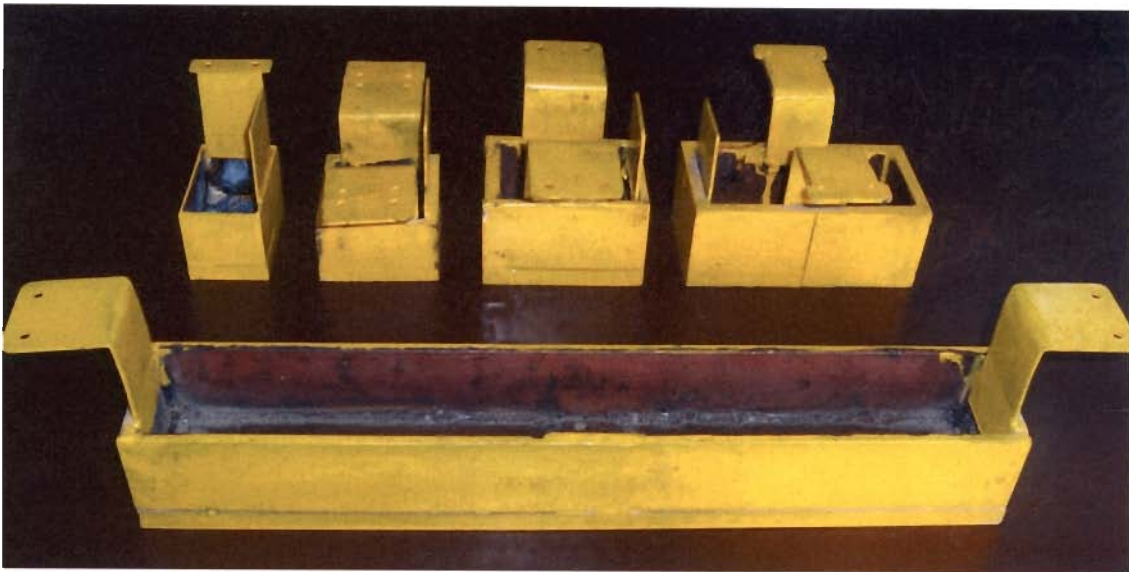


Figure 3.4 A view of model footings

3.5.2 Test Setup

The size of tank, used for conducting the model tests, was decided according to the sizes of the footings and the zone of influence (Ghumman, 1966). The dimensions of the tank, used for strip footings of sizes 50 mm x 75 mm, 75 mm x 75 mm and 100 mm x 75 mm in plane strain condition, were 800 mm long, 77 mm wide and 400 mm high and for strip footing of size 150 mm x 75 mm in plane strain condition, were 1200 mm long, 77 mm wide and 800 mm high. The dimensions of the tank, used for strip footings 75 mm x 450 mm, were 1000 mm long, 1000 mm wide, 1000 mm high in three dimensional tests.

The tank used for plain strain model footing tests consisted of thick timber planks strengthened by steel angles at the top and bottom sides. Steel stiffeners were also provided at the middle of tank walls. Perspex sheets were provided in front and back of tank as shown in Figure (3.5). Whereas the big tank for three dimensional tests (Figure 3.6), used for testing of strip footing was made up of heavy steel walls.



Figure 3.5 Test set-up arrangement for model tests (Plane strain condition)



Figure 3.6 Test set-up arrangement for model tests (three dimensional)

3.5.3 Loading Assembly

A loading device, developed by Murty (1967), was used to apply loads at different angles of inclination, throughout the model test programme. It consisted of two arcs of mild steel plates, 20 mm thick and making an angle of 50° at the centre. The two plates, being separated by a web, were cut at the top and bottom in V-grooves in order to facilitate the motion of ball bearings over which a cast iron block of 100 mm x 89 mm x 165 mm could slide.

A screw jack of 30 kN capacity was inserted into the cast iron block. The movement of the block was eased by the provision of a screw and a nut. The screw was hinged to the block, while passing through a rotating nut fixed to the plate. The angle of the applied load inclination was directly read from the plate, which was marked from 0° to 35° . A proving ring of required capacity was fixed in between the screw jack and a plunger tapered at one end. The whole assembly was fixed to a cross beam which, in turn, was fixed by bolts and nuts to the vertical supports, as shown in Figure 3.5.

Vertical settlement and horizontal displacement of the point of load of application of the footing, for each increment of applied load, were measured through a device consisting of two dial gauges for vertical displacement and one dial gauge for horizontal displacement. Specially designed tilt-meters were used to measure the tilts of the footing. Each tilt-meter was provided with a micrometer screw, with which tilt upto an accuracy of 10 seconds could be achieved. Two tilt-meters were mounted on each footing. One tilt-meter was fixed along a line parallel to the width of the footing to measure the tilt whereas, the other tilt-meter was fixed on a line parallel to the length of the footing to monitor the lateral tilt of the footing.

3.5.4 Preparation of Sand and RDFS below Footing

Sand or RDFS was placed in layers and compacted to achieve desired density. The amount of sand and fiber weight was calculated for each layer or zone of RDFS and fiber was mixed with sand by hand. Firstly, unreinforced sand was placed in the tank upto the desired height in layers of 75mm. Each layer was compacted by hammer to achieve the desired relative density of 30%, 50% or 70%. Then RDFS is placed in layers and compacted to achieve desired density. When RDFS is provided in particular zone, it is placed with the help of aluminum frame and by compaction after achieving desired density than aluminum frame is taken out. The top of RDFS or sand was properly leveled and the footing was placed in position for testing.

3.5.5 Test Procedure

The footing was placed on the surface of the leveled RDFS zone or sand. A proving ring with a plunger was fixed to the screw jack, which was adjusted at the desired angle of load application. Applied load was transferred through the plunger to the footing, seated in the desired groove depending on central or eccentric load.

Vertical settlement was measured at the point of load application by a dial gauge mounted on the horizontal plate, while, horizontal displacement was measured by another dial gauge placed at the vertical plate of the assembly. The magnetic bases of the dial gauges were fixed to a rigid beam supported by the walls of the test tank. One tilt-meter was mounted on the footing along its width, to measure the tilt, while, the other was mounted on the footing along its length to measure lateral tilting (if any) of the footing.

Prior to any test, the proving ring was driven downward by the screw jack until the plunger just touched the footing in desired groove. The bubbles of the tilt-meters were

brought to centre by the screws. Initial readings of all dial gauges and tilt-meters were recorded. The load was then applied by the screw jack in small increments and measured through the proving ring. The bubble of the tube becoming out of centre, indicates the tilting of assembly along with the footing. Bubbles of the tilt-meters were also brought back to centre. Readings of dial gauges and tilt-meters were then recorded. Similar procedure was repeated for the other load increments upto failure of footing tested.

For central vertical load, two dial gauges were mounted on the footing, and the average of the two readings was taken as the settlement of the footing.

Settlement, horizontal displacement and tilt were recorded when readings of dial gauges and tilt-meters became reasonably constant. Settlement, horizontal displacement and tilt due to each load increment were recorded and then utilized for obtaining pressure-settlement, pressure-horizontal displacement and pressure-tilt curves.

3.5.6 Tests Performed

Plane strain tests on model strip footings were conducted to study effect of fiber type, fiber content, density of sand, depth of RDFS zone, size of RDFS zone, scale effect, submergence of RDFS below footing, load eccentricity and inclination. Following variables were studied.

Effect of fiber type, fiber content, fiber length and fiber denier

1. Footing width = 75 mm
2. Depth of RDFS zone(R_d): full depth of tank $\approx 5B$
3. Width of RDFS zone(R_w): full width of tank $\approx 10B$
4. Relative density: 30%
5. Fiber content: 0, 0.25, 0.5 and 1%

6. Fibers / Mesh elements: **Monofilament:** 6 Denier 10 mm, 580 Denier 20 mm, 20 Denier 20 mm and 20 Denier 50 mm, **Fibrillated:** 1000 Denier 50 mm and 20 mm and **Mesh Elements:** Netlon CE121 mesh elements and Netlon advanced turf mesh elements (NAF).
7. Total number of tests conducted: 30

Effect of depth of RDFS layer

1. Footing width $B = 75\text{mm}$
2. Depth of RDFS layer (R_d): 0.5B, 1B, 2B and 3B
3. Relative density: 30, 50 and 70%
4. Fiber content: 0, 0.25, 0.5, 0.75 and 1%
5. Fibers: 1000 Denier 50 mm and 20 mm fibrillated.
6. Total number of tests conducted: 58

Effect of depth and width of RDFS zone

1. Footing width (B) = 75mm
2. Depth of RDFS zone (R_d): 0.5B, 1B, 2B and 3B
3. Width of RDFS zone (R_w): 1B, 2B, 3B, 4B, 6B and 8B
4. Relative density: 30, 50 and 70%
5. Fiber content: 0.25, 0.5, and 1%
6. Fibers: 1000 Denier 50 mm and 20 mm fibrillated, 360 Denier 20 mm fibrillated.
7. Total number of tests conducted: 80

Tank size effect

Four numbers three-dimensional tests were conducted in big tank (1 m x 1 m x 1 m) on strip footing of size 75 mm x 45 mm on 1000D 50mm long fibrillated fibers to compare the results with plane strain tests in small tank. It was observed that the effect of size of tank was insignificant.

Effect of submergence

1. Footing width (B) = 75mm
2. Depth of RDFS zone: 2B and full depth of tank
3. Width of RDFS zone: Full width of tank
4. Relative density: 30%
5. Fiber content: 0, 0.5 and 1%
6. Fibers: 1000 Denier 50 mm fibrillated.
7. Total number of tests conducted: 8

Test on sand reinforced with planar reinforcement for comparison

1. Footing width (B): 75mm
2. Relative density: 30%
3. Length of Geogrid: 3B, 5B and 8B
4. Depth of first Geogrid layer: 0.2B, 0.33B, 0.5B
5. Spacing of Geogrid: 0.33B
6. Number of Geogrid layer: 1,2,3,4 and 5
7. Total number of tests conducted: 12

Effect of load eccentric and inclination

1. Footing width (B): 75mm

2. Eccentricity: 0, 0.1 and 0.2B
3. Load inclination: 0, 10° and 20°
4. Depth of RDFS: 0.5B, 1B, 2B, 3B and full depth (5B)
5. Width of RDFS zone: 2B, 4B and 6B
6. Relative density: 30, 50 and 70%
7. Fiber content: 0.5, and 1%
8. Fibers: 1000 Denier 50 mm fibrillated.
9. Total number of tests conducted: 148

Scale Effect

1. Footing width (B): 50 mm, 100 mm, and 150 mm
2. Eccentricity: 0, 0.1 and 0.2B
3. Load inclination: 0, 10° and 20°
4. Depth of RDFS zone (Rd): 0.5B, 1B, 2B and 3B
5. Width of RDFS zone (Rw): 2B
6. Relative density: 30, 50 and 70%
7. Fiber content: 0.5, and 1%
8. Fibers: 1000 Denier 50 mm fibrillated
9. Total number of tests conducted: 40.

Chapter

4

RESULTS AND INTERPRETATION: STRENGTH AND DEFORMATION CHARACTERISTICS OF RDFS

4.1 GENERAL

In this chapter result of RDFS samples in triaxial compression test have been discussed. Strength-deformation characteristics of RDFS have been discussed in following sections which includes stress-strain behaviour, effect of various parameters, development of a predictive strength model for RDFS using non-linear multiple regression analysis and comparison with existing literature. Need of using constitutive laws is discussed instead of peak shear strength parameter obtained from triaxial tests. Nonlinear stress-strain curve were modeled using Kondner's constitutive laws and constitutive parameter of RDFS are determined.

4.2 RESULTS AND INTERPRETATION OF TRIAXIAL TESTS

4.2.1 Stress-Strain Behaviour

The deviator stress ($\sigma_1 - \sigma_3$) versus axial strain (ϵ %) curves for unreinforced sand at different confining pressure and at a relative density of 30% obtained in the drained triaxial tests are shown in Figure. 4.1. The deviator stress-axial strain curves for RDFS samples obtained for different monofilament fibers in the triaxial tests are shown in Figures 4.2 to 4.13. Comparing these figures it can be observed that the fiber-reinforced specimens showed ultimate strengths that were significantly increased for all confining

pressures. In RDFS samples, except RDFS samples prepared using 6 denier 10 mm long fiber, deviator stress has not shown a decreasing trend with increase in axial strain even up to 20% axial strain. They also showed a marked hardening behavior up to the end of the tests at axial strains of more than 20%, whereas for the unreinforced specimens, an almost perfectly plastic or brittle behavior was observed at large strains.

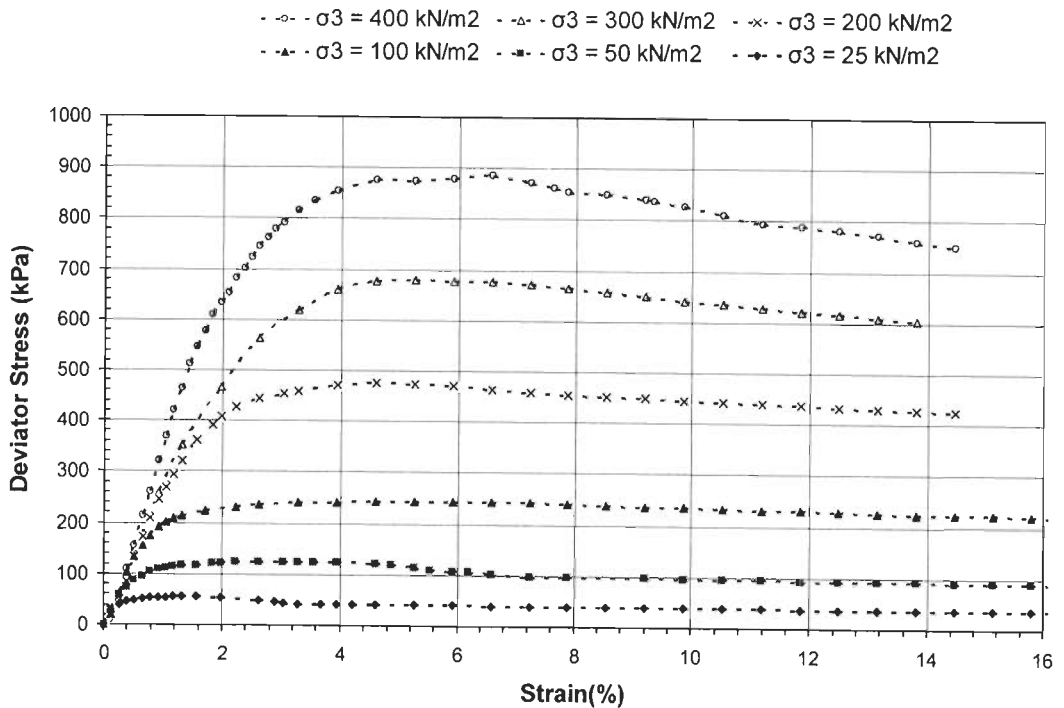


Figure 4.1 Stress- strain curves for sand ($D_r= 30\%$)

It is important to point out that, because of the strain hardening observed up to the end of the tests, the deviator stresses at failure for the fiber-reinforced specimens were taken at the axial strain of 20%.

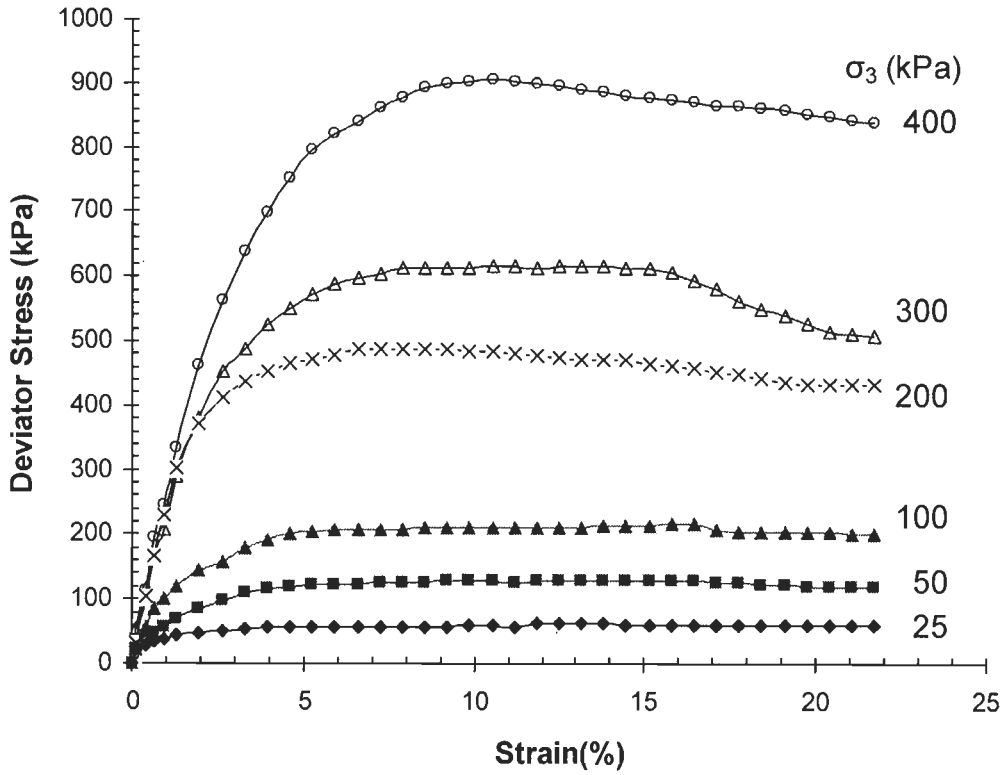


Figure 4.2 Stress- strain curves for sand ($D_r=30\%$) with 0.25% fiber (6D 10mm)

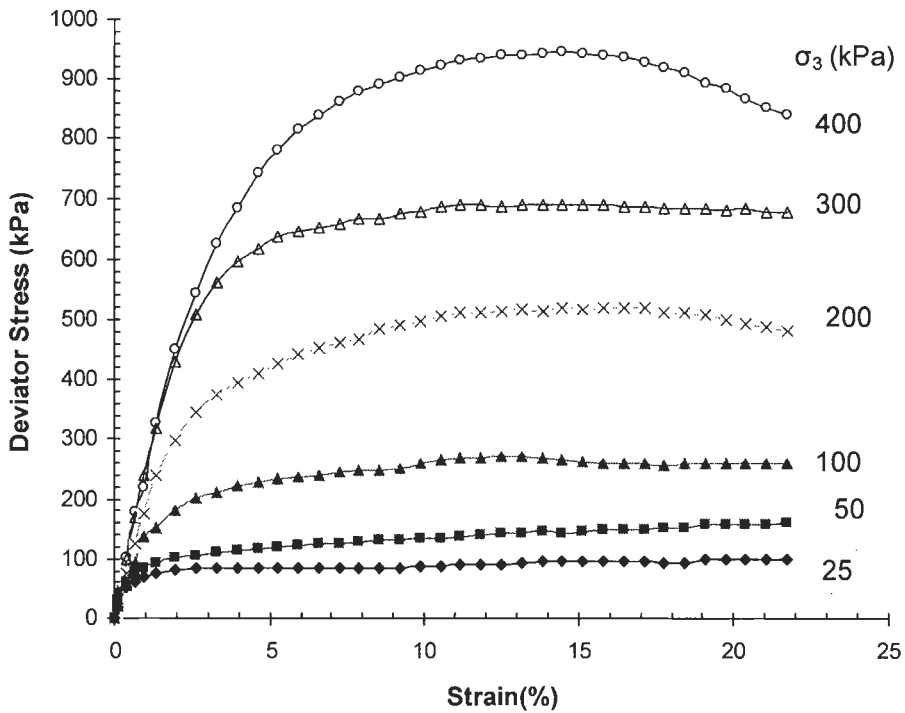


Figure 4.3 Stress- strain curves for sand ($D_r=30\%$) with 0.5% fiber (6D10mm)

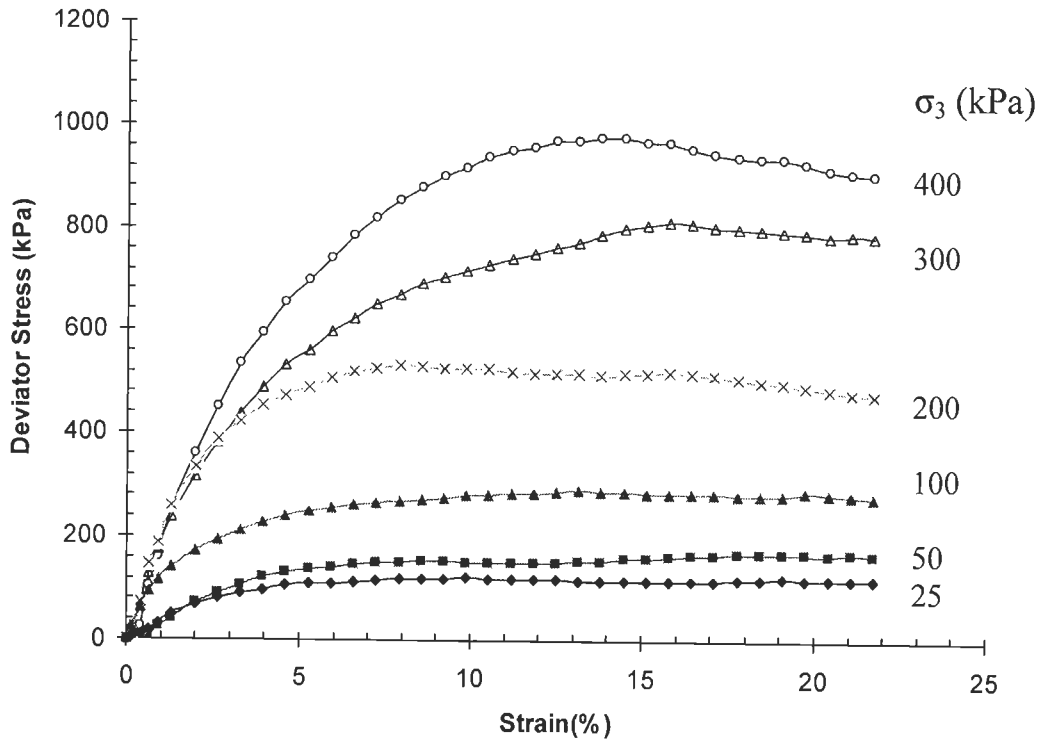


Figure 4.4 Stress- strain curves for sand ($D_r = 30\%$) with 0.75% fiber (6D10mm)

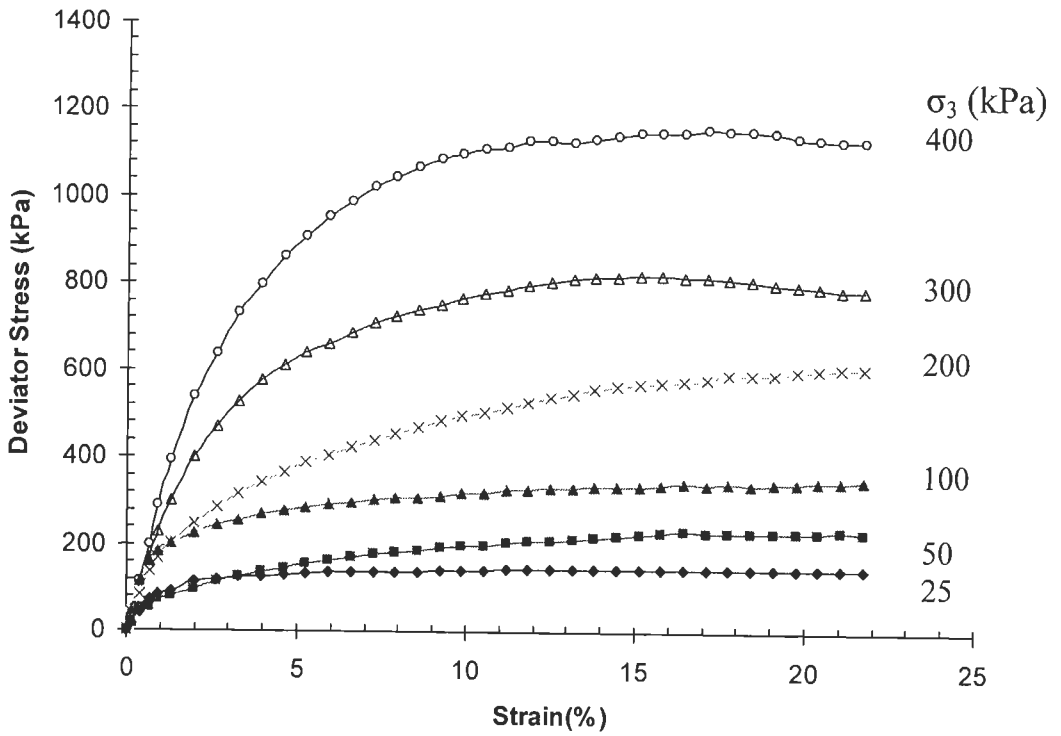


Figure 4.5 Stress- strain curves for sand ($D_r = 30\%$) with 1% fiber (6D 10mm)

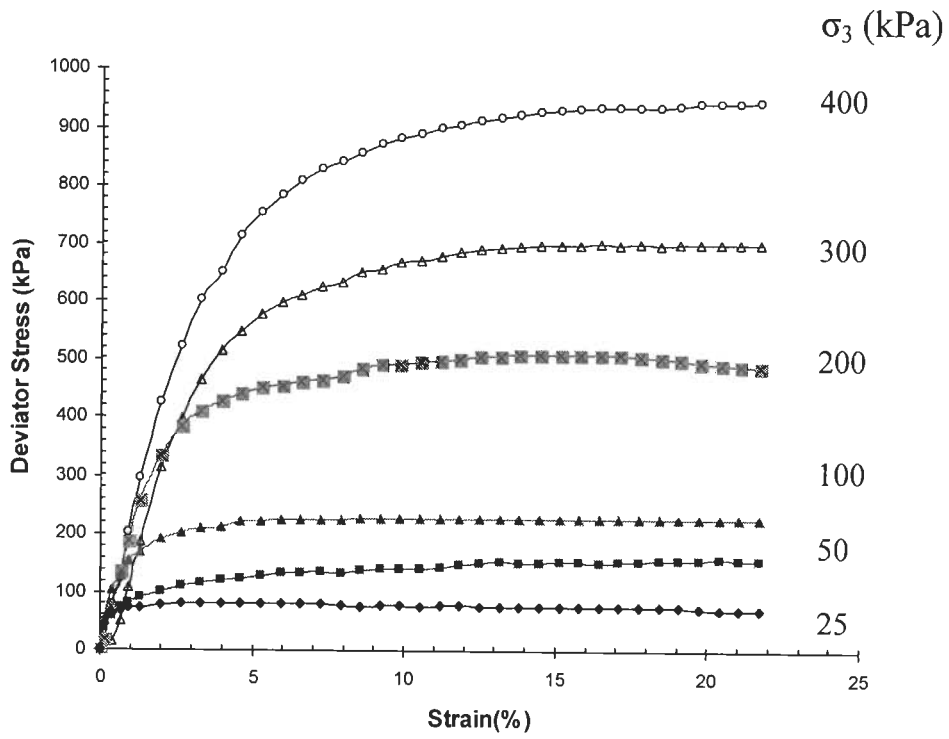


Figure 4.6 Stress- strain curve for sand ($D_r= 30\%$) with 0.25% fiber (20D 20mm)

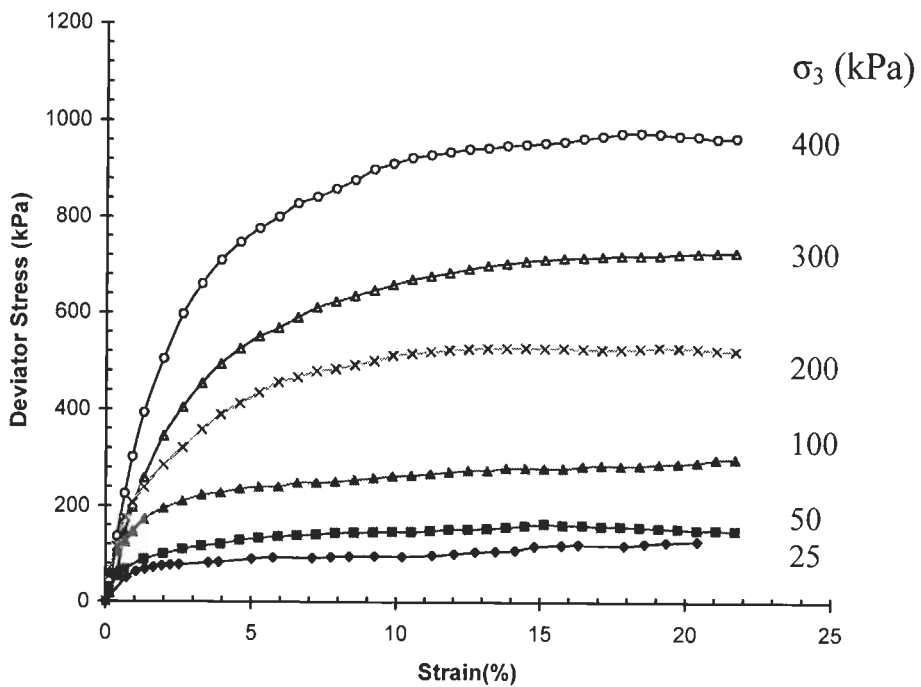


Figure 4.7 Stress- strain curves for sand ($D_r= 30\%$) with 0.5% fiber (20D 20mm)

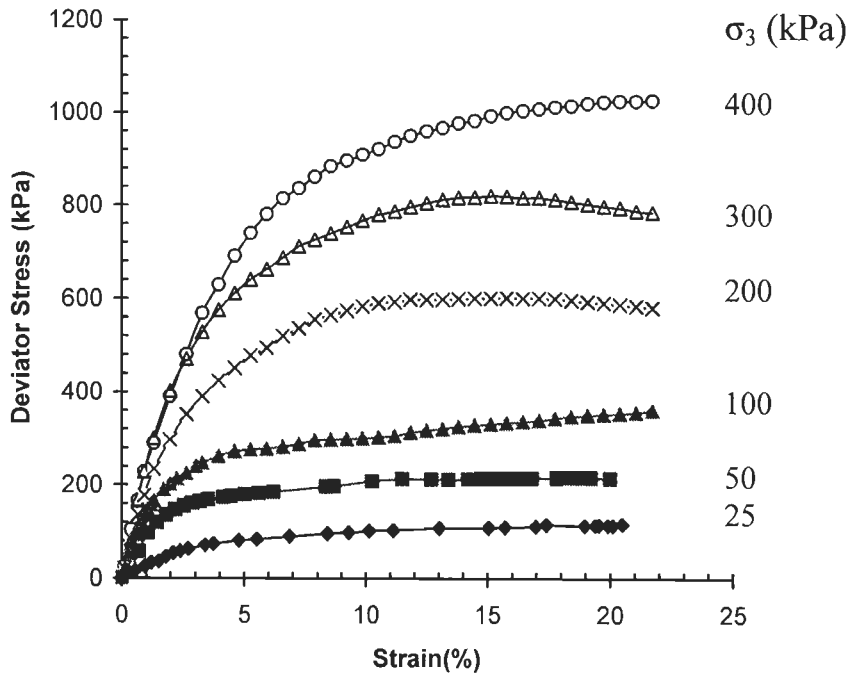


Figure 4.8 Stress- strain curves for sand ($D_r= 30\%$) with 0.75% fiber (20D 20mm)

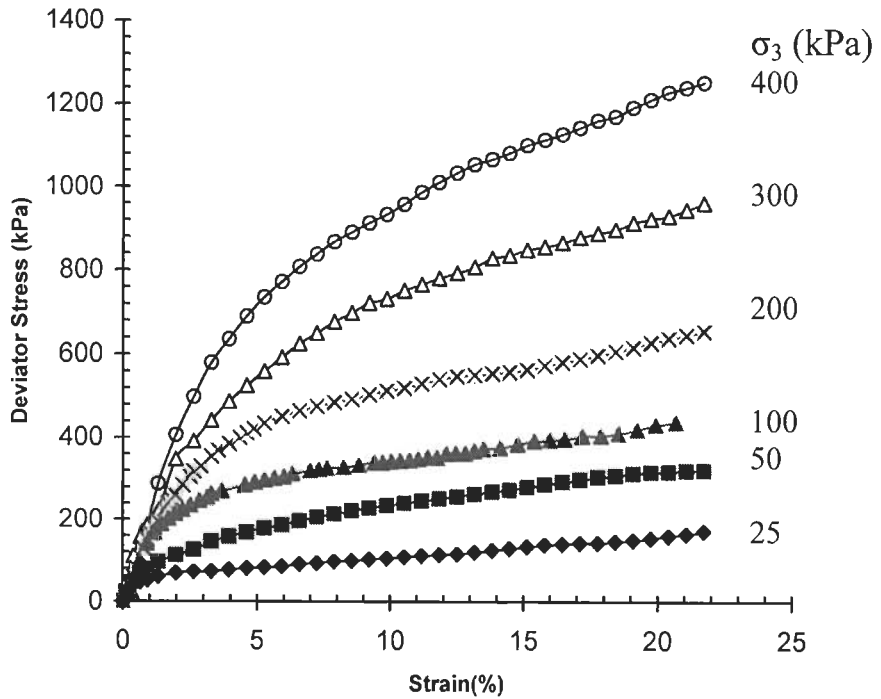


Figure 4.9 Stress- strain curves for sand ($D_r= 30\%$) with 1.0% fiber (20D 20mm)

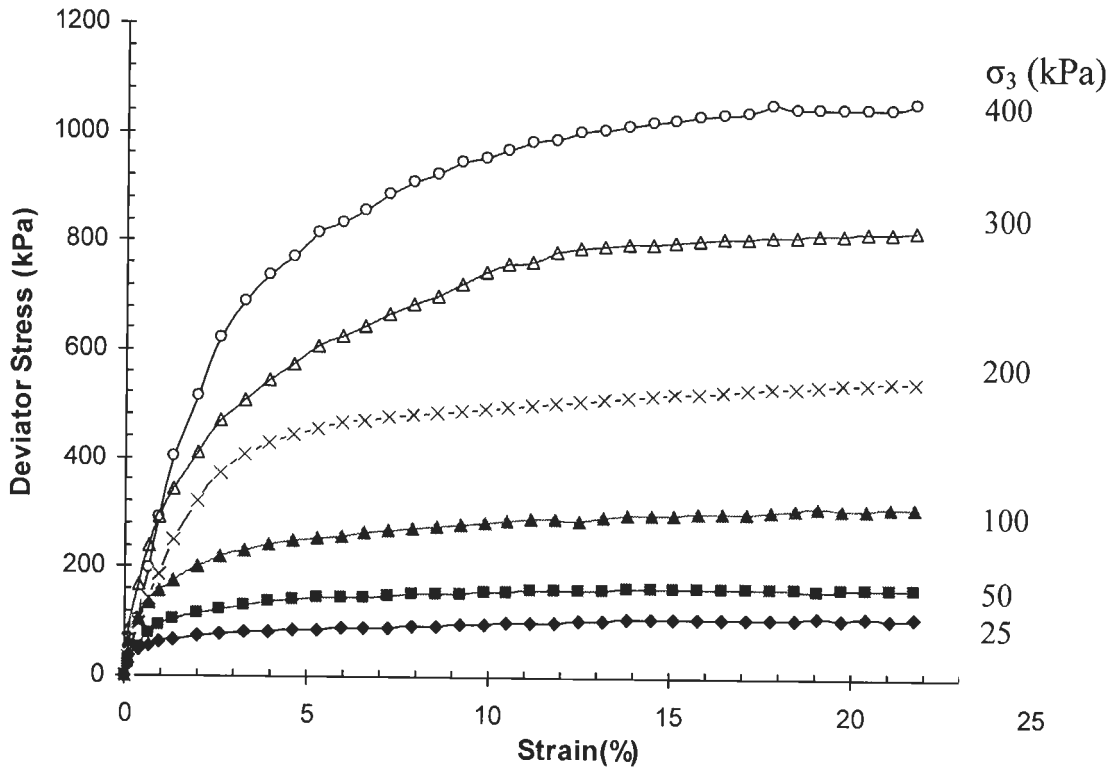


Figure 4.10 Stress- strain curves for sand ($D_r= 30\%$) with 0.25% fiber (20D 50mm)

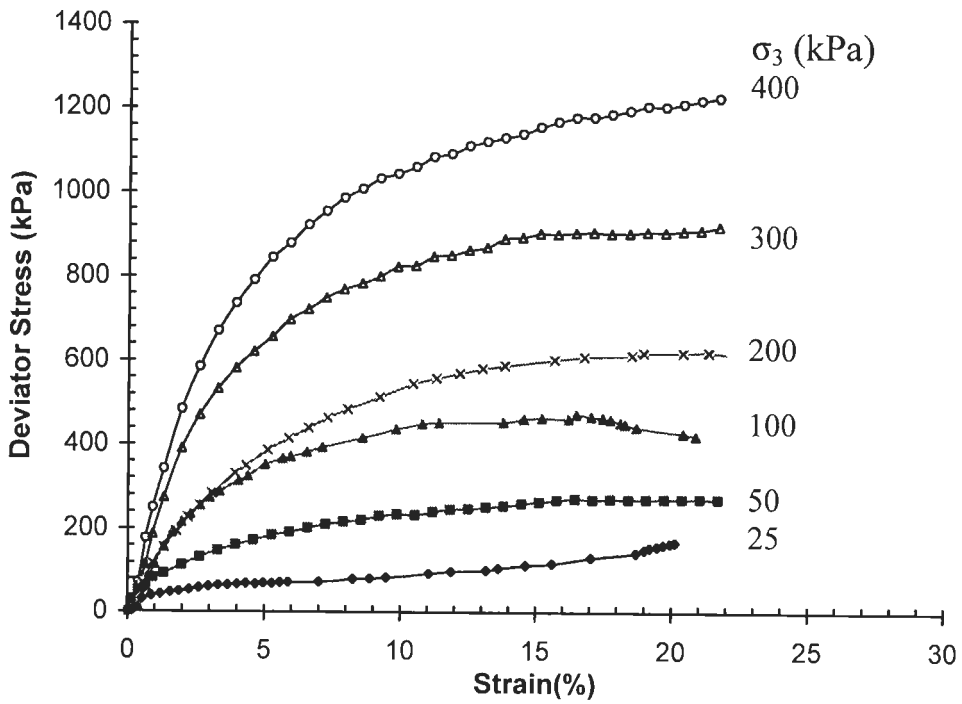


Figure 4.11 Stress- strain curves for sand ($D_r= 30\%$) with 0.5% fiber (20D 50mm)

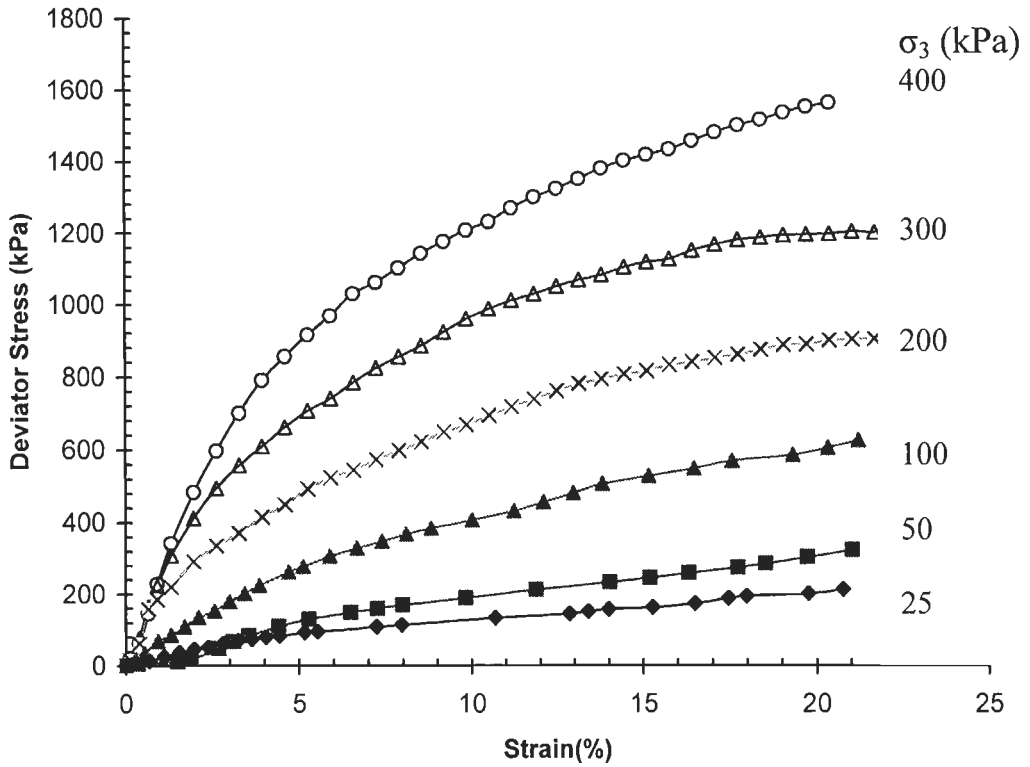


Figure 4.12 Stress- strain curves for sand ($D_r = 30\%$) with 0.75% fiber (20D 50mm)

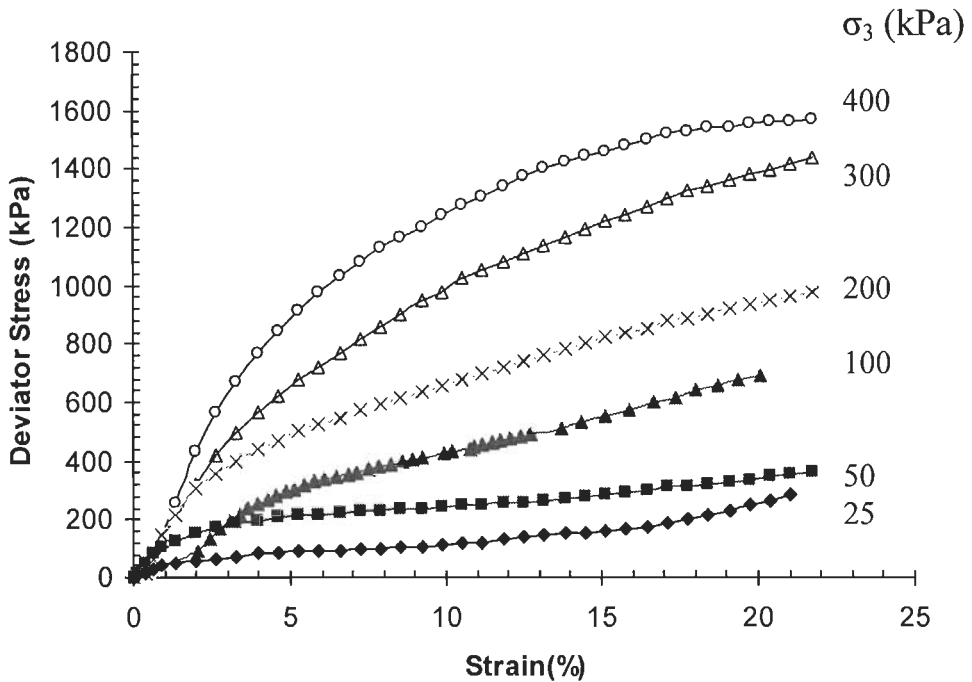


Figure 4.13 Stress- Strain Curve for sand ($D_r = 30\%$) with 1.0% fiber (20D 50mm)

A summary of the failure deviator stress obtained from the triaxial tests is presented in Table 4.1.

Table 4.1 Deviator Stress (kPa) at Failure for Unreinforced Sand (UR) and Different type of RDFS Sample - Experimental

D_r (30%)	Deviator Stress (kPa) at Failure						
	0	0.25	0.25	0.25	0.5	0.5	0.5
χ_w (%)→	UR	6D10mm	20D20mm	20D50mm	6D10mm	20D20mm	20D50mm
25	55.2	62.9	81.8	110.4	100.3	128.7	168.3
50	117.0	132.4	158.8	165.4	158.0	164.4	272.0
100	243.3	217.5	226.0	312.0	272.8	292.3	472.5
200	476.8	487.8	510.1	580.3	521.7	529.5	619.5
300	680.0	616.4	702.0	799.3	691.4	725.8	909.4
400	884.8	904.6	943.1	1053.4	946.7	976.5	1212.0
χ_w (%)→	0.75	0.75	0.75	1.0	1.0	1.0	
σ_3 (kPa) ↓	6D10mm	20D20mm	20D50mm	6D10mm	20D20mm	20D50mm	
25	120.7	140.0	212.5	146.3	159.0	267.0	
50	169.9	216.5	305.0	225.0	250.0	343.3	
100	290.0	354.4	606.4	345.9	437.9	691.7	
200	530.0	601.3	900.0	601.8	638.3	946.2	
300	811.0	819.8	1202.0	819.8	930.3	1395.9	
400	974.4	1023.1	1459.0	1157.6	1228.7	1559.7	

Fiber-reinforcement not only increases the shear strength of the soil, but also reduces the post-peak strength loss. The equivalent shear strength of the fiber-reinforced soil is a function of the shear strength of sand matrix and fiber-induced tension. Mobilization of fiber-induced tension requires the development of relative displacements between fiber and sand. Peak shear strength of fiber-reinforced sand comes from the peak

shear strength of the sand matrix and the full pullout resistance of the fibers. However, the peak shear strength of sand matrix and fiber-reinforced sand may be mobilized at different strain level.

The peak deviator stress increases approximately linearly with increasing fiber content. The post-peak shear strength loss is smaller in the reinforced specimens than in the unreinforced specimens. The Unreinforced sand appears to take most of the applied load at small strain levels, while the load resisted by the fibers is more substantial at higher strain levels. The larger strain corresponding to the peak deviator stress displayed by the fiber-reinforced specimens suggests that fibers increase the ductility of the reinforced soil specimen. For specimens prepared using high fiber content, the gradually mobilized fiber-induced distributed tension is enough to compensate the post-peak shear strength loss of the soil matrix. Therefore no post-peak shear strength loss is expected or maximum shear strength of the fiber-soil shear strength is mobilized at large strain level.

The effect of fiber length on the stress-strain behavior is shown in Figure 4.14. The specimens were prepared using fibers with different fiber types (6 denier 10mm and 20D 20mm) having same fiber content and similar aspect ratio but varying fiber lengths. As shown in the figure, the specimens reinforced with longer (20 mm) fibers displayed higher shear strength. The peak deviator stress increases linearly with increasing aspect ratio, which is consistent with the trend. The strain corresponding to the peak strength increases with increasing fiber length. When the governing failure mode is pullout, the fiber-induced distributed tension reaches its peak when the pullout resistance is fully mobilized. Longer fibers require a larger interface shear deformation to fully mobilize the interface strength. Consequently, the macroscopic axial strain at peak stress is expected to be larger for specimen reinforced with longer fibers.

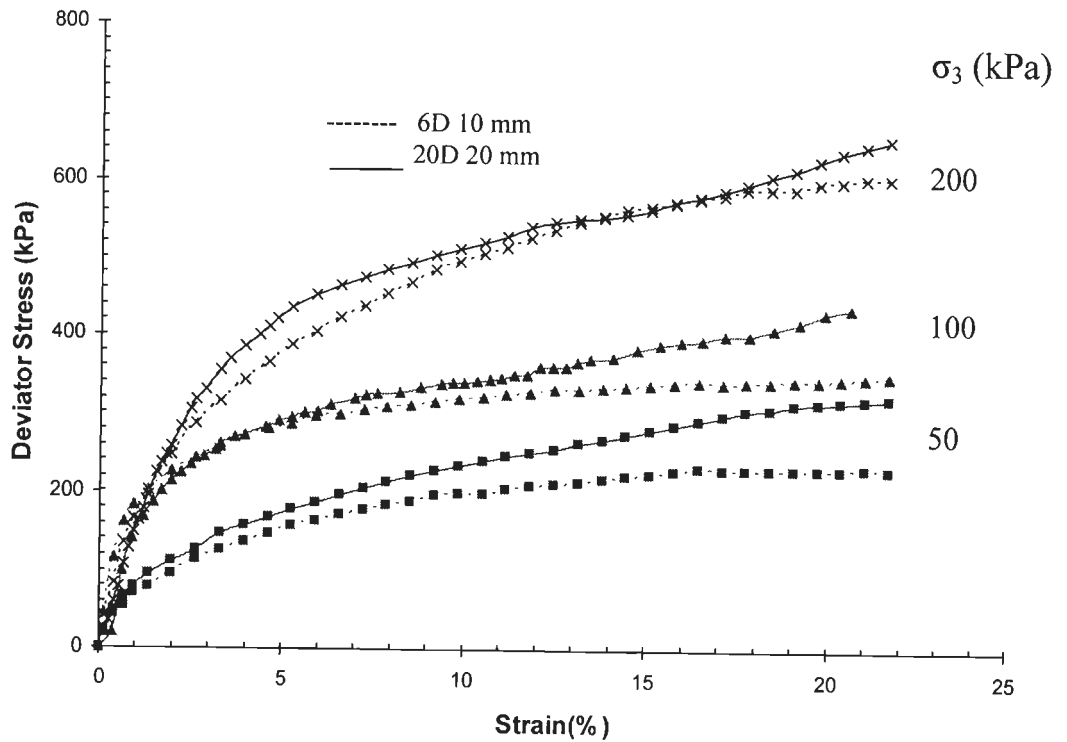


Figure 4.14 Comparison of stress - strain curves for RDFS sample with 1.0% fiber content for 6 Denier 10 mm and 20 Denier 20 mm

Fiber-reinforced specimens were prepared at two different relative densities (30% and 50%) with 6D 10 mm fibers. For the same 0.75% fiber content, specimens with higher densities display higher peak shear strength (Figure 4.15). At higher density strength is more and keeps on increasing with strain up to failure strain of 20%. The RDFS samples with relative density of 30% show a slight increase in shear strength beyond 10% axial strain. At the RDFS samples for 50% relative density, strain hardening was observed for all strains (up to 20%) tested in this study.

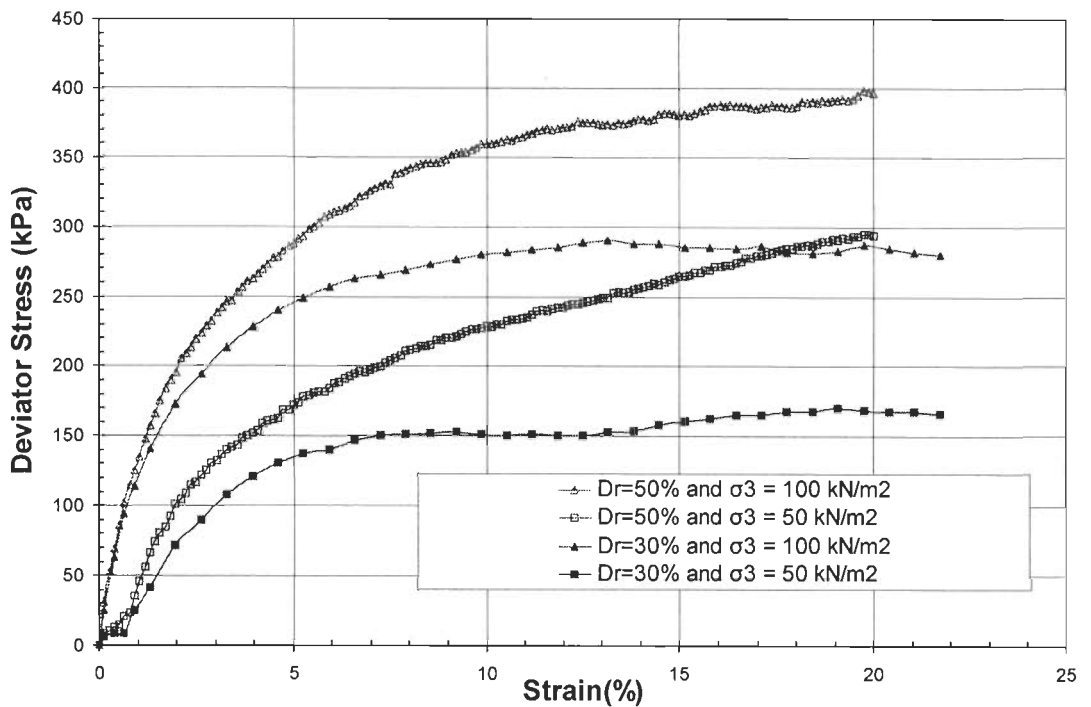


Figure 4.15 Stress- strain behaviour of fiber-reinforced sand with 0.75% fiber (6 Denier 10 mm) at different relative densities

It was interesting to note that RDFS samples with almost similar values of product of aspect ratio and fiber content ($\eta \cdot \chi_w$) (Table 4.2) have not only shown almost similar failure deviator stresses but also the shape of stress-strain curves (Figure 4.16).

Table 4.2 Some of RDFS samples with similar $\eta \cdot \chi_w$

RDFS Sample	$\eta \cdot \chi_w$
0.25%, 20 Denier 50mm long	$875 \times 0.25 = 219$
0.75%, 6 Denier 10mm long	$325 \times 0.75 = 244$

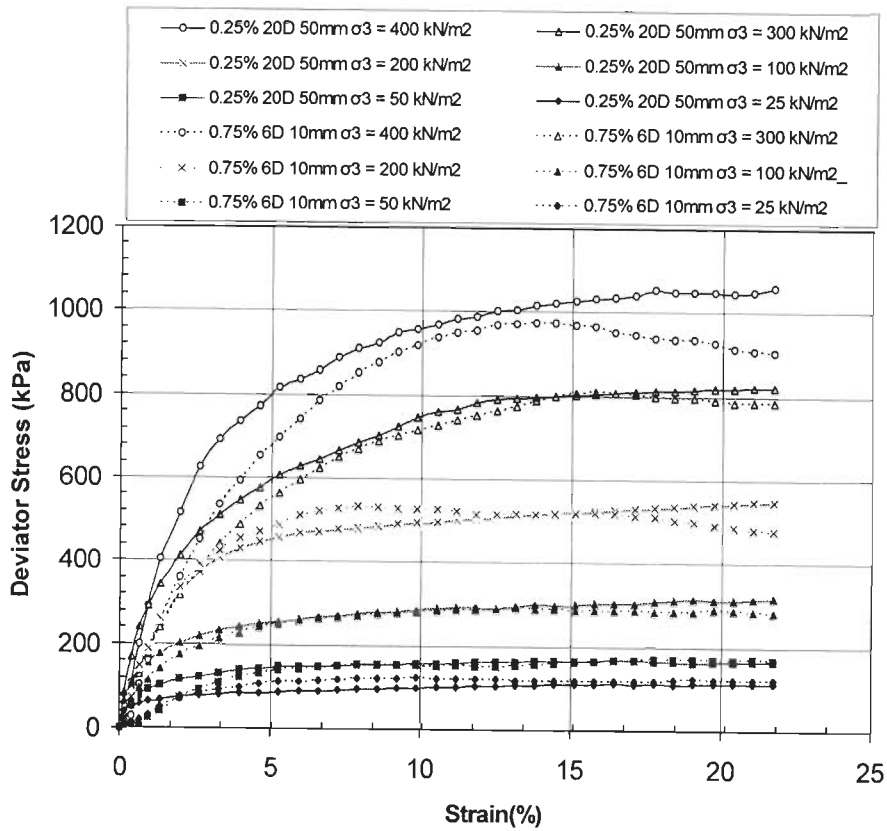


Figure 4.16 Comparison of Stress- Strain Curve for sand (RD= 30%) with 0.75% fiber of 6D10mm and 0.25% fiber of 20D50mm

One of the main advantages of the polypropylene fiber reinforcement is the strain hardening behavior induced, even at large strain deformations. This behavior suggests potential applications of the fiber-reinforced soils in shallow foundations subjected to eccentric – inclined load or located in seismic regions, that may suffer excessive deformations.

4.2.2 Applicability of Statistical Model for Prediction of Strength of RDFS

In present investigation critical normal stress ($\sigma_{n,crit}$) using Zornberg (2002) model worked out 643, 1531 and 2503 kPa for 6D 10 mm, 20D 20 mm and 20D 50 mm fibers respectively. These values are very high compared to confining pressure used in this experimental investigation (maximum $\sigma_3 = 400$ kPa) and encountered in shallow

foundations. Therefore, equation 2.10a (Ranjan et al. 1996) corresponding to $\sigma_3 < \sigma_{n,crit}$ is used for predicting deviator stress. Predicted values of deviator stress at failure using Ranjan et al. (1996) model with experimental values are shown in Table 4.3.

Table 4.3 Deviator Stress (kPa) at Failure - Predicted

	Fiber%	0.25%	0.25%	0.25%	0.50%	0.50%	0.50%
σ_3 (kPa)	UR	6D10mm	20D20mm	20D50mm	6D10mm	20D20mm	20D50mm
25	55.2	127.6	131.6	177.3	176.4	181.6	242.0
50	117.0	194.5	200.8	274.2	272.6	280.9	377.8
100	243.3	291.7	301.8	419.4	416.9	430.2	585.3
200	476.8	427.6	443.8	632.1	628.1	649.5	898.0
300	680.0	526.9	548.2	796.3	791.1	819.2	1146.6
400	884.8	605.5	631.5	933.2	926.8	961.0	1359.1
	Fiber%	0.75	0.75	0.75	1.0	1.0	1.0
σ_3 (kPa)	UR	6D10mm	20D20mm	20D50mm	6D10mm	20D20mm	20D50mm
25	55.2	211.8	217.9	289.0	240.7	247.6	327.3
50	117.0	329.4	339.2	453.1	375.7	386.7	514.4
100	243.3	507.9	523.6	706.0	582.1	599.6	804.3
200	476.8	774.0	799.1	1091.3	892.8	920.9	1248.8
300	680.0	983.2	1016.3	1401.3	1139.7	1176.8	1608.7
400	884.8	1160.4	1200.7	1668.8	1350.7	1395.9	1921.2

A comparison of experimental values of deviator stress of RDFS with predicted using Ranjan et al. (1996) model is made in Figure 4.17. Values predicted by model are on an average 25% higher. This difference may be due to high aspect ratio (325 to 875) of fibers used in experimentation. Ranjan et al. (1996) developed model using low aspect ratio of the order of 50 to 150 and no significant increase was observed beyond an aspect ratio of 120. Only for some cases of low fiber content of 0.25% the predicted values are

lower. Statistical model by Ranjan et al. (1996) was developed for fiber content of 0.5% to 4% may be the reason for such low values. Statistical model may be calibrated by conducting few tests for fibers or soil other than used for developing model. For example in present investigation a multiplying factor of 0.8 to equation 2.10a may yield good agreement between predicted and experimental values. Thus, statistical model can be used for prediction of strength of RDFS.

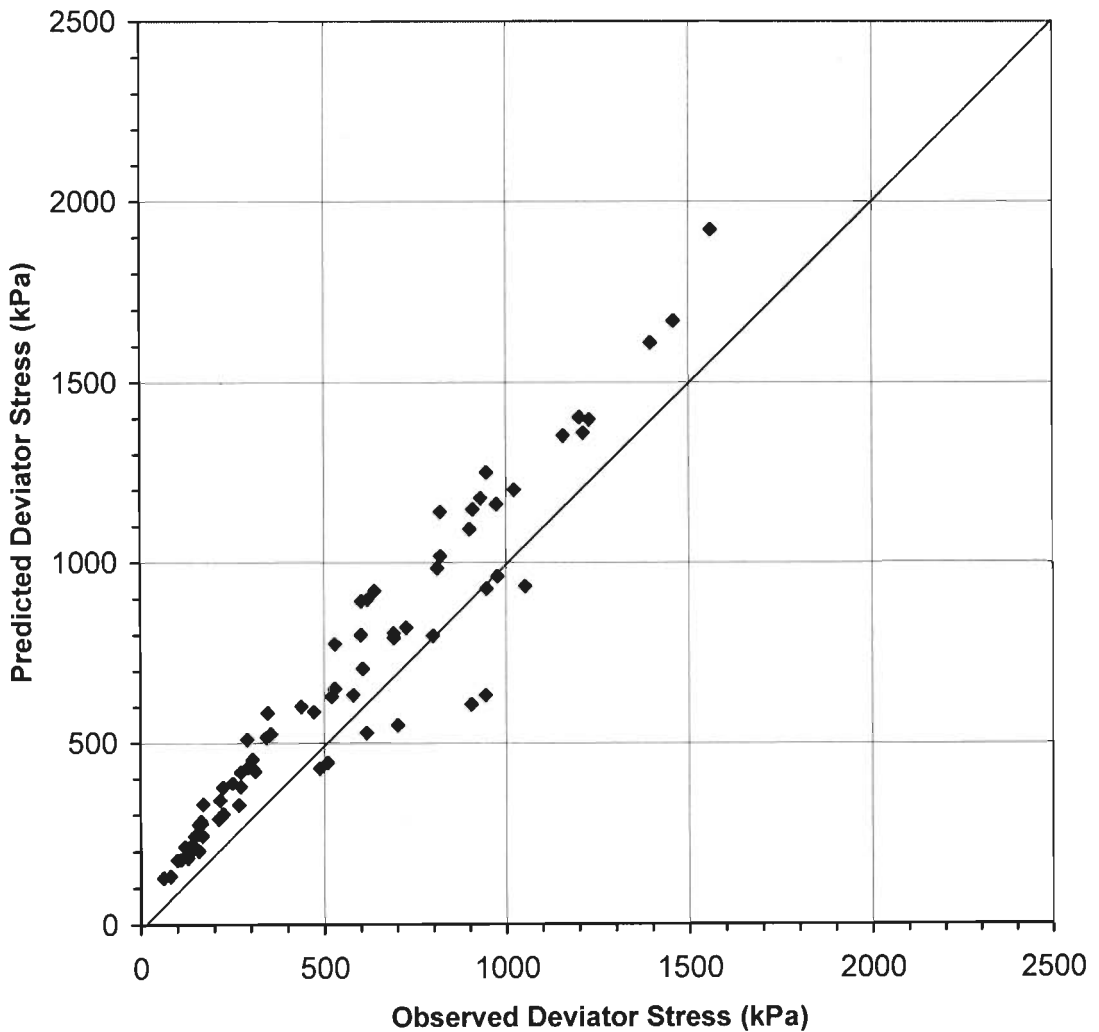


Figure 4.17 Experimental versus predicted deviator stress of RDFS using Ranjan et al. (1996)

4.3 CONSTITUTIVE LAWS OF RDFS

As noted earlier behaviour of RDFS is deformation (strain) dependent and in most of the cases maximum or failure stress was not observed. Such cases would be the obvious choice for application in field. Shear strength parameters (c and ϕ) are used to determine bearing capacity of unreinforced sand using available bearing capacity equations. However, in case of RDFS there are some difficulties in using such bearing capacity equations. For RDFS failure envelope is bilinear or curvilinear therefore selection of appropriate c and ϕ values are essential considering confining stress. Shear strength parameters (c - ϕ) are deformation dependent, hence which value of c - ϕ is to be used in case of RDFS, corresponding to peak or residual stresses or 15% or 20% strain is not certain. Relationships between friction angle and bearing capacity factors are given up to a friction angle of 50° only and depending upon soil and fibers used, friction angle for RDFS may exceeds 50° . Bearing capacity calculations are very sensitive to shear strength parameters (c and ϕ) particularly for $\phi > 35^\circ$. Hence, the question arises that which mode of failure is to be considered for footing resting on RDFS? Therefore, it is concluded that triaxial test results of RDFS can't be suitably applied for determination of bearing capacity using single c - ϕ value based on peak stresses or 20% strain or else. McGown et al. (1985) and Consoli et al. (2003b) reported that overall strength deformation behaviour represented by triaxial stress-strain curve of RDFS is similar to pressure-settlement curve of footing resting on RDFS. Therefore, it would be appropriate to develop a technique utilizing triaxial stress-strain data to predict pressure-settlement characteristics of footing resting on RDFS. The stress-strain curve simulates real behaviour of RDFS (such as increased stresses with increasing strain, strain hardening and ductile behaviour), therefore a constitutive law representing whole stress-strain curve

would be more appropriate technique to predict pressure-settlement characteristics of footing resting on RDFS.

To consider overall response of RDFS as given by stress-strain curve, attempts were made to model the stress-strain curves of RDFS using Kondner (1963) and Kondner & Zelasko (1963) constitutive laws.

Kondner (1963) and Kondner and Zelasko (1963) showed that the non-linear stress-strain curves, for both clay and sand, from triaxial tests, may be represented by hyperbola of the following form;

$$\frac{\varepsilon}{\sigma_1 - \sigma_3} = a + b\varepsilon \quad (4.1)$$

or

$$\varepsilon = \frac{a(\sigma_1 - \sigma_3)}{1 - b(\sigma_1 - \sigma_3)} \quad (4.2)$$

Where; ε = axial strain

$\sigma_1 - \sigma_3$ = deviator stress

a & b = constants of the hyperbola

The plot of $\varepsilon/(\sigma_1 - \sigma_3)$ versus ε gives a straight line, where 'a' is the intercept on the y-axis and 'b' is the slope of the line, as shown in Figure 4.18a, b.

At very small strain, equation (4.1) becomes

$$\sigma_1 - \sigma_3 = \varepsilon/a \quad (4.3)$$

Thus $1/a$ is the initial Young's modulus E_i . At very large strain the relation becomes;

$$\sigma_1 - \sigma_3 = 1/b \quad (4.4)$$

Where, $1/b$ is the ultimate compressive strength of the soil, which is larger than the failure compressive strength.

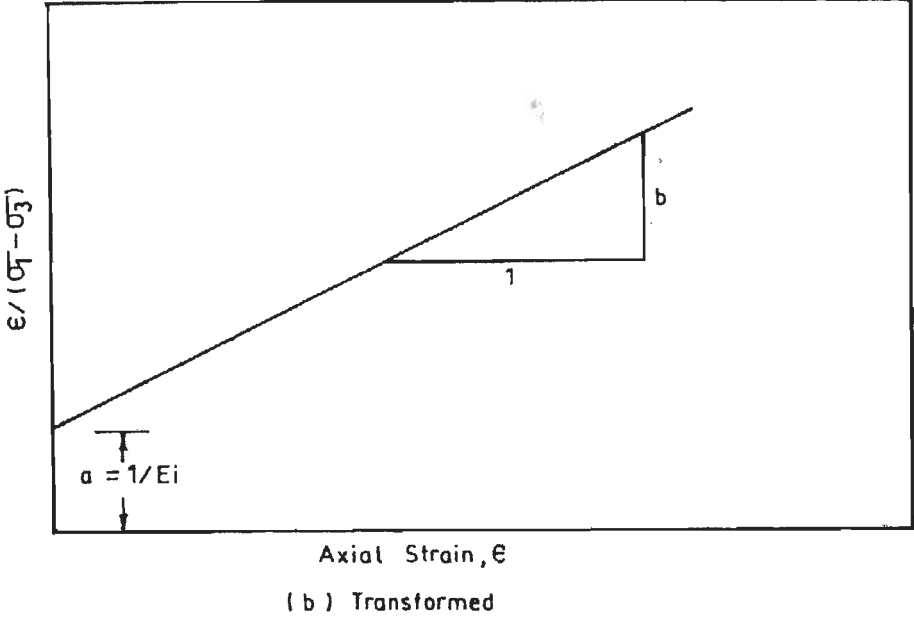
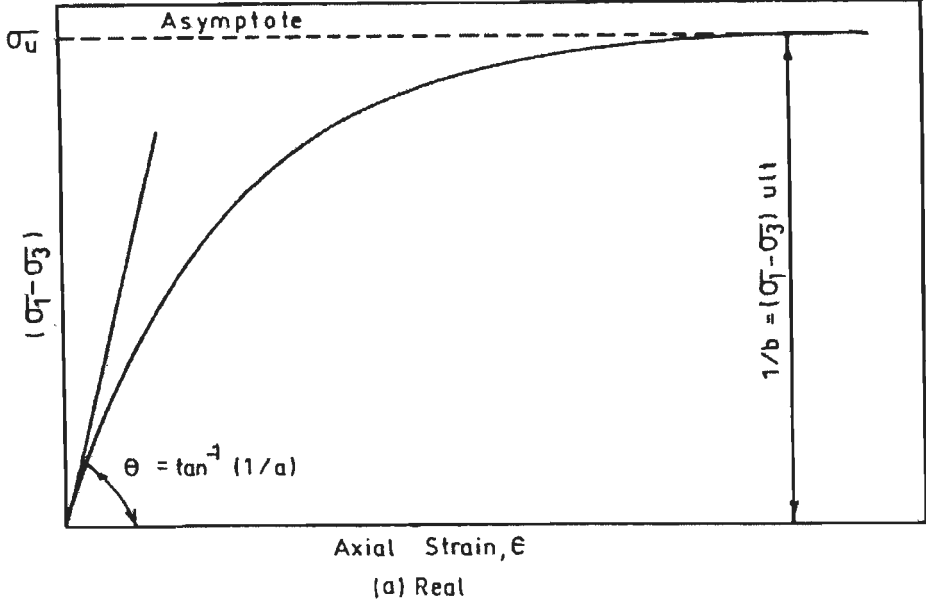


Figure 4.18 a, b Hyperbolic stress-strain representation (after Kondner, 1963)

The deviator stress-axial strain data were analyzed to determine the hyperbolic model parameters. Figures 4.19 and 4.20 show typical transformed hyperbolic stress-strain plots for RDFS obtained from triaxial test results. Transformed data fit very well to a straight line in the $[\varepsilon, \varepsilon/(\sigma_1 - \sigma_3)]$ co-ordinates system as the coefficient of determination R^2 approached unity and were in the range of 0.99 to 0.999.

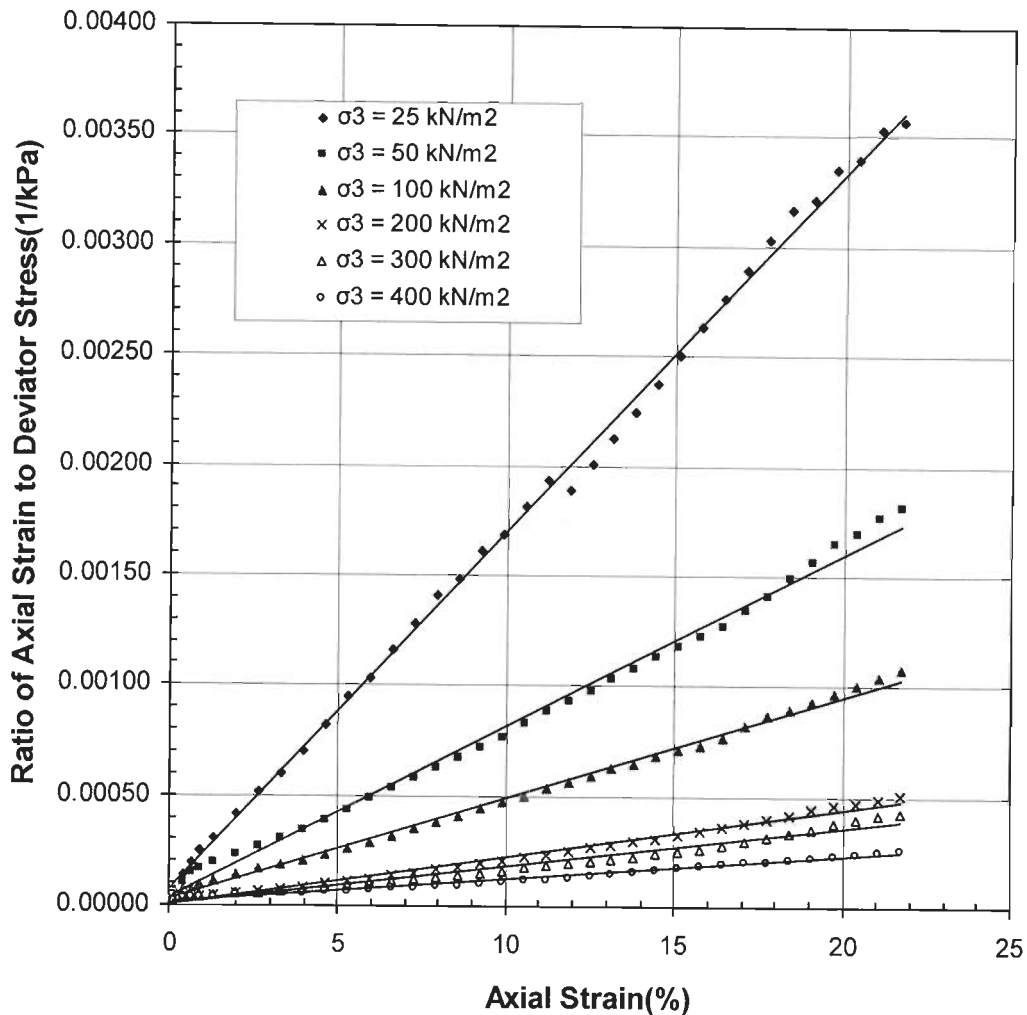


Figure 4.19 Transformed hyperbolic stress-strain plot for RDFS ($D_r = 30\%$) with 0.25% fiber content (6D 10 mm)

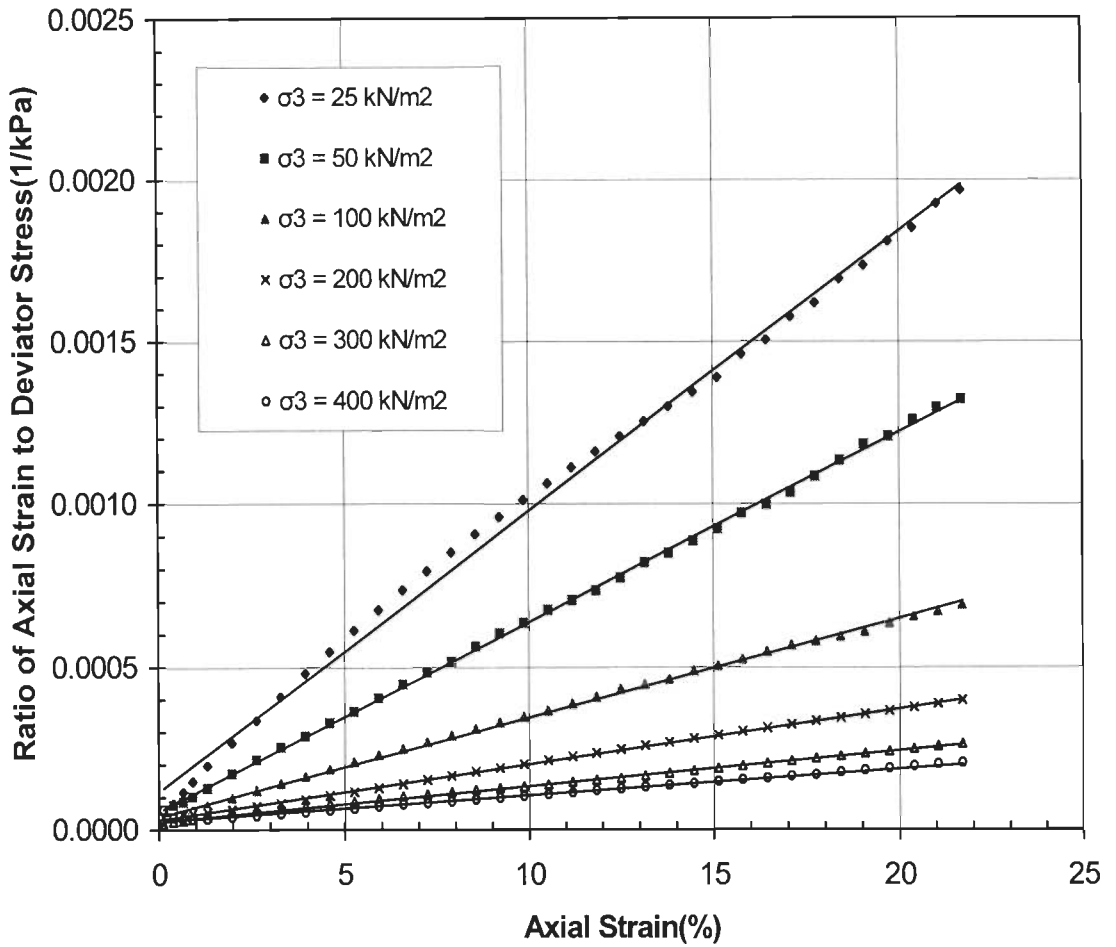


Figure 4.20 Transformed Hyperbolic Stress-Strain plot for RDFS ($D_r = 30\%$) with 0.25% fiber content (20D 50 mm)

The parameter 'a' (or $1/E_i$) and 'b' (or $1/\sigma_u$) of the hyperbola were correlated with confining pressures (σ_3) as shown in typical plots in Figures 4.21 and 4.22 respectively for 0.25% fiber content of 6 denier 10 mm fiber reinforced sand. The following relationships were found to hold good for RDFS.

$$1/a = k_1 (\sigma_3)^n \quad (4.5)$$

$$1/b = k_2 + k_3 \sigma_3 \quad (4.6)$$

where, σ_3 is the confining pressure (kN/m^2).

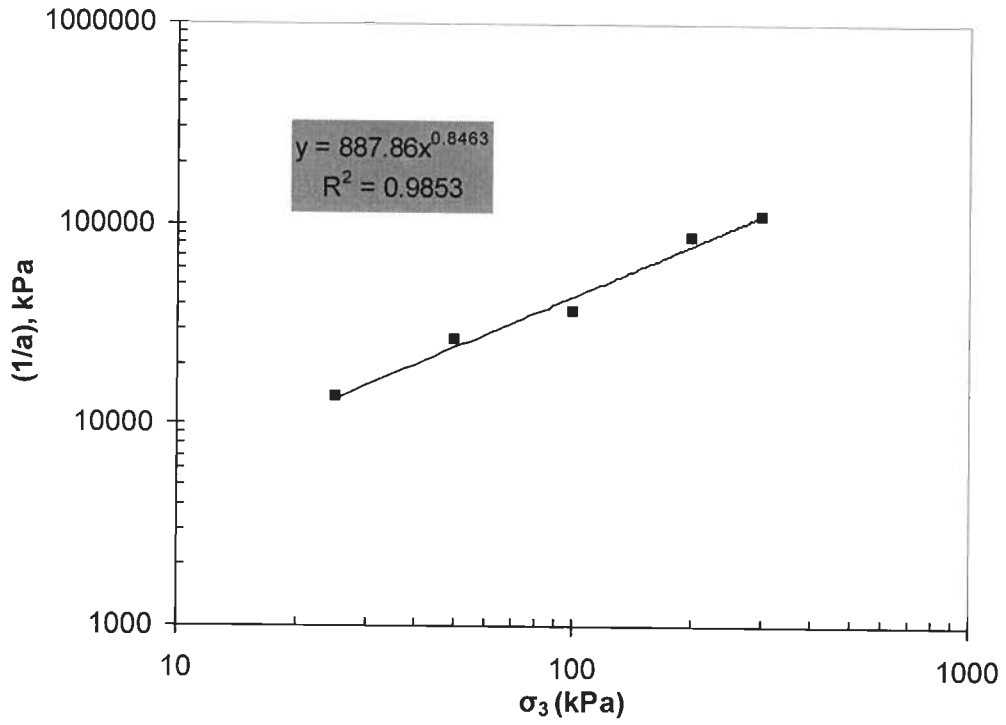


Figure 4.21 1/a for 0.25% 6D10mm fiber

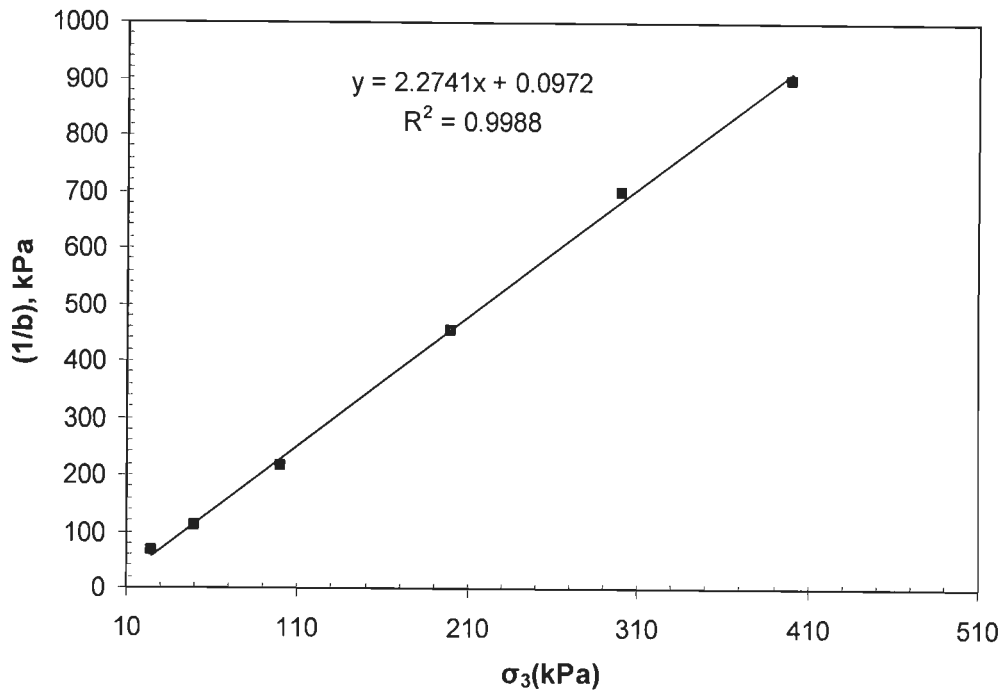


Figure 4.22 1/b for 0.25% 6D10mm fiber

McGown et al. (1985) conducted triaxial tests as well as model strip footing tests also in similar conditions. Figure 4.23 shows drained triaxial test results of Mid-Ross sand randomly reinforced with polypropylene mesh elements 50 mm x 50 mm. Triaxial test data of McGown et al. (1985) were analyzed to determine the hyperbolic model parameters. It was found that transformed data fit very well to a straight line in the $[\epsilon, \epsilon/(\sigma_1 - \sigma_3)]$ co-ordinates system as the coefficient of determination R^2 approached unity and were in the range of 0.99 to 0.999 (Figure 4.24).

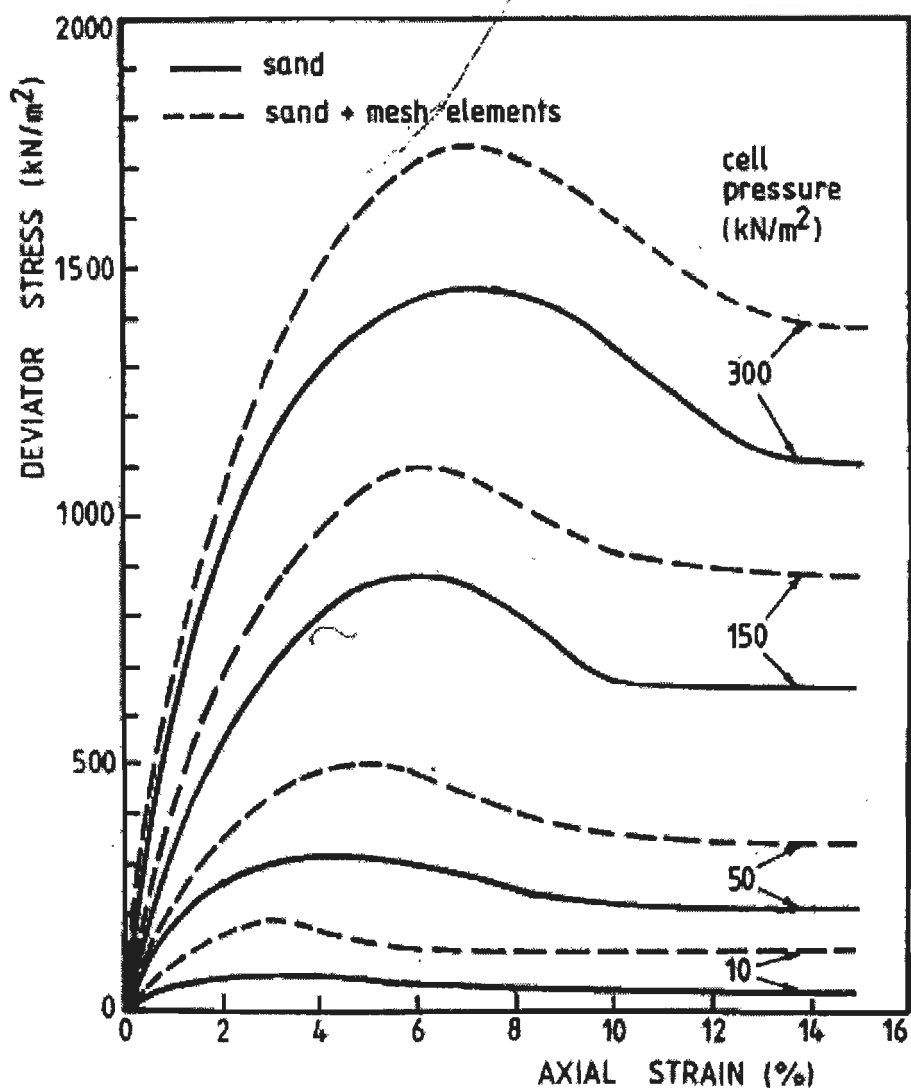


Figure 4.23 Stress-strain plot for Mid Ross sand and randomly reinforced with 0.18% mesh elements

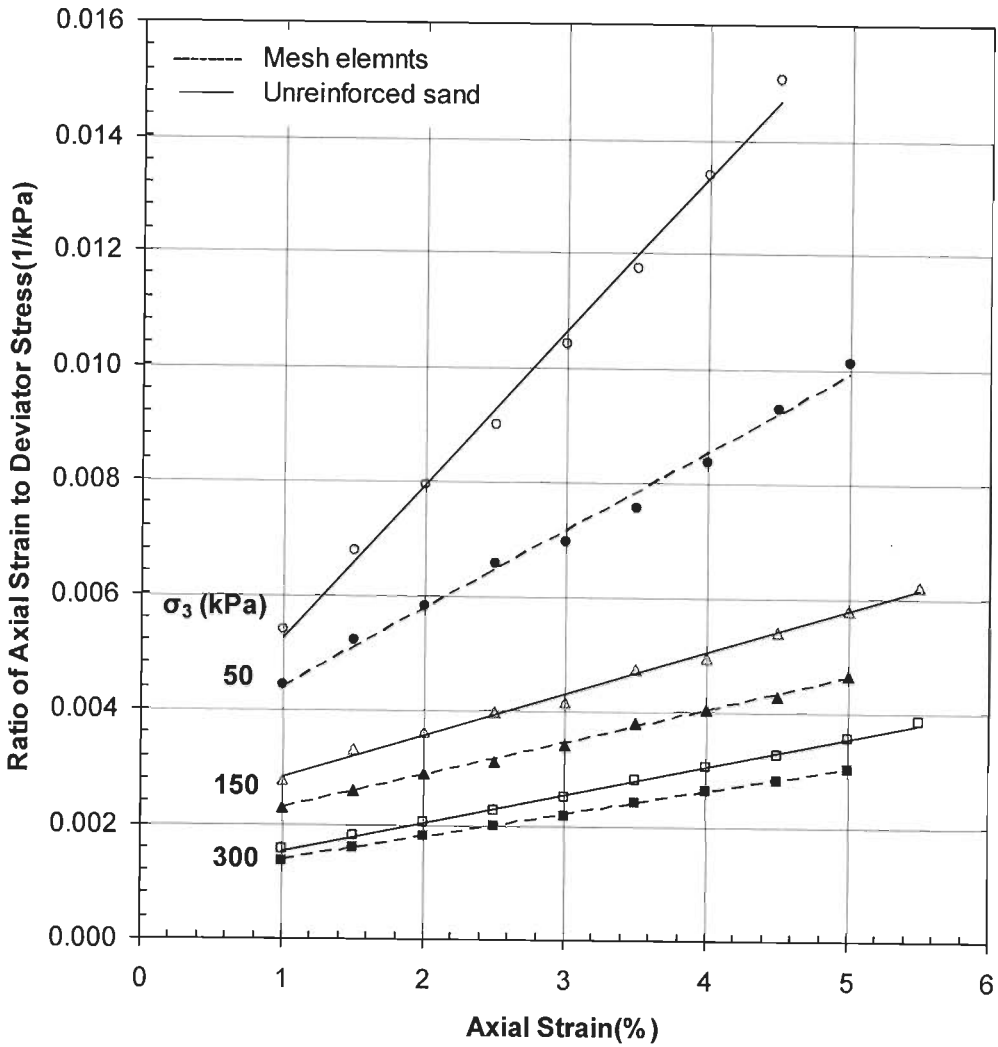


Figure 4.24 Transformed hyperbolic stress-strain plot for Mid Ross sand and randomly reinforced with 0.18% mesh elements

4.4 SUMMARY

The effect of fiber content and fiber length on the stress-strain behavior of the fiber-reinforced soil was evaluated. The stress-strain behavior of fiber-reinforced specimen prepared using different densities is also compared. Based on the experimental results, a discussion regarding use of whole stress-strain data instead of peak shear strength parameters of RDFS to predict the bearing capacity or pressure

settlement characteristics is presented. The following conclusions can be drawn from this evaluation:

1. The addition of fibers can increase significantly the peak shear strength and limit the post-peak shear strength loss of soil. In most of the RDFS samples strain hardening behaviour was observed. An increase in fiber content leads to increasing strain at failure and, consequently, to a more ductile behavior.
2. The peak shear strength increases with increasing aspect ratio. The strain at maximum strength increases with increasing fiber aspect ratio.
3. Mobilization of fiber-induced tension requires relatively high strain level, often beyond the peak for unreinforced soil.
4. The relative density has significant influence on the shear strength of RDFS. At higher relative density shear strength is much higher compared to that at lower relative density. For RDFS samples at 50% relative density strain hardening was observed for all strains (up to 20%).
5. Statistical model can be used for prediction of strength of RDFS within the range of large data base by which it is developed. For other fibers and soil, statistical model can be easily modified by conducting a few tests.
6. Using experimental data, hyperbolic stress-strain parameters were determined and it was found that hyperbolic stress-strain relationships are valid for RDFS.

5.1 GENERAL

Results and interpretation of model footing tests have been presented, in this chapter. Effect of various parameters (type of fiber/ mesh elements, fiber content, fiber length, fiber aspect ratio, fiber denier, depth of RDFS layer, density of RDFS, size of RDFS zone below footing, submerged condition, footing size etc.) on behaviour (pressure - settlement characteristic, bearing capacity ratio, tilt and horizontal displacement etc.) of strip footing under different loading conditions (central - vertical load, central – inclined load, eccentric - vertical load and eccentric – inclined load) resting on RDFS is evaluated. A cost comparison is also made with strip footing resting on planar reinforcement. Using nonlinear, multiple regression analysis, a mathematical model is developed using model tests to predicted bearing capacity, settlement and tilt of footing resting on RDFS.

**5.2 BEHAVIOUR OF STRIP FOOTING ON RDFS: CENTRAL – VERTICAL
LOAD**

Effect of various parameters (type of fiber/ mesh elements, fiber content, fiber length, fiber aspect ratio, fiber denier, depth of RDFS layer, density of RDFS, size of RDFS zone below footing, submerged condition etc.) on behaviour of strip footing (B=75 mm) under central - vertical load resting on RDFS is evaluated in this section.

5.2.1 Evaluation of Ultimate Bearing Capacity and Bearing Capacity Ratio

The three principal modes of shear failure under foundations have been described in literature as, general shear failure, local shear failure and punching shear failure. In the case of general shear failure, there is no difficulty in determining the ultimate bearing capacity from pressure-settlement curves. In contrast to this, in the case of the other failure models, local and punching shear, the point of failure is less clearly defined and often difficult to establish.

The ultimate bearing capacity is the load (Q) for which in the load settlement(s) curve ($Q=f(s)$) the gradient $\Delta s / \Delta Q$ become infinite. In cases where a peak load cannot be established with certainty (i.e. $\Delta s / \Delta Q = \infty$), the conventional ultimate bearing capacity is defined as the load causing a relative settlement 10% of the footing width (B) (Vesic, 1973; De Beer, 1970, 1987; Briaud & Jeanjean, 1994 and Lutenegger & Adams, 1998). In the present study, pressure-settlement curves did not show the point of failure clearly for most of the cases, therefore, for comparison ultimate bearing capacity (q_u) values were taken as the bearing pressure causing a relative settlement 10% of the footing width (B). Ultimate bearing capacity ratio (BCR) is defined as ratio of bearing capacity of footing on RDFS at 10% settlement ratio to sand alone at 10% settlement ratio.

5.2.2 Behaviour of Strip Footing on RDFS using Different Type of Fiber/ Mesh Elements

Improvement in engineering properties of RDFS is influenced by the fiber/ mesh element type, fiber content, fiber length, aspect ratio etc. Model footing tests were conducted on different type of fibers and mesh elements on a strip footing of 75 mm width at different fiber content. Randomly distributed fiber or mesh elements reinforced sand was placed

throughout the test tank (i.e. $R_d = 5B$, $R_w = 10B$). In all tests a relative density of 30% was maintained.

Pressure – settlement curves are shown in Figure 5.1 to 5.3 for different fiber content and bearing capacity ratios are given in table 5.1. Comparison of BCR values are shown in Figure 5.4 to 5.6. Performance and increase in bearing capacity of RDFS vary significantly with fiber or mesh type. At all fiber content, lowest improvement is given by mesh elements from Netlon CE121 and highest improvement is given by fibrillated fibers. Only, NAF 25 mm x 50 mm mesh elements performed better than 1000D 20 mm fibrillated fibers at 0.25%, but lower than 1000D 50 mm fibrillated fibers. With increase in percentage of mesh content mixing become difficult for NAF 25 mm x 50 mm mesh elements and segregation of mesh elements occur and performance decrease. At 0.5 % and 1% fiber content BCR of NAF 25 mm x 50 mm mesh elements is less than 1000D 20 mm fibrillated fibers. There was no difficulty in mixing fibrillated fibers. Some tests were conducted at 1.5 and 2% fiber content also. However for field application it is recommended to use up to 1% fiber content to get a uniform distribution of fibers.

NAF 25 mm x 50 mm mesh elements also given very good performance comparable to thin monofilament fibers but could not perform better than fibrillated fibers. Thus mesh elements perform better than fiber may not be taken as a general conclusion as reported by various investigators (Al-Refeai 1991, Uysal 1993, Wasti and Butun 1996 and McGown et al. 2004). However, mesh elements perform better compare to straight fiber cut from same mesh as reported by Wasti and Butun (1996) and Dash et al. (2004). Fibrillated fibers have shown improvement even at very low values of strain such as 2-3% of footing width also.

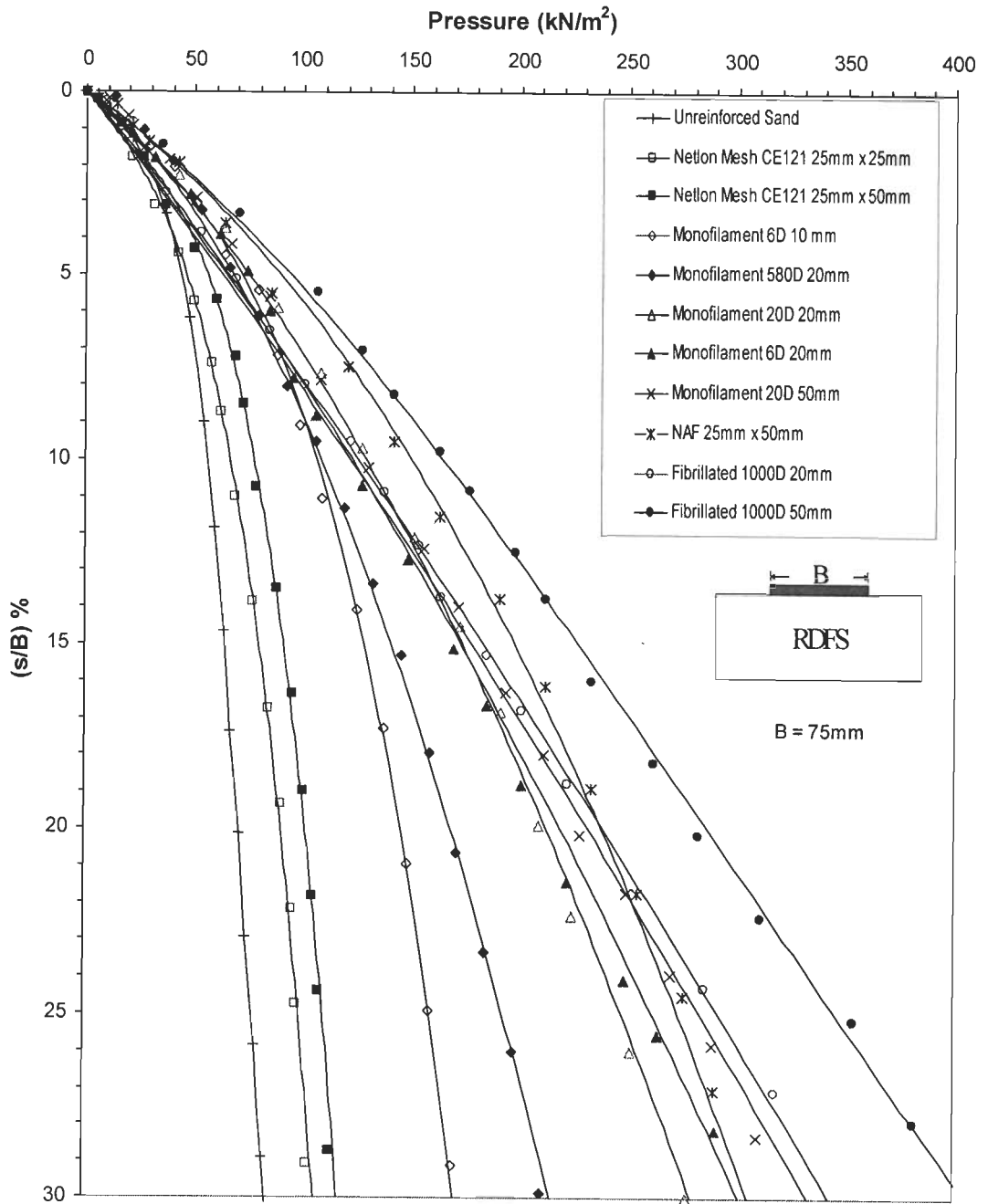


Figure 5.1 Pressure-settlement curves for different fibers/ mesh elements for 0.25% fiber content ($R_w=10B$, $R_d=5B$ and $D_r = 30\%$)

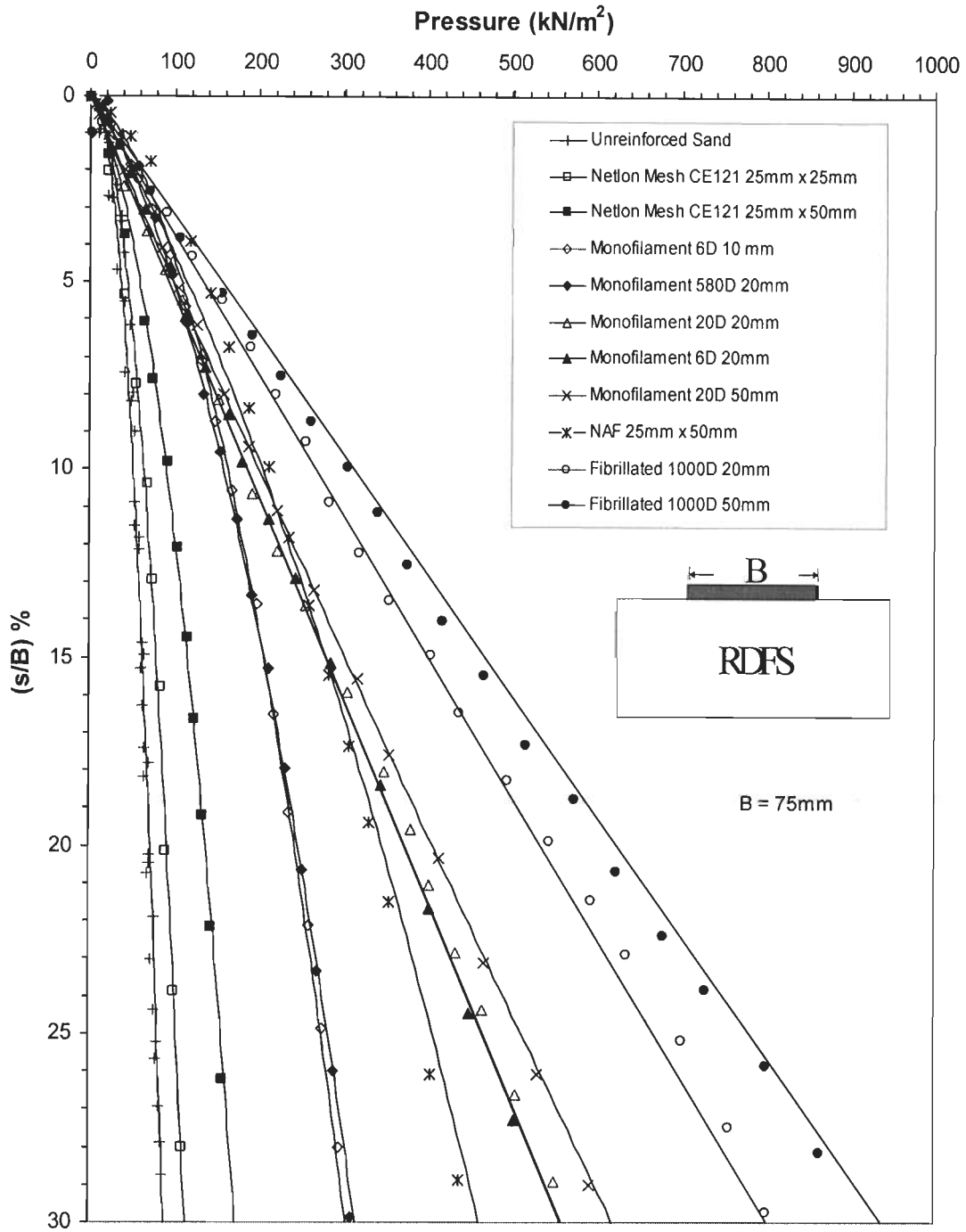


Figure 5.2 Pressure-settlement curves for different fibers/ mesh elements for 0.5% fiber content ($R_w=10B$, $R_d=5B$ and $D_r = 30\%$)

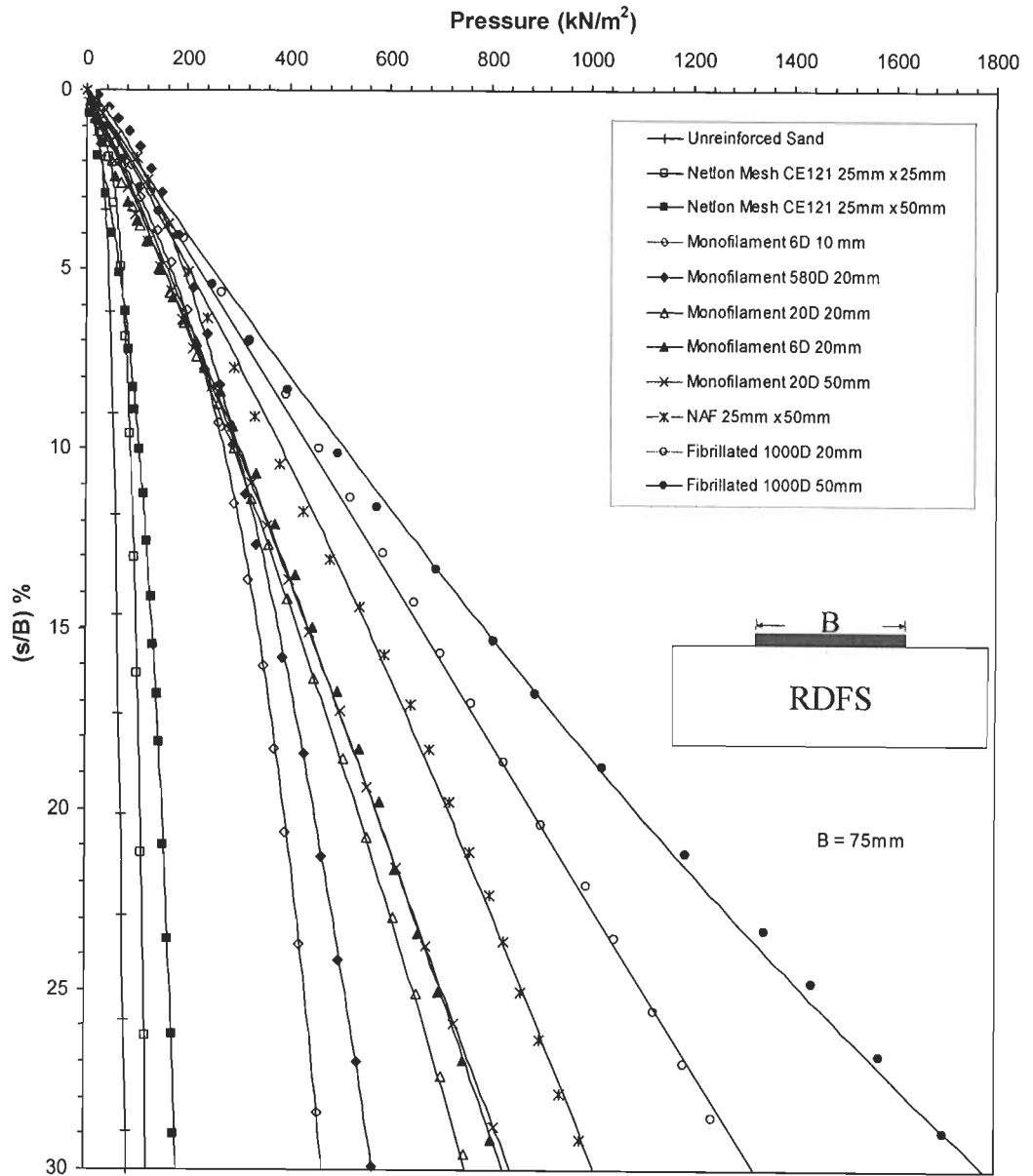


Figure 5.3 Pressure-settlement curves for different fibers/ mesh elements for 1% fiber content ($R_w=10B$, $R_d=5B$ and $D_r = 30\%$)

Table 5.1 Bearing Capacity Ratio (BCR) values for different type of fibers and mesh elements

Fiber content →	Bearing Capacity Ratio (BCR)		
	0.25%	0.50%	1%
Fiber/ Mesh element details ↓			
Netlon Mesh CE 121, 25 mm x 25 mm	1.2	1.3	1.6
Netlon Mesh CE 121, 25 mm x 50 mm	1.4	1.7	1.9
Monofilament 6D 10 mm	1.9	2.9	4.9
Monofilament 580D 20 mm	2.0	2.9	5.3
Monofilament 20D 20 mm	2.3	3.3	5.3
Monofilament 6D 20 mm	2.3	3.3	5.4
Monofilament 20D 50 mm	2.4	3.6	5.4
NAF 25 mm x 50 mm	2.7	3.8	6.7
Fibrillated 1000D 20 mm	2.5	5.0	8.4
Fibrillated 1000D 50 mm	3.0	5.6	9.2

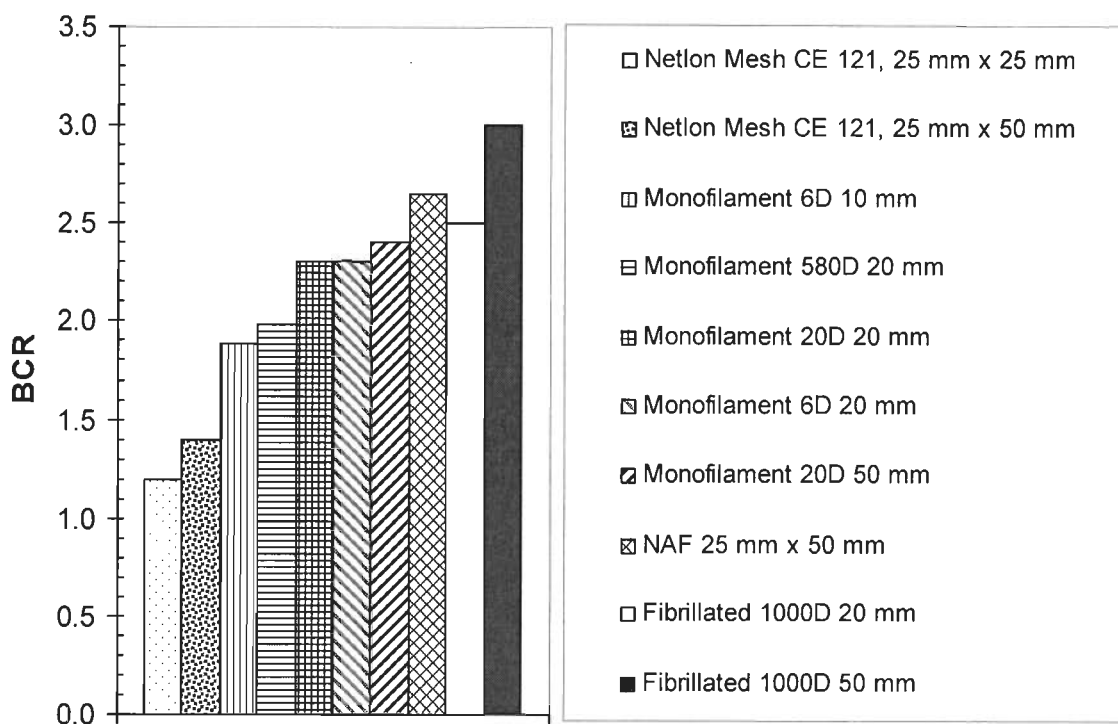


Figure 5.4 BCR for different fibers/ mesh elements at 0.25% fiber content ($R_w=10B$, $R_d=5B$ and $D_r = 30\%$)

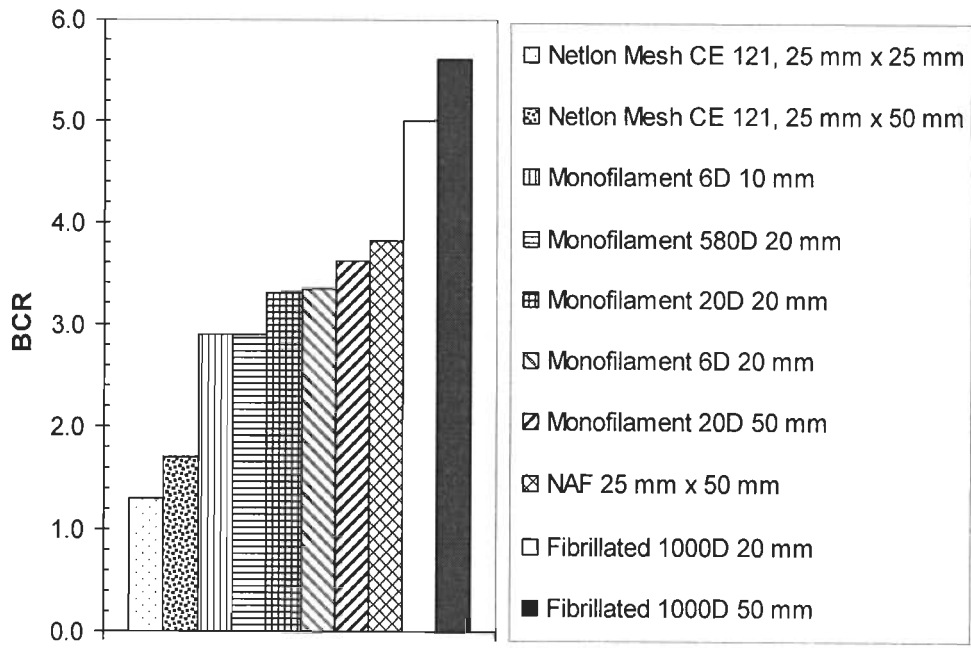


Figure 5.5 BCR for different fibers/ mesh elements at 0.5% fiber content ($R_w=10B$, $R_d=5B$ and $D_r = 30\%$)

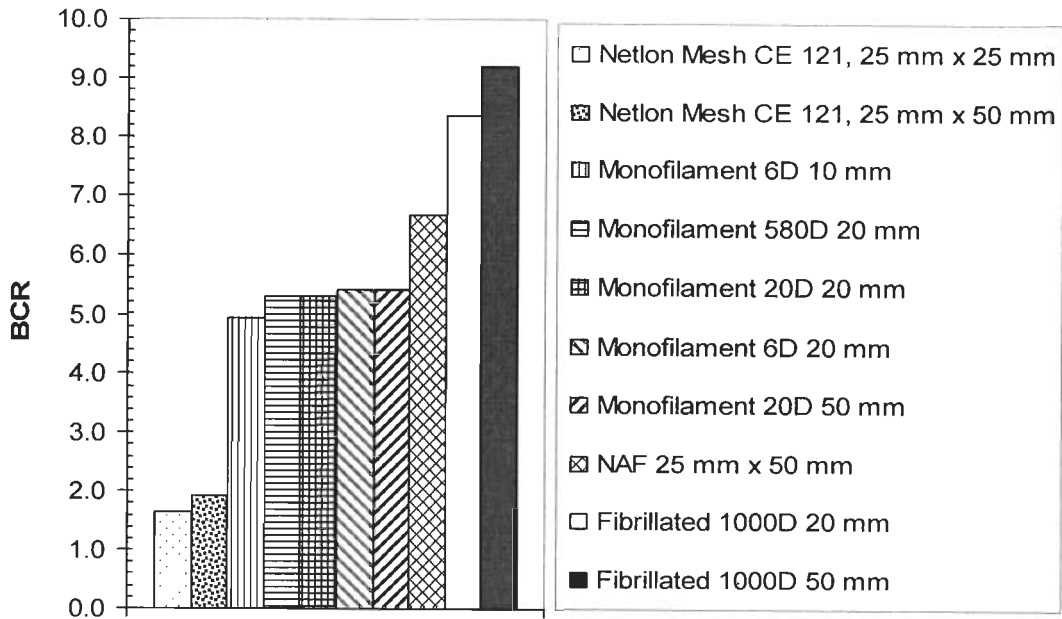


Figure 5.6 BCR for different fibers/ mesh elements at 1% fiber content ($R_w=10B$, $R_d=5B$ and $D_r = 30\%$)

Cost of NAF mesh elements is more than twice compared to monofilament and fibrillated fibers. In general it can be concluded that fibrillated fiber is best choice for shallow foundation.

With increase in length and aspect ratio BCR increases. Length of fiber was found to be an important factor. Longer fibers performed better compare to smaller one. The 50 mm long fibers performed better compare to 20 mm and 10 mm fibers, keeping other factors same. With increase in aspect ratio BCR increases. Monofilament 6 denier 10 mm ($\eta = 325$) fibers given lowest strength but monofilament 20D 20 mm fibers having similar aspect ratio ($\eta = 350$) has shown significantly high strength compare to monofilament 6D 10 mm fibers. Which suggest that fiber length should not be less than a critical value. For sands a range of 20-50 mm is suggested for its application to shallow foundations. Fiber lengths greater than 50 mm are not suitable due to difficulty in mixing in the field with a self- propelled rotary mixer or other mixing equipment. Triaxial test results reported by Al-Refeai, 1991 and unconfined compression test results reported by Santoni et al., 2001; Sobhan & Mashnad 2003, also indicated that the strength of the RDFS increased with increased length of fibers up to a length of 50 mm after that strength decreases or remain same. For field applications 50 mm length is most suitable. Effect of denier of fiber was studied by varying denier of monofilament fibers of 20 mm long keeping all other conditions same. It was found that with decrease in denier, BCR increases slightly. Monofilament, 580 denier 20 mm fiber has shown slight decrease in BCR compare to 6 denier 20 mm and 20 denier 20 mm fiber. Results of 6 denier 20 mm and 20 denier 20 mm are almost similar. With decrease in denier for same fiber content number of fibers increases consequently increased surface area is responsible for increase in BCR.

However, after certain limiting value of denier number of fibers are too large that surface area of fibers actively contributing to strength may not increase. Results suggest that there is a limiting value of fiber denier below which their no further increase in bearing capacity.

The bearing capacity increases with increase in fibre content for all type of fibers and mesh elements. For a given pressure intensity, the settlement of unreinforced sand is more than that of the RDFS and the settlement reduces with the increase in the fibre content. Maximum increase in BCR and reduction in settlements are found by 1000D 50 mm fibrillated fibers.

In general it can be concluded that fibrillated fiber is best choice for its application to shallow foundation. For detailed study of effect of various parameters such as relative density, depth of RDFS layer, size of RDFS zone below footing, submerged condition etc. on behaviour of strip footing resting on RDFS, fibrillated fibers were selected. Results and interpretation are discussed in subsequent sections.

5.2.3 Effect of Fiber Content and Relative Density:

Figure 5.7 to 5.9 show pressure – settlement curves for different fiber content at relative density of 30%, 50% and 70% respectively. All tests were conducted in two dimensional tank on a strip footing of 75 mm width. Whole tank was filled with RDFS (i.e. $R_w = 10B$ and $R_d = 5B$). With increase in fiber content over all pressure –settlement curve improved and shifted upward. Similar trends were observed at all three densities. Pressure –settlement curves are almost linear and showing strain hardening at higher fiber content. No failure was observed even up to 30% settlement ratio. Figure 5.10 shows

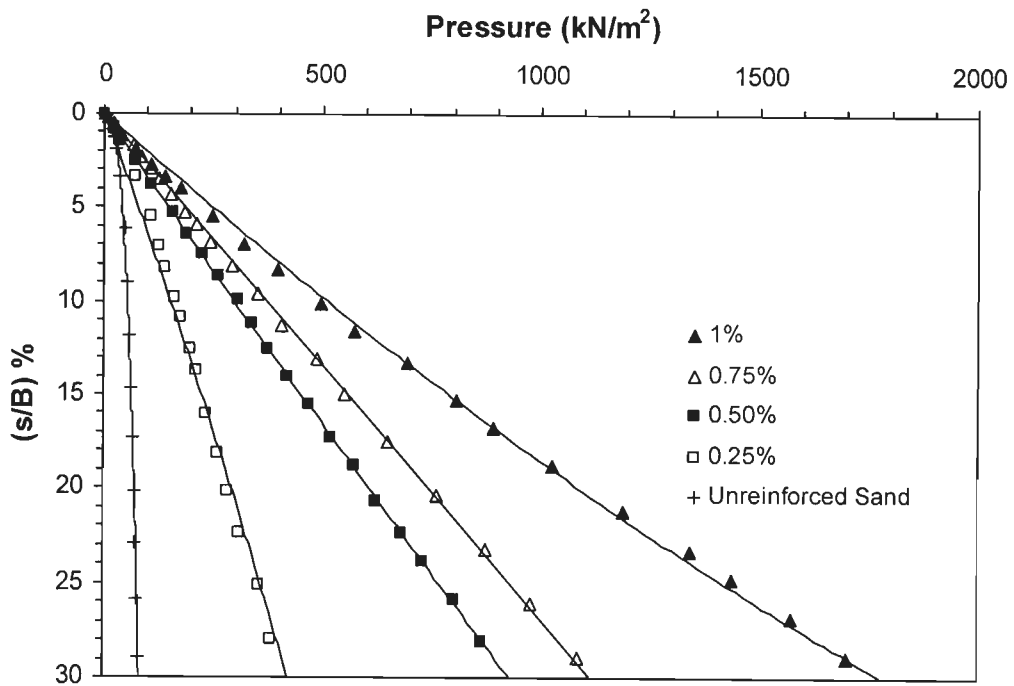


Figure 5.7 Pressure - settlement curves for different fiber content for 1000D 50 mm fibrillated fiber ($R_w=10B$, $R_d=5B$ and $D_r = 30\%$)

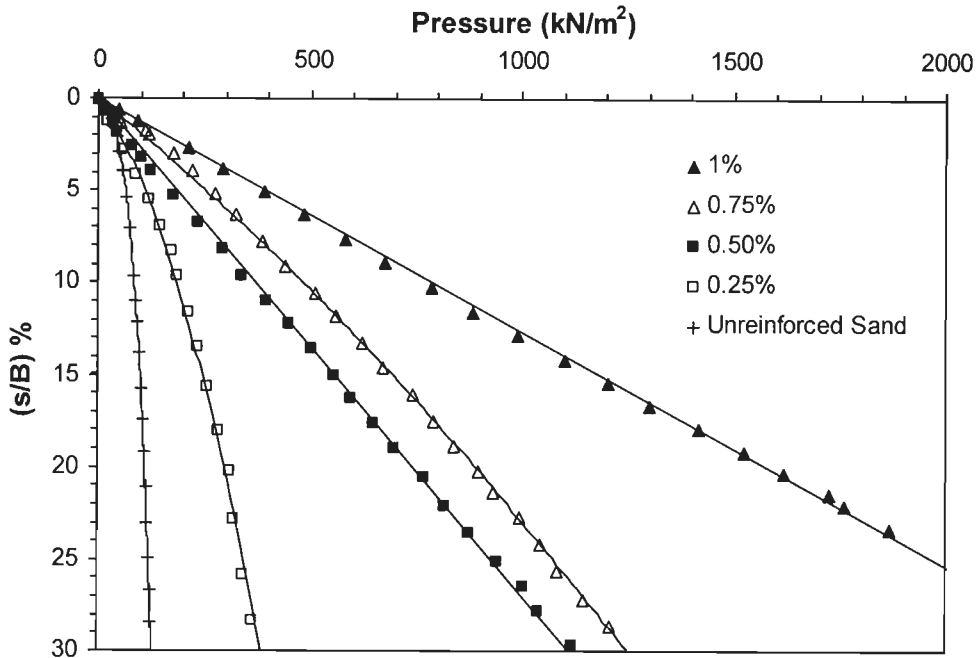


Figure 5.8 Pressure - settlement curves for different fiber content for 1000D 50 mm fibrillated fiber ($R_w=10B$, $R_d=5B$ and $D_r = 50\%$)

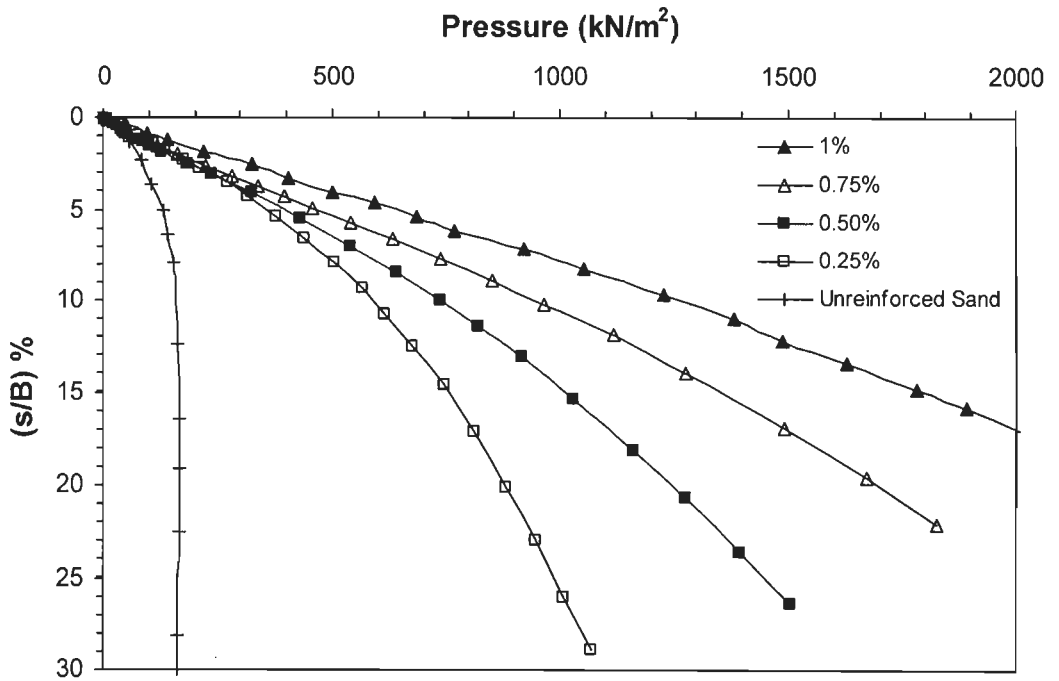


Figure 5.9 Pressure - settlement curves for different fiber content for 1000D 50 mm fibrillated fiber ($R_w=10B$, $R_d=5B$ and $D_r = 70\%$)

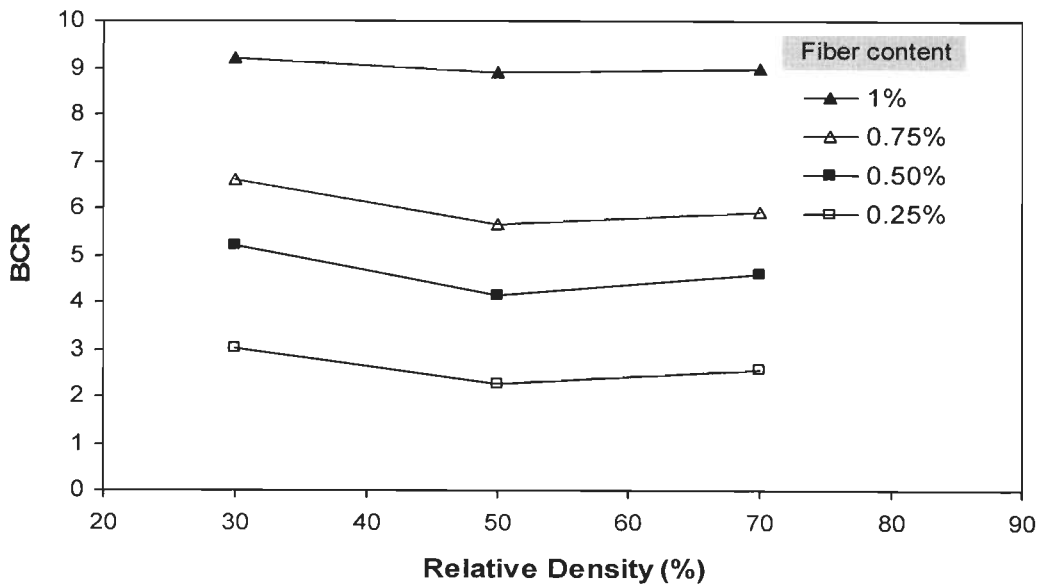


Figure 5.10 Variation of BCR with relative density for 1000D 50mm fibrillated fiber at different fiber content

variation of BCR with relative density at different fiber content. In loose condition ($D_r = 30\%$) maximum increase in BCR was observed. BCR values in dense condition ($D_r = 70\%$) are slightly less compare to loose condition ($D_r = 30\%$). BCR values in medium dense ($D_r = 50\%$) are further slightly less compare to dense condition ($D_r = 70\%$). No consistent decreasing trend was observed with increase in relative density. Figure 5.11 shows variation of BCR with fiber content at different relative densities. BCR values keeps on increasing with fiber content and BCR values are order of 9 at 1% fiber content at three relative densities. This suggests that this technique is equally applicable in loose and dense condition. Compaction of loose RDFS further enhances its performance in field. Results indicates that by increasing relative density of loose sand as well randomly reinforcing with fibers benefits will be further enhanced several times.

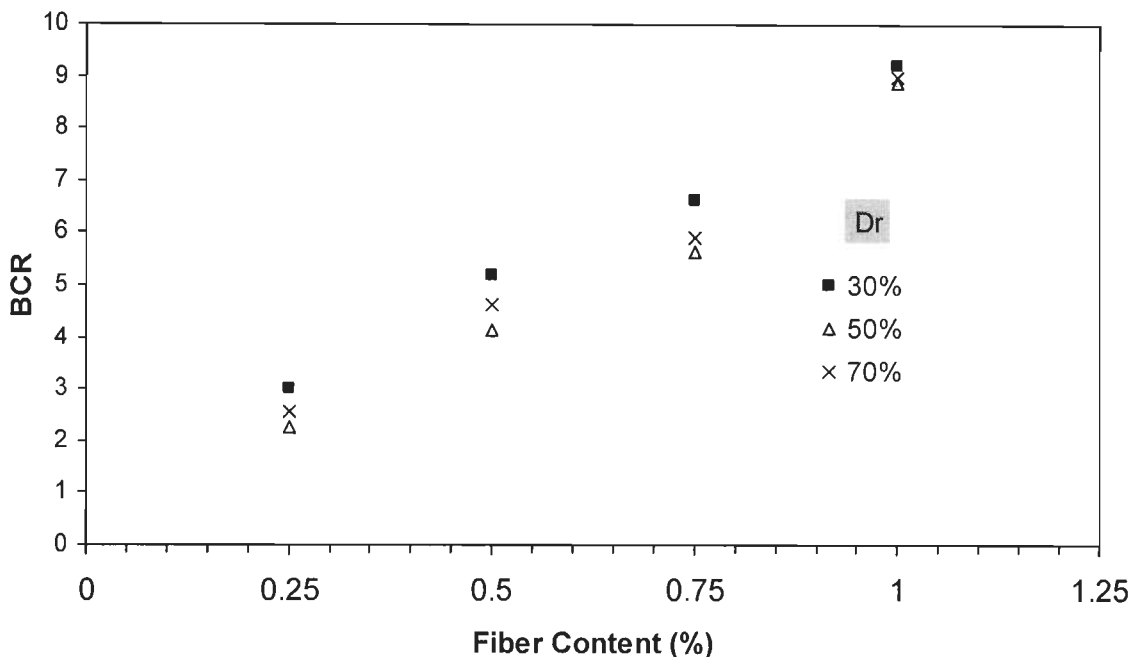


Figure 5.11 Variation of BCR with fiber content for 1000D 50mm fibrillated fiber at different relative density

5.2.4 Effect of Depth of RDFS Layer:

Figure 5.12 shows effect of depth of RDFS layer (R_d) below footing at 1% fiber content for 30% relative density. With increase in R_d bearing capacity increases and settlement decreases. Beyond $R_d = 3B$ increase in bearing capacity ($q_{10\%}$) is not significant. At, $R_d = 0.5B$, BCR is 3.4. At $R_d = 3B$, BCR becomes 6.4, while in this case the quantity of fiber at the rate of 1% fiber content becomes six times in comparison to fibers used in the case of $R_d = 0.5B$. Thus providing RDFS in deeper layer is not economical for ultimate bearing capacity improvement. Deeper layer of RDFS contribute at large strains when relative deformation take place between fibers and sand particles. Results suggest that to resist large deformations deeper layer of RDFS may be effective such as during an earthquake. Figure 5.13 shows similar trends for 1% fiber content at 70% relative density. It was interesting to note that BCR values are slightly more for 30% relative density compared to 70% relative density. Figure 5.14 shows pressure settlement curves for different depth of RDFS layer (R_d) below footing at 0.25% and 1% fiber content ($R_w = 10B$ and $D_r = 30\%$). For 0.25% fiber content in $R_d = 5B$ amount of fibers used is 2.5 times and 1.25 times compare to 1% fiber content in $R_d = 0.5B$ and $1B$ respectively. Therefore, it is more beneficial to reinforce shallow depths with high fiber content compare to low fiber content in deeper depth.

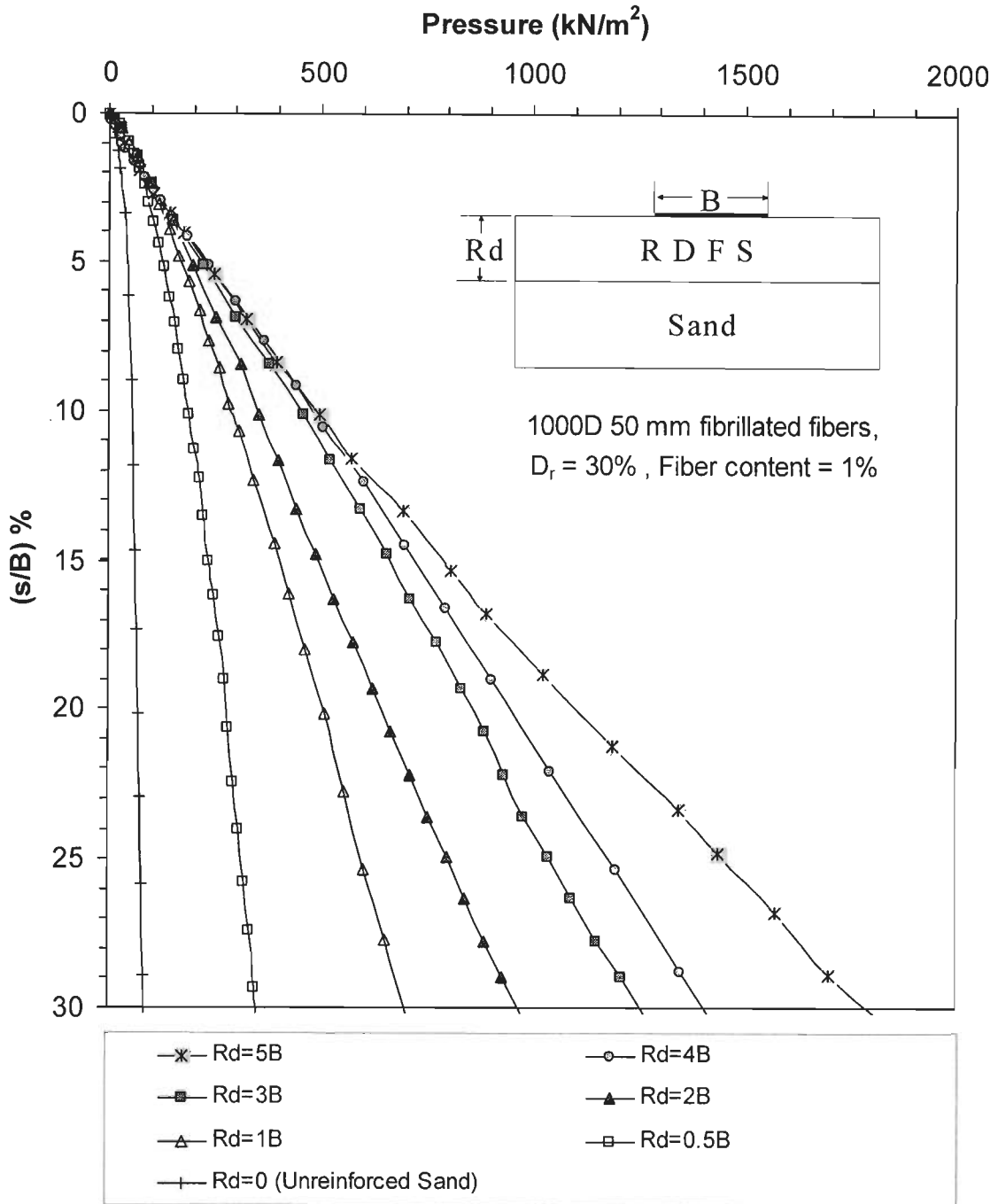


Figure 5.12 Pressure settlement curves for different depths of RDFS layer (Rd) below footing ($R_w = 10B$ and $D_r = 30\%$)

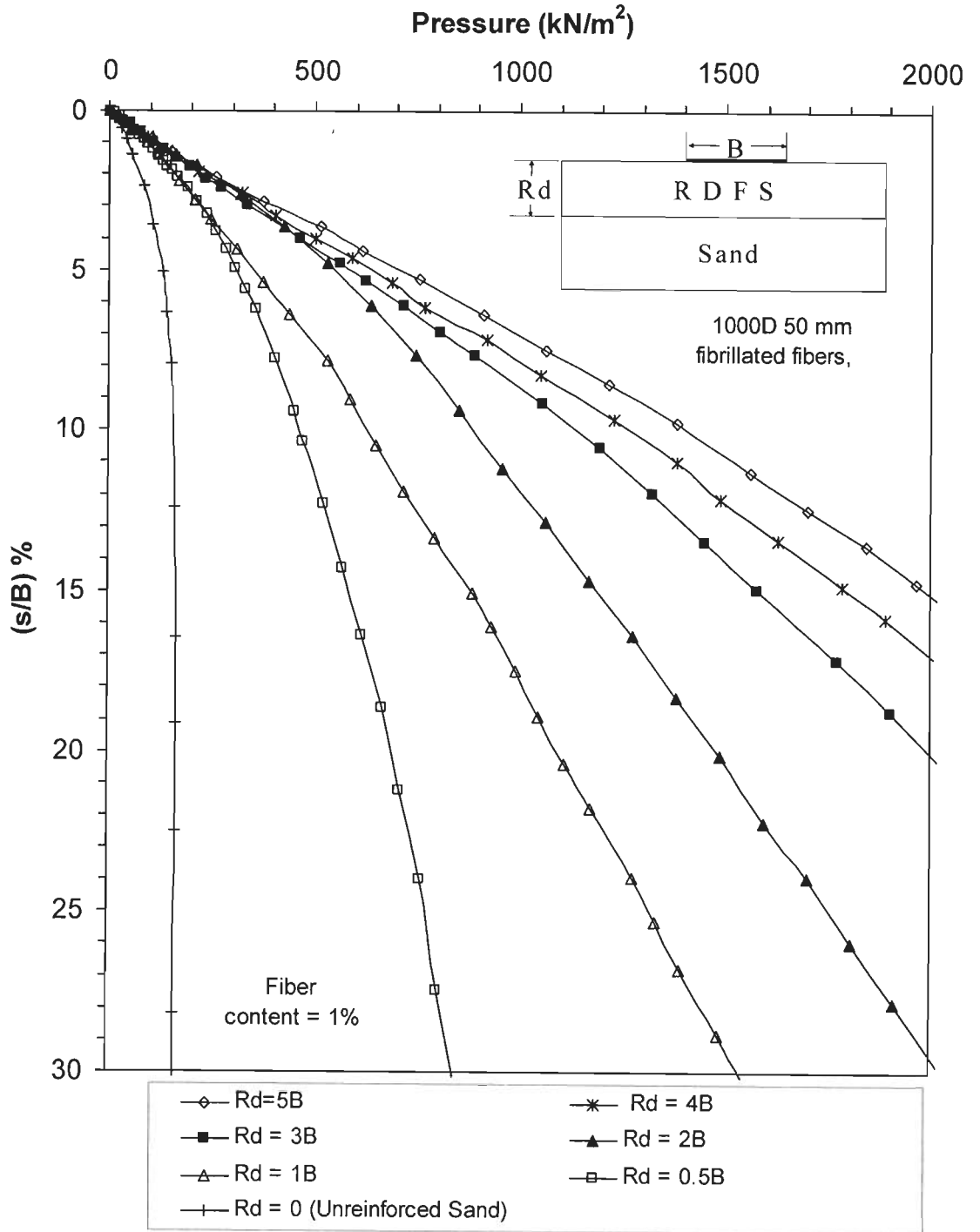


Figure 5.13 Pressure settlement curves for different depths of RDFS layer (Rd) below footing ($R_w = 10B$ and $D_r = 70\%$)

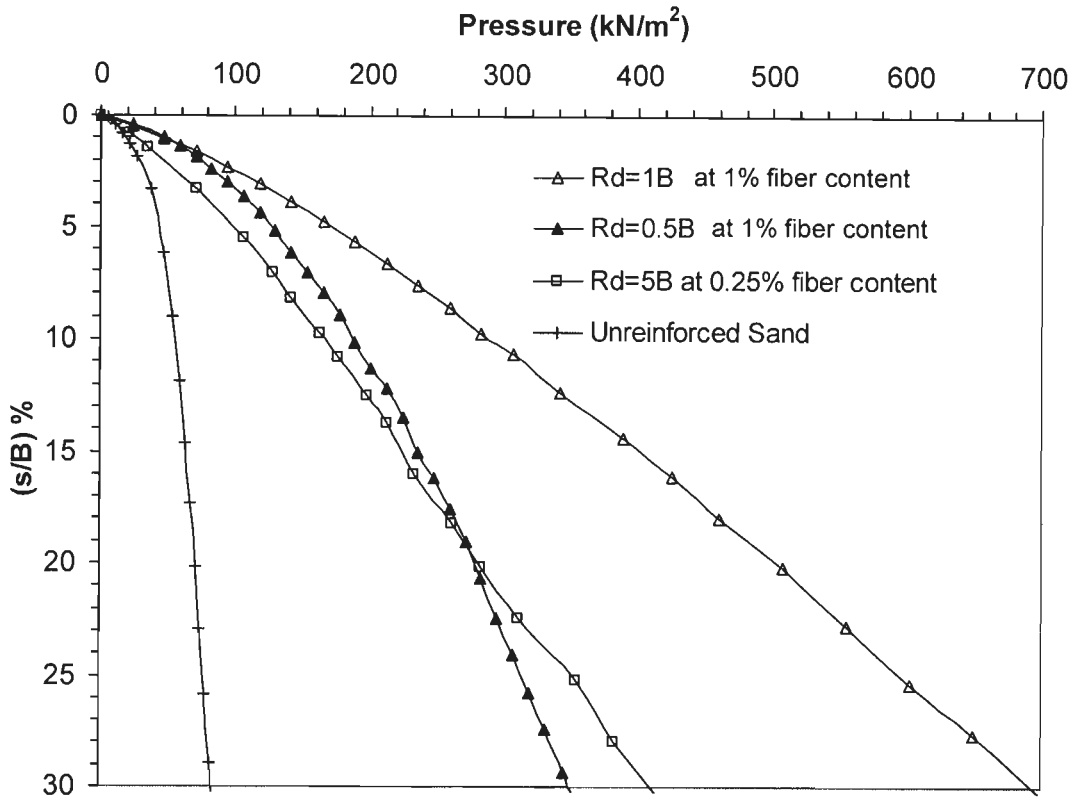


Figure 5.14 Comparison of pressure - settlement curves for different depth of RDFS layer (R_d) below footing ($R_w = 10B$ and $D_r = 30\%$)

5.2.5 Effect of Size of RDFS Zone below Footing

To find optimum zone of reinforcement below footing tests were conducted on varying width and depth of RDFS zone. Figure 5.15 shows effect of variation of width of RDFS zone (R_w) for 1% fibrillated fiber for depth of RDFS zone 1B. No significant improvement was observed beyond $R_w = 3B$ in this case. Figure 5.16 shows effect of variation of width of RDFS zone (R_w) for 1% fibrillated fiber for depth of RDFS zone 2B. No significant improvement was observed beyond $R_w = 4B$. Figure 5.17 also shows that for $R_d = 3B$, no significant improvement was observed beyond R_w equal to 6B.

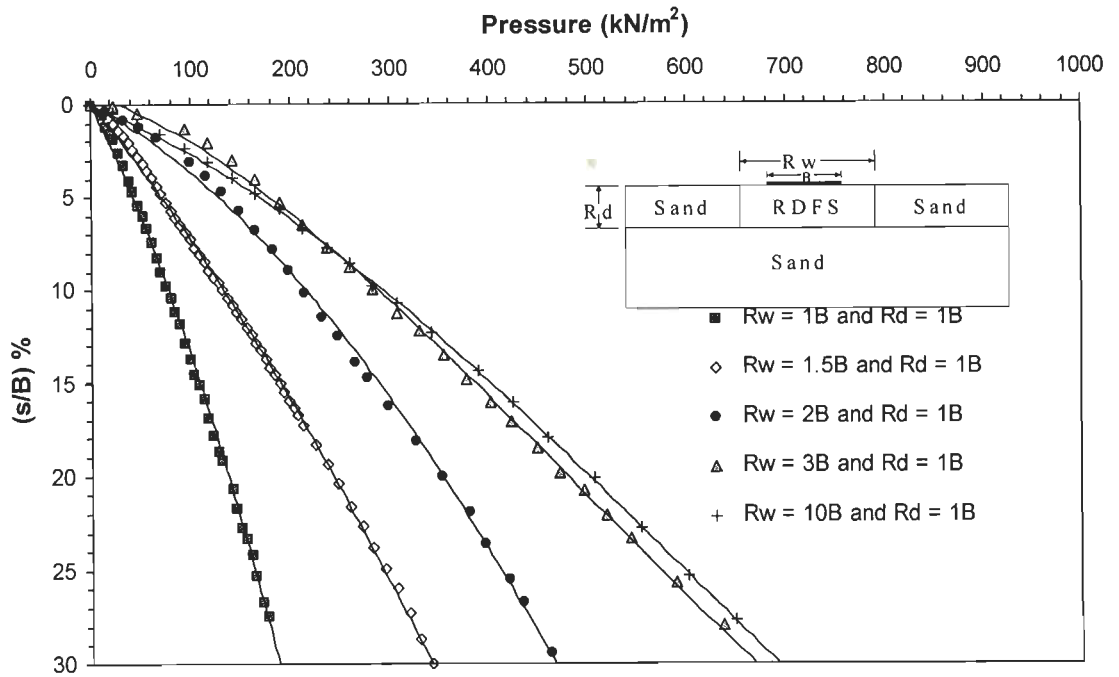


Figure 5.15 Effect of variation of width of RDFS zone (R_w) below Footing for 1% fiber content of fibrillated fiber ($R_d = 1B$ and $D_r = 30\%$)

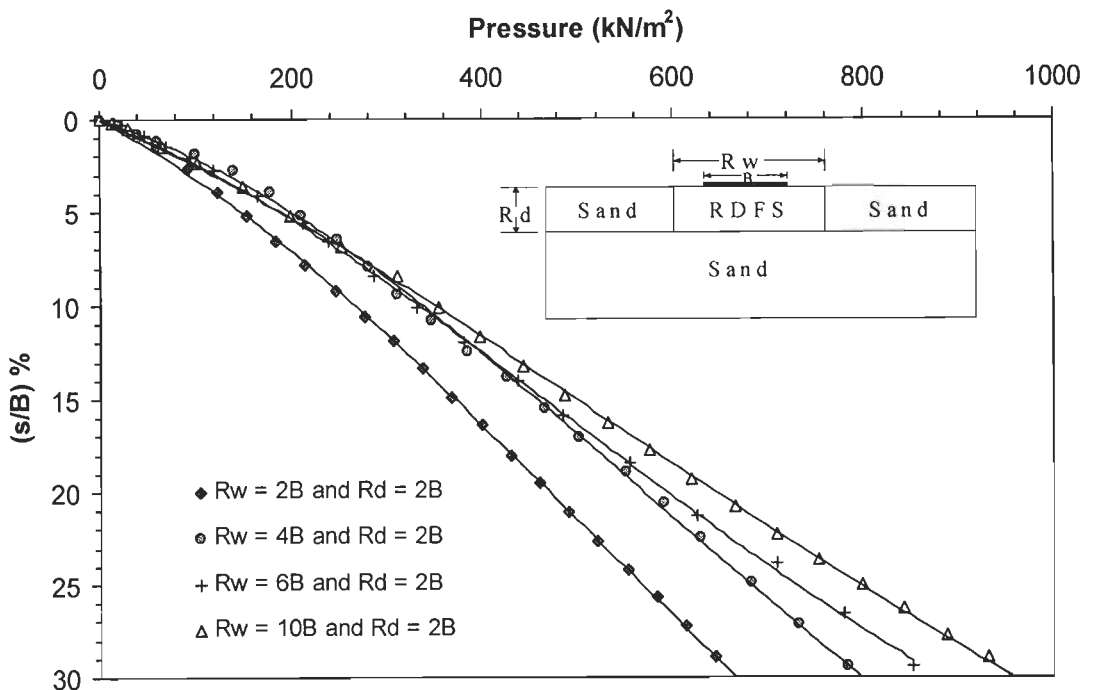


Figure 5.16 Effect of variation of width of RDFS zone (R_w) below Footing for 1% fiber content of fibrillated fiber ($R_d = 2B$ and $D_r = 30\%$)

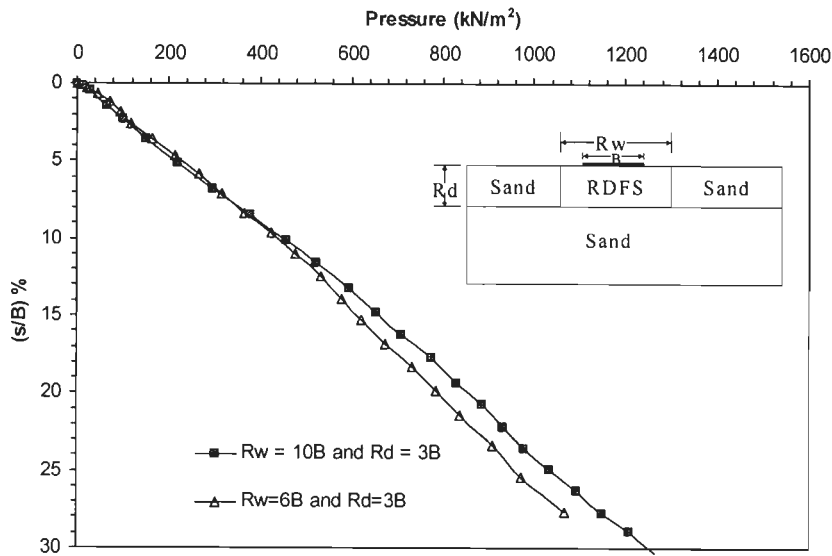


Figure 5.17 Effect of variation of width of RDFS zone (R_w) below Footing for 1% fiber content of fibrillated fiber ($R_d = 3B$ and $Dr = 30\%$)

No improvement was observed by increasing width of RDFS zone from 2B to 3B in case of $R_d = 0.5B$ for 1% fiber content at 30% relative density. Thus RDFS should be provided within optimum width only according to depth of RDFS zone. Figure 5.18 shows comparison of pressure – settlement curves for 1% fiber content in 1.5B width and 1B depth ($BCR = 2.4$) and 0.25% fiber content in 2B width and 1B depth ($BCR = 2.46$). Figure 5.19 shows comparison of pressure – settlement curves for 1% fiber content in 1B width and 1B depth ($BCR = 1.4$) and 0.25% fiber content in 2B width and 0.5B depth ($BCR = 2.1$). Figure 5.20 shows that when $R_w < 2B$ a sharp decrease in BCR was observed for $R_w = 1.5 B$ and 1B. Thus it is recommended to provide RDFS zone at least in 2B width. Providing RDFS below footing in zone of 2B deep and 3B wide found most effective beyond that range improvements will be less. It would be more beneficial to reinforce sand in shallow depths with high fiber content as compare to low fiber content for deeper depth. Providing RDFS in a depth of 0.5B and 2B wide below footing is found very effective and economical.

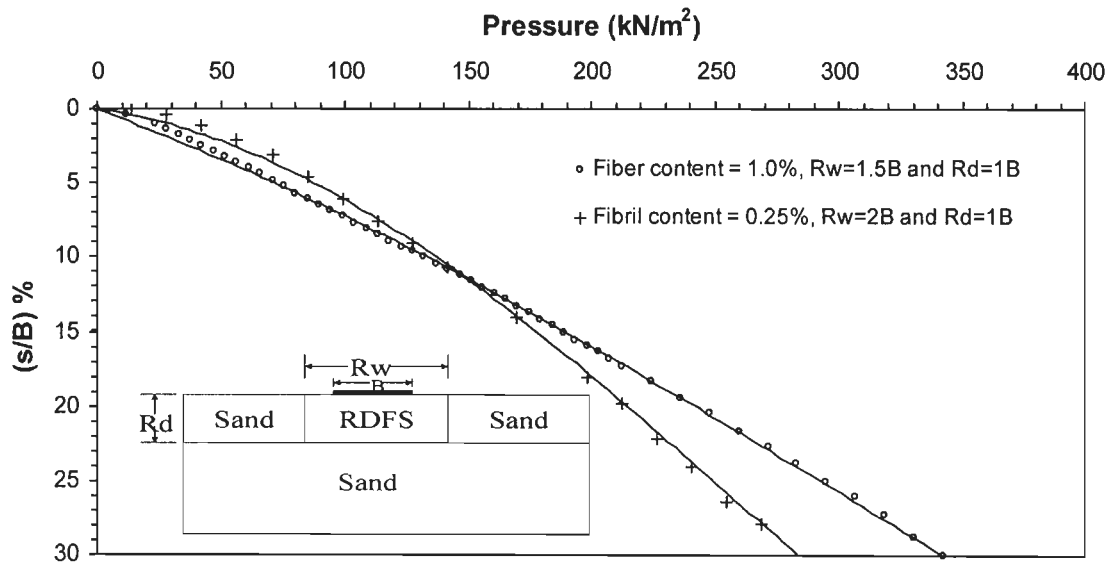


Figure 5.18 Comparison of pressure–settlement curves for 1% fiber content in 1.5B width and 1B depth and 0.25% fiber content in 2B width and 1B depth

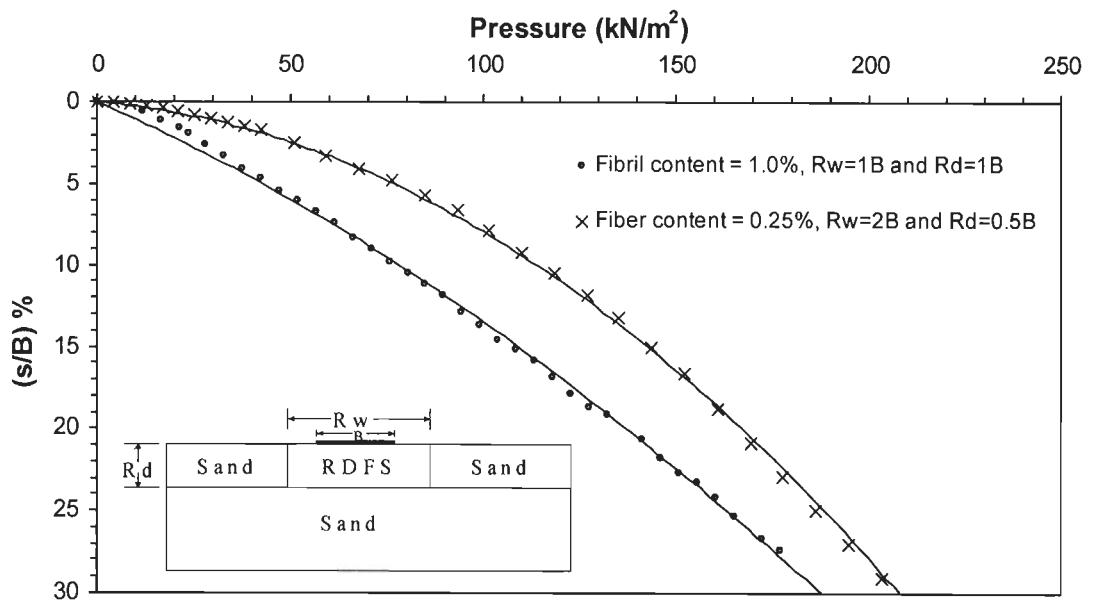


Figure 5.19 Comparison of pressure – settlement curves for 1% fiber content in 1B width and 1B depth and 0.25% fiber content in 2B width and 0.5B depth

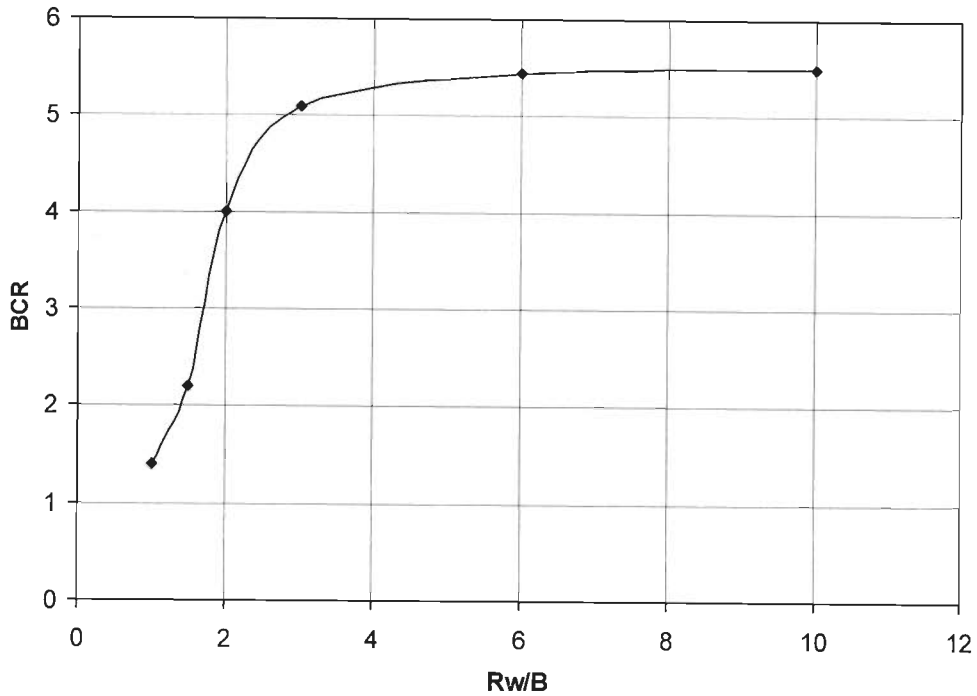


Figure 5.20 Variation of BCR with relative width (R_w/B) for 1% fiber content of 1000D 50mm fibrillated fiber ($R_d = 1B$ and $D_r = 30\%$)

5.2.6 Effect of Aspect Ratio of Fiber

Fibrillated fibers of three aspect ratio of 50 (1000D 20 mm), 80 (360D 20 mm) and 125 (1000D 50 mm) were used. Figure 5.21 shows pressure-Settlement curves for 0.25% fiber content, fibrillated fibers, $R_w = 2B$, $R_d = 1B$ at 30% relative density for different aspect ratio. Keeping all other factors constant with increase in aspect ratio pressure – settlement behaviour improves. Bearing capacity increases and settlement reduces. Similar trends were obtained at 70% relative density curves for 0.25% fiber content, fibrillated fibers, $R_w = 2B$, $R_d = 1B$ (Figure 5.22). Figure 5.23 and 24 shows, BCR versus aspect ratio curve for 0.25% fiber content, fibrillated fibers, $R_w = 2B$, $R_d = 1B$, 30% and 70% relative density respectively. BCR increases with increase in aspect ratio and slightly higher BCR were obtained for 30% relative density compared to 70% relative density.

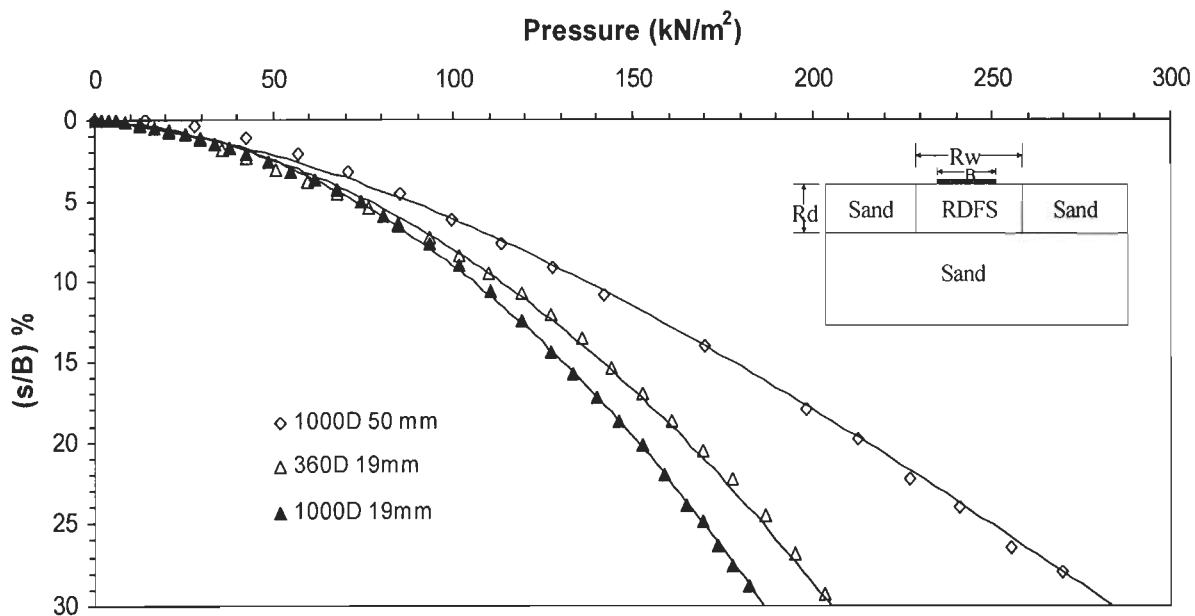


Figure 5.21 Pressure-Settlement Curve for 0.25% fiber content, fibrillated fibers, $R_w = 2B$, $R_d = 1B$ and $D_r = 30\%$

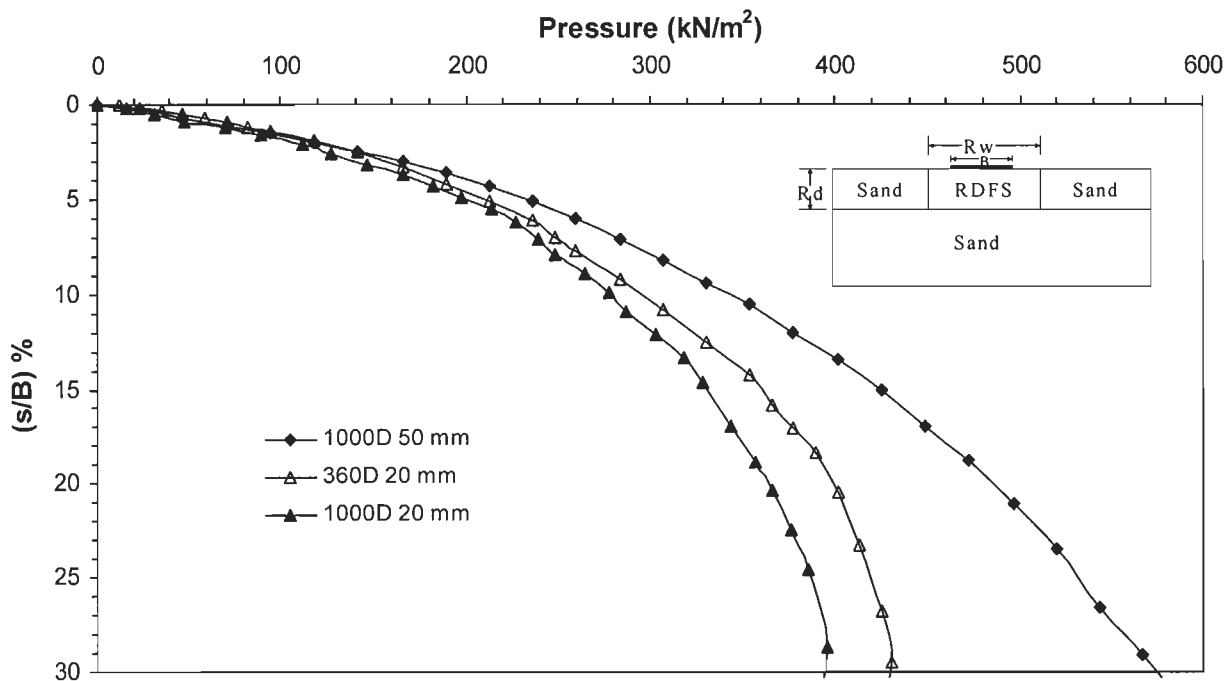


Figure 5.22 Pressure-Settlement Curve for 0.25% fiber content, fibrillated fibers, $R_w = 2B$, $R_d = 1B$ and $D_r = 70\%$

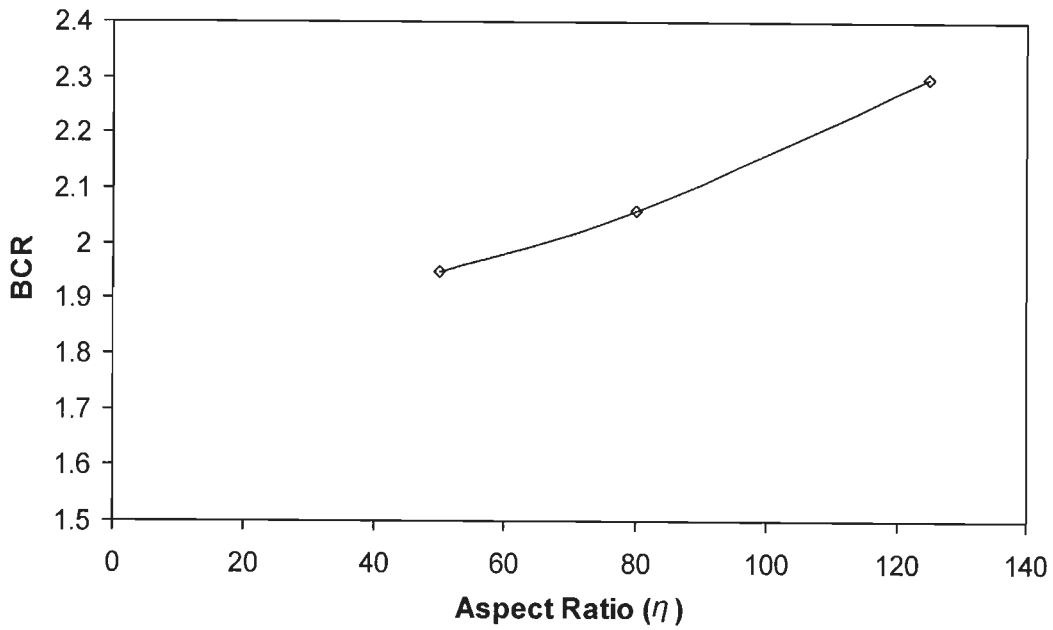


Figure 5.23 BCR versus aspect ratio curve for 0.25% fiber content, fibrillated fibers, $R_w = 2B$, $R_d = 1B$ and $Dr = 30\%$

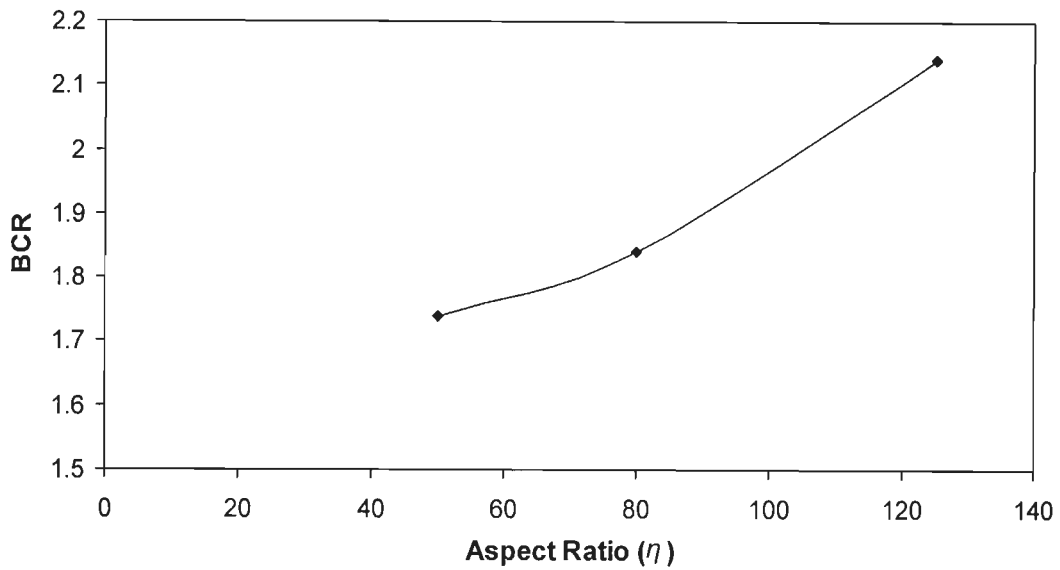


Figure 5.24 BCR versus aspect ratio curve for 0.25% fiber content, fibrillated fibers, $R_w = 2B$, $R_d = 1B$ and $Dr = 70\%$

5.2.7 Effect of Denier/ Diameter of Fiber

Fibrillated fibers of two different denier 1000D 20 mm and 360D 20 mm were used. Keeping all other factor same, with decrease in denier (or equivalent diameter) there is some improvement in pressure – settlement behaviour. BCR values increased slightly from 1.95 to 2.06 with decrease in denier from 1000 to 360 for 0.25% fiber content, $R_w = 2B$, $R_d = 1B$ at 30% relative density (Figure 5.21) and from 1.74 to 1.84 with decrease in denier from 1000 to 360 for 0.25% fiber content, $R_w = 2B$, $R_d = 1B$ at 70% relative density (Figure 5.24). With decrease in denier (diameter) for same fiber content numbers of fibers increased and provide additional resistance along fiber surface may be the reason for additional strength.

5.2.8 Effect of Submergence

Figure 5.25 shows typical plots of tests conducted under dry and submerged condition for sand reinforced with 0.5% of 1000D 50 mm fibrillated fibers ($R_d = 2B$ and $R_w = 10B$). Due to submergence bearing capacity of unreinforced sand decreased by 40%, similar decrease was observed for RDFS. This decrease was expected due to decrease in unit weight of sand due to submergence. Figure 5.26 shows comparison of BCR at different settlement ratios (s/B). Similar values of BCR are obtained in both dry and submerged condition. Thus during submerged condition beneficial effects of RDFS remain same as in case of dry conditions. Thus submergence under water has no adverse effect on improvements gained by RDFS. Similar trends were obtained for other fiber content, R_d and R_w cases.

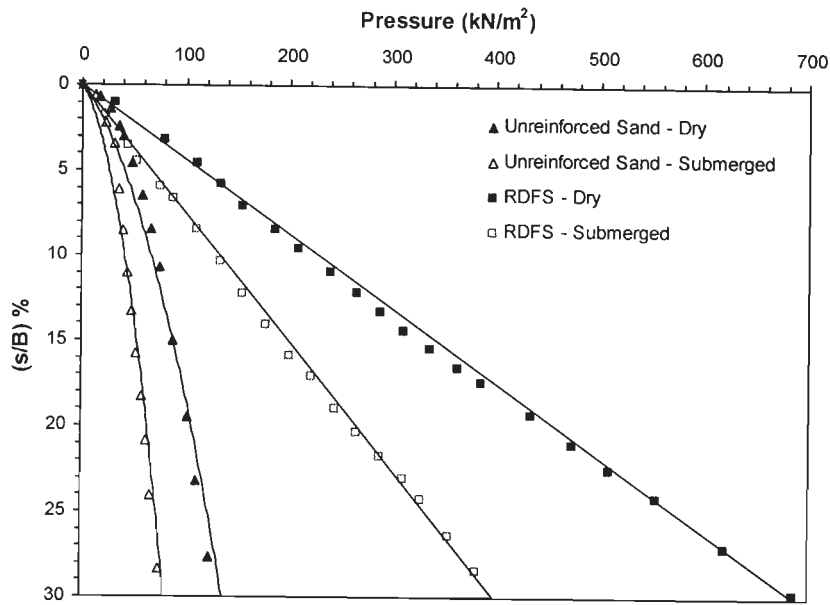


Figure 5.25 Pressure – settlement curves for dry and submerged conditions for unreinforced sand and RDFS (0.5% of 1000D 50 mm fibrillated fibers, $R_d = 2B$ and $R_w = 10B$)

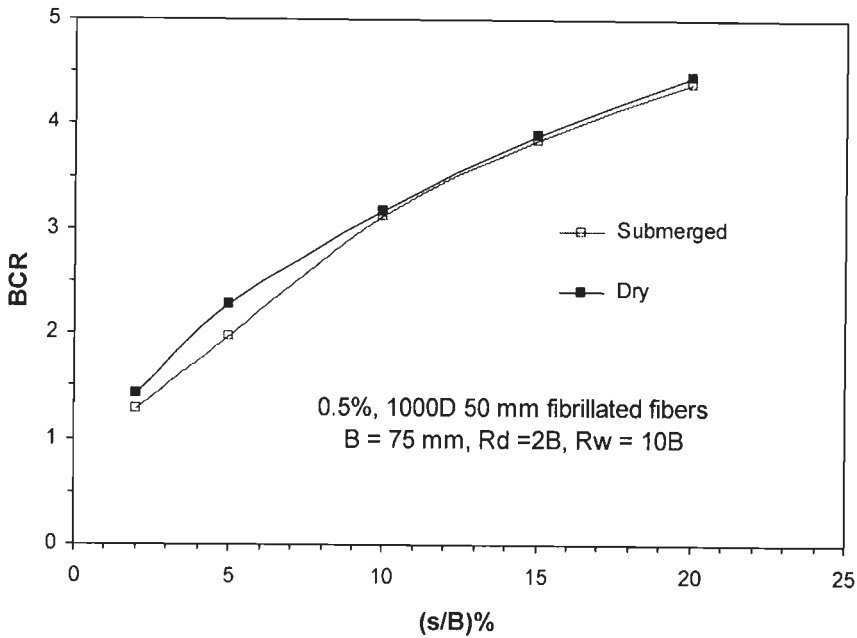


Figure 5.26 BCR versus (s/B) % for dry and submerged conditions for RDFS (0.5% of 1000D 50 mm fibrillated fibers, $R_d = 2B$ and $R_w = 10B$)

5.3 COMPARISON OF RDFS WITH PLANAR REINFORCEMENT

Tests were conducted on sand reinforced with Netlon CE 121 geogrid single layer reinforcement of different width ($R_w = 8B, 5B$ and $3B$) and depth below footing ($u = 0.2B, 0.33B$ and $0.5B$). Most optimum conditions were obtained for $R_w = 3B$ and $u = 0.33B$. Figure 5.27 shows pressure – settlement curves for sand reinforced with different geogrid layers of Netlon CE 121. Spacing between planar reinforcement (S_v) was $0.33B$.

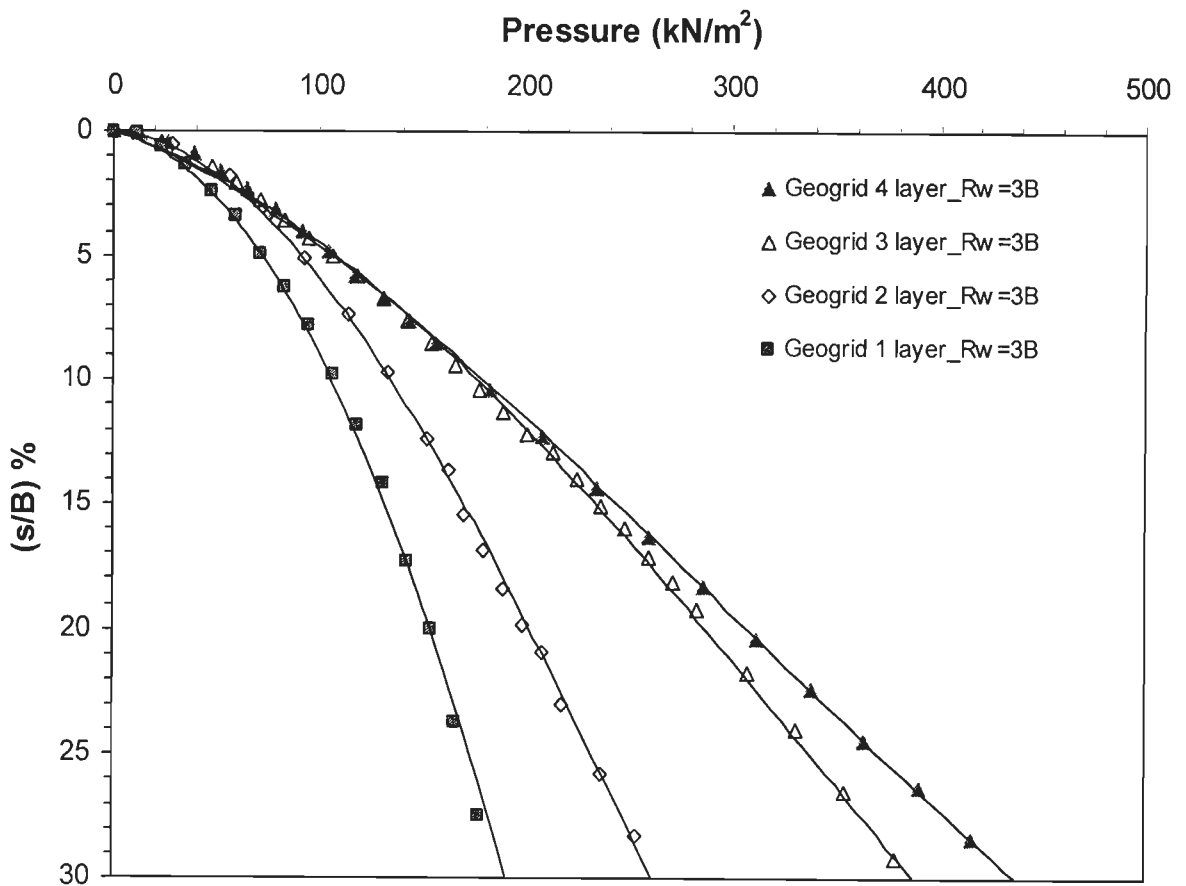


Figure 5.27 Pressure-Settlement curve for sand reinforced with Netlon CE 121, Geogrid layer at $u = S_v = 0.33B$ for $D_r = 30\%$

No significant improvements were noticed beyond 3 layer of planar reinforcement. A comparison of pressure –settlement curves of sand reinforced with three geogrid layer ($R_w = 3B$ and $u = S_v = 0.33B$) and RDFS (0.5% 1000D 50 mm fibrillated fibers in $R_w = 2B$ and $R_d = 1B$) is shown in Figure 5.28. Pressure – settlement curve for RDFS (BCR=3.4) shows somewhat better improvement compare to geogrid layers (BCR=3.2).

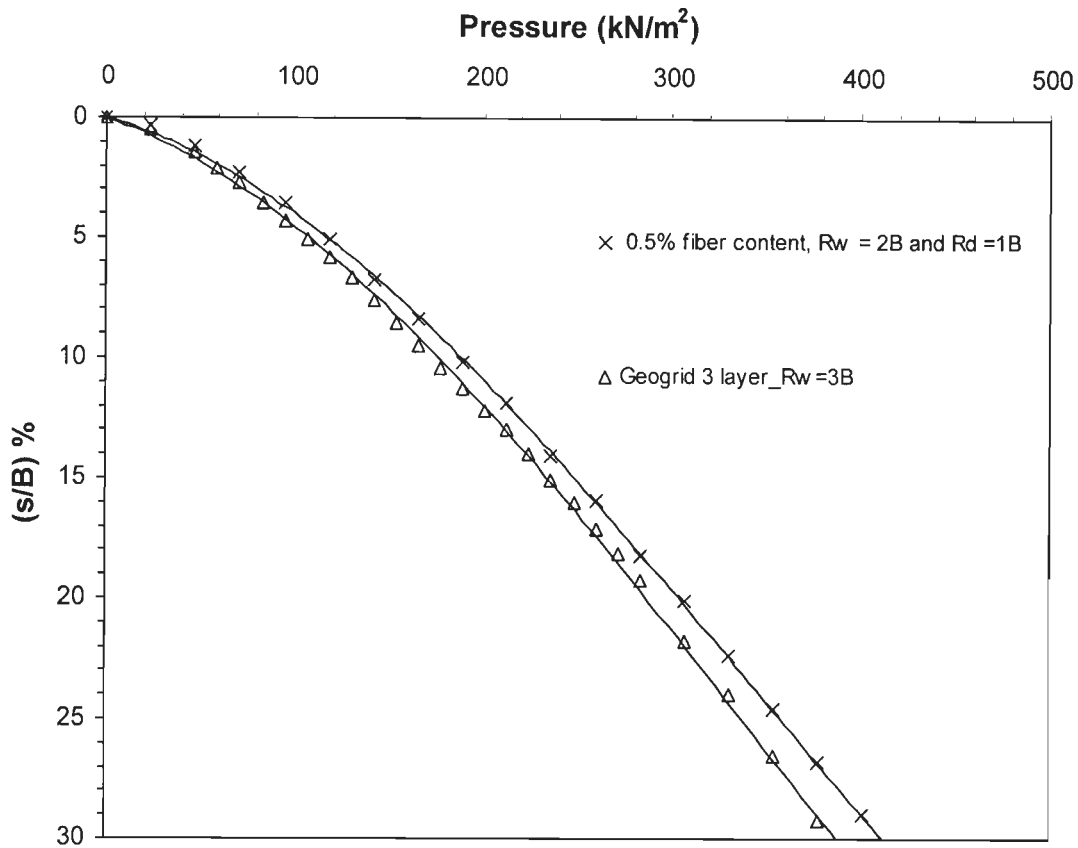


Figure 5.28 Comparison of pressure - settlement curves for sand reinforced with Netlon CE 121, three Geogrid layer at $u = S_v = 0.33B$ and 0.5% 1000D 50 mm fibrillated fibers in $R_w = 2B$ and $R_d = 1B$ ($D_r = 30\%$)

Cost Comparison

Area of 1 geogrid layer = $0.075 \text{ m} \times 0.0225 \text{ m} = 0.0169 \text{ m}^2$

Cost of 1 geogrid layer = $\text{Rs. } 100 \times 0.0169 = \text{Rs. } 1.69$

Cost of 2 geogrid layer = $\text{Rs. } 100 \times 2 \times 0.0169 = \text{Rs. } 3.38$

Cost of 3 geogrid layer = $\text{Rs. } 100 \times 3 \times 0.0169 = \text{Rs. } 5.06$

Weight of 0.5% fibers used in 2B width and 1B depth = 6.6 grams = 0.0066 kg

Cost of fibers = $\text{Rs. } 120 \times 0.0066 = \text{Rs. } 0.80$

Weight of 0.25% fibers used in 2B width and 0.5B depth = 0.00165 kg

Cost of fibers = $\text{Rs. } 120 \times 0.00165 = \text{Rs. } 0.20$

For same improvements cost of RDFS is much less compare to three layer of planar reinforcement. Even cost of single layer planar reinforcement (BCR=2) is also double compare to fiber (BCR=3.4). However, improvements are much higher for RDFS compare to single layer and double layer planar reinforcements (Figure 5.29).

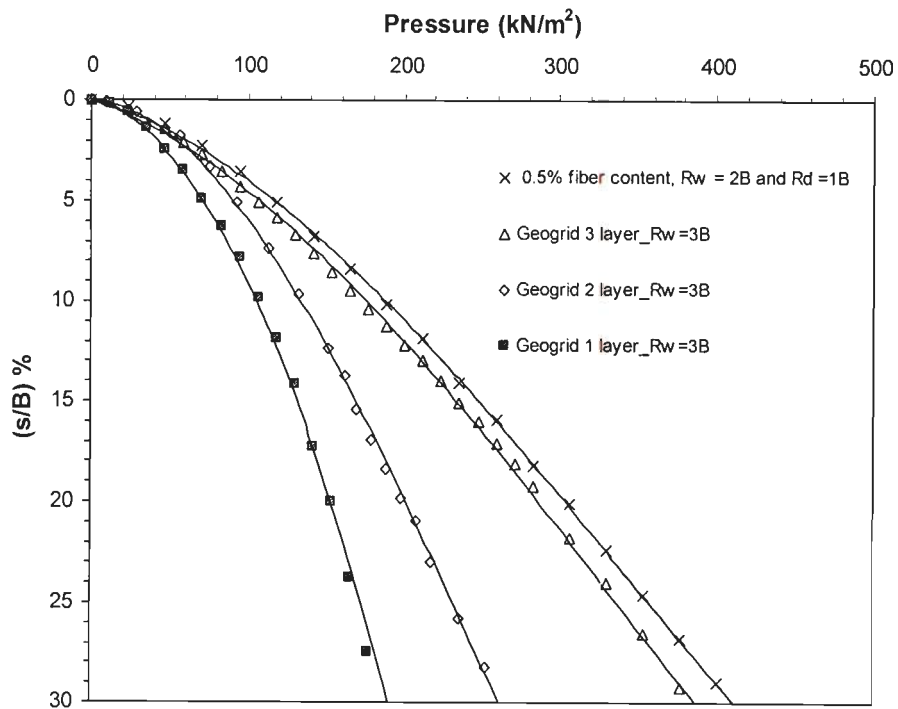


Figure 5.29 Comparison of pressure - settlement curves for sand reinforced with Netlon CE 121, Geogrid layer(s) at $u = Sv = 0.33B$ and 0.5% 1000D 50 mm fibrillated fibers in $R_w = 2B$ and $R_d = 1B$ ($D_r = 30\%$)

Figure 5.30 shows comparison of pressure - settlement curves for sand reinforced with Netlon CE 121, one Geogrid layer at $u = 0.33B$ and RDFS of 0.25% 1000D 50 mm fibrillated fibers in $R_w = 2B$ and $R_d = 0.5B$. For similar improvements ($BCR=2$) cost of RDFS is much less compare to one layer of planar reinforcement. Cost of single layer planar reinforcement is eight times compared to fiber.

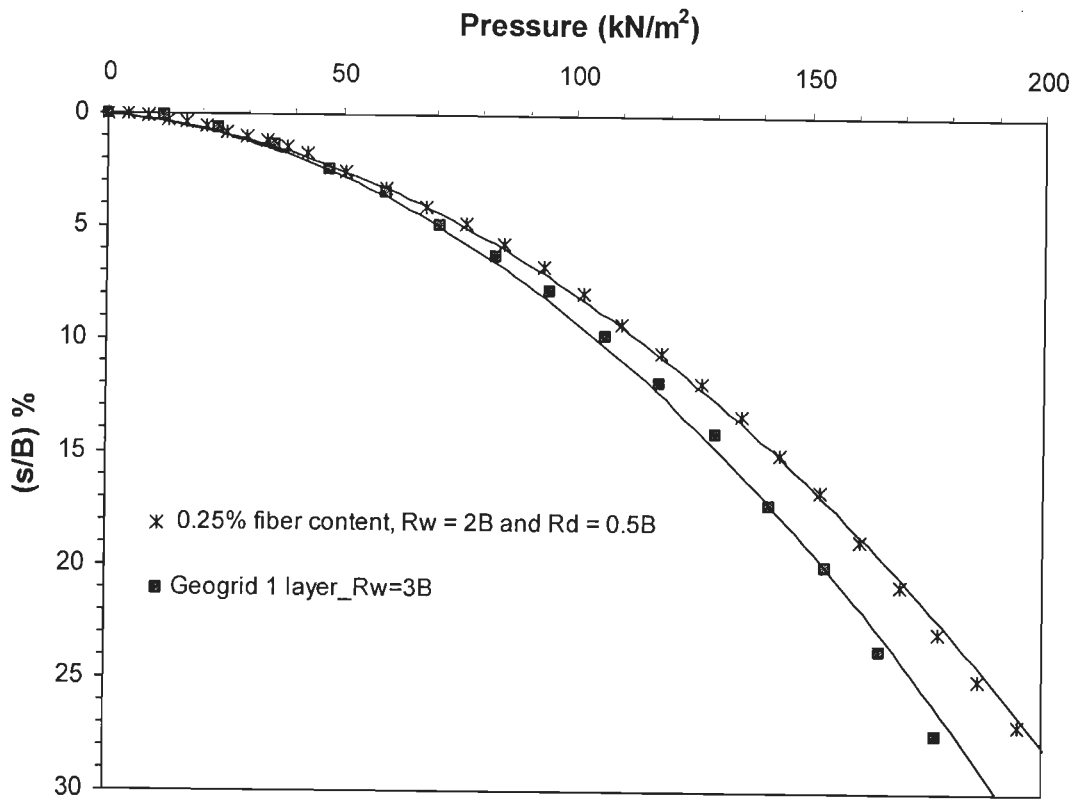


Figure 5.30 Comparison of pressure - settlement curves for sand reinforced with Netlon CE 121, one Geogrid layer at $u = 0.33B$ and 0.25% 1000D 50 mm fibrillated fibers in $R_w = 2B$ and $R_d = 1B$ ($D_r = 30\%$)

Based on results of model footing tests, Shamsher, (1992), reported that a single layer of planar geogrid (Netlon CE 121) reinforcement is more economical compare to sand randomly reinforcement by mesh elements of same geogrid. Adi (1996) also reported that 0.2% by weight of horizontal layers of mesh sheets have given much higher improvements compare to 0.3% of randomly reinforced mesh elements. Dash et al. (2004) also reported that the system is to be designed for settlements between 5% and 10% of the footing width, planar reinforcement may be ideal, based on cost economy. For settlements in excess of 10% of footing width, the geocell reinforcement is the clear choice. Shamsher, (1992), Adi (1996) and Dash et al. (2004) provided random reinforcement throughout the width of tank and used mesh elements of same geogrid which is the main reason for higher cost of random reinforcement compare to planar reinforcement. Therefore, important finding of this study is that if RDFS is provided in optimized zone than it may prove to be economical compare to planar reinforcement.

5.4 BEHAVIOUR OF STRIP FOOTING ON RDFS: ECCENTRIC – INCLINED LOAD

In this section results of model strip footing (75 mm x 75 mm) tests in two dimensional tank (plane strain condition) resting on unreinforced sand and RDFS under eccentric-inclined load have presented. Tests were conducted at eccentricity ratio $e/B = 0.0, 0.1, 0.2$, load inclinations $i = 0^\circ, 10^\circ, 20^\circ$ and relative density of 30%, 50% and 70%. Fibrillated fibers of 1000 deniers 50 mm long have been used in all tests on RDFS. Some tests were conducted on 1000 deniers 20 mm and 360 deniers 20 mm fibrillated fibers also. The pressure-settlement, pressure-horizontal displacement and the pressure-tilt curves have been obtained for each model test.

5.4.1 Behaviour of Strip Footing on Unreinforced Sand Subjected to Eccentric – Inclined Load

Figure 5.31 to 5.33 shows pressure- settlement, pressure – tilt and pressure – horizontal displacement curves for footings resting on unreinforced sand at different load eccentricities and inclinations. Pressure-settlement behaviour of footings resting on unreinforced sand under eccentric-inclined load was very poor; failure took place at very small deformations and for any further increase in deformation, sharp decrease in bearing pressure was observed.

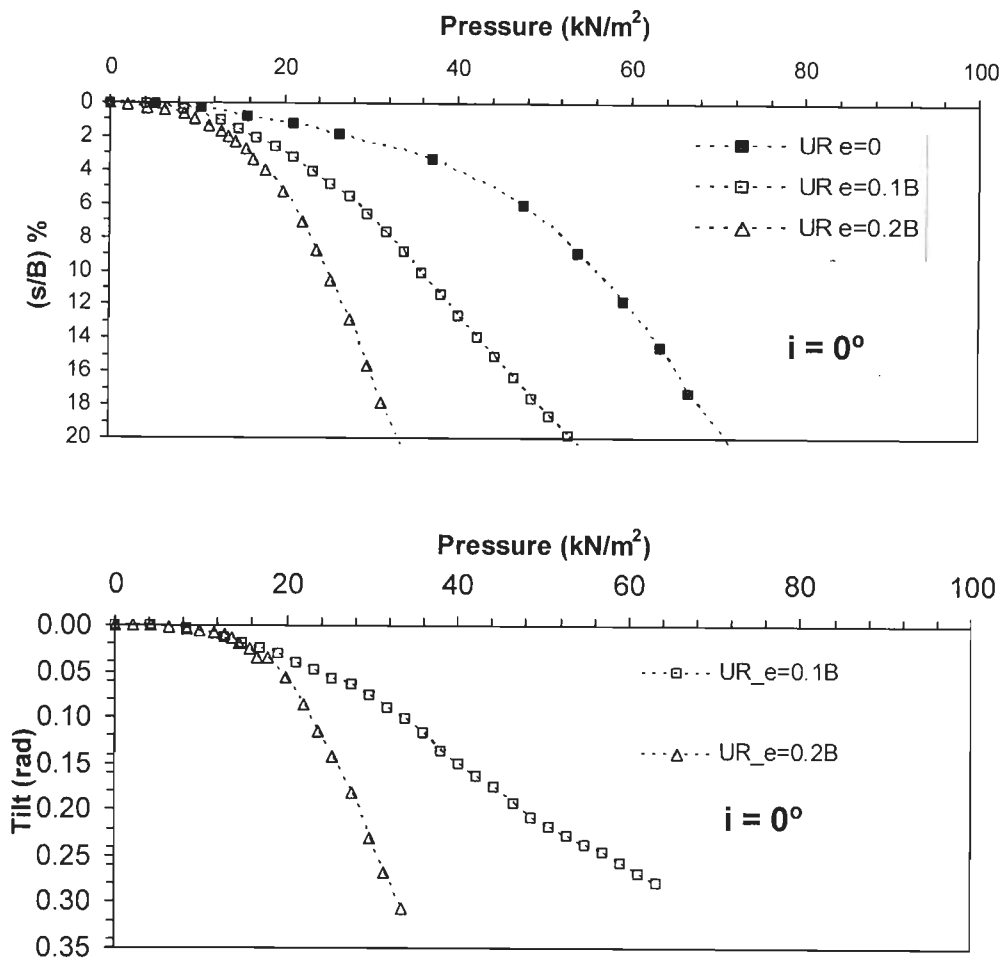


Figure 5.31 Pressure- settlement and tilt, curves for unreinforced sand (UR) for different load eccentricity at $i=0^\circ$ ($D_r=30\%$)

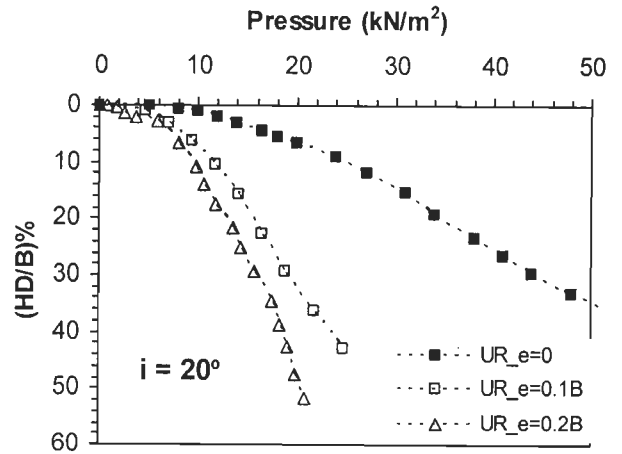
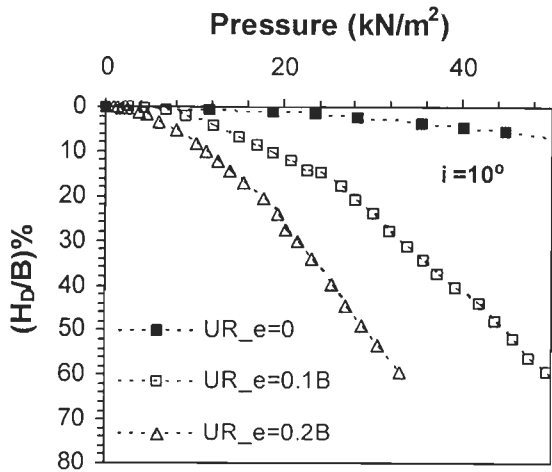
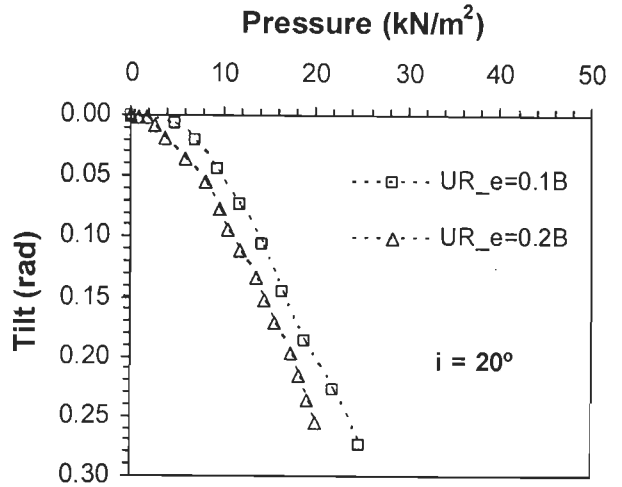
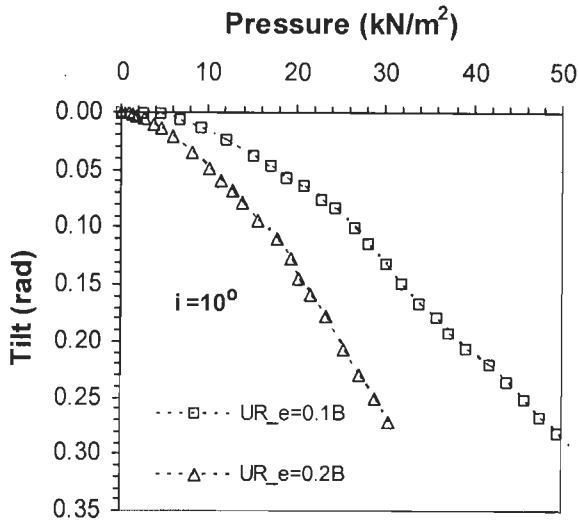
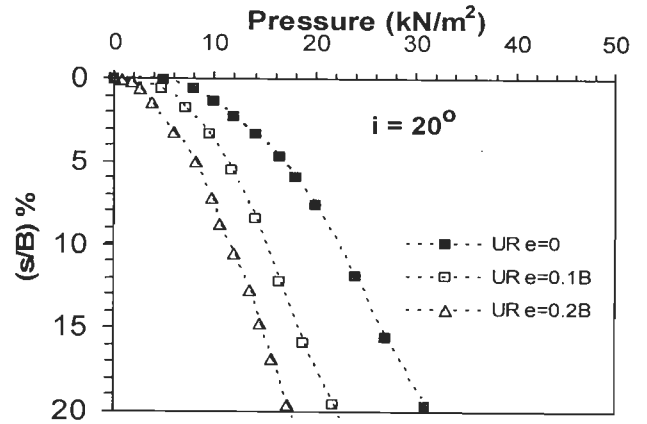
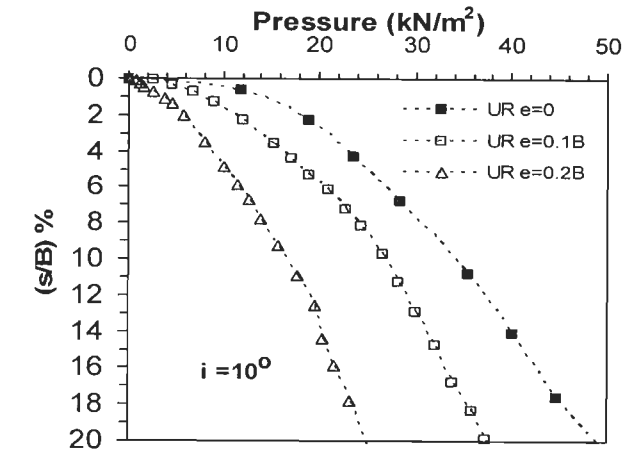


Figure 5.32 Pressure v/s settlement, tilt, H_D/B curves for unreinforced sand (UR) for different load eccentricity at $i=10^\circ$ ($D_r=30\%$)

Figure 5.33 Pressure v/s settlement, tilt, H_D/B curves for unreinforced sand (UR) for different load eccentricity at $i=20^\circ$ ($D_r=30\%$)

5.4.2 Behaviour of Strip Footing on RDFS Subjected to Eccentric – Inclined Load

Figure 5.34 to 5.36 shows pressure- settlement curves for footings resting on RDFS at 1% fiber content different load eccentricities and inclinations. In case of footings resting on RDFS, pressure–settlement behaviour improved substantially. There was no sudden decrease in bearing pressure with increase in settlement. With increase in settlement bearing pressure keeps on increasing and strain hardening behaviour was observed. This behaviour is particularly useful for resisting large deformations during earthquake. In pseudo static analysis of footing located in seismic regions earthquake forces are converted to equivalent horizontal forces and moment. During earthquake major reduction in bearing capacity and deformations comes from load inclination and eccentricity of the equivalent resultant load on the foundation. Thus RDFS is particularly more beneficial in seismic region.

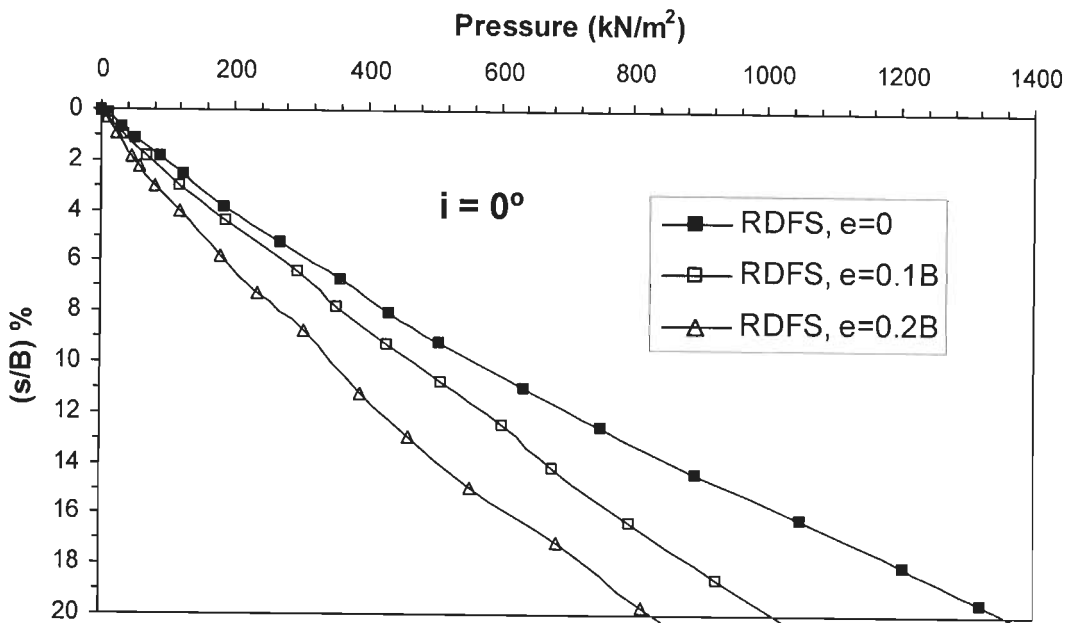


Figure 5.34 Pressure settlement curves for RDFS (1% fiber content) for different load eccentricity at $i=0^\circ$ ($R_w=10B$, $R_d=5B$ and $D_r=30\%$)

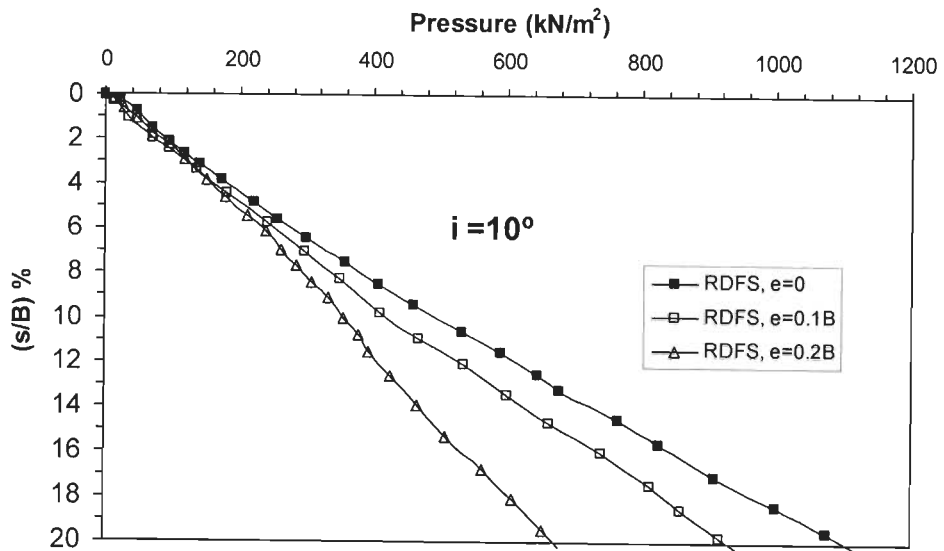


Figure 5.35 Pressure settlement curves for RDFS (1% fiber content) for different load eccentricity at $i=10^\circ$ ($R_w=10B$, $R_d=5B$ and $D_r=30\%$)

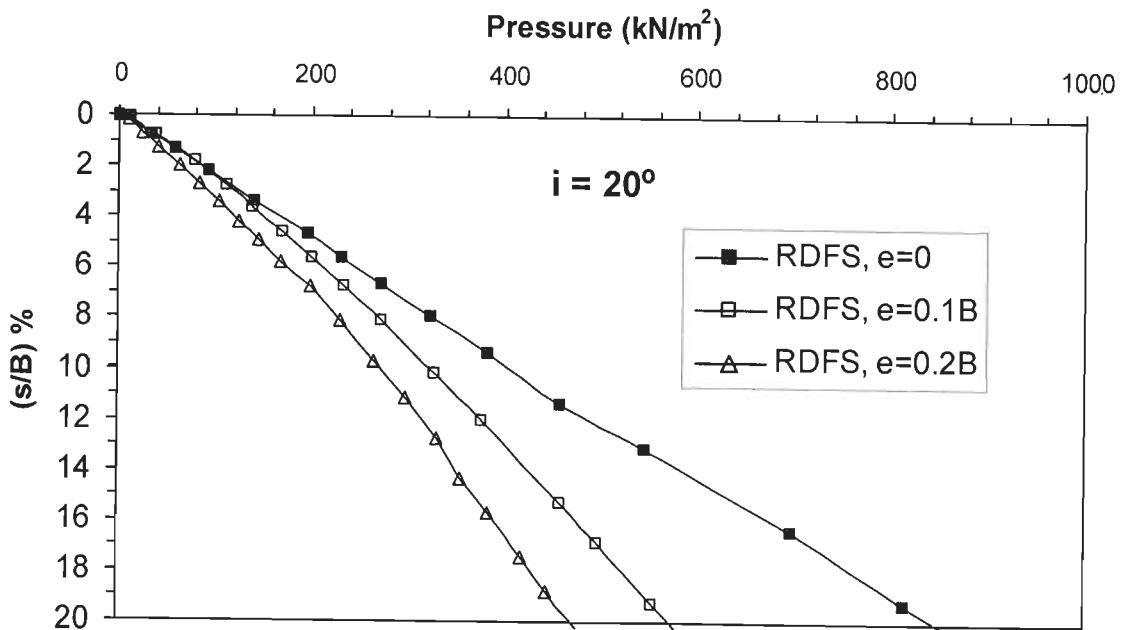


Figure 5.36 Pressure settlement curves for RDFS (1% fiber content) for different load eccentricity at $i=20^\circ$ ($R_w=10B$, $R_d=5B$ and $D_r=30\%$)

5.4.3 Effect of Eccentricity and Load Inclination

From figures 5.34 to 36 it is evident that in case of footing resting on RDFS subjected eccentric-inclined load also no failure is observed. Therefore, ultimate load is taken corresponding to 10% settlement ratio. Figure 5.37 and 5.38 shows variation of BCR with load eccentricities for $R_w=10B$, $R_d=5B$ and $D_r=30\%$, at 0.5% and 1% fiber content respectively. BCR keeps on increasing as load eccentricity increases. Figure 5.39 and 5.40 shows variation of BCR with load inclinations for $R_w=10B$, $R_d=5B$ and $D_r=30\%$, at 0.5% and 1% fiber content respectively. BCR keeps on increasing as load inclinations increases. At $e=0.2B$ and $i=20^\circ$ for 1% fiber content BCR increased to around 25. For central vertical load under same conditions BCR increased to around 10. It suggests that for eccentric-inclined loads beneficial effects of RDFS increased further in comparison to central-vertical loads.

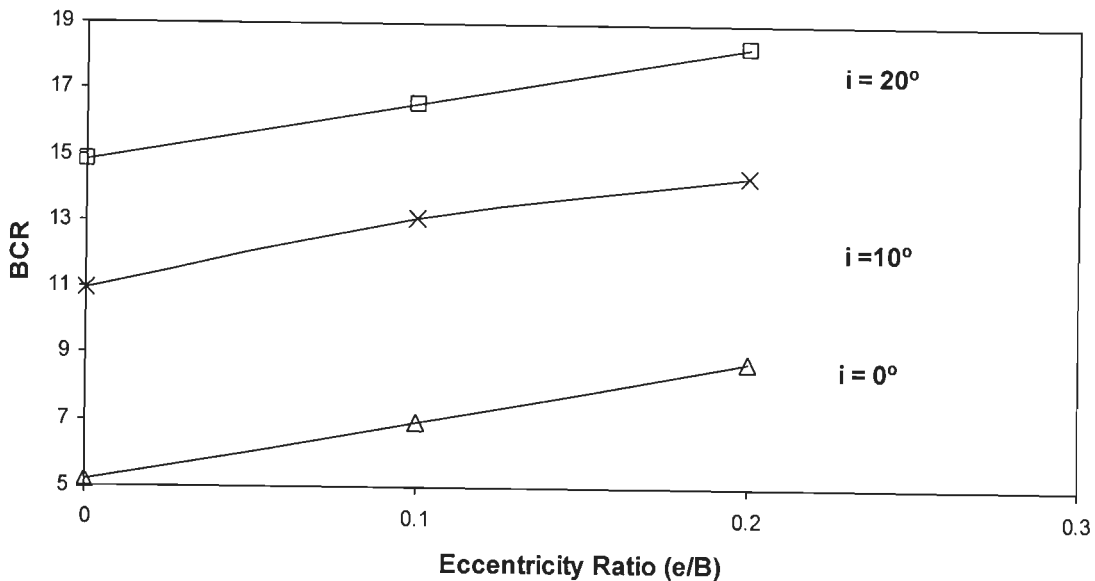


Figure 5.37 BCR for different load eccentricity ($\chi_w = 0.5\%$, $R_w=10B$, $R_d=5B$ and $D_r=30\%$)

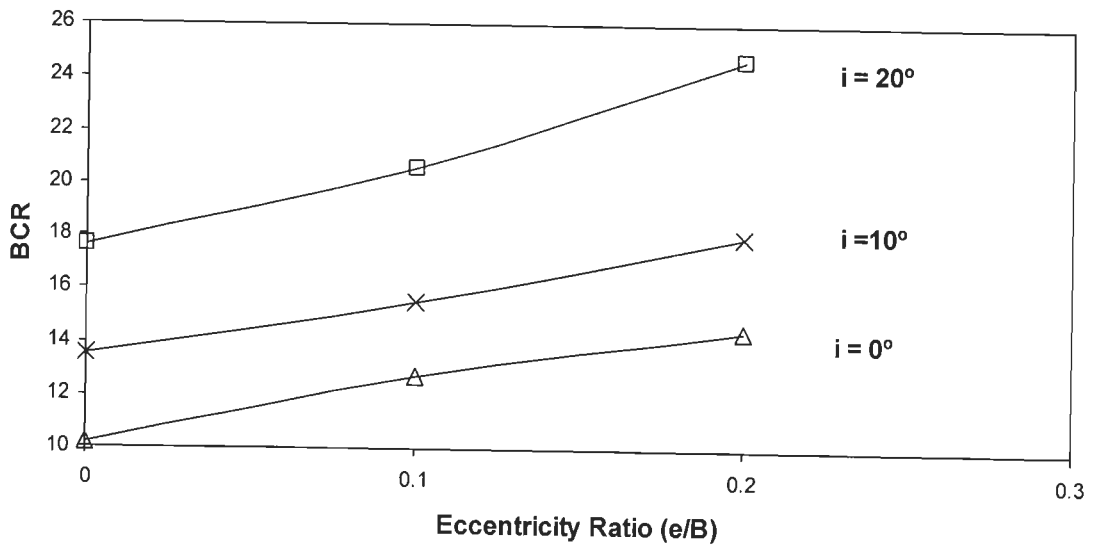


Figure 5.38 BCR for different load eccentricity ($\chi_w = 1\%$, $R_w=10B$, $R_d=5B$ and $D_r=30\%$)

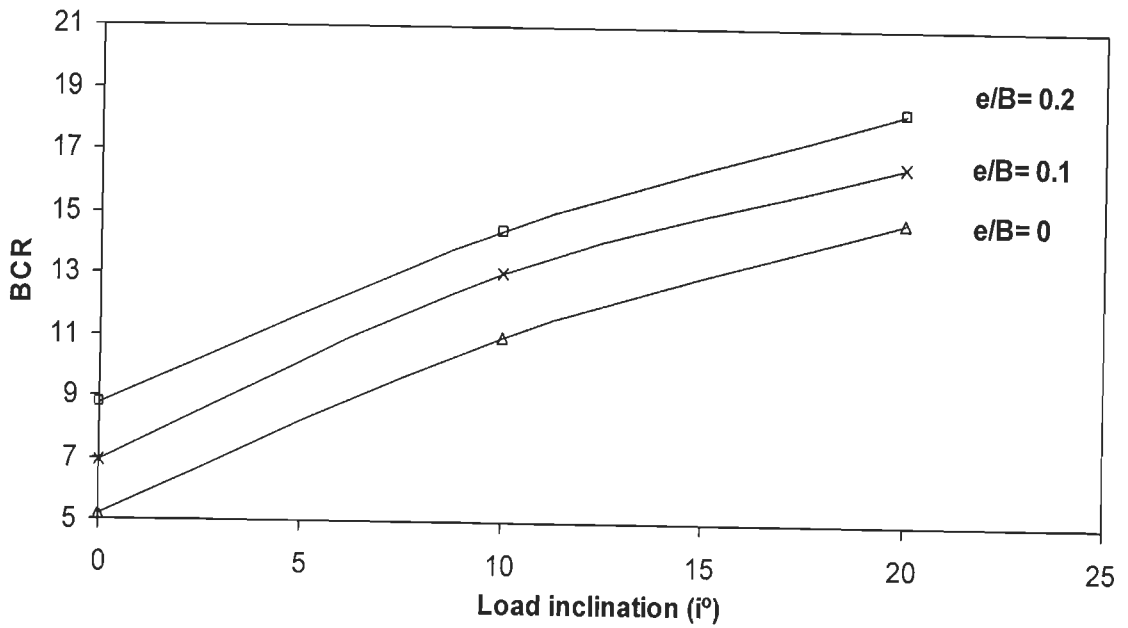


Figure 5.39 BCR for different load inclinations ($\chi_w = 0.5\%$, $R_w=10B$, $R_d=5B$ and $D_r=30\%$)

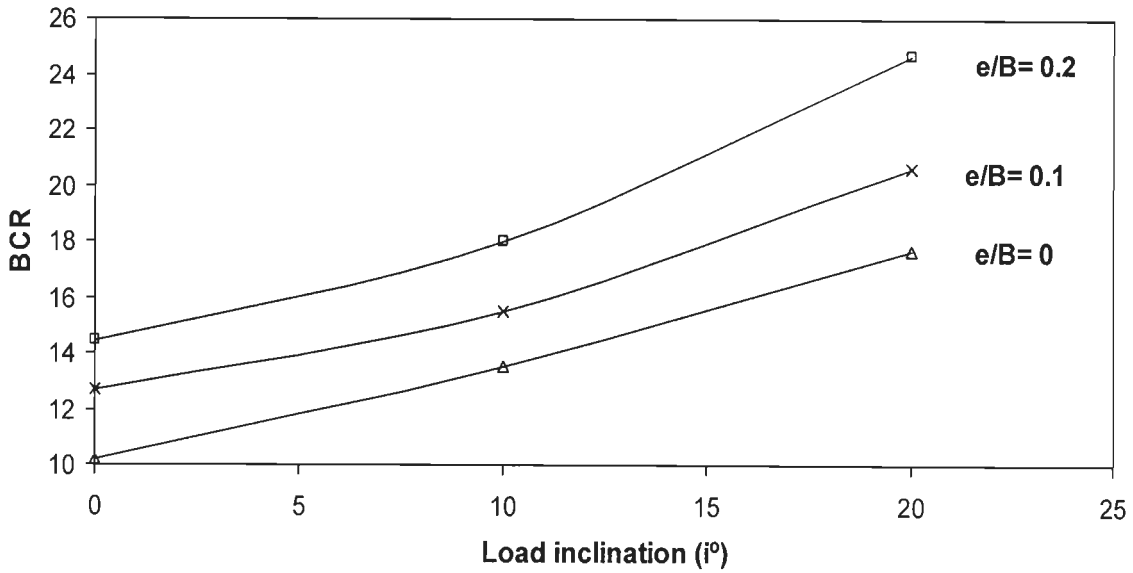


Figure 5.40 BCR for different load inclinations ($\chi_w = 1\%$, $R_w=10B$, $R_d=5B$ and $D_r=30\%$)

5.4.4 Effect of Depth of RDFS Layer

The depth of the fiber-reinforced layer had been varied from $0.5B$ to $5B$. Figure 5.41 shows typical plots for pressure- settlement curves for different depth of RDFS zone for 1.0% 1000D 50mm fibrillated fiber at $e=0.2B$ and $i=20^\circ$ for 30% relative density. Pressure settlement curve for $R_d=3B$ and $R_d=5B$ are almost same upto 10% settlement ratio. In case of $R_d=2B$ amount of fibers used is twice compare to $R_d=1B$, however BCR increase is not significant. Thus reinforcing deeper than $1B$ will not be economical in case of eccentric inclined load. As eccentricity and load inclinations increases depth rupture surface decreases. Thus as eccentricity and load inclinations increases much shallow depths are required compare to central-vertical load. Figure 5.42 and 5.43 shows pressure- tilt and pressure-horizontal displacement curves respectively. Tilt and horizontal displacement decreased substantially. Here also similar trends were obtained.

Most of the beneficial decrease in tilt and horizontal displacements are observed with in 1B depth.

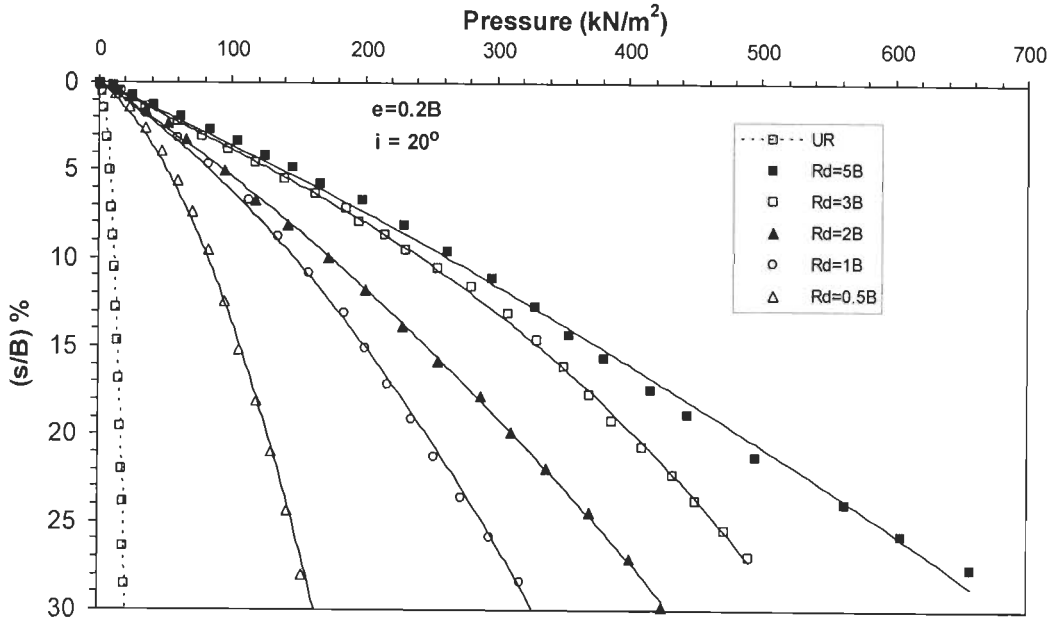


Figure 5.41 Pressure- settlement curves for different relative depth (1.0% 1000D 50mm fibrillated fiber, $e=0.2B$, $i=20^\circ$ and $Dr = 30\%$)

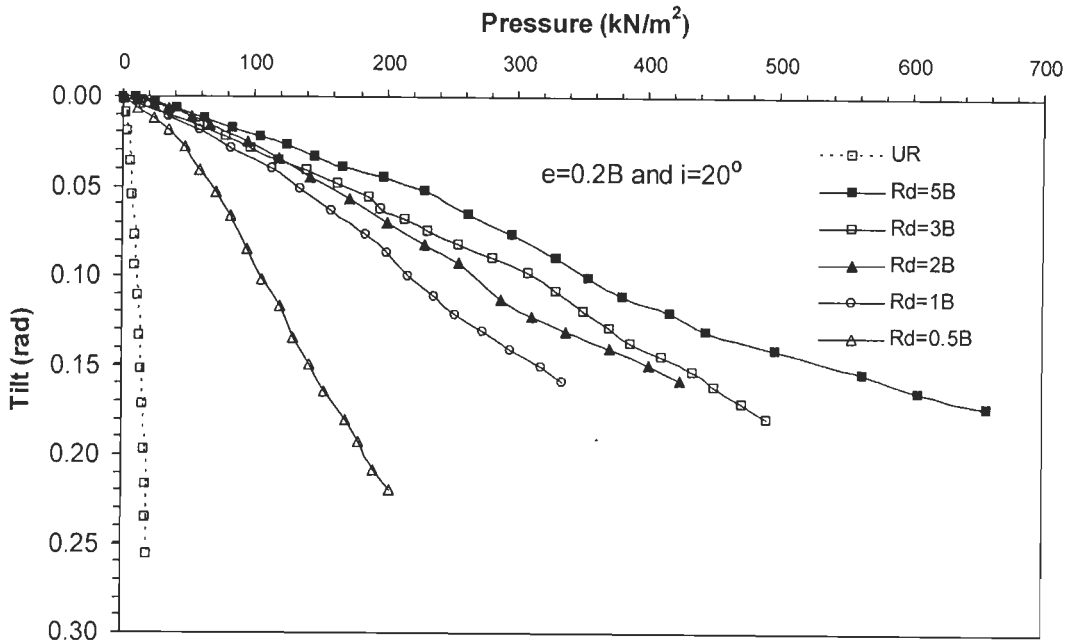


Figure 5.42 Pressure-tilt curves for different relative depth (1.0% 1000D 50mm fibrillated fiber, $e=0.2B$, $i=20^\circ$ and $Dr = 30\%$)

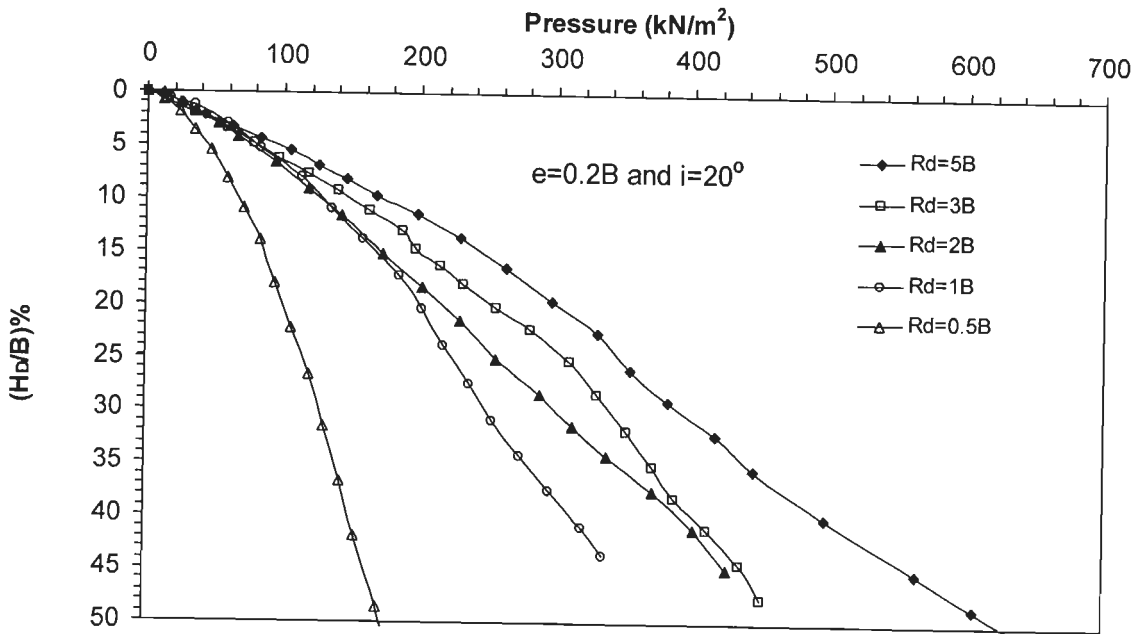


Figure 5.43 Pressure-horizontal displacement curves for different relative depth (1.0%, 1000D 50mm fibrillated fiber, $e=0.2B$, $i=20^\circ$ and $D_r = 30\%$)

5.4.5 Effect of RDFS Zone below Footing

The depth and width of the fiber-reinforced zone had been varied. Figure 5.44 shows pressure- settlement curves for different sizes of RDFS zone for 1.0% 1000D 50mm fibrillated fiber at $e=0.2B$ and $i=20^\circ$ for 30% relative density. Pressure settlement curve for $Rd=1B$ and $Rw=6B$ is highest compare to other curves. However, in case of $Rd=2B$ and $Rw = 4B$ amount of fibers used is more compare to $Rd=1B$ and $Rw=6B$. It was found that most optimum zone for eccentric-inclined load is 6 B wide and 1 B deep below footing. Figure 5.45 and 5.46 shows pressure- tilt and pressure-horizontal displacement curves respectively. Tilt and horizontal displacement decreased substantially. In case of unreinforced sand even at a pressure of 40 kPa footing is subjected to large settlements, tilts and horizontal displacements while for footing on RDFS settlements, tilts and horizontal displacements are with in limit at very low values.

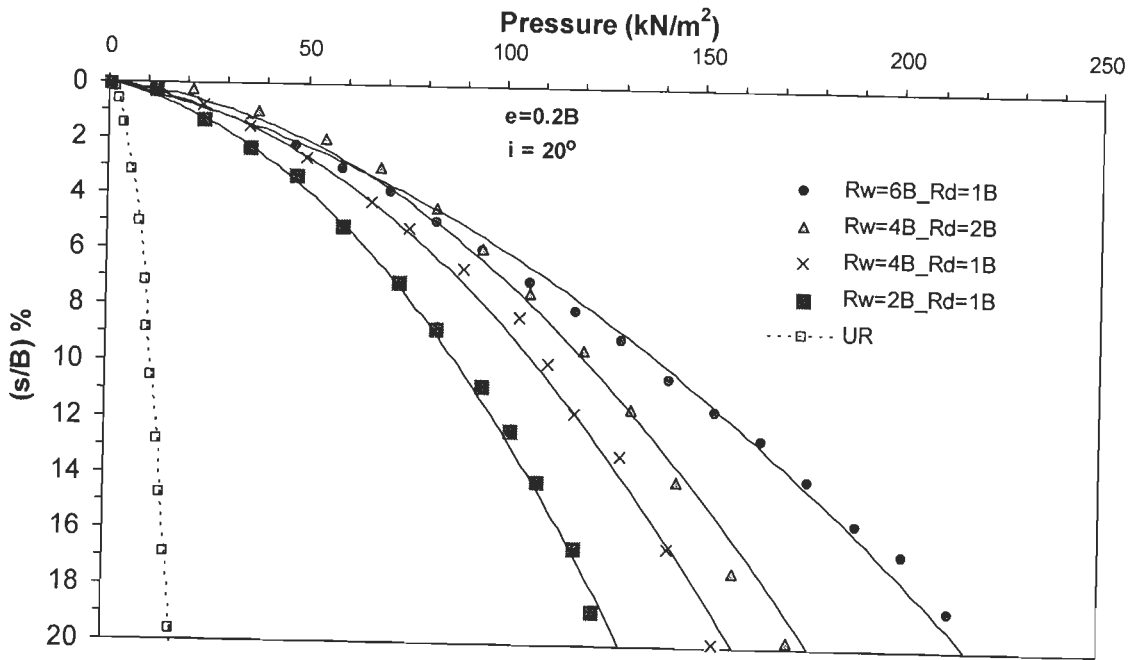


Figure 5.44 Pressure- settlement curves for different sizes of RDFS zone (1.0% 1000D 50mm fibrillated fiber, $e=0.2B$, $i=20^\circ$ and $D_r = 30\%$)

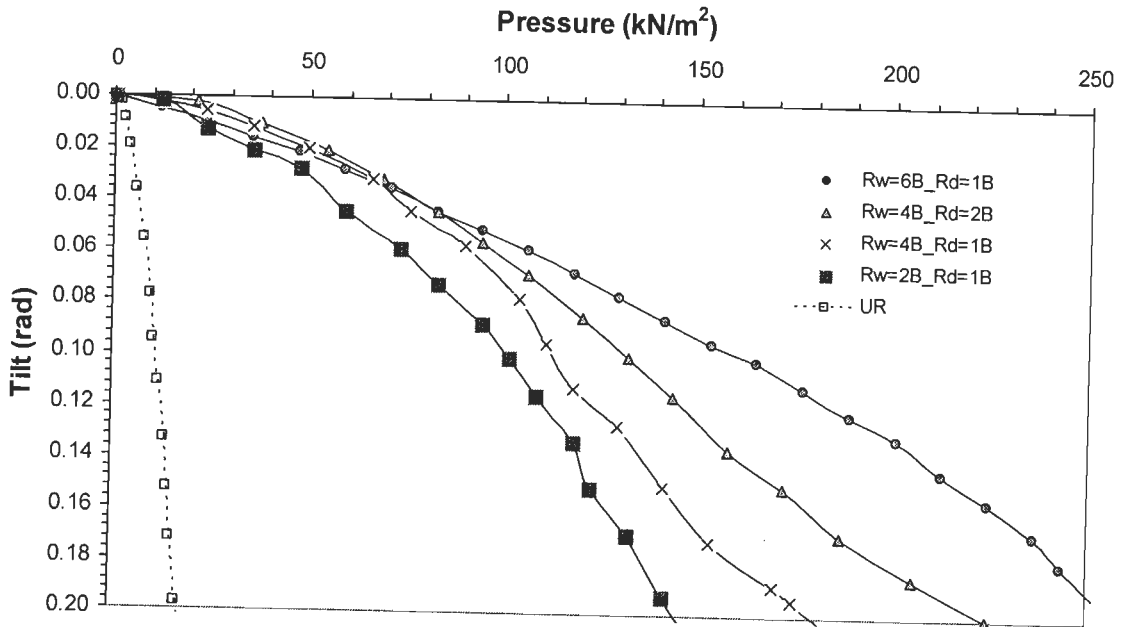


Figure 5.45 Pressure-tilt curves for different relative depth (1.0% 1000D 50mm fibrillated fiber, $e=0.2B$, $i=20^\circ$ and $D_r = 30\%$)

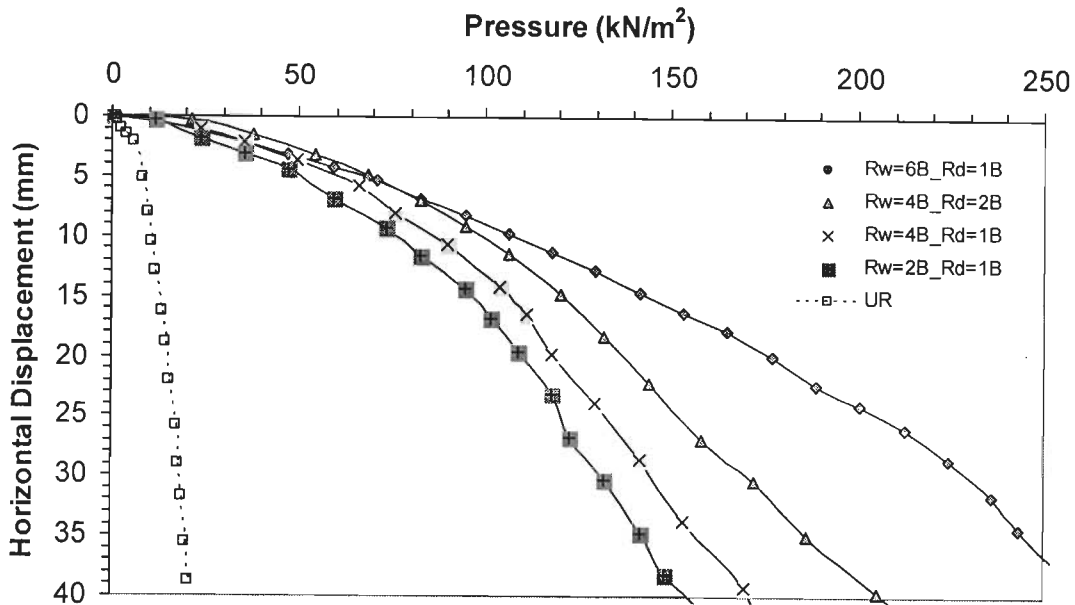


Figure 5.46 Pressure-horizontal displacement curves for different relative depth (1.0% 1000D 50mm fibrillated fiber, $e=0.2B$, $i=20^\circ$ and $Dr = 30\%$)

As in central vertical load similar trends were obtained for 50% and 70% relative density in case of eccentric – inclined load also.

5.5 THE INFLUENCE OF SIZE OF FOOTING ON BEARING CAPACITY – SETTLEMENT – TILT BEHAVIOUR

The size effects of footings referred as scale effects on the bearing capacity of unreinforced soil are well understood (DeBeer, 1963, 1965; Graham and Stuart, 1971; Vesic, 1973; Shiraishi, 1990; Clark, 1998; Ueno et al. 1998; Perkins and Madson, 2000). No study has yet made to determine this effect for footings resting on RDFS. For this purpose, model footing tests on unreinforced sand and RDFS have been carried out using four different sizes of footing. Figure 5.47 shows the pressure – settlement relationship for different sizes of the footings resting on sand at 30 % relative density. Figure 5.48 shows typical plot for pressure – settlement curves for different sizes

of the footings resting on RDFS (1% 1000D 50mm fibrillated fibers in $R_d=1B$ and $R_w=2B$) at 30% relative density.

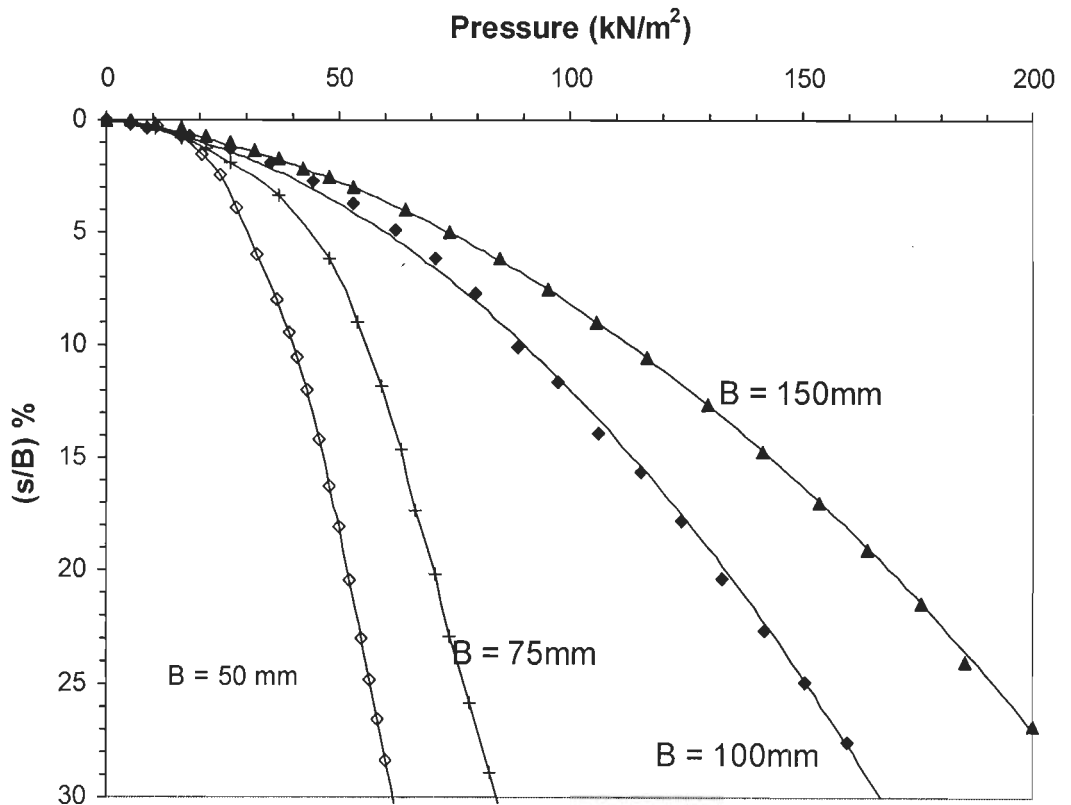


Figure 5.47 Pressure – settlement curves for different sizes of the footings resting on sand at 30 % relative density.

Bearing capacity increases with increase in foundation width for both footing resting on unreinforced and RDFS. However, BCR remain same for all footing widths.

The reliability of model test results will be of great importance for actual field design if the size effects are delineated. Bearing capacity ratio will prove to be an important parameter in such case. Table 5.2 shows the comparison of bearing capacity ratio (BCR) for different footing sizes.

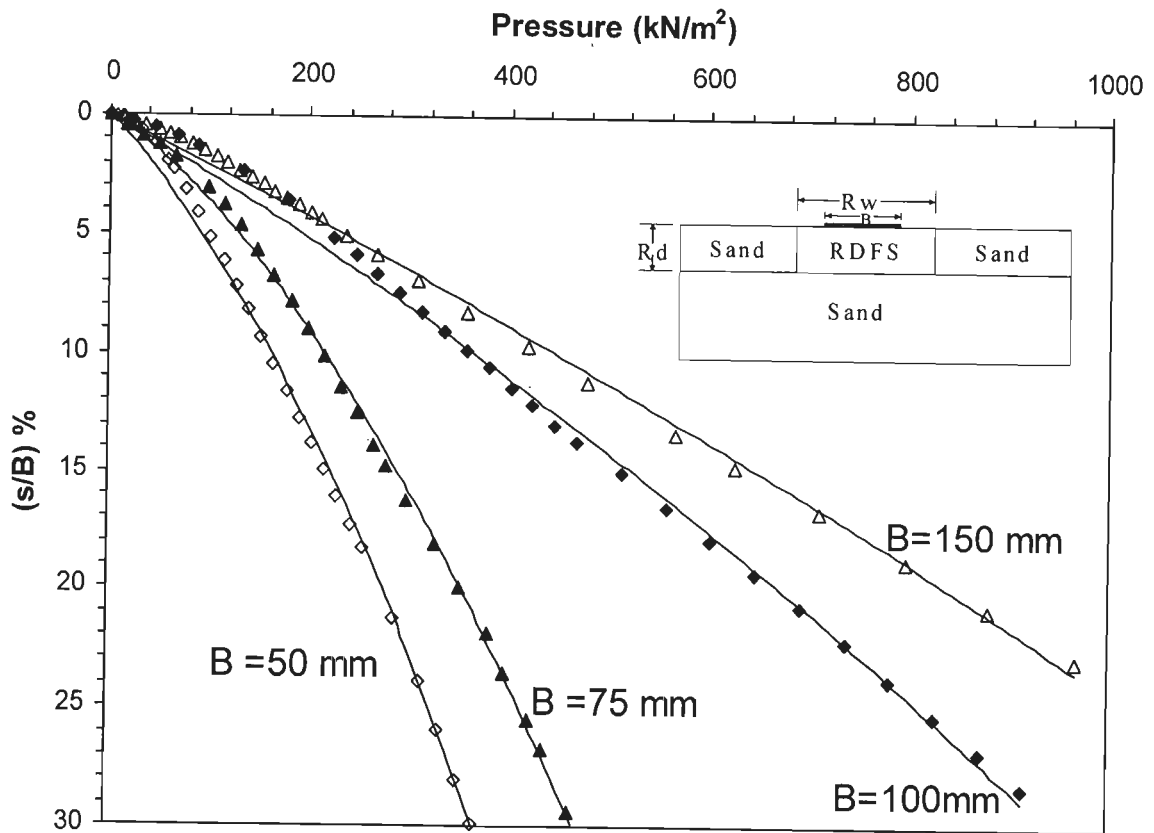


Figure 5.48 Pressure – settlement curves for different sizes of the footings resting on RDFS (1% 1000D 50mm fibrillated fibers in $R_d=1B$ and $R_w=2B$, $D_r= 30\%$)

Table 5.2 Comparison BCR values obtained for different footing sizes (B) of 50 mm, 100 mm and 150 mm

Sl. No.	D_r (%)	χ_w (%)	Rw	Rd	e/B	i	B (mm)	BCR
1	30	1	2	1	0	0	50	4.1
2	30	1	10	2	0	0	50	7
3	30	0.5	10	2	0	0	50	6.1
4	50	1	2	1	0	0	50	3.3
5	70	1	2	1	0	0	50	3.5
6	30	1	10	5	0	0	50	9
12	70	1	10	5	0	0	50	7.9
13	70	1	10	1	0	0	50	3.5
14	30	1	2	1	0	0	100	4.1
15	30	1	10	2	0	0	100	5.2
16	30	0.5	10	2	0	0	100	3.4
17	50	1	2	1	0	0	100	3.5
18	70	1	2	1	0	0	100	2.9
19	30	1	10	5	0	0	100	9.0
20	30	1	6	1	0.2	20	100	9.9
21	30	1	2	1	0	0	150	3.8
22	30	1	10	2	0	0	150	5.8
23	30	0.5	10	2	0	0	150	4.2
24	50	1	2	1	0	0	150	3.8
25	70	1	2	1	0	0	150	3.9
26	30	1	10	5	0	0	150	7.0
28	30	1	10	2	0.1	0	150	10.7
29	30	0.5	10	2	0.1	0	150	3.8
30	30	1	10	2	0.2	0	150	15.1
31	30	0.5	10	2	0.2	0	150	5.5
32	70	1	10	5	0	0	150	9.5
33	70	1	10	1	0	0	150	4.2
34	70	0.25	10	1	0	0	150	2.4

It was very interesting to note that BCR remain almost same for all footing widths. This indicates that if the fiber content and RDFS zone are uniquely defined in dimension less form resulting dimensionless bearing capacity (i.e. BCR) will not be affected by size of footing. Thus, results of model footing tests in dimensionless form can be used for field applications. This finding is of great relevance to field applications of RDFS for shallow foundations. Behaviour of footing resting on RDFS is material (soil and fiber) and construction (e.g. anisotropy of RDFS) specific problem and some parameters are difficult to assess (e.g. number of fiber intersecting rupture surface and out of these how many fibers are active at particular deformation level). Also it is dependent on large number of parameters which makes difficult to produce a generalised solution free from problems mentioned and amenable to practicing geotechnical engineers. In the view of these facts best solution to estimate accurately improvements for prototype foundation is to conduct laboratory model footing tests or field plate load tests on existing ground and improved with discrete fibers in non-dimensional form.

5.6 DEVELOPMENT OF MODELS FOR PREDICTION OF BEARING CAPACITY RATIO, SETTLEMENT AND TILT OF STRIP FOOTING RESTING ON RDFS

Empirical estimation methods are common in Geotechnical Engineering. Multiple variable regression analysis is one of the very useful tool most commonly used in case of complex geotechnical problem such liquefaction. Liquefaction occurrence and resulting lateral spreading depends on the large number of factors and no complete theoretical solution is possible till date. Therefore, currently the most widely used method for the prediction of lateral displacements is the multi-linear regression equations developed by Youd et al. 2002. In such cases, models are developed using observed data in laboratory model tests and/ or from field tests etc. Generally, a function is assumed

to estimate a relationship between the dependent variable and independent variables. The coefficients of the function are estimated by regression analysis using the observed data. If variables are expressed in terms of dimensionless form it can be applied for field applications by taking advantage of scaling laws of continuum mechanics. Analysis of footings resting on RDFS is also a very complicated problem because behaviour of footings resting on RDFS is also dependent on many variables such as fiber content, fiber aspect ratio, width and depth of RDFS zone, density of existing ground and RDFS etc. Further, in the case of RDFS, the position, the direction and the number of fibers at any plane is quite uncertain which makes difficult to produce a closed form solution. Thus, for analysis of strip footing resting on RDFS a statistical analysis using multiple regression would be more appropriate. No model is available in literature to predict bearing capacity, settlement and tilt of footings resting on RDFS. In following sections models are developed for prediction of bearing capacity, settlement and tilt of footings resting on RDFS.

5.6.1 Models For Prediction of Bearing Capacity Ratio, of Strip Footing Resting on RDFS

In the present study first time an attempt has been made to develop a model on the basis of the experimental data, for estimating the BCR of strip footing on RDFS. In the present investigation a non-linear power model, to estimate the bearing capacity of strip footing on RDFS, has been developed considering BCR as a function of different parameters in non-dimensional form as shown below:

$$\text{BCR} = f(\chi_w\%, \text{Rd/B}, \text{Rw/B}, i, e/B, l/d) \quad (5.1)$$

where, BCR is the predicted value of the criterion (dependent) variable $\chi_w\%$, Rd/B, Rw/B, i, e/B, l/d are predictors (independent) variables.

In present modeling experimental data of strip footing (B=75mm) on fibrillated fibers is used. Table 5.3 shows BCR values from experimental data for strip footing (B=75 mm) resting on RDFS under central-vertical load at 30% relative density. Various forms of models have been attempted and following form was found best giving highest value of R^2 .

$$BCR = 1.42 (\chi_w\%)^{0.564} (Rd/B)^{0.365} (Rw/B)^{0.18} (l/d)^{0.21} \quad (5.2)$$

The coefficient of determination (R^2), obtained for equation (2) is 0.98. A comparison of predicted versus experimental (observed) values of BCR is shown in figure 5.49. It is found that predicted values are in good agreement with observed values. Hence equation 5.2 can be used for predicting BCR.

Similarly table 5.4 and 5.5 shows BCR values from experimental data for strip footing (B=75 mm) resting on RDFS under central-vertical load at 50% and 70% relative density respectively. Following models were developed for 50% and 70% relative density.

$$BCR=1.35 (\chi_w\%)^{0.5} (Rd/B)^{0.332} (Rw/B)^{0.16} (l/d)^{0.18} \text{ for } D_r=50\% \quad (5.3)$$

$$BCR=1.4 (\chi_w\%)^{0.57} (Rd/B)^{0.44} (Rw/B)^{0.14} (l/d)^{0.2} \text{ for } D_r=70\% \quad (5.4)$$

A comparison of predicted versus experimental (observed) values of BCR is shown in figure 5.50 & 5.51 for 30% and 70% relative density respectively. It is found that predicted values are in good agreement with observed values. Hence equation 5.2, 5.3 and 5.4 can be used for predicting BCR of strip footing subjected to central-vertical load at 30%, 50% and 70% relative density respectively. A linear interpolation may be done for intermediate cases.

Table 5.3 BCR values for different tests under central vertical load for ($D_r=30\%$)

Sl. No.	χ_w % ↓	Rd/B	Rw/B	l/d	BCR
1	0.25	5	10	125	3.6
2	0.5	5	10	125	5.5
3	0.5	5	10	125	5.9
4	0.75	5	10	125	7.0
5	0.75	5	10	125	8.0
6	1	5	10	125	10.8
7	1	5	10	125	9.8
8	1	5	10	125	9.4
9	1	0.5	10	125	3.6
10	1	1	10	125	5.6
11	1	2	10	125	6.2
12	1	2	10	125	6.8
13	1	4	10	125	9.6
14	0.5	2	10	125	3.7
15	0.5	4	10	125	4.7
16	0.5	5	10	125	5.5
17	0.25	0.5	2	125	2.1
18	0.25	1	2	125	2.3
19	0.5	1	2	125	3.3
20	1	1	3	125	5.2
21	1	1	2	125	4.4
22	1	0.5	2	125	2.8
23	1	1	3	50	3.8
24	1	1	2	50	3.5
25	1	0.5	2	50	2.5
26	0.25	0.5	2	50	1.4
27	0.25	1	3	50	2.0
28	0.25	1	2	50	1.8
29	0.25	0.5	2	50	1.4
30	1	1	3	80	4.2
31	1	1	2	80	4.0
32	1	0.5	2	80	3.2
33	0.25	0.5	2	80	1.6
34	0.25	1	3	80	2.1
35	0.25	1	2	80	1.9
36	0.25	0.5	2	80	1.6
37	0.5	1	3	80	2.8
38	0.5	1	2	80	2.7
39	0.5	0.5	2	80	2.2
40	0.5	0.5	3	80	2.4

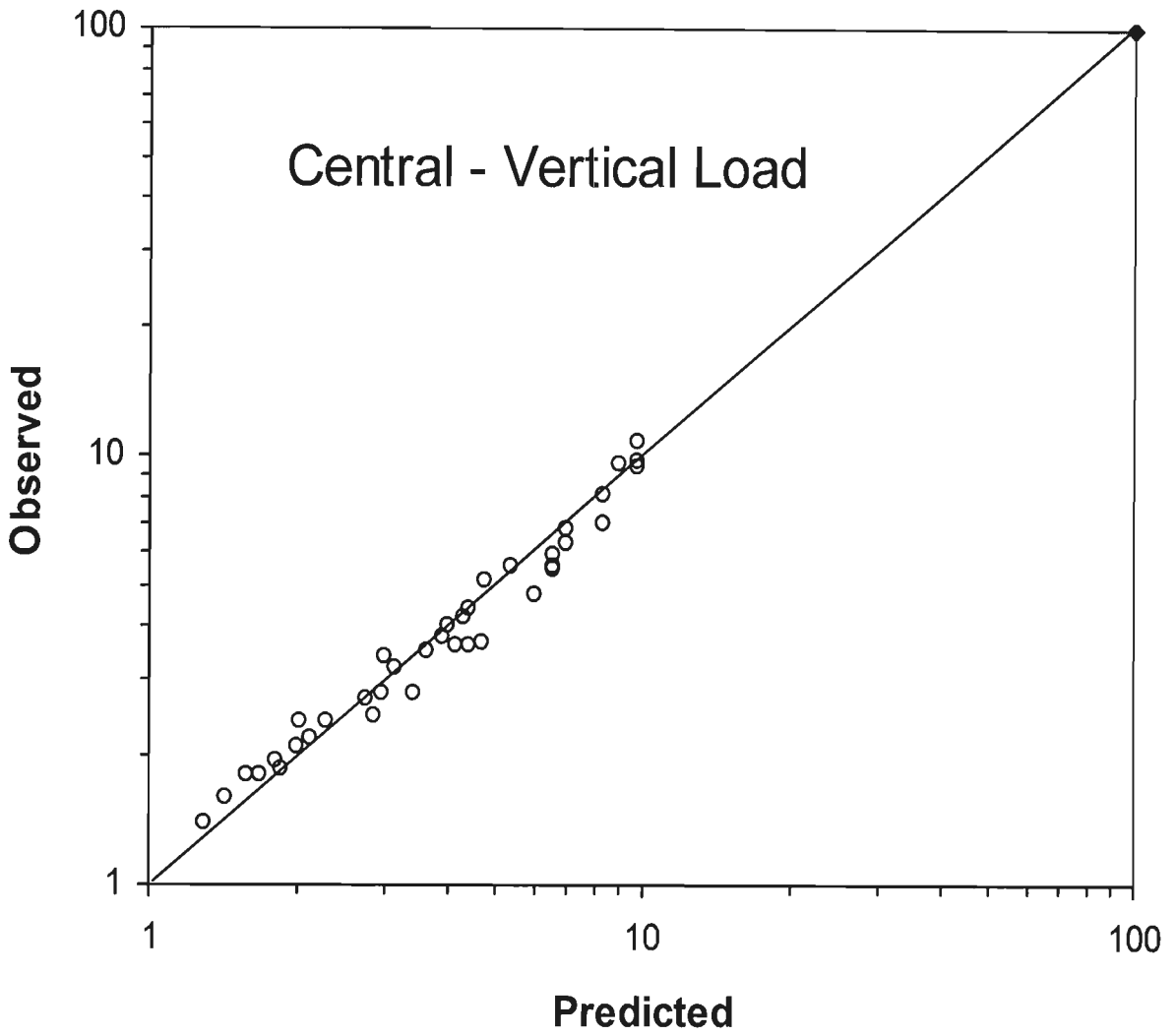


Figure 5.49 Observed BCR versus Predicted BCR for $D_r = 30\%$

Table 5.4 BCR values for different tests under central vertical load for ($D_r=50\%$)

Sl. No.	BCR	χ_w %	Rd/B	Rw/B	l/d
1	2.2	1	0.5	2	125
2	3.08	1	1	2	125
3	3.85	1	1	6	125
4	2.45	0.5	1	2	125
5	1.83	0.5	0.5	2	125
6	1.63	0.25	0.5	2	125
7	1.71	0.25	0.5	2	125
8	2.19	0.25	1	2	125
9	1.27	0.25	0.5	2	125
10	1.27	0.25	0.5	2	50
11	1.4	0.25	0.5	2	80
12	2.96	1	0.5	6	125
13	3.2	0.5	2	6	125
14	5.76	1	2	6	125
15	3	0.25	5	6	125
16	3.94	0.5	5	6	125
17	5.38	0.75	5	6	125
18	7.4	1	5	6	125
19	6.3	1	3	6	125
20	4.7	0.5	3	6	125
21	3.9	1	1	3	125
22	2.6	0.5	1	3	125
23	2	0.25	1	3	125
24	6	1	5	6	50
25	4.5	0.5	5	6	50

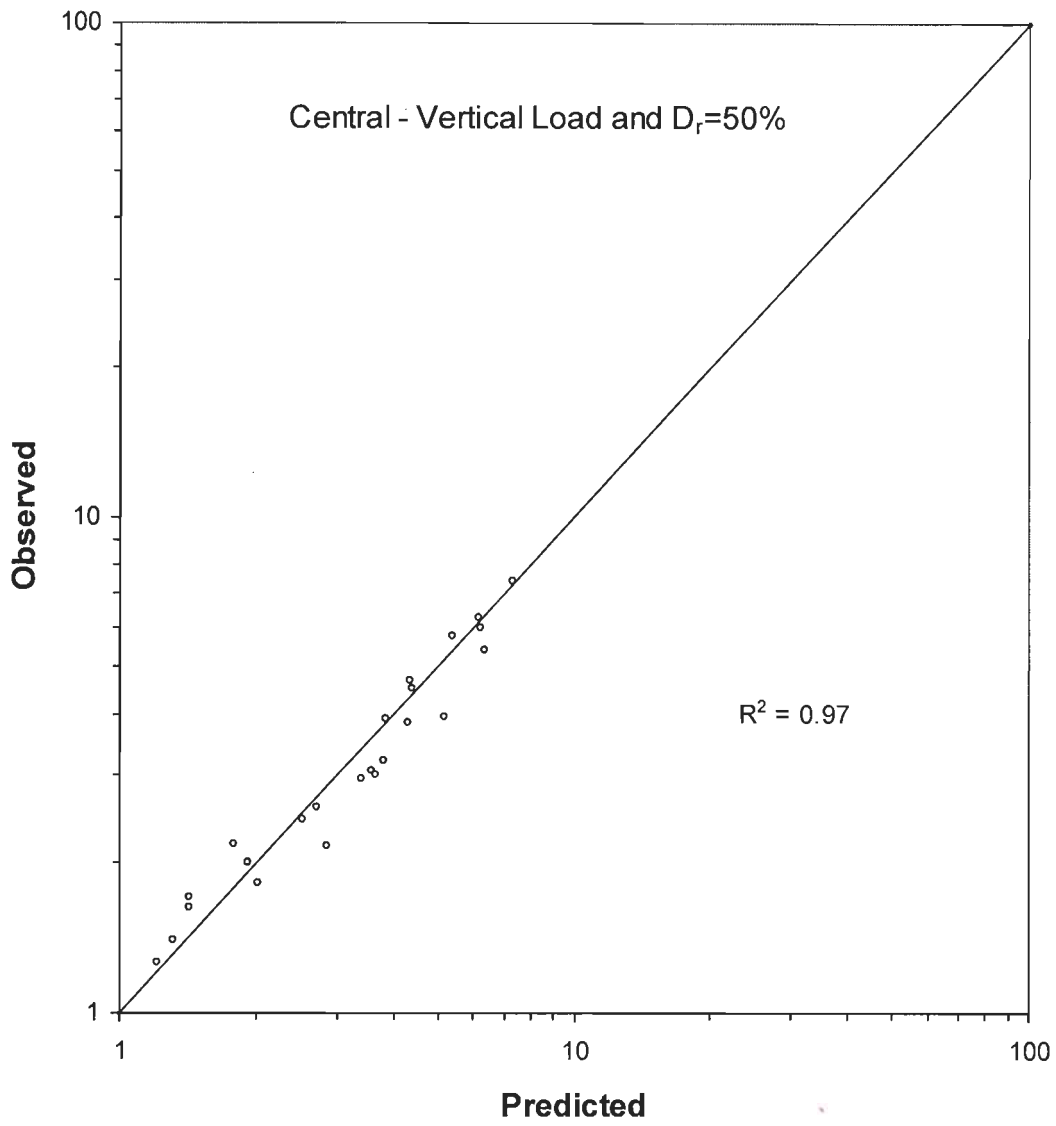


Figure 5.50 Observed BCR versus Predicted BCR for $D_r = 50\%$

Table 5.5 BCR values for different tests under central vertical load for ($D_r=70\%$)

Sl. No.	BCR	$\chi_w \% \downarrow$	Rd/B	Rw/B	l/d
1	1.48	0.25	0.5	2	125
2	1.41	0.25	0.5	2	125
3	2.14	0.25	1	2	125
4	6.09	0.5	5	6	125
5	3.67	0.5	3	6	125
6	2.89	0.5	2	4	125
7	2.58	0.5	1	2	125
8	3.00	0.5	2	2	125
9	3.05	0.5	2	2	125
10	3.04	0.5	2	2	125
11	3.20	0.5	2	2	125
12	2.95	0.5	1	3	125
13	2.89	1	0.5	10	125
14	2.70	0.25	1	10	125
15	6.07	1	5	6	125
16	9.16	1	5	8	125
17	8.80	1	5	8	125
18	6.00	1	3	6	125
19	4.19	1	2	4	125
20	2.24	1	0.5	2	125
21	3.34	1	1	2	125
22	6.50	1	4	2	125
23	5.60	1	2	2	125
24	3.94	1	1	3	125
25	4.25	1	3	3	125
26	9.00	1	5	10	125
27	5.21	1	1	10	125
28	2.56	0.25	5	10	125
29	3.33	0.25	5	10	125
30	4.61	0.5	5	10	125
31	1.30	0.25	0.5	2	50
32	1.74	0.25	1	2	50
33	2.72	1	1	10	50
34	1.43	0.25	0.5	2	80
35	1.84	0.25	1	2	80
36	2.15	1	1	2	80
37	2.74	1	1	10	80

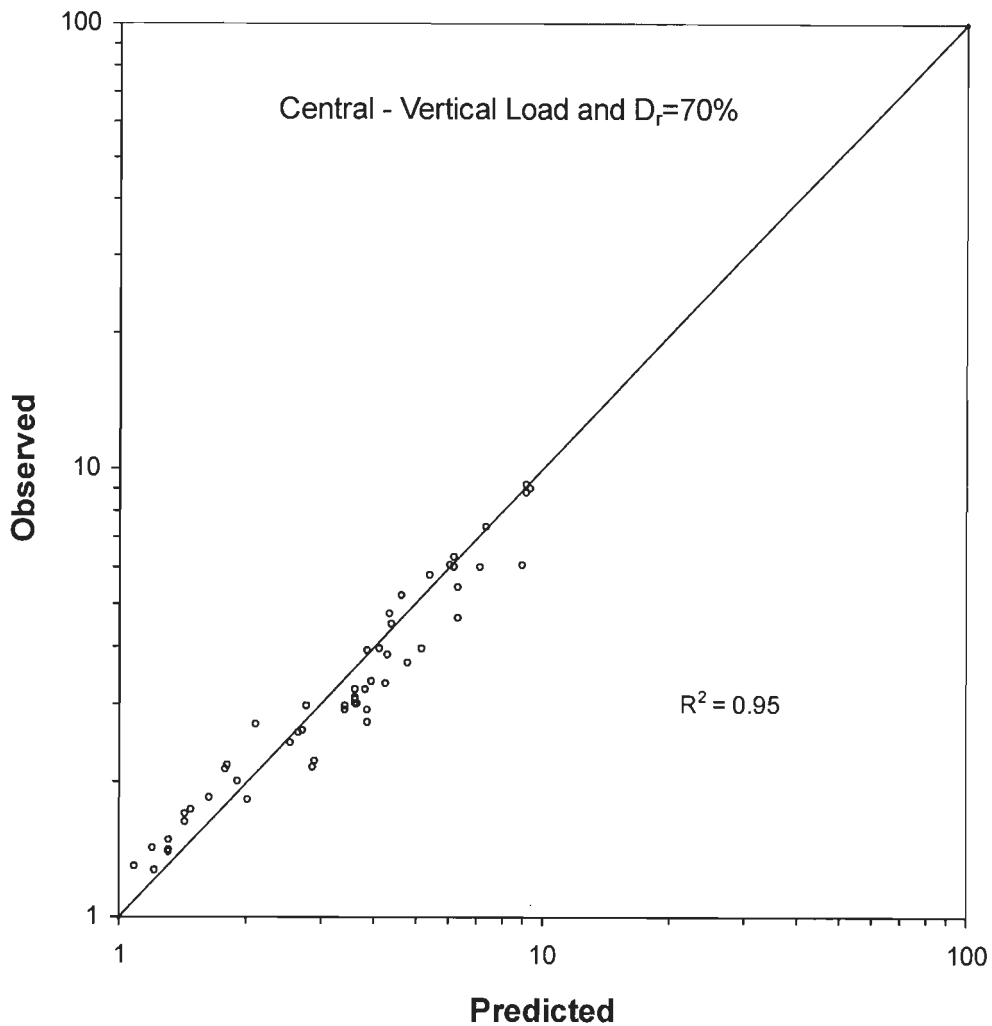


Figure 5.51 Observed BCR versus Predicted BCR for $D_r = 70\%$

Table 5.6 shows BCR values from experimental data for strip footing ($B=75$ mm) resting on RDFs under eccentric-inclined load at 30% relative density. Various forms of models have been attempted and following form was found best giving highest value of R^2 .

$$\text{BCR}=1.1*(\chi_w\%)^{0.68}*(Rd/B)^{0.49}*(Rw/B)^{0.23}*(1.034)^i*(1.8)^{e/B}*(l/d)^{0.21} \text{ for } D_r=30\% \quad (5.5)$$

The coefficient of determination (R^2), obtained for equation (5.5) is 0.97. A comparison of predicted versus experimental (observed) values of BCR is shown in figure 5.52. It is found that predicted values are in good agreement with observed values. Hence equation 5.5 can be used for predicting BCR.

Similarly table 5.7 and 5.8 shows BCR values from experimental data for strip footing ($B = 75 \text{ mm}$) resting on RDFS under eccentric-inclined load at 50% and 70% relative density respectively. Following models were developed for 50% and 70% relatively density.

$$\text{BCR}=0.7*(\chi_w\%)^{0.8}*(Rd/B)^{0.35}*(Rw/B)^{0.22}*(1.06)^i*(3)^{e/B}*(l/d)^{0.24} \text{ for } D_r=50\% \quad (5.6)$$

$$\text{BCR}=0.9*(\chi_w\%)^{0.71}*(Rd/B)^{0.45}*(Rw/B)^{0.2}*(1.04)^i*(3.2)^{e/B}*(l/d)^{0.18} \text{ for } D_r=70\% \quad (5.7)$$

A comparison of predicted versus experimental (observed) values of BCR is shown in figure 5.53 and 5.54. It is found that predicted values are in good agreement with observed values. Hence equation 5.5, 5.6 and 5.7 can be used for predicting BCR of strip footing subjected to eccentric-inclined load at 30%, 50% and 70% relative density respectively. A linear interpolation may be done for intermediate cases.

Table 5.6 BCR values for all tests under eccentric - inclined load for ($D_r=30\%$)

Sl. No.	χ_w %	Rd/B	Rw/B	i	e/B	l/d	BCR
1	0.5	5	10	0	0.1	80	5.9
2	0.5	5	10	0	0.1	125	7.3
3	1	5	10	0	0.1	125	13.6
4	0.5	5	10	0	0.2	125	8.1
5	1	5	10	0	0.2	125	13.4
6	0.5	5	10	10	0	125	11.0
7	1	5	10	10	0	125	13.5
8	0.5	5	10	10	0.1	125	11.6
9	1	5	10	10	0.1	125	13.7
10	0.5	5	10	10	0.2	125	12.6
11	1	5	10	10	0.2	125	18.0
12	0.5	5	10	20	0	125	15.7
13	1	5	10	20	0	125	21.6
14	0.5	5	10	20	0.1	125	16.6
15	1	5	10	20	0.1	125	25.9
16	0.5	5	10	20	0.2	125	17.1
17	1	5	10	20	0.2	125	28.0
18	1	2	10	10	0.1	125	10.0
19	1	4	10	10	0.1	125	14.8
20	1	2	10	20	0.2	125	17.3
21	1	3	10	20	0.2	125	22.2
22	1	1	10	10	0.1	50	4.8
23	1	1	10	10	0.2	50	5.1
24	1	1	10	20	0.1	50	7.1
25	1	1	10	20	0.2	50	7.7

Table Contd/---

Table 5.6 (contd.)

26	1	2	10	10	0.1	50	7.2
27	1	2	10	10	0.2	50	7.9
28	1	2	10	20	0.1	50	11.0
29	1	2	10	20	0.2	50	11.9
30	1	2	10	20	0	125	15.0
31	1	2	10	10	0.1	125	10.0
32	0.5	3	10	10	0.1	125	10.0
33	0.5	3	10	10	0.2	125	9.0
34	1	3	10	10	0.2	125	14.0
35	0.5	3	10	20	0	125	9.0
36	1	3	10	20	0	125	17.0
37	0.5	3	10	20	0.1	125	11.0
38	1	3	10	20	0.1	125	18.0
39	1	3	10	20	0.2	125	15.0
40	0.5	4	10	10	0.1	125	11.6
41	1	4	10	10	0.1	125	13.7
42	0.5	4	10	10	0.2	125	10.3
43	1	4	10	10	0.2	125	16.0
44	0.5	4	10	20	0	125	11.5
45	1	4	10	20	0	125	21.6
46	0.5	4	10	20	0.1	125	13.0
47	1	4	10	20	0.1	125	21.0
48	0.5	4	10	20	0.2	125	13.0
49	1	4	10	20	0.2	125	20.0

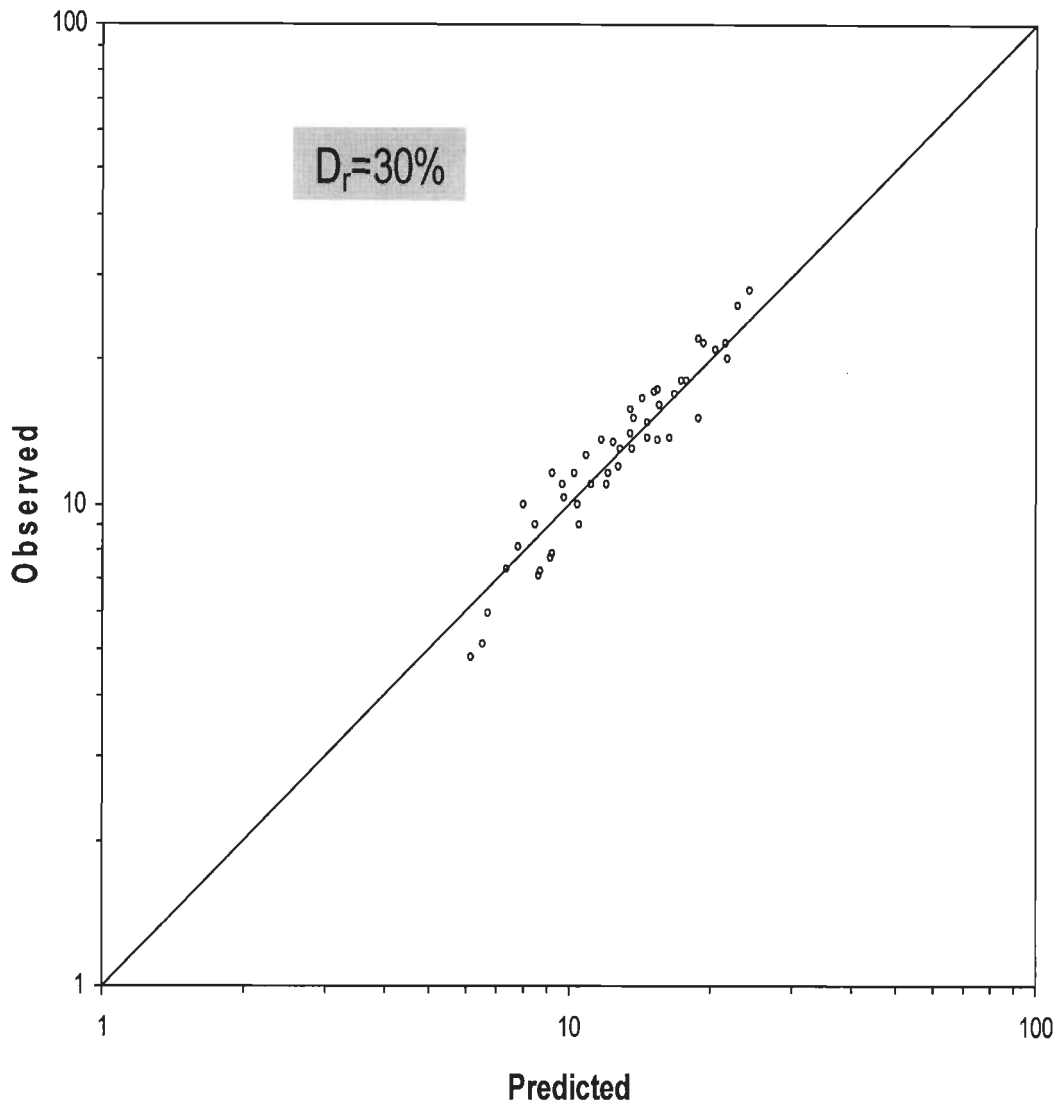


Figure 5.52 Observed BCR versus Predicted BCR for under eccentric - inclined load for ($D_r=30\%$)

Table 5.7 BCR values for tests under eccentric - inclined load for ($D_r=50\%$)

Sl. No.	BCR	χ_w %	Rd/B	Rw/B	i	e/B	l/d
1	3.6	0.5	1	10	10	0.1	125
2	5	0.5	1	10	10	0.2	125
3	7	1	1	10	10	0.1	125
4	9.3	1	1	10	10	0.2	125
5	6.2	0.5	1	10	20	0.1	125
6	10.5	0.5	1	10	20	0.2	125
7	10.9	1	1	10	20	0.1	125
8	14	1	1	10	20	0.2	125
9	5	0.5	2	10	10	0.1	125
10	6.5	0.5	2	10	10	0.2	125
11	9.5	1	2	10	10	0.1	125
12	11.5	1	2	10	10	0.2	125
13	9	0.5	2	10	20	0.1	125
14	11.5	0.5	2	10	20	0.2	125
15	17	1	2	10	20	0.1	125
16	18	1	2	10	20	0.2	125
17	6	0.5	3	10	10	0.1	125
18	7.4	0.5	3	10	10	0.2	125
19	8.5	1	3	10	10	0.1	125
20	13	1	3	10	10	0.2	125
21	11	0.5	3	10	20	0.1	125
22	13.8	0.5	3	10	20	0.2	125
23	19	1	3	10	20	0.1	125
24	22	1	3	10	20	0.2	125
25	11.9	1	1	10	20	0.2	50
26	7	1	2	10	10	0.1	50
27	8	1	3	10	10	0.1	50
28	14.7	1	2	10	20	0.2	50
29	5.4	1	1	10	10	0.1	80
30	13.1	1	1	10	20	0.2	80
31	4.7	0.5	1	6	10	0.1	125
32	8	0.5	1	6	20	0.2	125
33	5.5	1	1	6	10	0.1	125
34	14	1	1	6	20	0.2	125
35	9	1	1	2	20	0.2	125
36	12	1	1	4	20	0.2	125
37	6	1	1	4	10	0.1	125
38	7.5	1	1	4	10	0.2	125
39	10	1	1	4	20	0.1	125
40	4	1	1	4	0	0.1	125
41	4.5	1	1	4	0	0.2	125

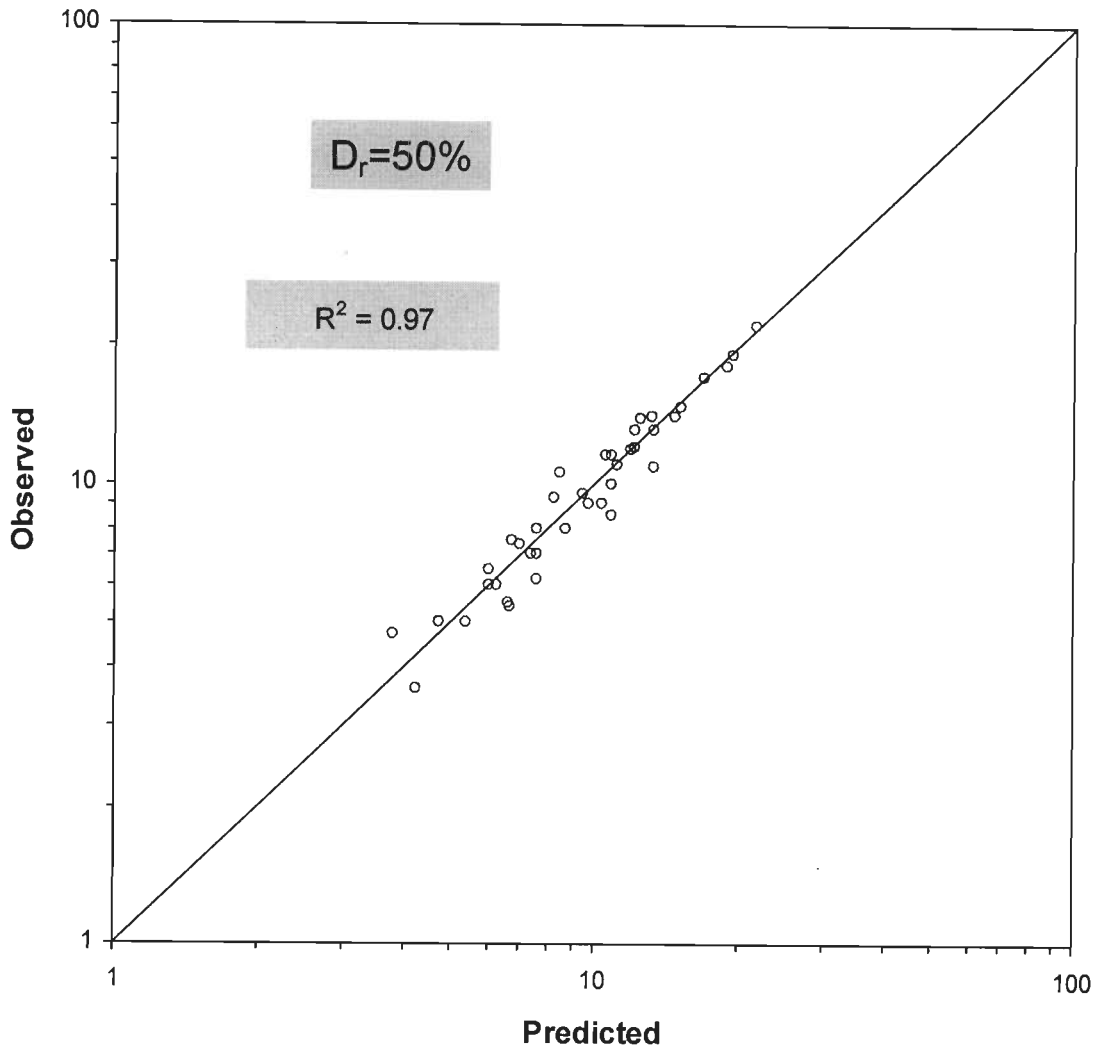


Figure 5.53 Observed BCR versus Predicted BCR for under eccentric - inclined load for ($D_r=50\%$)

Table 5.8 BCR values for tests under eccentric - inclined load for ($D_r=70\%$)

Sl. No.	BCR	χ_w %	Rd/B	Rw/B	i	e/B	l/d
1	3.20	0.5	1	10	10	0.1	125
2	3.00	0.5	1	10	10	0.2	125
3	6.00	1	1	10	10	0.1	125
4	6.20	1	1	10	10	0.2	125
5	4.80	0.5	1	10	20	0.1	125
6	5.60	0.5	1	10	20	0.2	125
7	8.60	1	1	10	20	0.1	125
8	9.20	1	1	10	20	0.2	125
9	4.80	0.5	2	10	10	0.1	125
10	6.20	0.5	2	10	10	0.2	125
11	8.20	1	2	10	10	0.1	125
12	9.00	1	2	10	10	0.2	125
13	7.20	0.5	2	10	20	0.1	125
14	7.70	0.5	2	10	20	0.2	125
15	11.30	1	2	10	20	0.1	125
16	13.39	1	2	10	20	0.2	125
17	5.30	0.5	3	10	10	0.1	125
18	6.50	0.5	3	10	10	0.2	125
19	9.10	1	3	10	10	0.1	125
20	10.10	1	3	10	10	0.2	125
21	8.40	0.5	3	10	20	0.1	125
22	9.20	0.5	3	10	20	0.2	125
23	13.60	1	3	10	20	0.1	125
24	14.98	1	3	10	20	0.2	125
25	9.00	1	1	10	20	0.2	50
26	8.00	1	2	10	10	0.1	50
27	8.00	1	3	10	10	0.1	50
28	12.00	1	2	10	20	0.2	50
29	6.00	1	1	10	10	0.1	80
30	9.50	1	1	10	20	0.2	80
31	4.00	0.5	1	6	10	0.1	125
32	7.00	0.5	1	6	20	0.2	125
33	6.00	1	1	6	10	0.1	125
34	8.00	1	1	6	20	0.2	125
35	7.00	1	1	2	20	0.2	125
36	8.20	1	1	4	20	0.2	125

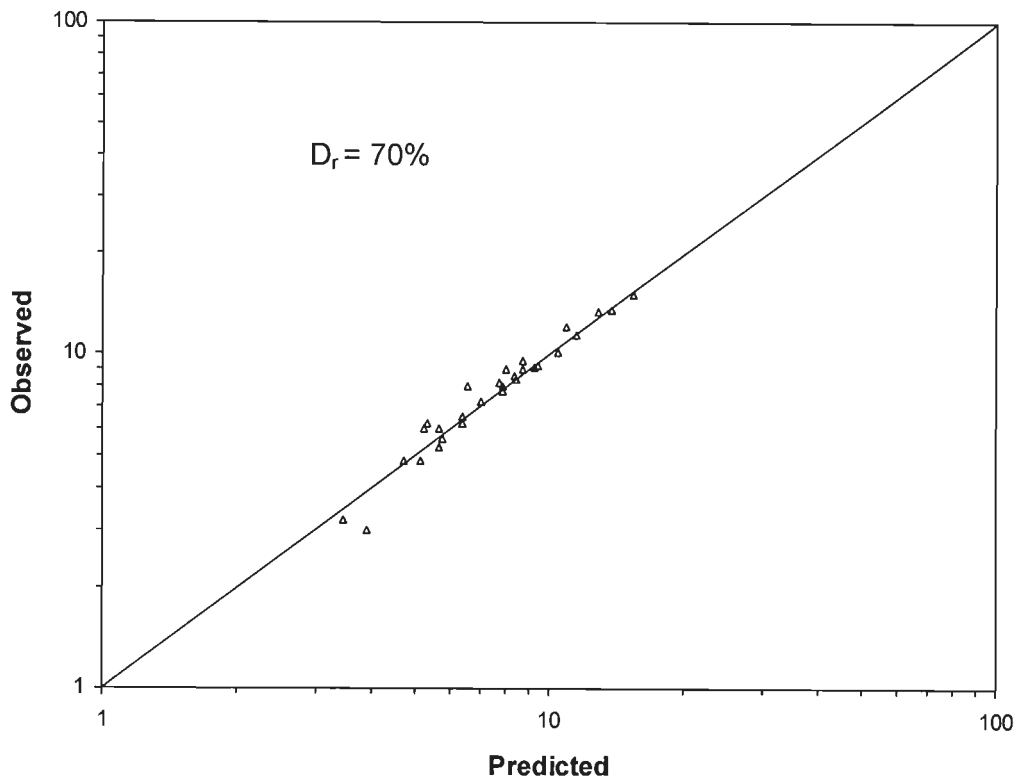


Figure 5.54 Observed BCR versus Predicted BCR for under eccentric - inclined load for ($D_r=30\%$)

5.6.2 Models For Prediction of Settlement of Strip Footing Resting on RDFS Subjected to Central Vertical load

Using the model test data non-dimensional correlation for S_{ORDFS} / S_{OUR} have been developed, where S_{ORDFS} and S_{OUR} is settlement under central vertical load for footing resting on RDFS and sand respectively at same factor of safety. Overall pressure – settlement curves of RDFS are very high compare to unreinforced sand, therefore settlements of unreinforced sand and RDFS can not be compared at equal bearing pressure corresponding to improved values of bearing pressure in RDFS. S_{ORDFS} / S_{OUR} values are compared at same factor of safety of 1,2 and 3. As discussed in section 5.2.1

ultimate bearing capacity (q_u) for both unreinforced and RDFS is taken at 10% settlement ratio. Therefore, at factor of safety 1 (i.e. corresponding to q_u) S_{oRDFS} / S_{oUR} value will be 1 for all cases. Table 5.9 shows values of S_{oRDFS} / S_{oUR} at factor of safety 1,2 & 3 for fibrillated fibers under central-vertical load for $R_w=2B$ and $R_d=1B$ for different fiber content for 30% relative density. Fig. 5.55 shows variation of S_{oRDFS} / S_{oUR} with fiber content for $R_w=2B$ and $R_d=1B$ at 30%.

Table 5.9 Settlement Computation at Factor of Safety 1,2 & 3 for Fibrillated Fibers under Central-Vertical Load for $R_w=2B$ and $R_d=1B$ at $D_r=30\%$

Test No	$\chi_w\%$	l/d	FOS=1	FOS=2			FOS=3		
			q_u (kPa)	q_u (kPa)	S_o (mm)	$\frac{S_{oRDFS}}{S_{oUR}}$	q_u (kPa)	S_o (mm)	$\frac{S_{oRDFS}}{S_{oUR}}$
1	0(UR)		55	27.5	1.52	1.00	18.3	0.85	1.00
2	0.25	125	135.2	67.6	2.5	1.64	45.1	1.5	1.76
3	0.5	125	186.4	93.2	2.65	1.74	62.1	1.42	1.67
4	1	125	241.3	120.7	2.55	1.68	80.4	1.45	1.71
5	0.25	80	113.2	56.6	2.72	1.79	37.7	1.45	1.71
6	0.5	80	165.2	82.6	2.53	1.66	55.1	1.44	1.69
7	1	80	200.1	100.0	2.5	1.64	66.7	1.5	1.76
8	0.25	50	107.2	53.6	2.28	1.50	35.7	1.3	1.53
9	0.5	50	158.3	79.2	2.56	1.68	52.8	1.5	1.76
10	1	50	190.3	95.2	2.56	1.68	63.4	1.5	1.76

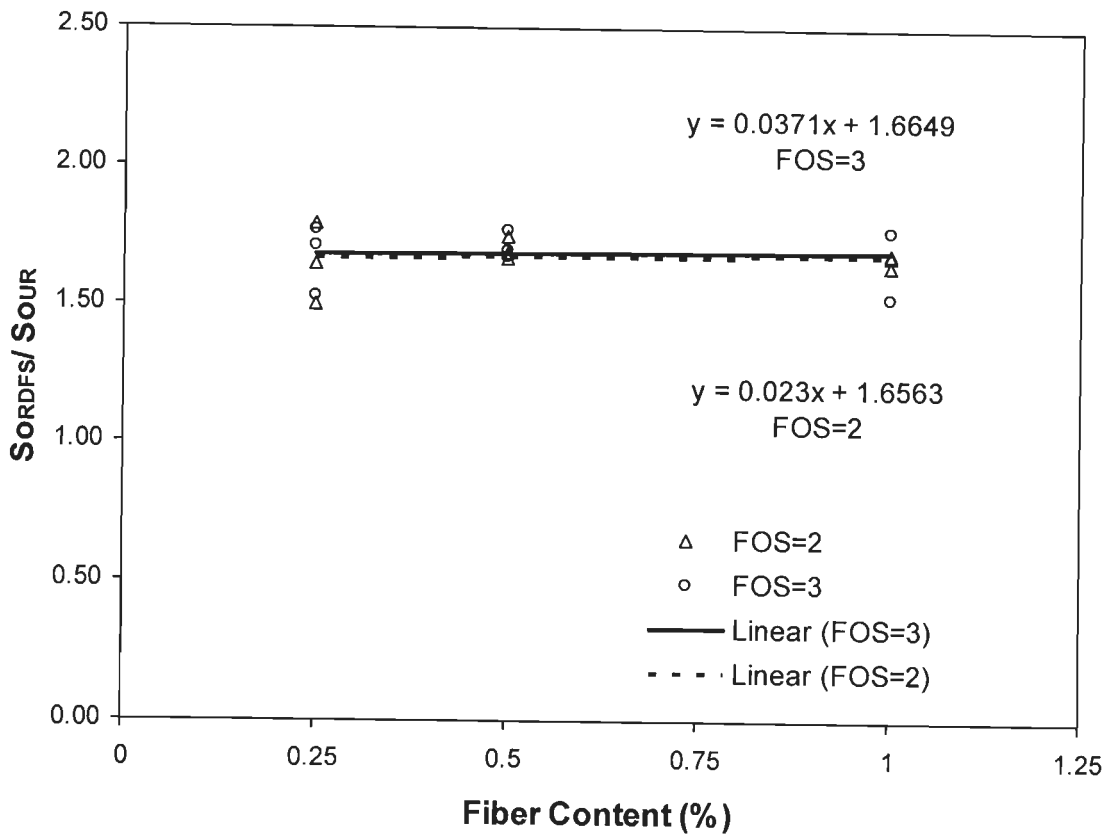


Figure 5.55 S_{0RDFS} / S_{0UR} versus fiber content for $R_w=2B$ and $R_d=1B$ at $Dr=30\%$

It is evident from table 5.9 and figure 5.55 that almost same value is obtained for S_{0RDFS} / S_{0UR} irrespective of factor of safety and fiber content. S_{0RDFS} / S_{0UR} can be expressed by following simple relation considering results slightly on safer side.

$$\frac{S_{0RDFS}}{S_{0UR}} = 1.7 \quad (5.8)$$

It was interesting to note that above relationship was found valid for different fiber content in $R_w = 2B$ and $R_d = 0.5B$ and $R_d = 3B$ and $R_d = 1B$ also. Same relationship was found valid for 50% and 70% relative density data also. By knowing S_{0UR} from conventional field plate load test on sand, S_{0RDFS} can be determined using equation 5.8.

5.6.3 Models for Prediction Settlement and Tilt of Strip Footing Resting on RDFS Subjected to Eccentric - Inclined Load

Using the model test data non-dimensional correlation for S_{eRDFS} / S_{oRDFS} and S_{mRDFS} / S_{oRDFS} have been developed, where S_{eRDFS} is settlement of footing under eccentric-inclined load and S_{mRDFS} is maximum settlement of the footing under eccentric-inclined load for footing resting on RDFS. S_{oRDFS} is settlement of footing under central vertical load for footing resting on RDFS.

Where,
$$S_{mRDFS} = S_{eRDFS} + (B/2 - e) \text{ sint} \tag{5.9}$$

S_{eRDFS} / S_{oRDFS} versus e/B plots and S_{mRDFS} / S_{oRDFS} versus e/B plots for different load inclinations are shown in figures 5.56 to 5.61.

Table 5.10 Settlement & Tilt Computation at Factor of Safety 2 & 3 for

Fibrillated Fibers under Eccentric Vertical Load

Rw	Rd	$\chi_w\%$	I	e/B	FOS=2				FOS=3			
					S_e	$\frac{S_{eRDFS}}{S_{oRDFS}}$	S_m	$\frac{S_{mRDFS}}{S_{oRDFS}}$	S_e	$\frac{S_{eRDFS}}{S_{oRDFS}}$	S_m	$\frac{S_{mRDFS}}{S_{oRDFS}}$
4	1	1%	0	0	2.6	1.00	2.60	1.00	1.45	1.00	1.45	1.00
4	1	0.5%	0	0	2.6	1.00	2.60	1.00	1.45	1.00	1.45	1.00
4	1	0.5	0	0.1	2.52	0.97	3.10	1.19	1.3	0.90	1.46	1.01
4	1	1	0	0.1	2.54	0.98	3.10	1.19	1.28	0.88	1.48	1.02
4	1	0.5	0	0.2	2.36	0.91	2.86	1.10	1.28	0.88	1.52	1.05
4	1	1	0	0.2	2.4	0.92	2.90	1.12	1.25	0.86	1.53	1.06

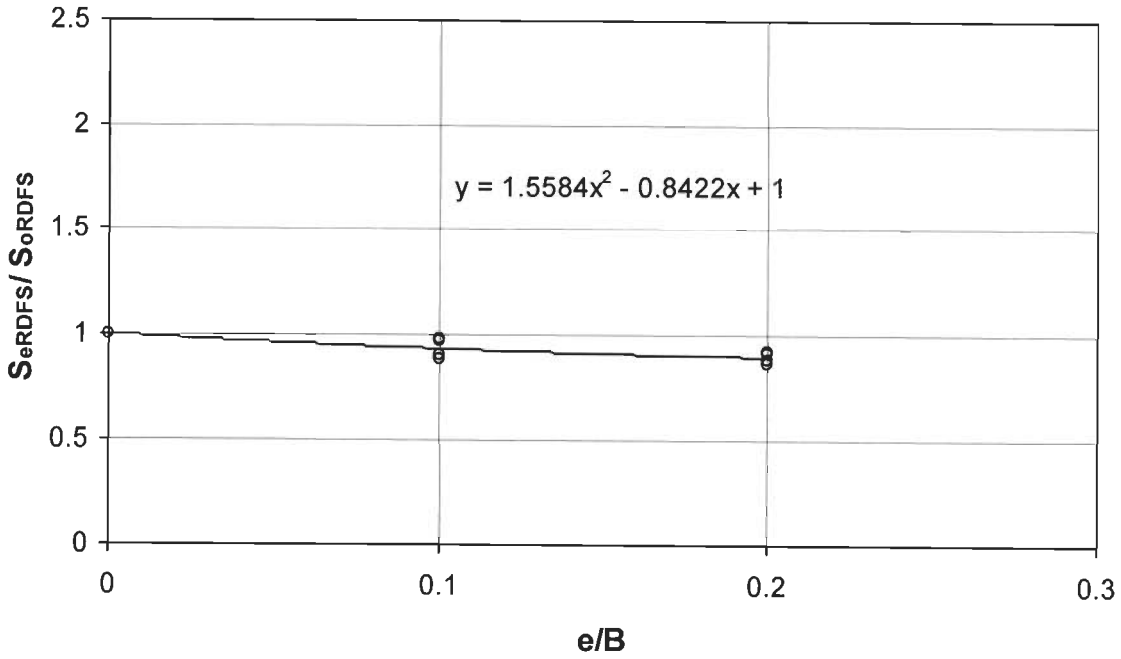


Figure 5.56 S_{eRDFS} / S_{oRDFS} versus e/B plot for $i=0$ ($R_w=4B$ and $R_d=1B$ at $Dr=30\%$)

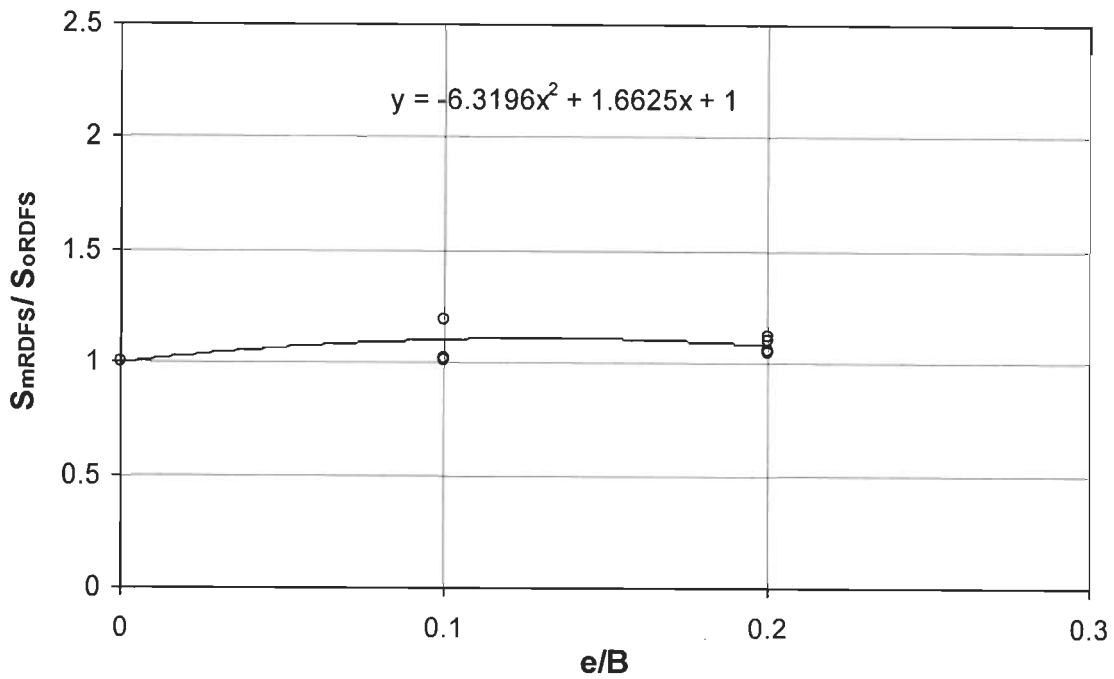


Figure 5.57 S_{mRDFS} / S_{oRDFS} versus e/B plot for $i=0$ ($R_w=4B$ and $R_d=1B$ at $Dr=30\%$)

Table 5.11 Settlement & Tilt Computation at Factor of Safety 2 & 3 for Fibrillated Fibers under Eccentric Inclined Load, for Load Inclination of 10^0

					FOS=2	FOS=2	FOS=2	FOS=2	FOS=3	FOS=3	FOS=3	FOS=3
Rw	Rd	χ_w %	i	e/B	S_e	$\frac{S_{eRDFS}}{S_{oRDFS}}$	S_m	$\frac{S_{mRDFS}}{S_{oRDFS}}$	S_e	$\frac{S_{eRDFS}}{S_{oRDFS}}$	S_m	$\frac{S_{mRDFS}}{S_{oRDFS}}$
4	1	0.5	0	0	2.6	1.00	2.60	1.00	1.45	1.00	1.45	1.00
4	1	1	0	0	2.6	1.00	2.60	1.00	1.45	1.00	1.45	1.00
4	1	0.5	10	0	2.55	0.98	2.55	0.98	1.4	0.97	1.4	0.97
4	1	1	10	0	2.58	0.99	2.58	0.99	1.42	0.98	1.42	0.98
4	1	0.5	10	0.1	2.53	0.97	2.90	1.12	1.33	0.92	1.58	1.09
4	1	1	10	0.1	2.54	0.98	3.10	1.19	1.32	0.91	1.58	1.09
4	1	0.5	10	0.2	2.52	0.97	2.90	1.12	1.3	0.90	1.6	1.10
4	1	1	10	0.2	2.53	0.97	3.00	1.15	1.3	0.90	1.5	1.03

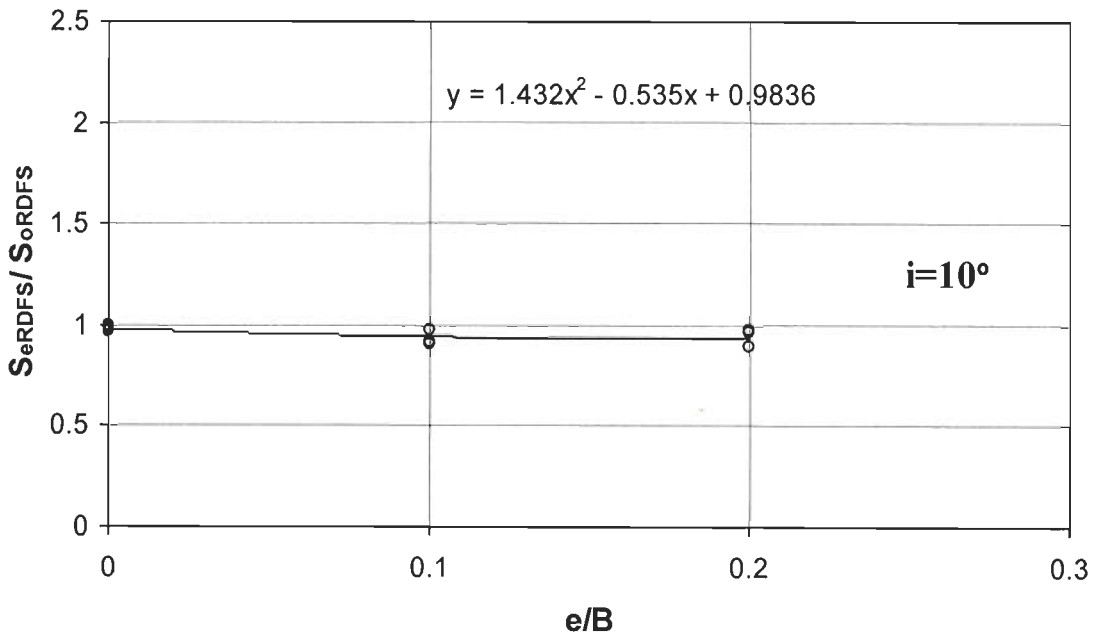


Figure 5.58 S_{eRDFS} / S_{oRDFS} versus e/B plot for $i=10^0$ ($R_w=4B$ and $R_d=1B$ at $D_r=30\%$)

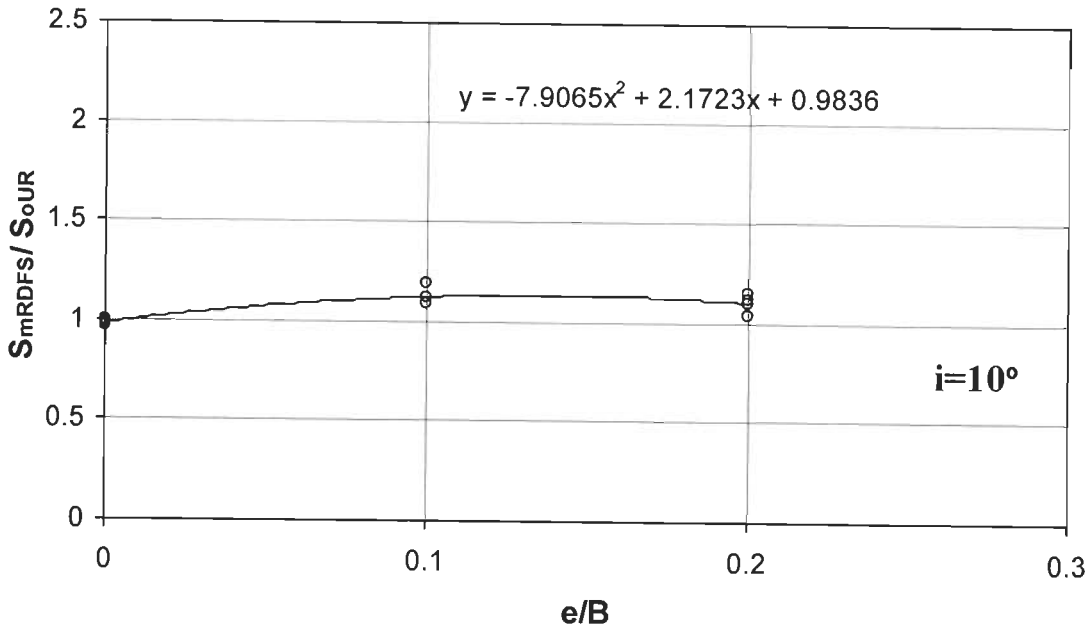


Figure 5.59 S_{mRDFS} / S_{oRDFS} versus e/B plot for $i=10^\circ$ ($R_w=4B$ and $R_d=1B$ at $D_r=30\%$)

Table 5.12 Settlement & Tilt Computation at Factor of Safety 2 & 3 for Fibrillated Fibers under Eccentric Inclined Load, for Load Inclination of 20°

Rw	Rd	$\chi_w\%$	i	e/B	FOS=2	FOS=2	FOS=2	FOS=2	FOS=3	FOS=3	FOS=3	FOS=3
					S_e	$\frac{S_{eRDFS}}{S_{oRDFS}}$	S_m	$\frac{S_{mRDFS}}{S_{oRDFS}}$	S_e	$\frac{S_{eRDFS}}{S_{oRDFS}}$	S_m	$\frac{S_{mRDFS}}{S_{oRDFS}}$
4	1	0.5	0	0	2.6	1.00	2.60	1.00	1.45	1.00	1.45	1.00
4	1	1	0	0	2.6	1.00	2.60	1.00	1.45	1.00	1.45	1.00
4	1	0.5	20	0	2.54	0.98	2.54	0.98	1.4	0.97	1.4	0.97
4	1	1	20	0	2.56	0.98	2.56	0.98	1.42	0.98	1.42	0.98
4	1	0.5	20	0.1	2.5	0.96	2.90	1.12	1.4	0.97	1.6	1.10
4	1	1	20	0.1	2.52	0.97	2.98	1.15	1.4	0.97	1.62	1.12
4	1	0.5	20	0.2	2.25	0.87	2.73	1.05	1.32	0.91	1.64	1.13
4	1	1	20	0.2	2.36	0.91	2.80	1.08	1.28	0.88	1.52	1.05

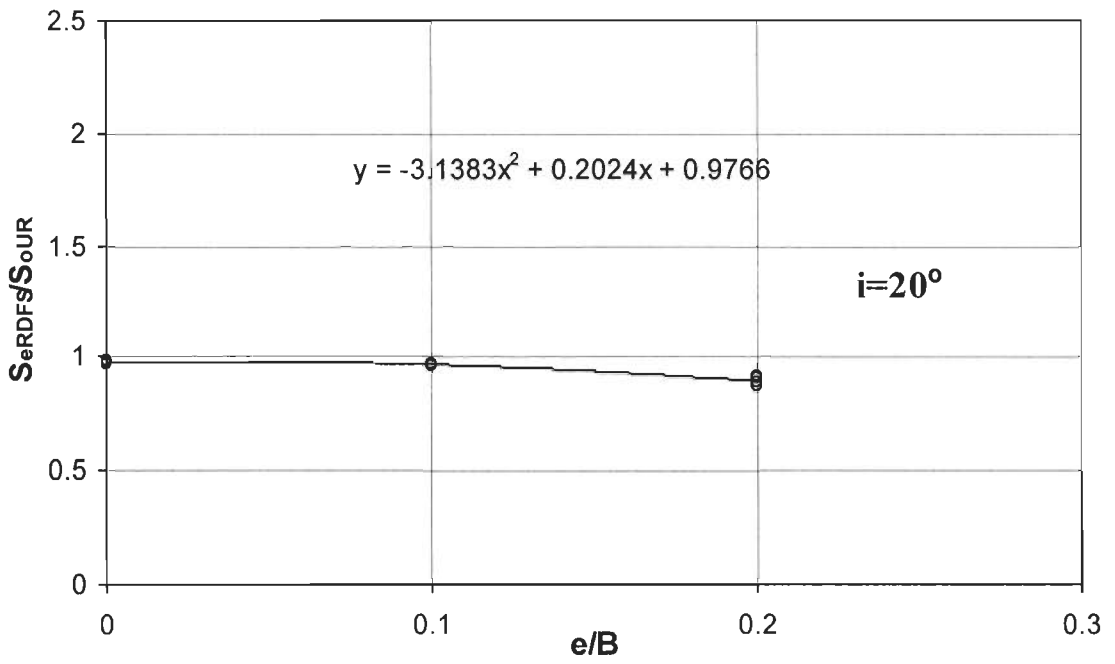


Figure 5.60 S_{eRDFS} / S_{oRDFS} versus e/B plot for $i=20^\circ$ ($R_w=4B$ and $R_d=1B$ at $D_r=30\%$)

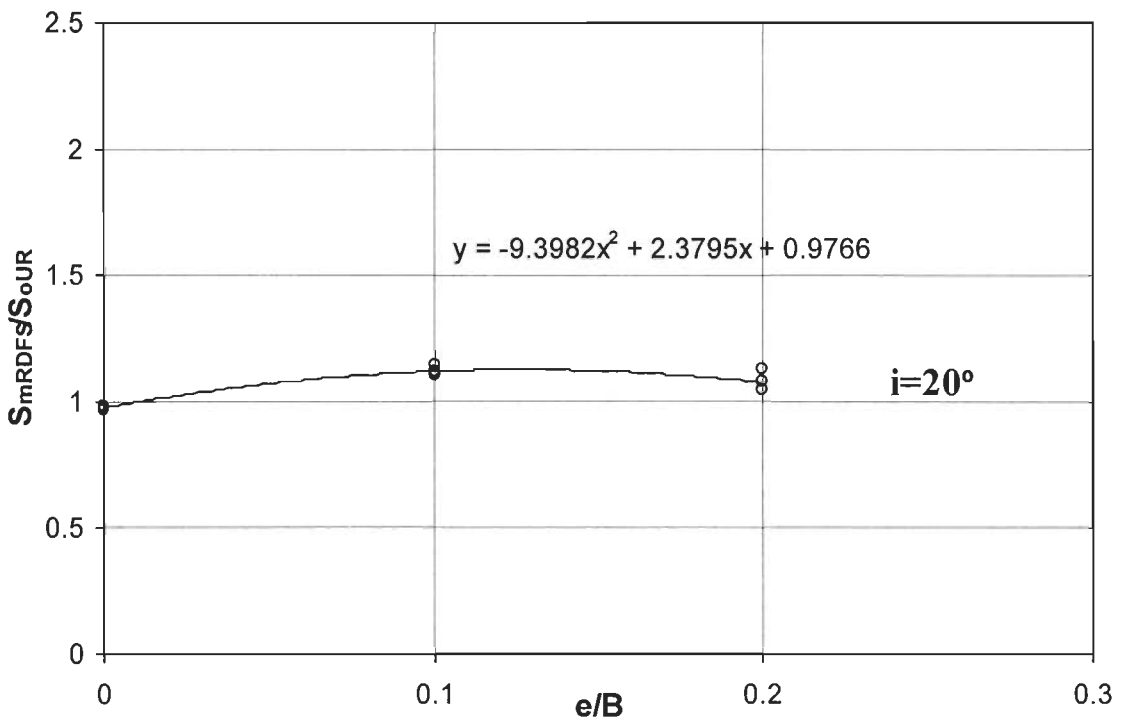


Figure 5.61 S_{mRDFS} / S_{oRDFS} versus e/B plot for $i=20^\circ$ ($R_w=4B$ and $R_d=1B$ at $D_r=30\%$)

It is evident from tables 5.10 to 5.12 and figures 5.56, 5.58 and 5.60 that almost same value is obtained for S_{eRDFS} / S_{oRDFS} irrespective of factor of safety, fiber content, load eccentricity and inclination. S_{eRDFS} / S_{oRDFS} can be expressed by following simple relation considering results slightly on safer side.

$$\frac{S_{eRDFS}}{S_{oRDFS}} = 1 \quad (5.10)$$

similarly for S_{mRDFS} / S_{oRDFS}

$$\frac{S_{mRDFS}}{S_{oRDFS}} = 1.1 \quad (5.11)$$

Above relationship was found valid for $R_w = 6B$ and $R_d = 1B$ and $R_d = 2B$ and $R_d = 1B$ also. Same relationship was found for 50% and 70% relative density data also.

5.7 VALIDATION OF MODEL DEVELOPED FOR PREDICTED BEARING CAPACITY – SETTLEMENT – TILT BEHAVIOUR

Finally, the real test, of how good the resulting regression model is depends on the ability of the model to predict the dependent variable for observation on the independent variables that were not used in estimating the regression coefficients. The general applicability of the models for estimating BCR, settlement and tilt have been tested with additional 34 experimental data on RDFS that were not used in developing the model. The results are presented in Table 5.13. A comparison of predicted versus experimental (observed) values of BCR is shown in figure 5.62. It is found that predicted values are in good agreement with observed values. Thus models developed for BCR are free from footing size effect and can be used for prototype foundations.

Table 5.13 Observed and Predicted BCR values using models developed by 75 mm width footing data for footing sizes (B) of 50 mm, 100 mm and 150 mm

Sl. No.	D_r (%)	χ_w (%)	Rw	Rd	e/B	i	Width of footing (mm)	BCR Observed	BCR Predicted
1	30	1	2	1	0	0	50	4.1	4
2	30	1	10	2	0	0	50	7	6.9
3	30	0.5	10	2	0	0	50	6.1	5.2
4	50	1	2	1	0	0	50	3.3	3.6
5	70	1	2	1	0	0	50	3.5	3.9
6	30	1	10	5	0	0	50	9	9.7
12	70	1	10	5	0	0	50	7.9	9.3
13	70	1	10	1	0	0	50	3.5	5
14	30	1	2	1	0	0	100	4.1	4
15	30	1	10	2	0	0	100	5.2	6.9
16	30	0.5	10	2	0	0	100	3.4	5.2
17	50	1	2	1	0	0	100	3.5	3.6
18	70	1	2	1	0	0	100	2.9	3.9
19	30	1	10	5	0	0	100	9.0	9.7
20	30	1	6	1	0.2	20	100	9.9	9.9
21	30	1	2	1	0	0	150	3.8	4
22	30	1	10	2	0	0	150	5.8	6.9
23	30	0.5	10	2	0	0	150	4.2	5.2
24	50	1	2	1	0	0	150	3.8	3.6
25	70	1	2	1	0	0	150	3.9	3.9
26	30	1	10	5	0	0	150	7.0	9.7
28	30	1	10	2	0.1	0	150	10.7	7.5
29	30	0.5	10	2	0.1	0	150	3.8	4.7
30	30	1	10	2	0.2	0	150	15.1	7.9
31	30	0.5	10	2	0.2	0	150	5.5	5
32	70	1	10	5	0	0	150	9.5	9.3
33	70	1	10	1	0	0	150	4.2	4.8
34	70	0.25	10	1	0	0	150	2.4	2.3

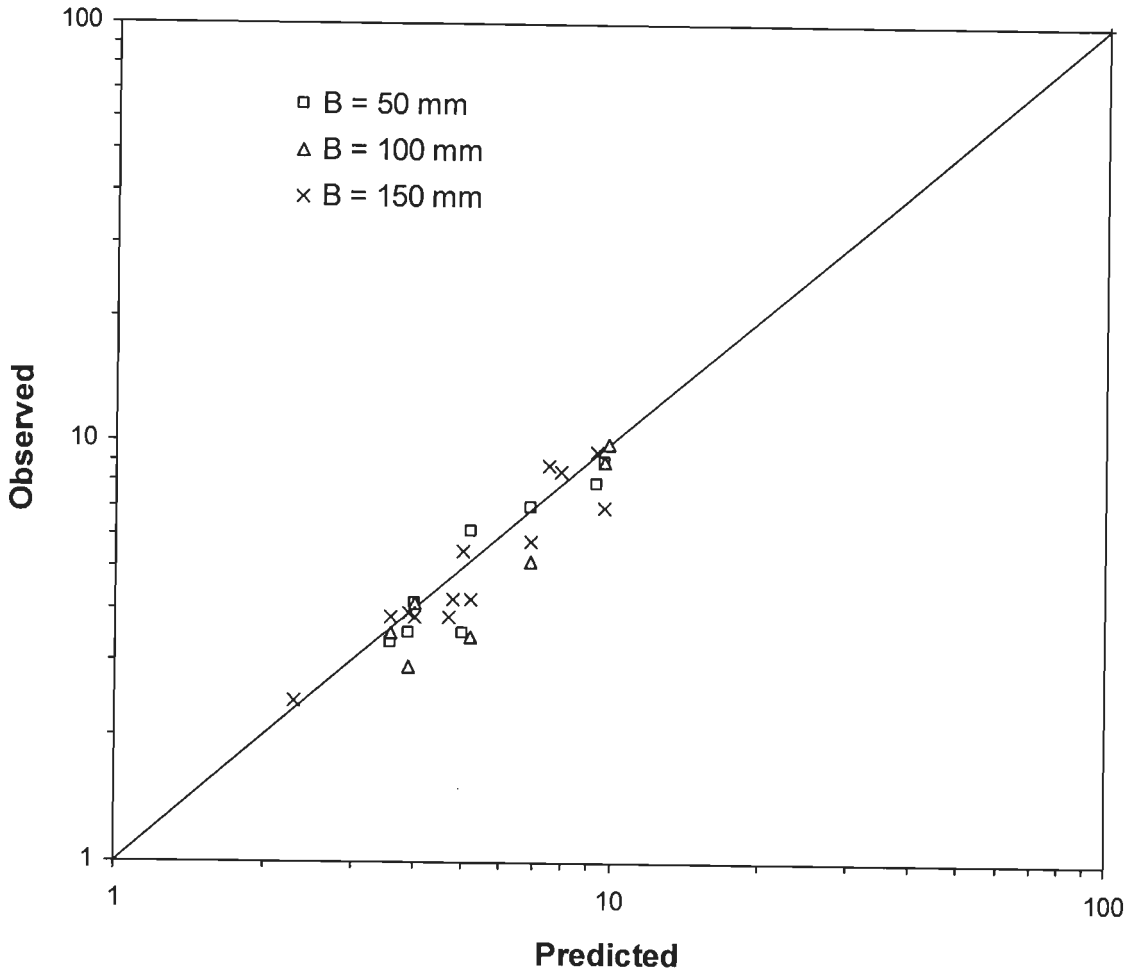


Figure 5.62 Observed BCR versus Predicted BCR for footing sizes (B) of 50 mm, 100 mm and 150 mm

To predict settlement of footing resting on RDFS, settlement data of different size of footing is shown in Table 5.14. This table shows settlement computation at factor of safety 1,2 & 3 for 1000 Denier 50 mm fibrillated fibers under central-vertical load for $R_w=2B$ and $R_d=1B$, for different width of footing at $D_r=30\%$. From Table 5.14, it is evident that $S_{o\ RDFS}/S_{o\ UR}$ values are less than 1.7 or nearly equal to 1.7. The equation 5.7 can be used for predicting settlement of footings resting on RDFS for prototype foundations.

Table 5.14 Settlement Computation at Factor of Safety 1,2 & 3 for 1000Denier 50 mm Fibrillated Fibers under Central-Vertical Load for $R_w=2B$ and $R_d=1B$, for different width of footing at $D_r=30\%$

B (mm)	D_r (%)	R_w	R_d	χ_w (%)	FOS=1		FOS=2		FOS=3	
					S_o (mm)	$\frac{S_{oRDFS}}{S_{oUR}}$	S_o (mm)	$\frac{S_{oRDFS}}{S_{oUR}}$	S_o (mm)	$\frac{S_{oRDFS}}{S_{oUR}}$
50	30	-	-	0 (UR)	5	-	0.95	-	0.48	-
50	30	2	1	1	5	1	1.70	1.78	0.86	1.79
50	70	-	-	0(UR)	5	-	1.3	-	0.75	-
50	70	2	1	1	5	1	2.0	1.54	1.3	1.73
100	30	-	-	0 (UR)	10	-	2.7	-	1.5	-
100	30	2	1	1	10	1	3.75	1.4	2.1	1.4
100	70	-	-	0 (UR)	10	-	2.5	-	1.3	-
100	70	2	1	1	10	1	3.5	1.4	1.84	1.4
150	30	-	-	0(UR)	15	-	4.9	-	2.7	-
150	30	2	1	1	15	1	6.8	1.4	4.0	1.48

5.8 ILLUSTRATIVE EXAMPLES

Two examples are presented to illustrate the procedure for designing strip footing resting on RDFS by using design equations developed.

5.8.1 Strip Footing on RDFS under Central-Vertical Load

Design Example 1

Design a strip footing resting on sand to carry a central vertical load ' P_v ' of 300 kN/m. The density of the sand is 15 kN/m^3 and angle of internal friction is 35° . The

pressure settlement curve for a strip footing of 60 cm width on sand is given in the figure

5.63. Footing width is restricted to 1m.

Case I: Central Vertical load only and surface footing, $D_f = 0$

$$P_v = 300 \text{ kN/m}, \quad \phi = 35^\circ, \quad \gamma = 15 \text{ kN/m}^3$$

$$B = 1 \text{ m fixed}, \quad N_\gamma = 45.41 \text{ (Terzaghi)}$$

$$q_u = 0.5 \gamma \cdot B \cdot N_\gamma = 0.5 \times 15 \times 1 \times 45.41 \\ = 340.6 \text{ kPa}$$

$$\text{F.O.S. against shear failure} = \frac{340.6}{300} = 1.1 < 3 \quad \text{not safe}$$

$$\text{Desired B.C.R.} = \frac{3 \times 300}{340.6} = 2.64 \approx 2.7 \text{ (for F.O.S. = 3)}$$

From load settlement curve of field plate load test it appears that existing ground is in dense condition thus equation 5.4 is used for design.

$$\text{Option I} \quad \text{BCR} = 1.4 (\chi_w \%)^{0.57} (\text{Rd/B})^{0.44} (\text{Rw/B})^{0.14} (l/d)^{0.2}$$

$$\text{Rd/B} = 1, \text{ Rw/B} = 2, \quad l/d = 125$$

$$2.7 = 1.4 (\chi_w \%)^{0.57} (1)^{0.44} (2)^{0.14} (125)^{0.2}$$

$$\chi_w \% = 0.43, \text{ provide } 0.45\%$$

$$\text{Amount of fibers / m} = 2 \text{ m} \times 1 \text{ m} \times 15 \frac{\text{kN}}{\text{m}^3} \times \frac{0.45}{100}$$

$$= 0.0675 \text{ kN} \times 2 \approx 6.75 \text{ kg} \times 2 = 13.5 \text{ kg}$$

$$\text{Cost} = 2 \times 6.75 \times 120 = 2 \times \text{Rs. } 810 / \text{m} = \text{Rs. } 1620 / \text{m}$$

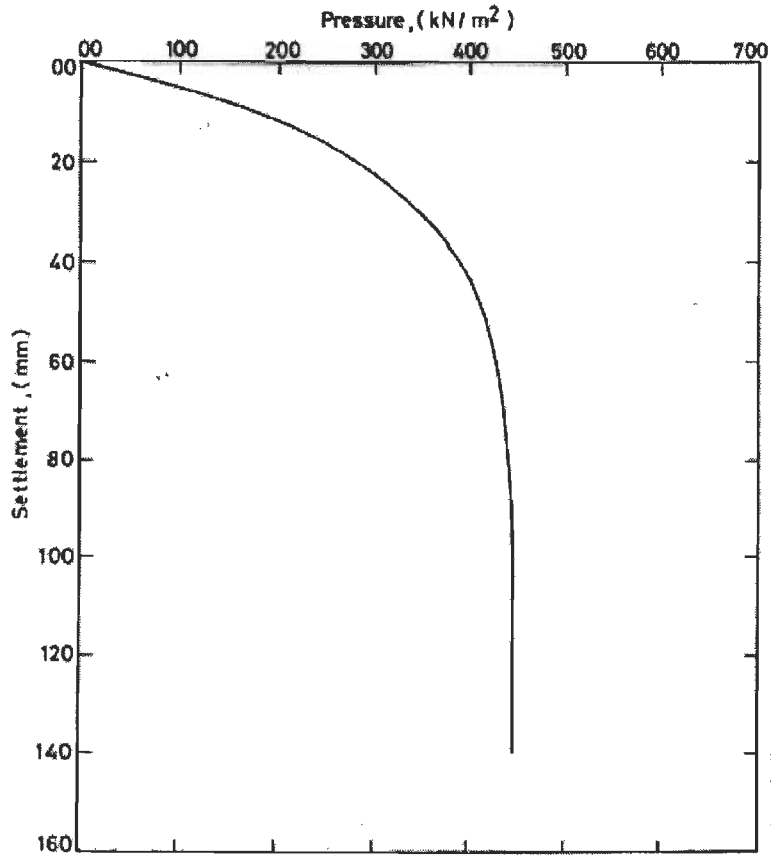


Figure 5.63 Pressure - settlement curve for strip footing of 60 cm width

Option-II $R_d / B = 0.5$ $\frac{R_w}{B} = 2$ $l/d = 125$

$$2.7 = 1.4 (\chi_w \%)^{0.57} (0.5)^{0.44} (2)^{0.14} (l/d)^{0.2}$$

$$\chi_w \% = 0.7$$

Provide 0.7% fiber content

$$\text{Amount of fibers / m} = 2 \text{ m} \times 0.5 \times 15 \times \frac{0.7}{100}$$

$$= 0.105 \text{ kN} = 10.5 \text{ kg}$$

$$\text{Cost} = \text{Rs. } 1260 / \text{m}$$

Option II is more economical, therefore providing higher fiber content in shallow depth is more economical.

Pressure intensity on footing for F.O.S. 3

$$= \frac{900}{3 \times 1 \text{ m} \times 1 \text{ m}} = 300 \text{ kN/m}^2$$

For unreinforced sand for same factor of safety pressure is $\frac{340.6}{2} = 114 \text{ kPa}$.

From plate load test data of 60 cm size plate corresponding to pressure intensity of 114 kN/m² settlement is 6 mm.

Settlement of 1 m wide foundation for same pressure intensity on sand is

$$S_f = S_p \left[\frac{B_f (B_p + 30)}{B_p (B_f + 30)} \right]^2$$

$$= 6 \times \left[\frac{100(60 \times 30)}{60(100 + 300)} \right]^2$$

Thus $S_{oUR} \cong 8 \text{ mm}$

Settlement for footing resting on RDFS

$$\frac{S_{oRDFS}}{S_{oUR}} = 1.7$$

$$S_{oRDFS} = 8 \times 1.7 = 13.6 \text{ mm} < 50 \text{ mm}$$

O.K.

Case II: Footing placed at depth of 0.5 B below ground level

$$D_f = 0.5 B = 0.5 \text{ m}$$

$$\begin{aligned} \text{Desired, } q_u &= 900 = 0.5 \cdot \gamma \cdot B \cdot N_\gamma + \gamma \cdot D_f \cdot N_q \\ &= 0.5 \times 15 \times 1 \times N_\gamma + 15 \times 0.5 \times N_q \\ &= 7.5 \times N_\gamma + 7.5 N_q \\ &= 7.5 (N_\gamma + N_q) \end{aligned}$$

for $\phi = 38^\circ$ $N_q = 48.93$ $N_\gamma = 64.7$

$$N_\gamma + N_q = 113$$

$$\phi = 39^\circ \quad N_\gamma + N_q = 56 + 77 = 133$$

Say target $\phi = 39^\circ, N_\gamma = 77$

Required q_u for surface footing

$$q_u = 0.5 \times \gamma \times 1 \times 77 = 577.5$$

Required $BCR = \frac{577.5}{340.6} = 1.7,$

Selecting, $R_d / B = 0.5,$ $\frac{R_w}{B} = 2$ and $l/d = 125$

$$1.7 = (1.4) \cdot (\chi_w\%)^{0.57} (0.5)^{0.44} (2)^{0.14} (125)^{0.2}$$

$$\chi_w\% = 0.37 \approx 0.4\%$$

Thus 0.4% is sufficient

5.8.2 Strip Footing on RDFS under Eccentric - Inclined Load

Design Example 2

Design a strip footing to carry a central vertical load ' P_v ' of 200 kN/m, a horizontal shear load ' P_h ' of 35 kN/m and moment M of 20 kN/m. The density of sand is 15 kN/m³ and angle of internal friction is 35°. The pressure settlement curve for a strip footing of 60 cm width on sand is given in the figure 5.63.

(i) Surface footing taking $B = 1$ m width footing

(ii) $e = \frac{M}{P_v} = \frac{20}{200} = 0.1m$

(iii) Equivalent eccentric - inclined load P

$$P = \sqrt{200^2 + 35^2} = 203 \text{ kN/m}$$

(iv) Inclination of eccentric - inclined load from vertical

$$i = \tan^{-1} \left(\frac{P_h}{P_v} \right) = \tan^{-1} \left(\frac{35}{200} \right) = 9.93^\circ \approx 10^\circ$$

(v) $q_u = 0.5 \gamma \cdot B \cdot N_\gamma \cdot R_{e\gamma} \cdot R_{i\gamma}$

$$= 0.5 \times 15 \times 1 \times 45.41 \times 0.64 \times 0.51$$

$$= 111.64 \text{ kN/m}^2$$

$$\text{F.O.S. against shear} = \frac{111.64}{203} = 0.55 < 3 \quad \text{not safe}$$

$$\text{Desired BCR} = \frac{203 \times 3}{111.64} \cong 5.5$$

$$\text{BCR} = 0.9 (\chi_w\%)^{0.71} (R_d/B)^{0.45} (R_w/B)^{0.2} (1.04)^i (3.2)^{e/B} (l/d)^{0.18}$$

$$\text{Selecting} \quad R_d/B = 1 \quad R_w/B = 4$$

$$\text{BCR} = 0.9 \times (\chi_w\%)^{0.71} \times 7.4 = 5.5$$

$$\chi_w\% = 0.754\%$$

Say provide $\chi_w\% = 0.8\%$ in 4B width and 1B deep.

$$\text{Pressure intensity on actual footing} = \frac{203 \times 3}{3 \times 1 \times 1} = 203 \text{ kN/m}^2 \text{ for a factor of safety of 3.}$$

From plate load test data of 60 cm size plate settlement is 6 mm corresponding to a pressure of 114 kN/m² for same factor of safety of 3, under central – vertical load. For 1m wide footing on sand, under central vertical load.

$$S_f = 6 \times \left[\frac{100(60 + 3)}{60(100 + 300)} \right]^2$$

$$= 8 \text{ mm}$$

Thus $S_{oUR} = 8 \text{ mm}$.

For footing on RDFS under central vertical load

$$\frac{S_{oRDFS}}{S_{oUR}} = 1.7 \Rightarrow S_{oRDFS} = 1.7 \times 8 = 13.6 \text{ mm}$$

$$\frac{S_{eRDFS}}{S_{oRDFS}} = 1 \Rightarrow S_{eRDFS} = 13.6 \text{ mm}$$

$$\frac{S_{mRDFS}}{S_{oRDFS}} = 1.1 \Rightarrow S_{mRDFS} = 1.1 \times 13.6 = 15 \text{ mm} < 50 \text{ mm}$$

$$e = 0.1 \text{ m}$$

$$S_{int} = \frac{S_{mRDFS} - S_{eRDFS}}{\frac{B}{2} - e} = \frac{(15 - 13.6) \times 10^{-3}}{(0.5 - 0.1)} \quad \text{O.K.}$$

$$t = 0.2^0 < 1^0 \quad \text{O.K.} \quad \text{Hence, design is safe.}$$

6.1 GENERAL

In this chapter a methodology has been presented, to predict the pressure - settlement characteristic of strip footing under central - vertical loads resting on RDFS, using its constitutive laws.

6.2 ANALYSIS OF STRIP FOOTING ON RDFS

6.2.1 Introduction

In general, settlement is the governing criterion for designing a footing resting on granular material. Usually, for a given settlement, the load that a footing can carry is obtained either by using plate load test data or standard penetration test. Prediction of pressure-settlement characteristics becomes necessary in advance for footing resting on improved ground with randomly reinforced sand to workout its structural suitability and economic viability. In this chapter the method proposed by Sharan (1977) and Prakash et al. (1984) based on constitutive laws of soil, which gives pressure-settlement characteristics of a footing resting on unreinforced soil, has been extended to predict pressure - settlement characteristic of strip footing under central - vertical loads resting on RDFS. The mathematical model proposed by Kondner (1963) has been used to describe the constitutive laws of the soil. Sharan (1977) and Prakash, et al., (1984) studied the behaviour of surface strip and square footings on clay and sand, subjected to

central - vertical load using the non-linear constitutive laws of soils. One of the main findings of their studies was that, the pressure versus average settlement characteristics of a flexible smooth footing was practically the same as the average pressure versus average settlement of the rigid rough footing.

The proposed analysis, as outlined in the subsequent section, makes use of the theory of elasticity for calculation of stresses, whereas, the stress - strain relations of soil required for the calculation of strains, have been obtained from the experimental data.

This method has two advantages:

- (i) It eliminates the use of costly field tests, and (ii) it gives directly the pressure–settlement characteristics of actual footing.
- (ii) The proposed method of the analysis has been attempted to predict the model test results of this study and reported by Mercer et al. (1984), and McGown et al. (1985) in the literature.

6.2.2 Assumptions

Assumptions made in the analysis are as given below:

The analysis has been developed for studying the pressure–settlement characteristics of strip footings resting on RDFS using non-linear constitutive laws of soil. Constitutive laws of a soil define its mechanical behaviour, and is of prime importance for analysing almost all applied non-linear problems of soil mechanics. One of the popular models for describing a constitutive law of a soil is two constants hyperbola suggested by Kondner (1963), Kondner and Zelasko (1963). The constants of this model can be obtained by performing triaxial tests on the RDFS simulating field conditions. The stress–strain behaviour of sands and RDFS is dependent on confining

pressure. This fact has been taken into account in developing the analysis. The analysis is based on the following assumptions:

- (i) The base of the footing has been assumed smooth, as the effect of roughness on pressure–settlement characteristics has been found very small (Sharan, 1977).
- (ii) RDFS is assumed to be an isotropic and semi-infinite medium.
- (iii) The footing is considered flexible, and therefore the contact pressure distribution is considered uniform.
- (iv) Stresses in soil mass have been computed using theory of elasticity. Strains have been computed from the hyperbolic soil model defined by Kondner (1963).
- (v) The soil mass supporting the footing has been divided into a large number of thin horizontal layers, to a depth beyond which the stresses become very small. Proposed method is applicable when RDFS is provided in large area upto influence zone below footing.
- (vi) The effect of soil weight has been taken into consideration for the determination of stresses in soil mass. The vertical stress component due to weight of soil has been taken as γz , where γ is the unit weight of soil and z is the depth to centre of soil layer. The horizontal stress components (in the x and y – directions) due to the weight of the soil have been taken equal to $K_o\gamma z$, where K_o is the coefficient of earth pressure at rest ($K_o = 1 - \sin \phi$), ϕ being the angle of internal friction.
- (vii) A factor of safety ‘F’ has been introduced, so that, at all stress levels, the following relationship is satisfied.

$$\frac{q_u}{q} = \frac{\sigma_v}{\sigma_1 - \sigma_3} = F \tag{6.1}$$

where,

q_u = ultimate bearing capacity

q = intensity of surface load

σ_u = ultimate stress from hyperbola relation ($1/b$)

σ_1 and σ_3 , = the major and minor principal stresses due to q and the weight of the soil

(viii) Modulus of elasticity (E_s) at stress levels of σ_u/F has been taken as secant modulus (Figure 6.1).

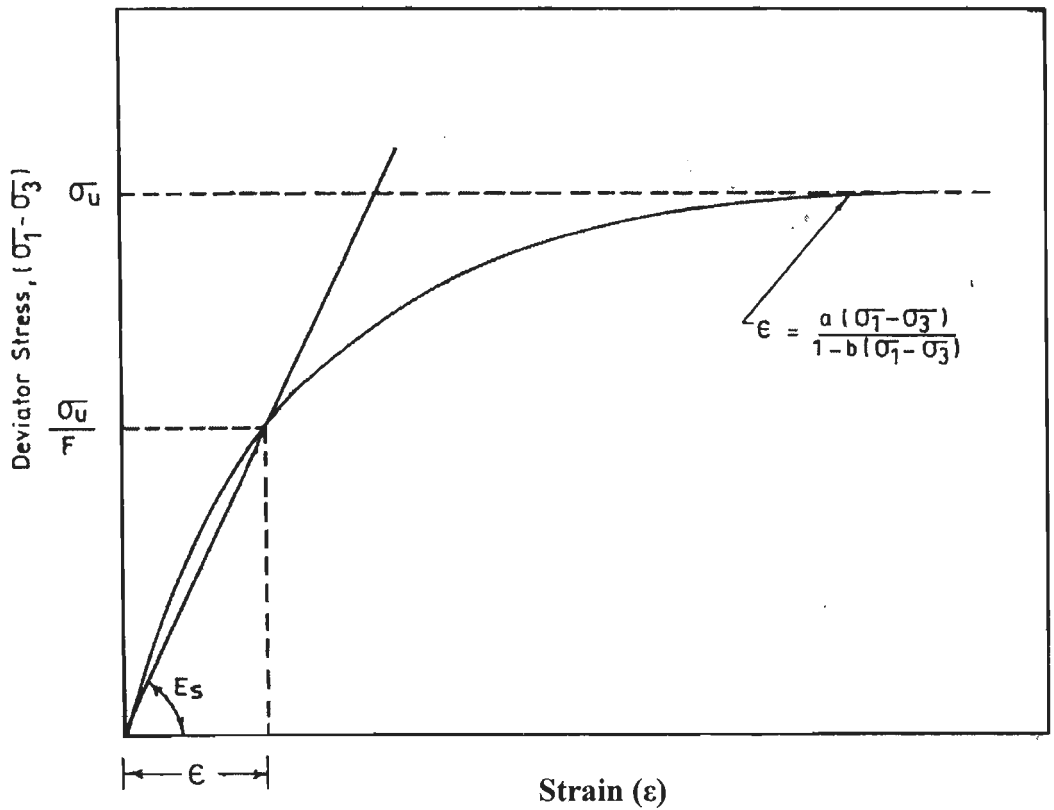


Figure 6.1 Hyperbolic stress-strain representation (Kondner, 1963)

The strain at stress level of (σ_u/F) is given by;

$$\text{Strain} = \frac{a(\sigma_u/F)}{1-b(\sigma_u/F)} \quad (6.2)$$

hence,

$$E_s = \frac{\text{Stress}}{\text{Strain}} = \frac{1-b(\sigma_u/F)}{a} \quad (6.3)$$

where, $\sigma_u (=1/b)$ and $E_s (=1/a)$ are dependent on the confining pressure.

6.2.3 Prediction of Pressure – Settlement Curve

The proposed analytical procedure for predicting the pressure – settlement characteristics of strip footing, subjected to central – vertical load resting on sand or RDFS is described in the following steps.

Step 1: The whole RDFS supporting the footing, of width B , is divided into a large number of thin layers e.g., n layers, up to a depth of $5B$ beyond which the vertical stresses become almost negligible (Figure 6.2). The thickness of each layer was taken as $0.25B$. The normal and shear stresses at the centre of each layer of soil mass along the vertical section have been computed using theory of elasticity (Poulos and Davis, 1974). The effect of weight of soil has been incorporated by adding γz to σ_z and $K_o \gamma z$ to σ_x , where $K_o = 1 - \sin \phi$. The value of angle of internal friction ϕ is determined from drained triaxial tests on RDFS.

Step 2: The principal stresses (σ_1, σ_3) at a point in the RDFS and their directions (θ_1, θ_3) with respect to vertical Z -axis (Figure 6.3) have been computed using equations of the theory of elasticity (Harr, 1966 and Poulos and Davis, 1974, presented by Sharan, 1977). Stresses for uniform vertical loading on an infinite strip are given below.

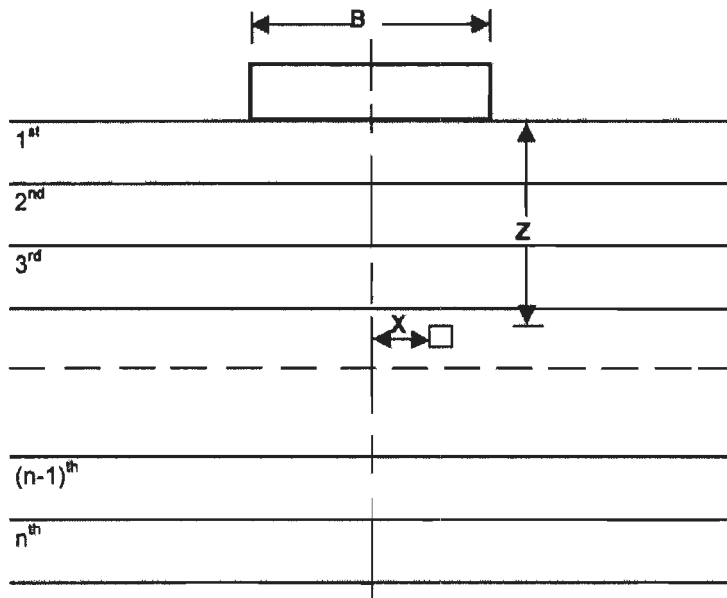


Figure 6.2 RDFS below footing divided into n layers

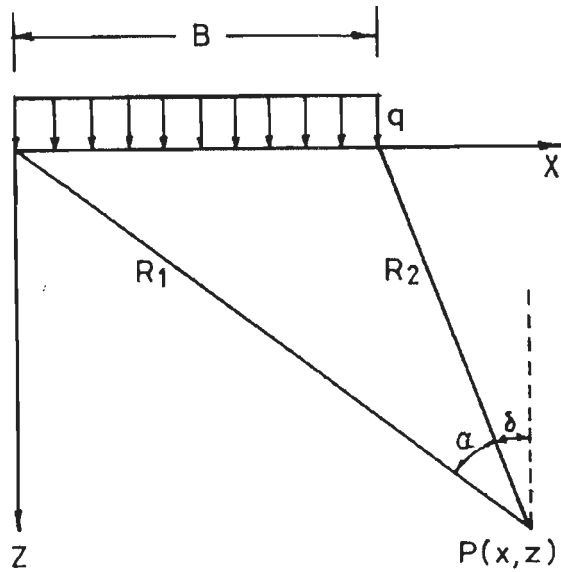


Figure 6.3 Uniform vertical loading on an infinite strip

$$\sigma_z = \frac{q}{\pi} [\alpha + \sin\alpha \cos(\alpha + 2\delta)] \quad (6.4)$$

$$\sigma_x = \frac{q}{\pi} [\alpha - \sin\alpha \cos(\alpha + 2\delta)] \quad (6.5)$$

$$\tau_{xz} = \frac{q}{\pi} [\sin\alpha \sin(\alpha + 2\delta)] \quad (6.6)$$

where; x and z are orthogonal coordinates

σ_z = vertical stress

σ_x = stress in direction of x-axis

τ_{xz} = shear stress

q = Uniform vertical load

$$\sigma_1 = \frac{\sigma_z + \sigma_x}{2} + \sqrt{\left[\frac{\sigma_z - \sigma_x}{2}\right]^2 + \tau_{xz}^2} \quad (6.7)$$

$$\sigma_3 = \frac{\sigma_z + \sigma_x}{2} - \sqrt{\left[\frac{\sigma_z - \sigma_x}{2}\right]^2 + \tau_{xz}^2} \quad (6.8)$$

$$\tan 2\theta = \frac{2\tau_{xz}}{\sigma_z - \sigma_x} \quad (6.9)$$

Positive value of θ is measured in counter clockwise with direction of σ_z , where σ_1 and σ_3 are major and minor principal stresses (Figure 6.4).

Step 3: The value of Poisson's ratio ' μ ' and the coefficient of earth pressure at rest ' K_0 ' have been obtained from the following relationships.

$$K_0 = 1 - \sin \phi \quad (6.10)$$

$$\mu = K_0 / (1 + K_0) \quad (6.11)$$

where,

ϕ = angle of internal friction of RDFS/ sand

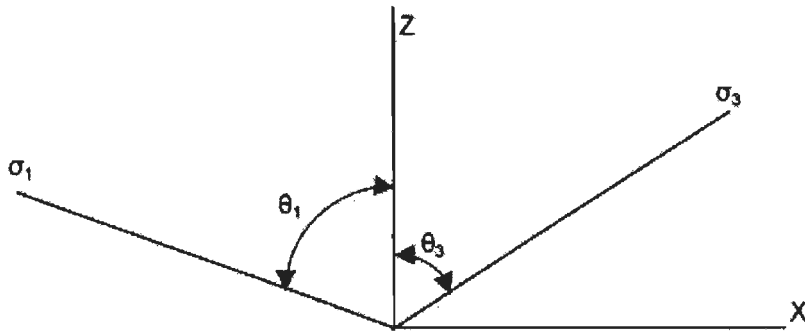


Figure 6.4 Principal stresses at a point and their directions in the RDFS

Step 4: The ultimate bearing pressure ' q_u ' for RDFS has been computed from the equations developed for computation of BCR in Chapter 5.

Step 5: The factor 'F' for the given surface load intensity 'q' has been obtained from the relation:

$$F = \frac{q_u}{q} \quad (6.12)$$

Step 6: Modulus of elasticity ' E_s ' has been determined by using the following equation:

$$E_s = \frac{1 - b(\sigma_u/F)}{a} \quad (6.13)$$

where, 'a' and 'b' are the constants of the hyperbola, values of which are dependent on the confining pressure.

Step 7: Principal strains ϵ_1 and ϵ_3 in each layer in the directions of principal stresses, i.e., the major and minor principal stresses (σ_1 and σ_3) respectively, can be computed using the following formulae.

$$\varepsilon_1 = (\sigma'_1 - \sigma'_3)/E_s \quad (6.14)$$

$$\varepsilon_3 = -\mu_2 \cdot \varepsilon_1 \quad (6.15)$$

where; $\mu_2 = \frac{-\sigma_3 + \mu_1\sigma_1}{\sigma_1 - \mu_1\sigma_3}$

$$\mu_1 = \frac{\mu}{1 - \mu}$$

μ = Poisson's ratio

and E_s = modulus of elasticity

Step 8: The strain in the vertical direction ε_z in each layer along a vertical section is computed using the following equation;

$$\varepsilon_z = \varepsilon_1 \cos^2\theta_1 + \varepsilon_3 \cos^2\theta_3 \quad (6.16)$$

where θ_1 and θ_3 are the directions of principal strains with respect to the vertical z-axis, as shown in Figure 6.4.

Step 9: The vertical settlement 's' of any layer along a vertical section is computed by multiplying the vertical strain ε_z in each layer by the thickness of the layer, dz.

$$s = \varepsilon_z dz \quad (6.17)$$

Step 10: The total settlement 'S' along any vertical section is computed by numerically integrating the expression up to the depth of influence.

$$S = \int_0^l \varepsilon_z dz \quad (6.18)$$

Step11: Settlements are computed for different applied load intensities by repeating step 1 through step 10. Consequently pressure versus settlement curves can be

obtained. The Total settlement is computed along all vertical sections for each pressure intensity.

Step 12: The average settlement is computed by dividing the area of settlement diagram by width of footing.

6.3 RESULTS AND VALIDATION OF PROPOSED METHOD

To validate proposed method for strip footing resting on unreinforced and RDFS, results of experimental data reported in this thesis and literature are utilised. Results have been obtained using the above procedure for unreinforced sand and RDFS by using its constitutive laws. The properties and the hyperbolic constants (a and b) for Solani river sand are taken from Saharan (1977) and Agarwal (1986).

Predicted pressure – settlement (S_e) curve, for strip footing resting on Solani river sand obtained for $B = 50$ mm is presented in Figure 6.5 and comparison with experimental pressure – settlement data is also presented. Predicted values of settlement have shown good agreement with experimental values. This again validates its applicability to unreinforced sand.

To validate proposed method for RDFS, triaxial tests results reported in Chapter 4 are utilized to predict pressure – settlement curve for strip footing ($B = 75$ mm) on RDFS ($D_r=30\%$) reinforced with 1%, 20D 20mm, monofilament polypropylene fiber (Figure 6.6). Experimental pressure – settlement curve is also obtained and plotted in same figure. Predicted values of settlement have shown good agreement with experimental values. This validates applicability of proposed method to RDFS.

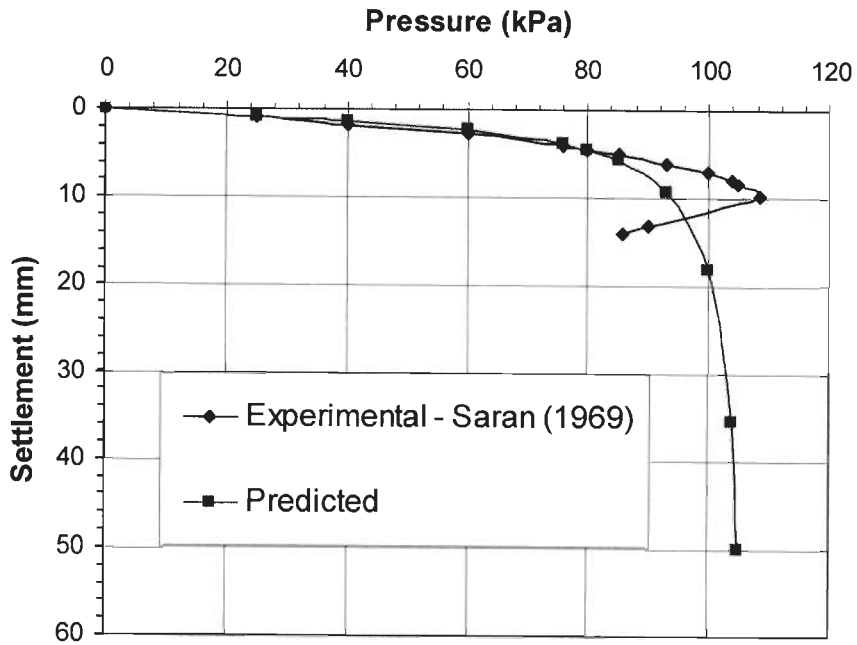


Figure 6.5 Pressure versus settlement curves for strip footing on Ranipur Sand ($B=50$ mm, $D_r=84\%$), considering 5B Depth

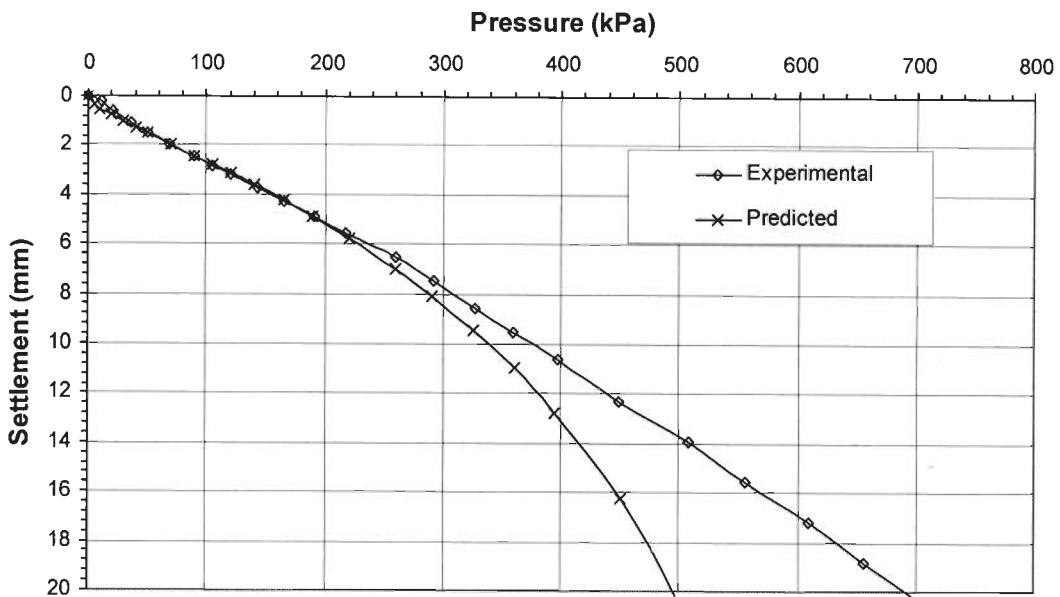


Figure 6.6 Pressure versus settlement curves for strip footing ($B = 75$ mm) on RDFS 1% fiber content of 20D 20mm ($D_r=30\%$)

The proposed method of the analysis has been attempted to predict the model test results of Mercer et al. (1984) and McGown et al. (1985) reported in the literature. Transformed Hyperbolic Stress-Strain plot for Mid Ross sand and randomly reinforced with 0.18% mesh elements were worked and plotted in Figure 4.24.

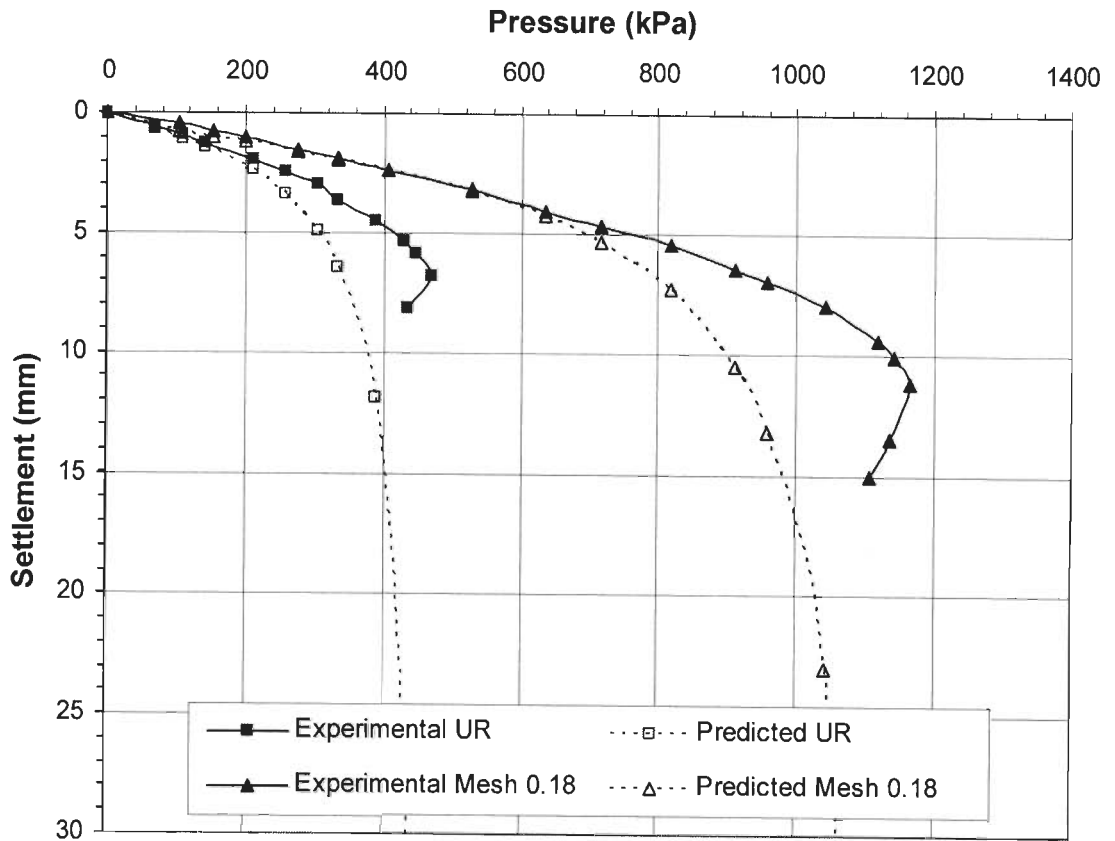


Figure 6.7 Pressure - settlement curve for strip footing ($B = 75$ mm) resting on Mid Ross sand with 0.18% mesh elements considering $4B$ depth in 40 layers (experimental data from McGown et al., 1985)

A good agreement, between experimental results reported in literature and predicted settlements, is obtained for both footing resting on unreinforced sand and sand randomly reinforced with 0.18% mesh elements as shown in Figure 6.7.

6.4 SUMMARY

A good agreement, between experimental results of this study and reported in literature and predicted settlements, is obtained. This suggests suitability of proposed method for predicting the pressure–settlement characteristics of a strip footing resting on RDFS.

In this chapter main findings are presented based on analysis and interpretation of test data carried out in earlier chapters. The findings are presented in the following sections:

7.1 STRENGTH –DEFORMATION CHARACTERISTICS

1. Fiber-reinforcement not only increases the shear strength of the soil, but also reduces the post-peak strength loss.
2. Main advantage of the polypropylene fiber reinforcement is the inducement of strain hardening behavior, even at large strain deformations.
3. RDFS samples with similar values of product of aspect ratio and fiber content ($\eta \cdot \chi_w$) have not only shown similar failure deviator stresses but also whole stress-strain curve. Selecting a high value of aspect ratio (η) may result in lower value of fiber content (χ_w) for a required strength of RDFS.
4. The relative density has significant influence on the shear strength of RDFS. At higher relative density shear strength is much higher compare to lower one.
5. Behaviour of RDFS is deformation (strain) dependent, and in most of the cases maximum or failure stress was not observed. Such cases would be the obvious choice for application in field.

7.2 FOOTING ON RDFS SUBJECTED TO CENTRAL – VERTICAL LOAD

1. In general, fibrillated fiber is best choice for its application to shallow foundation considering performance, cost and easy mixing. However, depending upon availability and cost the monofilament fiber may prove to be economical. Use of mesh elements from Netlon CE-121 in RDFS indicated that it is not a suitable alternative for bearing capacity improvement. However, mesh elements of Netlon Advance Turf (NAF) increases the behaviour of footing on RDFS comparable to polypropylene fibers.
2. The bearing capacity increases with increase in fibre content for all type of fibers and mesh elements. Depending upon mixing difficulties it is found that for monofilament and fibrillated fibers upper limit is 1%. For low fiber content, smaller denier is useful as it will give high strength. For high fiber content a suitable fiber denier should be chosen so that good mixing of fibers is achieved. For mesh elements (NAF), upper limit is 0.5%.
3. Mixing of fibers in soil plays an important role in improving its behaviour. It is found that there is an upper limit of fiber content beyond which proper mixing becomes difficult. It depends on the type of fiber.
4. Longer fibers performed better compare to smaller one. The 50 mm long fibers performed better compare to 20 mm and 10 mm fibers, keeping other factors same. For field applications 50 mm length is most suitable.
5. It was found that with decrease in denier (diameter) of fiber, BCR increases.
6. With increase in fiber content, over all pressure - settlement curve improved and shifted upward. Significant improvements in the bearing capacity and

reduction in the settlement of footing resting on RDFS was observed. Similar trends were observed at all three densities. Pressure –settlement curves were almost linear and showing strain hardening effect. No failure was observed even up to 30% settlement ratio.

7. RDFS is equally applicable in loose and dense condition. Bearing capacity ratio (BCR) values in loose conditions are on an average 15% higher compare to dense condition. However, absolute increase in bearing pressure is much more in dense condition compared to in loose condition.
8. Below strip footing, significant improvements in bearing capacity take place within a depth of $3B$. To resist large deformations deeper layer of RDFS up to $5B$ also found effective.
9. It would be more beneficial to reinforce sand in shallow depths with high fiber content as compared to low fiber content for deeper depth.
10. No significant improvements were noticed by providing RDFS zone width (R_w) more than $6B$.
11. It is recommended to provide RDFS zone at least in $2B$ width. Providing RDFS in a depth of $0.5B$ and width of $2B$ below footing is found very effective and most economical. In this case BCR gets increased to around 2.5 for 1% fibrillated fibers. For higher increase in BCR one can select for deeper layer of RDFS (e.g. for 1% fiber content in $R_d=1B$ and $R_w=3B$, BCR may increase upto 5). Width of RDFS zone should not be more than optimum considering depth of RDFS layer. Providing RDFS below footing in zone of

2B deep and 3B wide found most effective beyond that range rate of improvements will be less compare to increased amount of fiber (cost).

12. Under submerged condition beneficial effects of RDFS remain same as in case of dry conditions.
13. One of the important findings is that RDFS may prove to be much economical compared to planar reinforcement if RDFS is provided in optimum zone below footing.
14. Another important finding is that BCR remains same for all footing widths. Results of field plate load test or model footing tests in dimensionless form (e.g. size of RDFS zone in terms of footing width, R_d and R_w ; percentage fiber content by weight of sand in RDFS zone etc.) can be used for prototype footings.
15. Model test results have been analyzed and correlations have been developed to predict the BCR and settlement of strip footing subjected to central – vertical load resting on RDFS, using the non-linear multiple regression analysis.

7.3 STRIP FOOTING ON RDFS SUBJECTED TO ECCENTRIC – INCLINED LOAD

1. Pressure-settlement behaviour of footings resting on un-reinforced sand under eccentric-inclined load was very poor; failure took place at very small deformations.

2. In case of RDFS, pressure–settlement behaviour improved substantially. There was no sudden decrease in bearing pressure with increase in settlement. Strain hardening behaviour was observed.
3. BCR keeps on increasing as load eccentricity and inclination increases. For eccentric-inclined loads beneficial effects of RDFS increased further in comparison to central–vertical loads.
4. Most optimum RDFS zone below footing for eccentric-inclined load is 6 B wide and 1 B deep below footing.
5. Settlement, tilt and horizontal displacement decreased substantially.
6. Randomly distributed fiber-reinforced sand, is a viable and effective ground improvement technique for especially for sites located in seismic area.
7. Model test results have been analyzed and correlations have been developed to predict the BCR, settlement and tilt of strip footing subjected to eccentric-inclined load resting on RDFS, using the non-linear multiple regression analysis.

7.4 PREDICTION OF PRESSURE – SETTLEMENT CURVE FOR STRIP FOOTING ON RDFS USING CONSTITUTIVE LAWS OF RDFS

1. A methodology has been developed to predict the pressure-vertical settlement characteristics of strip footing subjected to central – vertical load resting on RDFS, using the non-linear constitutive laws of RDFS. This approach, however, requires predetermination of the ultimate bearing capacity of footing resting on RDFS.

2. Comparison of the predicted settlements has shown very good agreement with observed (model test results of present work and reported in literature) settlements.
3. This approach is applicable when RDFS is provided in large zone covering whole influence zone below footing.

**SUGGESTIONS FOR FURTHER
RESEARCH WORK**

Present study is limited to behaviour of strip footing resting on randomly distributed fiber reinforced sand. Developed models in this study, using experimental data are limited in scope and taken as a first step in that direction. Behaviour of footing resting on RDFS is affected by large number of parameters and large number of experimentation is involved to study all aspects. To widen the scope of these models and study behaviour of different type of footings on different type of fiber reinforced soil, further research is recommended in the following areas.

- (1) Behaviour of footings resting on fiber reinforced silt and clay.
- (2) Behaviour of footings resting on randomly distributed fiber reinforced sand fills overlying on soft clays.
- (3) Behaviour of eccentrically-obliquely loaded footings on randomly distributed fiber reinforced sand fills overlying on soft clays.
- (4) Behavior of footings resting on RDFS for different shapes of footings.
- (5) Field tests on large size footings resting on RDFS.
- (6) Behaviour of footings on RDFS under dynamic loading.
- (7) Effect of inclusion of fibers on the liquefaction resistance.

REFERENCES

1. Adams, M.T. and Collin, J.G. (1997). "Large model spread footing load tests on geosynthetic reinforced soil foundation." *Journal of Geotechnical and Geoenvironmental Engineering*, ASCE, 123(1), 66 - 72.
2. Adi, A. D. (1996). "The use of polymeric mesh elements to strengthen a range of soil types" Ph.D. Thesis for University of Strathclyde, January 1996.
3. Agarwal, K.B. and Chandra, S. (1997). "Improvement in strength and bearing capacity of clay due to fibre reinforcement." *Indian Geotechnical Conference*, 1997, Vadodara, India, 269 – 272.
4. Agrawal, R.K. (1986). "Behaviour of shallow foundations subjected to eccentric-inclined loads." Ph.D. Thesis, University of Roorkee, Roorkee, U.P., India.
5. Akbulut, S., Arasan, S. and Kalkan, E. (2007). "Modification of clayey soils using scrap tire rubber and synthetic fibers." *Applied Clay Science*, in press, doi:10.1016/j.clay.2007.02.001.
6. Akinmusuru, J.O. and Akinbolade, J.A., (1981). "Stability of loaded footings on reinforced soil." *Journal of the Geotechnical Engineering*, ASCE, 107(6), 819 - 827.
7. Allan, M. L. and Kukacka, L. E. (1995). "Permeability of microcracked fibre-reinforced containment barriers." *Waste Management*, 15(2), 171-177.
8. Al-Refeai, T. and Al-Suhaibani, A., (1998). "Dynamic and static characterization of polypropylene fiber-reinforced dune sand." *Geosynthetics International*, 5(5), 443-458.
9. Al-Refeai, T.O. (1991). "Behaviour of granular soils reinforced with discrete randomly oriented inclusions." *J. Geotextiles and Geomembranes*, 10(4), 319-333.
10. Al-Smadi, M.M. (1998). "Behaviour of ring foundations on reinforced soil." Ph.D. Thesis, University of Roorkee, Roorkee, U.P., India.
11. Al-Wahab, R. M. and Al-Qurna, H. H. (1995). "Fiber reinforced cohesive soils for application in compacted earth structures." *Proceedings of Geosynthetics '95*, IFAI, Vol. 2, 433-446.

12. Al-Wahab, R. M. and El-Kedrah, M. A. (1995). "Using fibers to reduce tension cracks and shrink/ swell in compacted clay." *Geoenvironment 2000, Geotechnical Special Publication No. 46, ASCE, New York, Vol. 1, 791-805.*
13. Andersland, O.B. and Khattak A.S. (1979). "Shear strength of Kaolinite / fibre soil mixture." *Proc. 1st Int. Con. on Soil Reinforcement, Vol. I Paris, 11 – 16.*
14. Arenicz, R.M. and Choudhary, R.N. (1988). "Laboratory investigation of earth walls simultaneously reinforced by strips and random reinforcement." *Geotechnical Testing Journal, 11(4), 241-247.*
15. Bauer, G.E. and Fatani, M.N (1991). "Strength characteristics of sand reinforced with rigid and flexible elements." *Proc of 9th Asian Regional Conference on soil Mech. and Foundation Engg. Vol 1 Bangkok (Thailand), 471-474.*
16. Beena, K.S. (2002). "Study on engineering properties of coir pith mixed soil." *Indian Geotechnical Conference 2002, Allahabad, India.*
17. Benson, C.H. and Khire, M.V. (1994). "Reinforcing sand with strips of reclaimed high-density polyethylene." *Journal of Geotechnical Engineering, ASCE, 120(5), 838-855.*
18. Binquet, J. & Lee, K. L. (1975). "Bearing capacity tests on reinforced earth slabs." *Journal of Geotechnical Engineering Division, ASCE, 101, 1241–1255.*
19. Briaud, J.L. and Jeanjean, P. (1994). "Load settlement curve method for spread footings on sand." *Vertical and Horizontal Deformations of Foundations and Embankments, ASCE. Vol. 2, 1774-1804.*
20. Bueno, B. de S. (1997). "The Mechanical response of reinforced soils using short randomly distributed plastic strips." *Recent developments in Soil and Pavement Mechanics, Rotterdam, ISBN 9054108851, 401-407.*
21. Casagrande, M.D.T., Coop, M.R. and Consoli, N.C. (2006). "Behavior of a fiber-reinforced bentonite at large shear displacements." *Journal of Geotechnical and Geoenvironmental Engineering, ASCE, 132(11), 1505-1508.*
22. Cecich, V., Gonzales, L., Hoisaeter, A., Williams, J. and Reddy, K. (1996). "Use of shredded tires as lightweight backfill material for retaining structures." *Waste Management & Research, 14, 433-451.*

23. Charan, H.D. (1995). "Probabilistic analysis of randomly distributed fibre reinforced soil." Ph.D. Thesis, Deptt. of Civil Engg. I.I.T. Roorkee, Roorkee, India.
24. Choubane, B., Armaghani, J.M. and Ho, R.K. (2001). "Full scale laboratory evaluation of polypropylene fiber reinforcement of subgrade soils." Transportation Research Board Annual Meeting, Washington, D. C., 7-11 January 2001, Paper No. 01-2157.
25. Clark, J.I. (1998). "The settlement and bearing capacity of very large foundations on strong soils." The 1996 R. M. Hardy lecture." Canadian Geotechnical Journal, 35, 131-145.
26. Consoli, N.C., Casagrande, M.D.T. and Coop, M.R. (2005). "Effect of fiber-reinforcement on the isotropic compression behavior of sand." Journal of Geotechnical and Geoenvironmental Engineering, ASCE, 131(11), 1434-1436.
27. Consoli, N.C., Casagrande, M.D.T., Prietto, P.D.M. and Thome, A. (2003b). "Plate load test on fiber-reinforced soil." Journal of Geotechnical and Geoenvironmental Engineering, ASCE, 129(10), 951-955.
28. Consoli, N.C., Montardo, J.P. and Prietto, P.D.M (2002). "Engineering behaviour of sand reinforced with plastic waste." Journal of Geotechnical and Geoenvironmental Engineering, ASCE, Vol. 128 June 2002, 462-472.
29. Consoli, N.C., Montardo, J.P., Donato, M., and Prietto, P. D. M. (2004). "Effect of material properties on the behaviour of sand-cement-fibre composites." Ground Improvement, 8(2), 77-90.
30. Consoli, N.C., Prietto, P.D.M. and Ulbrich, L.A. (1998). "Influence of fibre and cement addition on behaviour of sandy soil." Journal of Geotechnical and Geoenvironmental Engineering, ASCE, 124(12), 1211-1214.
31. Consoli, N.C., Vendrucolo, M.A. and Prietto, P.D.M. (2003a). "Behaviour of plate load tests on soil layers improved with cement and fiber." Journal of Geotechnical and Geoenvironmental Engineering, ASCE, 129(1), 95-101.
32. Crockford, W.W., Grogan, W.P. and Chill, D. S. (1993). "Strength and life of stabilized pavement layers containing fibrillated poly propylene." Transportation Research Record, 1418, 60-66.

33. Dash, S.K., Rajagopal, K. and Krishnaswamy, N.R. (2004), "Performance of different geosynthetic reinforcement materials in sand foundations." *Geosynthetics International*, 11(1), 35-42.
34. De Beer, E.E. (1963). "The scale effect in the transposition of the results of deep-sounding tests on the ultimate bearing capacity of piles and caisson foundations." *Geotechnique*, London, 13(1), 39-75.
35. De Beer, E.E. (1965). "Bearing capacity and settlement of shallow foundations on sand." *Proc., Bearing Capacity and Settlement of Found. Symp., Duke University, Durham*, 15–34.
36. De Beer, E.E. (1970). "Experimental determination of the shape factors and bearing capacity factors of sand." *Geotechnique*, 20(4), 387–411.
37. De Beer, E.E. (1987). "Analysis of shallow foundations on sand." Chapter 6, in *Geotechnical Modeling and Applications*, S.M. Sayed, editor, Gulf Publishing Company, 212–321.
38. Dembicki, E., Jermolowicz, P. and Niemunis, A., (1986). "Bearing capacity of strip foundation on soft soil reinforced by geotextile." 3rd International Conference on Geotextiles, Vienna, Austria, Vol. 2A/6, 205 – 208.
39. Dixit, R.K. and Mandal, J.N. (1993). "Bearing capacity of geosynthetic reinforced soil using variational method." *Geotextiles and Geomembranes*, 12, 543 – 566.
40. Edil, T. B. and Bosscher, P. J. (1994) Engineering properties of tire chips and soil mixtures, *Geotechnical Testing Journal*, ASTM, 17(4), 453–464.
41. Falorca I.M.C.F.G. and Pinto M.I.M. (2002). "Sand reinforced with short length synthetic fibres randomly oriented." 7th International Conference on Geosynthetics, Nice, France, 1237-1240.
42. Falorca I.M.C.F.G., Pinto M.I.M. and Ferreira Gomes, L.M. (2006). "Residual shear strength of sandy clay reinforced with short polypropylene fibres randomly oriented." 8th International Conference on Geosynthetics, Yokohama (Japan), Vol. 4, 1663 – 1666.
43. Fatani, M.N., Bauer, G.E. and Al-Joulani, N. (1991). "Reinforcing soil with aligned and randomly oriented metallic fibres." *Geotechnical Testing Journal*, GTJODJ, ASTM, 14(1), 78–87.

44. Foose, G. J., Benson, C. H. and Bosscher, P. J. (1996). "Sand reinforced with shredded waste tires." *Journal of Geotechnical Engineering Division, ASCE*, 122(9), 760–767.
45. Fragaszy, R. J. & Lawton, E. (1984). "Bearing capacity of reinforced sand subgrades." *Journal of Geotechnical Engineering Division, ASCE*, 110, 1500–1507.
46. Frietag D.R. (1986). "Soil randomly reinforced with fibres." *Journal of Geotechnical Engineering, ASCE*, 112(8), 823-825.
47. Galav, B. (1997). "Behaviour of ring footings on reinforced sand under vertical and lateral loads." M.E. Thesis, University of Roorkee, Roorkee, U.P., India.
48. Ghiassian, H., Poorebrahim, G. and Gray, D.H. (2004). "Soil reinforcement with recycled carpet wastes." *Waste Management & Research*, 22(2), 108-114.
49. Ghumman, M.S., (1966). "Effect of bearing capacity of model footings on sand." M.E. Thesis, University of Roorkee, Roorkee, U.P., India
50. Gosavi, M., Patil, K.A, Mittal, S. and Saran, S. (2004). "Improvements of properties of black cotton soil subgrade through synthetic reinforcement." *Journal of Institution of Engineers (India)*, 84, 257-262.
51. Graham, J. and Stuart, J. G. (1971). "Scale and boundary effects in foundation analysis." *J. Soil Mech. and Found. Div., ASCE*, 97(11), 1533–1548.
52. Gray, D.H. (1974). "Reinforcement and stabilization of soil by vegetation." *Journal of the Geotechnical Engineering*, 100(6), 695-699.
53. Gray, D.H. (1978). "Role of woody vegetation in reinforcing soils and stabilising slope." *Proc. Symposium Soil Reinforcing and Stabilizing Techniques. Sydney, Australia*, 253-306.
54. Gray, D.H. and Ohashi, H. (1983). "Mechanics of fiber reinforcing in sand." *Journal of Geotechnical Engineering*. 109(3): 335-353.
55. Gray, D.H., and Al-Refeai, T. (1986). "Behavior of fabric-versus fiber-reinforced sand." *Journal of Geotechnical Engineering* 112(8): 804-820.
56. Gregory, G.H. and Chill, D.S. (1998). "Stabilization of earth slopes with fiber-reinforcement", *Proc. Sixth International Conference on Geosynthetics, Atlanta*, 1073-1078.

57. Grogan, W. P. and Johnson, W. G. (1993). "Stabilization of high plasticity clay and silty sand by inclusion of discrete fibrillated polypropylene fibers for use in pavement subgrades." Tech. Rep. CPAR-GL-93-3, U.S. Army Engineer Waterways Experiment Station, Vicksburg, Miss.
58. Guido, V. A., Chang, D. K. and Sweeney, M. A. (1986). "Comparison of geogrid and geotextile reinforced earth slabs." *Canadian Geotechnical Journal*, 23, 435–440.
59. Gupta, P.K., Saran, S. and Mittal, R.K. (2006). "Behaviour of fibre reinforced sand in different test conditions." *Indian Geotechnical Journal*, 36 (3), 272-282.
60. Hanna, A.M. and Meyerhof, G.G. (1980). "Experimental evaluation of bearing capacity of footing subjected to inclined loads." *Canadian Geotechnical Journal*, 18, 599 – 603.
61. Harr, M.E. (1966). "Foundations of theoretical soil mechanics." McGraw–Hill Book Company, New York, 3 - 54.
62. Hataf, N. and Rahimi, M.M. (2006). "Experimental investigation of bearing capacity of sand reinforced with randomly distributed tire shreds." *Construction and Building Materials*, 20(10), 910–916.
63. Heineck, K. S. and Consoli, N. C. (2004). "Discrete framework for limit equilibrium analysis of fibre-reinforced soil." *Discussion, Géotechnique*, 54(1), 72-73.
64. Heineck, K.S., Coop, M.R. and Consoli, N.C. (2005). "The effect of micro-reinforcement of soils from very small to large shear strains." *Journal of Geotechnical and Geoenvironmental Engineering, ASCE*, 131(8), 1024-1033.
65. Hoshiya, M. and Mandal, J.N. (1984). "Metallic powders in reinforced earth." *Journal of Geotechnical Engineering*, Vol. 110(10), 1507-1511.
66. Huang, C.C. and Menq, F.Y. (1997). "Deep footing and wide–slab effects in reinforced sandy ground." *Journal of Geotechnical and Geoenvironmental Engineering, ASCE*, 123(1), 30-36.
67. Huang, C.C. and Tatsuoka, F. (1990). "Bearing capacity of reinforced horizontal sandy ground." *Geotextiles and Geomembranes*, 9, 51-82.

68. IS: 2720-Part 14, (1983). "Determination of density index (relative density) of cohesionless soils." BIS, New Delhi, India.
69. Jumikis, A.R. (1956). "Rupture surface in sand under oblique loads." Proceeding ASCE, 8(1), 26.
70. Jumikis, A.R. (1961). "Shape of rupture surface in dry sand." Proceeding of 5th Int. Conference on SMFE Vol. 1, 693.
71. Kaniraj, S.R. and Gayatri, V. (2003). "Geotechnical behavior of fly ash mixed with randomly oriented fiber inclusions." Geotextiles and Geomembranes, 21, 123-149.
72. Kaniraj, S.R. and Havanagi, V.G. (2001). "Behavior of cement-stabilized fiber-reinforced fly ash-soil mixtures." Journal of Geotechnical and Geoenvironmental Engineering, ASCE, 127(7), 574-584.
73. Kezdi, A. (1961). "The effect of inclined loads on the stability of a foundation." 5th International Conference on SMFE, Vol.1, Div. 1-3A, 699 - 703.
74. Khan, S.A. (2005). "Stabilization of soil using bamboo industry waste." 6th International Conference on Ground Improvement Techniques, 18 - 19 July, 2005, Coimbra, Portugal, 357-362.
75. Khay, M., Gigan, J.P. and Ledelliou, M. (1990). "Reinforcement with continuous thread: technical developments and design methods." In: Proc. 4th International Conf on Geotextiles, Geomembranes and Related Products, The Hague Vol. 1, 21-26.
76. Khing, K.H., Das, B.M., Puri, V.K., Cook, E.E. and Yen, S.C. (1993). "The bearing capacity of a strip foundation on geogrid reinforced sand." Geotextiles and Geomembranes 12(4), 351-361.
77. Kondner, R.L. (1963). "Hyperbolic stress - strain response: cohesive soils." Journal of the Soil Mechanics and Foundation Engineering, ASCE, 89(SM1), 115-143.
78. Kondner, R.L. and Zelasko, J.S. (1963). "A Hyperbolic stress-strain formulation for sands." 2nd Pan American Conference on SMFE, Brazil, Vol. 1, 289-324.

79. Kudo, M., Ochiai, H. and Omine, K. (2001). "Mechanical properties in short-fibers mixture stabilized volcanic cohesive soil." Landmarks in Earth Reinforcement, Department of Civil Engineering, Kyushu University, Fukuoka, Japan, ISBN 90 26518528.
80. Kumar, A. and Saran, S. (2001). "Isolated strip footings on reinforced sand." Journal of Geotechnical Engineering, SEAGS, Bangkok, Thailand, 177-189.
81. Kumar, A. and Saran, S. (2002). "Isolated square footing on reinforced soil – a parametric study." Proc. A.I.C.M., R.E.C., Hamirpur.
82. Kumar, A. and Saran, S. (2003). "Bearing capacity of rectangular footing on reinforced soil." Journal of Geotechnical and Geological Engineering, Kluwer Academic Publishers, The Netherlands, 21, 201-224.
83. Kumar, P. and Sastry, M.V.B.R. (2001). "Strength behaviour of lateritic soils randomly reinforced with jute fibre." Landmarks in Earth Reinforcement, 127-130.
84. Kumar, S. and Tabor, E. (2003). "Strength characteristics of silty clay reinforced with randomly oriented nylon fibers." Electronic Journal of Geotechnical Engineering.
85. Kurian, P.N. (2001). "Fibre-reinforced backfills for retaining structures." 15th International Conference of Soil Mechanics and Geotechnical Engineering, Istanbul, Turkey, Vol.2, 1185-1188.
86. Ladd, R.S. (1978). "Preparing test specimens using undercompaction." Journal of Geotechnical Testing Journal, GTJODJ, 1(1), 16-23.
87. Lawton, E.C., Khire, M.V. and Fox, N.S. (1993). "Reinforcement of soils by multioriented geosynthetic inclusions." Journal of Geotechnical Engineering, ASCE, 119(2), 257-275.
88. Lee, I.K. (1965). "Footings subjected to moments." Proceedings of 4th International Conference of Soil Mechanics and Foundation Engineering, 2, 108.
89. Lee, K.L., Adams, B.D. and Vagneron (1973). "Reinforced earth retaining walls." Journal of the Soil Mechanics and Foundation Division, ASCE, 99(10), 745-764.

90. Leflaive, E. (1985). "Soil reinforced with continuous yarns: texsol." In: Proc. 11th International Conf. on Soil Mechanics and Foundation Engng, San Francisco Vol. 3, 1787-1790.
91. Li, G.X., Jie, Y.X. and Jie, G.Z. (2001). "Study on the critical height of fiber-reinforced slope by centrifuge test." Landmarks in Earth Reinforcement, Balkema, 239-241.
92. Lindh, E. and Eriksson, L. (1990). "Sand reinforced with plastic fibers, a field experiment." Performance of Reinforced Soil Structures, McGown, A., Yeo, K., and Andrawes, K.Z., Editors, Thomas Telford, Proceedings of the International Reinforced Soil Conference held in Glasgow, Scotland, September 1990, 471-473.
93. Loehr, J.E., Axtell, P.J. and Bowders, J.J. (2000). "Reduction of soil swell potential with fiber reinforcement." In Proceedings of Geo Eng 2000, Melbourne, Australia.
94. Lutenecker, A.J. and Adams, M.T. (1998). "Bearing capacity of footings on compacted sand." Proceedings of the 4th International Conference on Case Histories in Geotechnical Engineering, 1216-1224.
95. Maher, M. H. and Ho, Y.C. (1994). "Mechanical properties of kaolinite/fiber soil composite." Journal of Geotechnical Engineering Division, ASCE, 120(8), 1381-1393.
96. Maher, M.H. and Gray, D. H. (1990). "Static response of sands reinforced with randomly distributed fibres." Journal of Geotechnical Engineering, ASCE. 116 (11), 1661-1677.
97. Maher, M.H. and Woods, R.D. (1990). "Dynamic response of sand reinforced with randomly distributed fibers." Journal of Geotechnical Engineering, ASCE, 116(7), 1116-1131.
98. Mandal, J.N. and Murti, M.V.R. (1989). "Potential for use of natural fibres in geotextile engineering." International Workshops on Geotextiles 1989, Bangalore, India, 251-254.
99. Mandal, J.N. and Suresh, S.V. (2001). "Enhancement of slope stability of cover soils of landfills." Indian Geotechnical Journal, 31(3), 258-272.

100. Mandal, J.N., Kumar, S. and Meena, C.L. (2005). "Centrifuge modeling of reinforced soil slopes using tire chips." ASCE, GSP 140 Slopes and Retaining Structures under Seismic and Static Conditions, Geofrontier 2005 (in CD-ROM).
101. Manjunath, V.R. and Dewaikar, D.M. (1996). "Bearing capacity of inclined loaded footings on geotextile reinforced two-layer soil system." Earth Reinforcement, Balkema, Rotterdam, 619-622.
102. McGown, A., Andrawes, K.Z. and Al-Hasani, M.M. (1978). "Effect of inclusion properties on the behavior of sand." Geotechnique, 28(3), 327-346.
103. McGown, A., Andrawes, K.Z., Hytiris, N. and Mercer, F.B. (1985). "Soil strengthening using randomly distributed mesh elements." In: Proc. 11th International Conf: on Soil Mechanics and Foundation Engg., San Francisco, 3, 1735-1738.
104. McGown, A., Kanyoza, A. and Doctor, R. (2004). "A comparison of mesh elements and short fibres for the micro-reinforcement of granular soils." EuroGeo3, Third European Geosynthetics Conference, 569-574.
105. Mercer, F.B., Andrawes, K.Z., McGown, A. and Hytiris, N. (1984). "A new method of soil stabilization." Polymer Grid Reinforcement, Thomas Telford, 1985, Proceedings of a conference held in London, UK, March 1984, 244-249.
106. Meyerhof, G.G. (1953). "The bearing capacity of foundations under eccentric and inclined loads." 3rd International Conference on SMFE, Zurich, 1, 440-445.
107. Meyerhof, G.G. (1956). "Rupture surfaces in sand under oblique loads." Discussion, Journal of Soil Mechanics and Foundation Engineering, ASCE, 82(3), 1028 - 1050.
108. Michalowski, R.L. and Cermák, J. (2002). "Strength anisotropy of fiber-reinforced sand." Computers and Geotechnics, 29(4), 279-299.
109. Michalowski, R.L. and Cermák, J. (2003). "Triaxial compression of sand reinforced with fibres." Journal of Geotechnical and Geoenvironmental Engg., ASCE 129 (2), 125-136.
110. Michalowski, R.L. and Zaho, A. (1995). "Limit condition for fibres-reinforced granular soils". Transp. Res. Rec., 1474, Transportation Research Board. Washington D.C., 102-107.

111. Michalowski, R.L. and Zhao, A. (1996). "Failure of fiber-reinforced granular soils." *Journal of Geotechnical Geoenvironmental Engg.,ASCE*, 122(3), 226–234..
112. Miller, C.J. and Rifai, S. (2004). "Fiber reinforcement for waste containment soil liners." *Journal of Environmental Engineering, ASCE*, 130(8), 891-895.
113. Morel, J. C. and Gourc, J. P. (1997). "Mechanical behavior of sand reinforced with mesh elements." *Geosynthetics International*, 4(5), 481–508.
114. Muhs, H. and Weiss, K. (1969). "The influence of load inclination on bearing capacity of shallow footings." *Proceedings of 7th International Conference on SMFE*, 187.
115. Muhs, H. and Weiss, K. (1973). "Inclined load tests on shallow strip footings." *Proceedings of 8th International Conference on SMFE, Mockba, 1(Part-III, Session-2)*, 173.
116. Murty, A.V.S.R. (1967). "Bearing capacity of footings under inclined loads." M.E. Thesis, University of Roorkee, Roorkee, U.P., India.
117. Mutgi, R.P., Dewaikar, D.M. and Mohapatra, B.G. (2001). "Eccentrically - inclined loaded circular footing on reinforced sand bed." *Indian Geotechnical Conference, IGC-2001, Indore, 1*, 199-202.
118. Nataraj, M.S. and McManis, K.L. (1997). "Strength and deformation properties of soils reinforced with fibrillated fibers." *Geosynthetics International*, 4(1), 65-79.
119. Nataraj, M.S., Boutwell, G.P. and McManis, K.L. (2005). "Selected case studies in slope stability." *GEOPRACTICE – 2005, National Conference on Case Studies in Geotechnical Engineering, July 25 – 26, 2005*, 25-32.
120. Noorany, I. and Uzdavines, M. (1989). "Dynamic behaviour of saturated sand reinforced with geosynthetic fibres." In: *Proc. Geosynthetics '89 Conference North American Geosynthetics Society, San Diego* , 385–396.
121. Opoczky, L. and Pentek, L. (1975). "Investigation of the corrosion of asbestos fibres in asbestos cement sheets weathered for long time." *Proceedings of Fibre Reinforced Cement Concrete, RILEM, Symposium, Vol. 1*, 269-276.
122. Park, T. and Tan, S.A. (2005). "Enhanced performance of reinforced soil walls by the inclusion of short fiber." *Geotextiles and Geomembranes*, 23, 348–361.

123. Pinto, M.I.M. and Falorca, I.M.C.F.G. (2005). "Improvement of sand by short length polypropylene fibres randomly oriented." 6th International Conference on Ground Improvement Techniques, Coimbra, Portugal.
124. Pinto, M.I.M. and Falorca, I.M.C.F.G. (2006). "The influence of cement and polypropylene fibres addition on the behaviour of sand under shear loads." Geo – Singapore (2006), An International Conference on Geotechnical Engineering, 11-13 December (2006), Singapore, 37-46.
125. Poulos, H.G. and Davis, E.H. (1974). "Elastic solutions for soil and rock mechanics." John Wiley and Sons, Inc. New York.
126. Prabhakar, J. and Sridhar, R.S. (2002). "Effect of Random inclusion of sisal fibre on strength behaviour of soil." Construction and Building Materials, 16, 123-131.
127. Prakash, S. and Saran, S. (1971). "Bearing capacity of eccentrically loaded footings." Journal of the Soil Mechanics and Foundations, ASCE, 97(1), 95-118.
128. Prakash, S. and Saran, S. (1973). "A new method of designing eccentrically loaded rigid footings." Journal of Indian Geotechnical Society, New Delhi, India, 1-11.
129. Prakash, S., Saran, S. and Sharan, U.N. (1984). "Footings and constitutive laws." Journal of the Geotechnical Engineering, ASCE, 110(10), 1473-1488.
130. Punthutaecha, K., Puppala, A.J., Vanpalli, S.K. and Inyang, H. (2006). "Volume change behaviour of expansive soils stabilized with recycled ashes and fibers." Journal of Materials in Civil Engineering, ASCE, 18(2), 295-306.
131. Puppala, A.J. and Musenda, C. (2000). "Effects of fibre reinforcement on strength and volume change in expansive soils." Transportation Research Record, 1736, Paper No. 00-0716, 134-140.
132. Puppala, A.J., and Musenda, C. (2001). "Shrinkage potentials of fiber reinforced and raw expansive soils." Proceedings, International Symposium on Suction, Swelling, Permeability and Structure of Clays, Balkema Publishers, IS-Shizuoka, Shizuoka, Japan, January, 11-13, 2001.

133. Puppala, A.J., Hoyos, L., Viyanant, C. and Musenda, C. (2000). "Fiber and fly ash stabilization methods to treat soft expansive soils." ASCE Special Publication No. 112, Soft Ground Technology, Noordwijkerhout, The Netherlands, May 28 - June 2, 2000.
134. Puppala, A.J., Punthutaecha, K. and Vanapalli, S.K. (2006). "Soil-water characteristic curves of stabilized expansive soils." *Journal of Geotechnical and Geoenvironmental Engineering*, ASCE, 132(6), 736-751.
135. Purohit, D.G., Ameta, N.K., Sharma, V.S. and Singhvi, R. (1997a). "Behaviour of circular footing on dune sand reinforced with natural fiber" Second IISc National Seminar on Geotechnical Engineering 24-25 July 1997, Bangalore, India.
136. Purohit, D.G., Ohri, M.L. and Shukla, A. (1997b). "Behaviour of circular footing on dune sand reinforced with shredded waste tyres" Second IISc National Seminar on Geotechnical Engineering 24-25 July, 1997, Bangalore, India.
137. Purukayastha, R.D. and Char, A.N.R., (1977). "Stability analysis of eccentrically loaded footing." *Journal of Geotechnical Engineering*, ASCE, 103(6), 647.
138. Purukayastha, R.D., (1978), "Investigation of footing under eccentric load." *Journal of Indian Geotechnical Society*, 9, 220-234.
139. Ranjan, G., Singh, B. and Charan, H.D. (1999). "Experimental study of soft clay reinforced with sand-fiber core." *Indian Geotechnical Journal*, 29(4), 281-291.
140. Ranjan, G., Vasani, R.M. and Charan, H.D. (1994). "Behaviour of plastic-fibre-reinforced sand." *Geotextiles and Geomembranes*, 13, 555-565.
141. Ranjan, G., Vasani, R.M. and Charan, H.D. (1996). "Probabilistic analysis of randomly distributed fiber-reinforced soil". *Journal of Geotechnical Engineering*, ASCE, 122(6): 419-426.
142. Rao, A.S., Rao, K.V.N., Sabitha, G. and Suresh, K. (2006a). "Load deformation behaviour of fibre-reinforced gravel beds overlying soft clay." A National Conference on Corrective Engineering Practices in Troublesome Soils (CONCEPTS), Kakinada, 8 - 9 July, 2006, 187-190.
143. Rao, G. V. and Dutta, R. K. (2001). "Utilization of shredded tyres in highway engineering." In *Proceedings of the International Seminar on Sustainable Development in Road Transport*, New Delhi, I-257-I-268.

144. Rao, G. V., Dutta, R. K. and Ujwala, D. (2006b). "Strength characteristics of sand reinforced with coir fibers and coir geotextiles." *Electronic Journal of Geotechnical Engineering*.
145. Rao, G.V. and Dutta, R.K. (2004). "Sand plastic mixtures ground improvement." *International Conference on Geosynthetics and Geoenvironmental Engineering, I.I.T. Mumbai*, 189-194.
146. Rao, G.V. and Dutta, R.K. (2006). "Compressibility and strength behaviour of sand-tyre chip mixtures." *Geotechnical and Geological Engineering*, 24, 711-724.
147. Rao, G.V., Kate, J.M. and Shamsher, F.H. (1991). "Ground improvement with geogrids." 9th *Asian Regional Conference on SMFE, Thailand, Bangkok*, 531 – 534.
148. Rao, G.V., Kate, J.M. and Shamsher, F.H. (1994). "Soil improvement with geosynthetics." 13th *International Conference on SMFE, New Delhi, India*, 1237 - 1240.
149. Rao, S., Rao, K.K.V.N., Suresh, K. and Kumar, P. (2005). "Role of fibre-reinforcement in improving load carrying capacity of sand beds overlying soft marine clay." *Indian Geotechnical Conference, 2005, Ahmedabad, India*, 121 – 124.
150. Razani, R. and Behpour, L. (1970). "Some studies on improving the properties of earth materials used for construction of rural earth houses in seismic region of Iran." *Symp. on Earthquake .Engg., Roorkee*.
151. Rehsi, S.S. (1988), "Use of natural fibre concrete in India." *Natural Fibre Reinforced Cement and Concrete – Edited by R. N. Swamy, Blackie*.
152. Samatani, N.C. and Sonpal, R.C. (1989). "Laboratory tests of strip footing on reinforced cohesive soil." *Journal of Geotechnical Engg. Div., ASCE*, 115(9), 1326-1330.
153. Sambasivarao, P. and Mandal, J.N. (2004). "Finite element analysis of fiber reinforced fly ash slopes." *International Conference on Geosynthetics and Geoenvironmental Engineering, I.I.T. Mumbai*, 361-366.

154. Santoni, R.L. and Webster, S. L (2001). "Airfield and road construction using fiber stabilization of sands." *Journal of Transportation Engineering, ASCE*, 127(2), 96-104.
155. Santoni, R.L., Tingle, J.S. and Webster, S. L (2001). "Engineering properties of sand-fiber mixtures for road construction." *Journal of Geotechnical and Geoenvironmental Engineering, ASCE*, 127(3), 258-268.
156. Saran, S. (1969). "Bearing capacity of footings subjected to moments." Ph.D. Thesis, University of Roorkee, Roorkee, India.
157. Saran, S. (1971). "Bearing capacity of footings under inclined loads." *Seminar on Foundation Problems, New Delhi, Vol. 2, 5*.
158. Saran, S. and Agarawal, R.K. (1989). "Eccentrically – obliquely loaded footing." *Journal of Geotechnical Engineering Division, ASCE*, 115(11), 1673-1680.
159. Saran, S. and Agarawal, R.K. (1991). "Bearing capacity of eccentrically obliquely loaded footings." *Journal of Geotechnical Engineering Division, ASCE*, 117(11), 1169-1190.
160. Saran, S. and Singh, P. (1976). "Behaviour of footings subjected to two-way eccentric inclined loads." *Journal IGS*, 6(3), 160-175.
161. Saran, S., Kumar, S., Garg, K.G. and Kumar, A. (2007). "Analysis of square and rectangular footings subjected to eccentric-inclined load resting on reinforced sand." *Geotechnical and Geological Engineering*, DOI 10.1007/s10706-006-0010-7.
162. Saran, S., Rao, A.S.R. and Singh, H. (1985). "Behaviour of eccentrically loaded footing on reinforced earth slab." *Indian Geotechnical Conference, IGC-85, Roorkee, Vol.1, 117-122*.
163. Setty, K.R.N.S. and Chandrashekar, M. (1988). "Behaviour of fiber reinforced lateritic soil under circular footing." *First Indian Geotextile Conference on Reinforced soil and Geotextile, Mumbai, India, Part C, 41–46*.
164. Setty, K.R.N.S. and Rao, S.V.G. (1987). "Characteristics of fibre reinforced lateritic soil." *Indian Geotechnical Conference, Bangalore, 1, 329-333*.

165. Setty, K.R.N.S. and Shetty, P.P. (1989). "Reinforced soil layers in pavement construction." International Workshops on Geotextiles, Bangalore, India, 267-270.
166. Shamsher, F. H. (1992). "Ground improvement with oriented geotextiles and randomly distributed geogrid micro-mesh." Ph.D. Thesis, Deptt. of Civil Engg. I.I.T. Delhi, New Delhi, India.
167. Sharan, U.N. (1977). "Pressure settlement characteristics of surface footing from constitutive laws." Ph.D. Thesis, University of Roorkee, Roorkee, India.
168. Shiraishi, S. (1990). "Variation in bearing capacity factors of dense sand assessed by model loading tests." Soils and Found., Tokyo, 30(1), 17-26.
169. Shukla, S.K. and Chandra, S. (1994a) A study of settlement response of a geosynthetic reinforced compressible granular fill-soft soil system, Geotextiles and Geomembranes, 13, 627-639.
170. Shukla, S.K. and Chandra, S. (1994b). "A generalized mechanical model for geosynthetic reinforced foundation soil." Geotextiles and Geomembranes, 13, 813-825.
171. Sivakumar Babu, G.L. and Vasudevan, A.K. (2005). "Strength and stiffness behaviour of coir-fibre reinforced soil." Indian Geotechnical Conference, 2, 241-245.
172. Sobhan, K. and Mashnad, M. (2002). "Tensile strength and toughness of soil-cement-fly-ash composite reinforced with recycled high-density polyethylene strips." Journal of Materials in Civil Engg., ASCE, 2002, 14(2), 177-184.
173. Sobhan, K. and Mashnad, M. (2003). "Fatigue behaviour of a pavement foundation with recycled aggregate and waste HDPE strips." Journal of Geotechnical and Geoenvironmental Engineering, ASCE, 129(7), 630-638.
174. Sridharan, A., Murthy, B.R.S. and Singh, H.R. (1988). "Shape and size effects of foundations on the bearing capacity of reinforced soil beds." Indian Geotechnical Conference-1988, Allahabad, India, Vol. 1, 205-210.
175. Tang, C., Shi, B., Gao, W., Chen, F. and Cai, Y. (2007). "Strength and mechanical behavior of short polypropylene fiber reinforced and cement stabilized clayey soil." Geotextiles and Geomembrances, 25(3), 194-202.

176. Tingle, J. S., Santoni, R.S., and Webster, S.L. (2002). "Full-scale field tests of discrete fiber-reinforced sand." *Journal of Transportation Engineering, ASCE* 128(1), 9-16.
177. Tiwari, S.K. (2004). "Influence of randomly distributed fibres reinforced backfill on lateral earth pressure against model retaining walls." *International Conference on Geosynthetics and Geoenvironmental Engineering, I.I.T. Bombay, Mumbai, India*, 285-290.
178. Ueno, K., Miura, K., and Maeda, Y. (1998). "Prediction of ultimate bearing capacity of surface footings with regard to size effect." *Soils and Found.*, Tokyo, 38(3), 165-178.
179. Uysal, C. (1993). "Stress-strain behaviour of randomly distributed, discrete fibre and mesh reinforced sand." M.Sc. Thesis, Middle East Technical University, Ankara, Turkey (1993).
180. Van Impe, E. and Silence, P. (1986). "Improving of the Bearing Capacity of Weak Hydraulic Fills by Means of Geotextiles." *Proc. 3rd IGS Conf., Vienna, Austria*, pp.1411-1416.
181. Verma, B.P. and Char, A.N.R. (1978). "Triaxial tests on reinforced sand." *Proc. Symposium Soil Reinforcing and Stabilizing Techniques, Sydney, Australia*, 29-39.
182. Vesic, A.S. (1973). "Analysis of Ultimate Loads of Shallow Foundations." *Journal of the Soil Mechanics and Foundations Division, ASCE*. 99(1),45-73.
183. Vidal, H. (1969). "The principle of reinforced earth." *Highway Research Record* No. 282, 1-16.
184. Waldron, L.J. (1977). "The shear resistance of root-permeated homogeneous and stratified soil." *Soil Science Society of American Journal*, 41(3), 843-849.
185. Wasti, Y.W. and Butun, D. (1996). "Behaviour of model footings on sand reinforced with discrete inclusions." *Geotextiles and Geomembranes*. 14(10), 575-584.
186. Wu, T.H., Beal, P. E. and Lan, C. (1988). "In situ shear test of soil-root system." *Journal of Geotech. Engg., ASCE*, 114(12), 1376-1394.

187. Yetimoglu, T. and Salbas, O. (2003). "A study on shear strength of sands reinforced with randomly distributed discrete fibers." *Geotextiles and Geomembranes*, 21(2), 103-110.
188. Yetimoglu, T., Inanir, M. and Inanir, O.E. (2005). "A study on bearing capacity of randomly distributed fiber-reinforced sand fills overlying soft clay." *Geotextiles and Geomembranes*. 23(1), 174-183.
189. Yetimoglu, T., Wu, J.T.H. and Saglamer, A. (1994). "Bearing capacity of rectangular footings on geogrid-reinforced sand." *Journal of Geotechnical Engineering*, ASCE, 120, 2083–2099.
190. Youd, T.L., Hansen, C.M. and Bartlett, S.F. (2002). "Revised multilinear regression equations for prediction of lateral spread displacement." *Journal of Geotechnical and Geoenvironmental Engineering*, ASCE, 128(12), 1007-1017.
191. Ziegler, S. Leshchinsky, D. Ling, S.I. and Perry, E.B. (1998). "Effect of short polymeric fibers on crack development in clays." *Soils and Foundations*, 38(1), 247-253.
192. Zornberg, J.G. (2002). "Discrete framework for limit equilibrium analysis of fibre-reinforced soil." *Géotechnique*, 52(8), 593-604.
193. Zornberg, J.G. (2004). "Discrete framework for limit equilibrium analysis of fibre-reinforced soil." Closure, *Géotechnique*, 54(1), 72-73.
194. Zornberg, J.G. (2005). "Geosynthetic Reinforcement in Landfill Design: US Perspectives." *International Perspectives on Soil Reinforcement Applications*. ASCE, Geotechnical Special Publication No. 141, Zornberg, Gabr, and Bowders (Editors), January 2005, Austin, Texas (CD-ROM).
195. Zornberg, J.G., Somasundaram, S. and LaFountain, L. (2001). "Design of geosynthetic-reinforced veneer slopes." *Proceedings of the International Symposium on Earth Reinforcement (IS Kyushu 2001)*, Fukuoka, Japan, Ochiai, H., Otani, J., Yasufuku, N. and Omine, K. (Editors), A.A. Balkema, November 14-16, Vol. 1, 305-310.